



<http://researchcommons.waikato.ac.nz/>

Research Commons at the University of Waikato

Copyright Statement:

The digital copy of this thesis is protected by the Copyright Act 1994 (New Zealand).

The thesis may be consulted by you, provided you comply with the provisions of the Act and the following conditions of use:

- Any use you make of these documents or images must be for research or private study purposes only, and you may not make them available to any other person.
- Authors control the copyright of their thesis. You will recognise the author's right to be identified as the author of the thesis, and due acknowledgement will be made to the author where appropriate.
- You will obtain the author's permission before publishing any material from the thesis.

U-Pb Dating of Silicic Volcanic Rocks of the Eastern Coromandel Peninsula

A thesis submitted in partial fulfilment
of the requirements for the degree of

**Master of Science
in Earth and Ocean Sciences
at
The University of Waikato**

by
Kirsty Anne Vincent



THE UNIVERSITY OF
WAIKATO
Te Whare Wānanga o Waikato

2012

Abstract

The eastern Coromandel Volcanic Zone (CVZ) is an area of predominantly andesite-dacite-rhyolite volcanism which was erupted and subsequently hydrothermally altered in parts during the Late Miocene to Early Pleistocene. Many of the andesitic host rocks and products of hydrothermal alteration have been dated, but there are few ages on the rhyolites. This study was undertaken to help better constrain the age of selected rhyolite lavas and ignimbrites of the onshore eastern CVZ. 21 units were sampled for U-Pb dating of zircon using laser ablation inductively coupled plasma mass spectrometry (LA-ICP-MS). This method was chosen because most CVZ rhyolites are known to contain zircon. In this study, 18 of the 21 samples contained sufficient zircons for dating, and 18 new zircon U-Pb ages are presented. These ages are the age of crystallisation and therefore represent the maximum eruption age. This method has not previously been used in the CVZ, so was also chosen to assess if it is an appropriate method for dating CVZ rhyolites. This was determined by comparing the new ages generated in this study with any previous ages. They mostly agree, which supports the validity of the method, and also provides new age data of several units which had not previously been dated.

In order to set the new ages into a geological context, it was necessary to describe the units sampled. The petrography, mineralogy and petrochemistry were assessed by petrographic microscope, electron microprobe and whole rock X-ray diffraction and fluorescence. 21 new whole rock major and trace element XRF analyses are presented.

Acknowledgements

I would like to thank the following people who have been a part of this project:

Thanks first to my supervisors, Assoc. Professor Roger Briggs and Dr Adrian Pittari for suggesting the topic and being great mentors.

Dr Ganqing Xu, Annette Rodgers and Renat Radosinsky for help with sample preparation. Also Xu for running the XRD analyses and Annette for the XRF analyses. Thank you to everyone else in the department who has given me advice and support.

Steve Cameron and Megan Grainger from the Chemistry Department for guiding me through the use of the LA-ICP-MS.

Stephanie Lee and Sean Jones for advice on zircons and age data processing.

Ritchie Sims from the University of Auckland for assistance with the microprobe.

Dr Stuart Rabone from Broken Hills Mine for showing me around the mine and allowing me to take samples from it.

Rick Streiff and Lorrance Torckler from Martha Mine for advice about the Wharekirauponga Prospect.

Dr Fiona Petchey from the Carbon Dating Unit for advice about comparing radiometric ages.

My fellow graduates for all the fun times, lunch breaks, discussions and memories. Thanks to Megan, Anna and Sarah for helping me in the field. Thanks to Simon for help with GIS. Thanks to Kerri for help with proof reading.

My parents who have supported and encouraged me all this time. Thank you for just being there.

Funding was received from the University of Waikato Masters Research Scholarship, the Broad Memorial Fund, and the Minerals Industry Student Scholarship (AusIMM).

Table of Contents

Abstract	iii
Acknowledgements	v
Table of Contents	vii
List of Figures	xi
List of Tables.....	xiii
Chapter 1: Introduction	1
1.1 Introduction	1
1.2 Research objectives and methodology	1
1.3 Tectonic and geological setting	2
1.4 Previous work.....	7
1.5 Location of study area	9
Ferry Landing Ignimbrite	12
Shakespeare Ignimbrite	12
Wharepapa Ignimbrite.....	12
Paku Rhyolite	12
Pauanui Dome Complex	13
Timata Dome.....	13
Staircase Dome.....	13
Broken Hills Rhyolite	13
Broken Hills Mine Rhyolite	13
Hikuai Ignimbrite	14
Pokohino Dome Complex	14
The Knob.....	14
Pohakahaka Dome Complex	14
Te Karaka Rhyolite	15
Papakura Bay Dome.....	15
Maratoto Rhyolite – Wharekirauponga Dome	15
Homunga Rhyolite – Whale Bone Bay and Shark Bay Domes	15
Owharoa Ignimbrite	16

1.6 Thesis outline	16
Chapter 2: Petrography and Mineralogy 17	
2.1 Introduction and methodology	17
2.2 Slightly altered rhyolite lavas	18
2.2.1 Phenocrysts.....	18
Quartz	18
Plagioclase	18
Relict mafic minerals.....	18
Biotite	21
Opaques	21
Zircon	22
2.2.2 Groundmass	22
2.3 Intensively altered rhyolite lavas	23
2.3.1 Phenocrysts.....	24
Quartz	24
Altered plagioclase	24
Relict mafic minerals.....	24
Biotite	24
Opaques	24
Zircon	26
2.3.2 Groundmass	26
2.3.3 Effects of hydrothermal alteration.....	26
2.4 Ignimbrites	27
2.4.1 Ferry Landing Ignimbrite	27
2.4.2 Shakespeare Ignimbrite	27
2.4.3 Wharepapa Ignimbrite	30
2.4.4 Hikuai Ignimbrite	30
2.4.5 Owharoa Ignimbrite.....	32

Chapter 3: Petrochemistry.....	35
3.1 Introduction	35
3.2 Methodology	35
3.3 Major element chemistry.....	39
3.4 Trace element chemistry.....	40
 Chapter 4: U-Pb Dating of Zircons	45
4.1 Introduction	45
4.2 Methodology	47
4.2.1 Mineral separation.....	48
4.2.2 Grain selection	48
4.2.3 Laser Ablation Inductively Coupled Plasma Mass Spectrometry (LA-ICP-MS)	49
4.2.4 Data processing	50
4.3 Petrography of zircons.....	51
4.4 Results	53
4.4.1 U-Pb ages	53
4.4.2 Inherited zircons.....	54
 Chapter 5: Discussion	57
5.1 Introduction	57
5.2 Mineralogy and petrochemistry.....	57
5.2.1 K ₂ O vs. SiO ₂	57
5.2.2 Hydrothermal alteration	57
5.2.3 Petrography and petrochemistry of Broken Hills Rhyolite.....	59
5.3 U-Pb dating of zircons.....	60
5.3.1 Results from this study.....	60
5.3.2 Errors and uncertainties.....	61

5.3.3	Comparison with previous studies.....	62
5.3.4	Age of CVZ volcanics	65
5.3.5	Silicic centres of the CVZ	67
5.3.6	Origin of inherited zircons.....	68
5.3.7	Physical properties of zircons.....	70
5.3.8	Comparison to the TVZ.....	71
 Chapter 6: Summary and Conclusions		75
6.1	Introduction.....	75
6.2	Petrography, mineralogy and petrochemistry	75
6.2.1	Slightly altered rhyolite lavas	75
6.2.2	Intensively altered rhyolite lavas	76
6.2.3	Ignimbrites.....	76
6.3	U-Pb dating	76
 References		79
 Appendix I: Sample catalogue.....		89
Appendix II: Hand specimen and thin section descriptions		93
Appendix III: Microprobe analyses		99
Appendix IV: XRD traces		105
Appendix V: Equipment settings.....		117
Appendix VI: LA-ICP-MS specifications		119
Appendix VII: Certificates of authenticity		121
Appendix VIII: Isotope ratios.....		127
Appendix IX: Concordia and probability density plots.....		153
Appendix X: CVZ age data		191

List of Figures

Fig. 1.1: The Hauraki Volcanic Region, North Island, New Zealand..	3
Fig. 1.2: Simplified geology of the CVZ.....	5
Fig. 1.3: Division of the Hauraki Goldfield into the Northern, Eastern and Southern Epithermal Provinces.....	6
Fig. 1.4: Simplified geology of the eastern CVZ with sample sites marked.....	9
Fig. 1.5: Characteristic rhyolite sections of Eastern CVZ.	10
Fig. 2.1: Phenocrysts of slightly altered rhyolite lavas.....	19
Fig. 2.2: A) Orthoclase – albite – anorthite ternary diagram for plagioclase phenocrysts of rhyolite lavas. B) Composition of representative phenocrysts of plagioclase, ordered from north to south.....	20
Fig. 2.3: Al – Mg – Fe+Mn ternary diagram for biotite phenocrysts of Papakura Bay Dome and Owharoa Ignimbrite	21
Fig. 2.4: Groundmass features of slightly altered rhyolite lavas	23
Fig. 2.5: Phenocrysts and groundmass features of intensively altered rhyolite lavas.....	25
Fig. 2.6: Orthoclase – albite – anorthite ternary diagram for all plagioclase crystals (free matrix crystals, pumice phenocrysts and crystals in lithics) of ignimbrites analysed in this study, ordered from north to south.....	28
Fig. 2.7: Orthoclase – albite – anorthite ternary diagram for representative plagioclase crystals (free matrix crystals, pumice phenocrysts and crystals in lithics) of ignimbrites in this study, highlighting the variations between core (c) and rim (r) compositions	29
Fig. 2.8: Features of ignimbrites.....	31
Fig. 2.9: Wollastonite – enstatite – ferrosilite ternary diagram for pyroxene crystals of the Wharepapa Ignimbrite.	32
Fig. 3.1: Plot of K ₂ O vs. SiO ₂ wt % of all samples.	40
Fig. 3.2: Harker variation diagrams of selected major elements	41
Fig. 3.3: Harker variation diagrams of selected trace elements.....	42
Fig. 3.4: Selected element-element plots	43
Fig. 4.1: Typological classification of zircons.....	47
Fig. 4.2: Colourless, light pink and pink zircons, Wharekirauponga Dome, reflected light.	49
Fig. 4.3: Colour of zircon crystals that were ablated by LA-ICP-MS.....	52

Fig. 4.4: Morphology of crystals that were ablated and the percentage of each present.....	53
Fig. 5.1: Plot of K ₂ O vs. SiO ₂ of all samples in this study. Shaded areas show the range of compositions of CVZ and TVZ volcanics for comparison	58
Fig. 5.2: Map of the central Eastern CVZ and the samples that were dated in this study.	60
Fig. 5.3: Age of CVZ volcanics dated in this study, with respect to location from north to south.....	61
Fig. 5.4: Map of the igneous rocks of the CVZ that have been dated using all available data.	66
Fig. 5.5: Age versus distance through the CVZ of the igneous rocks of the CVZ that have been dated using all available data.....	67
Fig. 5.6: Tephra thickness at offshore site 1124 (Carter <i>et al.</i> 2003), including tephras from both CVZ and TVZ, and age of silicic centres in the CVZ.....	68
Fig. 5.7: Locations in New Zealand where inherited zircons of Late Cretaceous to Early Miocene age could have originated.	69
Fig. 5.8: Age of ablated zircons by location. Observed colour as indicated.....	71
Fig. 5.9: Silicic centres and calderas of the CVZ and TVZ	72

List of Tables

Table 1.1: Summary of regional stratigraphy of the CVZ	7
Table 1.2: A selection of previous studies that have dated volcanic rocks of the CVZ.....	8
Table 3.1: Whole rock XRF geochemical analyses of selected rhyolite lavas and ignimbrites, eastern CVZ	36
Table 4.1: Optical and physical properties of zircon crystals (Zr[SiO ₄].....	46
Table 4.2: U-Pb ages (My, 1 σ errors) for samples dated in this study, listed north to south.....	54
Table 5.1: Ages (My) from samples dated in this study with comparison to previous age estimates.....	62

Chapter 1

Introduction

1.1 Introduction

The Coromandel Volcanic Zone (CVZ) is the easternmost part of the Hauraki Volcanic Region (HVR), which is the largest and longest lived region of andesite-dacite-rhyolite volcanism in New Zealand. The CVZ was active from c. 18 to 1.9 Ma (Adams *et al.* 1994; Briggs *et al.* 2005). Many of the intermediate volcanics of the CVZ have been dated but the ages of the silicic volcanics are poorly constrained. Most silicic volcanism of the CVZ occurs in the central-east of the Coromandel Peninsula, where the landscape is dominated by rhyolite domes, flows and ignimbrites. In this study, 16 rhyolite lavas and 5 rhyolitic ignimbrites were sampled from the eastern CVZ to generate new U-Pb ages by dating of zircon.

1.2 Research objectives and methodology

The focus of this study was to determine eruption ages for selected silicic volcanic rocks of the eastern CVZ in order to constrain the geochronological evolution of the CVZ. Some of these samples have not previously been dated.

The objectives of the study were:

- To determine maximum eruption ages for selected rhyolite lavas and ignimbrites of the eastern CVZ by U-Pb dating of zircon using laser ablation inductively coupled plasma mass spectrometry (LA-ICP-MS).
- To assess the feasibility of the U-Pb dating of zircon method for dating silicic volcanic rocks of the CVZ.
- To determine if there is any relationship between the physical properties of zircon (i.e. colour and morphology) and age, location and host rock type.

These were achieved by:

- Characterising the rocks sampled to place them into a geological context by determining their chemical composition and mineralogy using a petrographic microscope, electron microprobe, whole rock X-ray diffraction and X-ray fluorescence spectrometry;
- Comparing the new ages generated in this study with any existing ages (fission track on zircon/obsidian, Ar-Ar on adularia, K-Ar on plagioclase/biotite/hornblende/whole rock, U-Pb on zircon). Prior to this study, the zircon U-Pb method had only been used on one sample in the CVZ by ion probe (Hoskin *et al.* 1998); and
- Identifying colour and morphology of zircons using a petrographic microscope.

1.3 Tectonic and geological setting

The CVZ is a continental volcanic arc more than 200 km long by 35 km wide within the HVR (Fig. 1.1). The HVR is the largest and longest lived region of andesite-dacite-rhyolite volcanism in New Zealand and includes the Kiwitahi Volcanic Zone (KVZ, active during the Late Miocene), central Hauraki Rift and the CVZ (Skinner 1986). Volcanism in the CVZ began c. 18 Ma in response to the southwest-dipping Hikurangi subduction zone (King 2000) where the Pacific Plate had already begun subducting beneath the Australian Plate c. 25 Ma (Furlong & Kamp 2009). The CVZ was active from the late-Early Miocene (c. 18 Ma, Adams *et al.* 1994) until the Early Pleistocene (1.9 Ma, Briggs *et al.* 2005). It extends from Great Barrier Island in the north to Te Puke in the south. The Coromandel Peninsula is not in itself a volcanic arc, but is the sub-aerial expression of Neogene volcanism and tectonics which have been superimposed on a fundamental horst structure (Skinner 1986). The CVZ was active at the same time as the off-shore Colville Ridge, a NE-SW trending ridge parallel and to the west of the Kermadec Ridge. When volcanism of the CVZ shifted to the Taupo Volcanic Zone (TVZ) in the Early Pleistocene, volcanism along the Colville Ridge shifted to the Kermadec Ridge (Wright 2008). The CVZ is considered to be a tectonic precursor to the presently active TVZ (Skinner 1986; Adams *et al.* 1994).

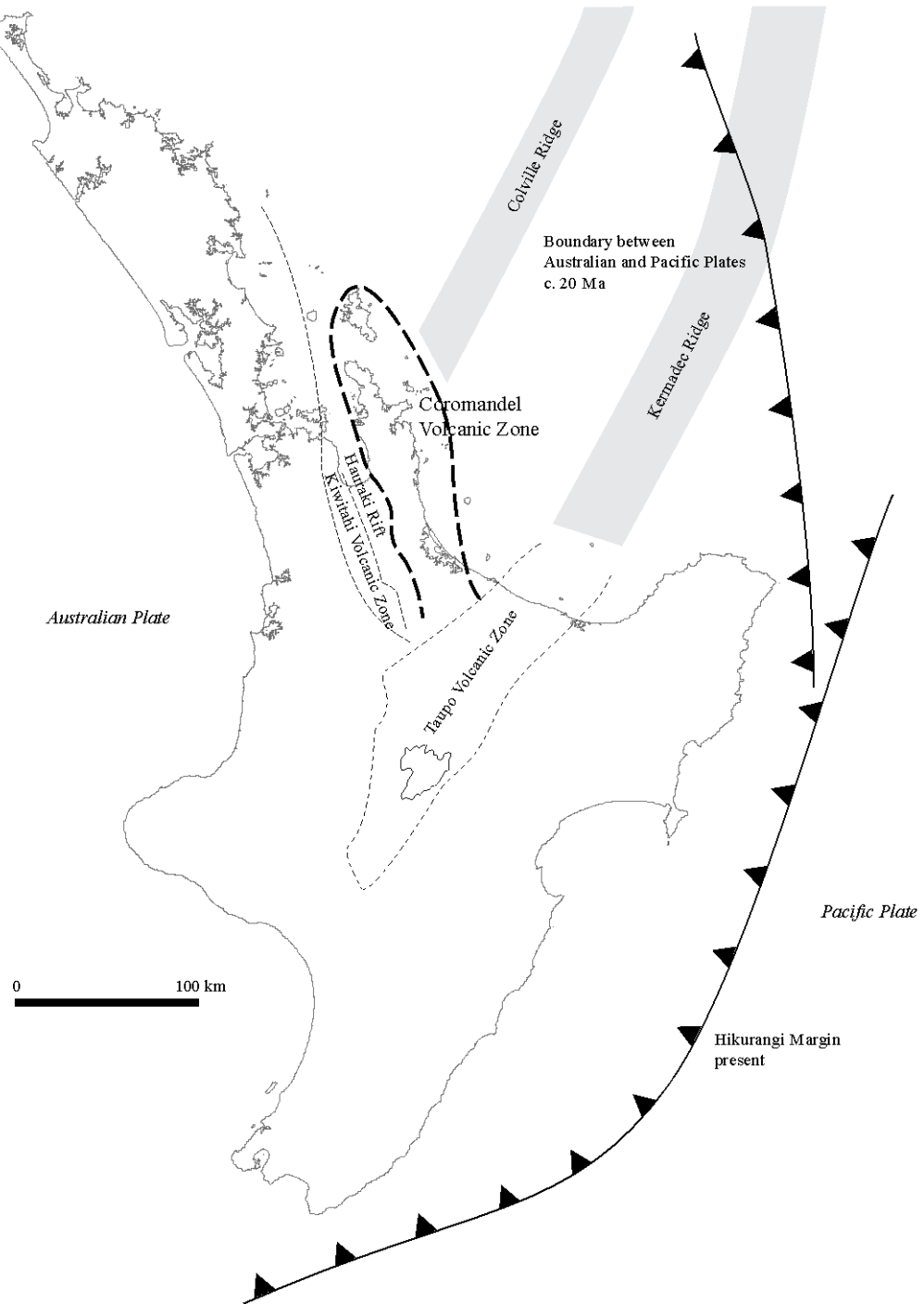


Fig. 1.1: The Hauraki Volcanic Region, North Island, New Zealand. The HVR includes the KVZ, Hauraki Rift and the CVZ. Plate boundary c. 20 Ma is prior to the commencement of the CVZ and is shown relative to the present day position of the CVZ. After Skinner (1986) and Furlong & Kamp (2009).

The CVZ basement is a Jurassic metagreywacke sequence (Manai Hill Group) which is exposed mainly in northwestern CVZ (Adams *et al.* 1994). The basement is overlain by Oligocene coal measures and calcareous marine rocks (Skinner 1986). Minor volcanogenic marine conglomerate, sandstone and siltstone of Early Miocene age (Colville Formation, Waitemata Group) precede the oldest exposed volcanic rocks of the CVZ (Skinner 1986).

The volcanic rocks of the CVZ range from basalt flows to rhyolite domes and ignimbrites, as well as hypabyssal and plutonic complexes (Cole *et al.* 1987) (Fig. 1.2). Volcanism began in the CVZ in the end of the Early Miocene with a predominantly andesitic-dacitic sequence throughout the west of the peninsula (Adams *et al.* 1994). Volcanism shifted to the east-central part of the peninsula in the Late Miocene (c. 12 Ma, Carter *et al.* 2003) with bimodal episodes of rhyolite and basalt/basaltic andesite. There was significant caldera formation and ignimbrite production during this time. The basaltic-andesitic cones and flows (Kerikeri Volcanic Group) of the Late Miocene to Pliocene are localised and occur on the Kuaotunu Peninsula, Mercury Islands, and south of Whitianga (Adams *et al.* 1994).

The youngest products of the CVZ are to the south of the peninsula, where andesitic eruptions continued into the Late Pliocene and dacitic-rhyolitic eruptions into the Early Pleistocene (Briggs *et al.* 2005). The Kaimai and Tauranga Volcanic Centres mark the end of rhyolitic volcanism in the CVZ, with the Papamoa Ignimbrite from the Tauranga Basin as the youngest dated product of the CVZ at 1.9 Ma (Briggs *et al.* 2005). There was a period of transition following this until the first rhyolitic eruption in the TVZ at c. 1.55 Ma from the Mangakino Volcanic Centre (Houghton *et al.* 1995). This time period with no recorded rhyolitic volcanism is also reflected in the offshore tephra record, which is often more complete than the onshore record (Carter *et al.* 2003). The proportion of mafic (basalt to andesite) versus silicic (dacite to rhyolite) volcanism is approximately 40:60 for the CVZ (Briggs *et al.* 2005). The locus of volcanism migrated irregularly c. 3 mm per year eastwards and c. 8 mm per year southwards over time (Adams *et al.* 1994).

Hydrothermal alteration and Au-Ag mineralisation took place episodically throughout the CVZ from at least 10 Ma in the northern Coromandel Peninsula (Christie *et al.* 2006a) until the Late Pliocene/Early Pleistocene near Te Puke (Rabone 2006b). The Hauraki Goldfield hosts the largest concentration of precious metal mineralisation in New Zealand (Brathwaite *et al.* 1989). The region has been divided into three epithermal provinces based on a number of factors, including age of the deposits, host rock type, alteration and vein minerals, Au:Ag ratios, and vein types and textures (Fig. 1.3) (Christie *et al.* 2006a).

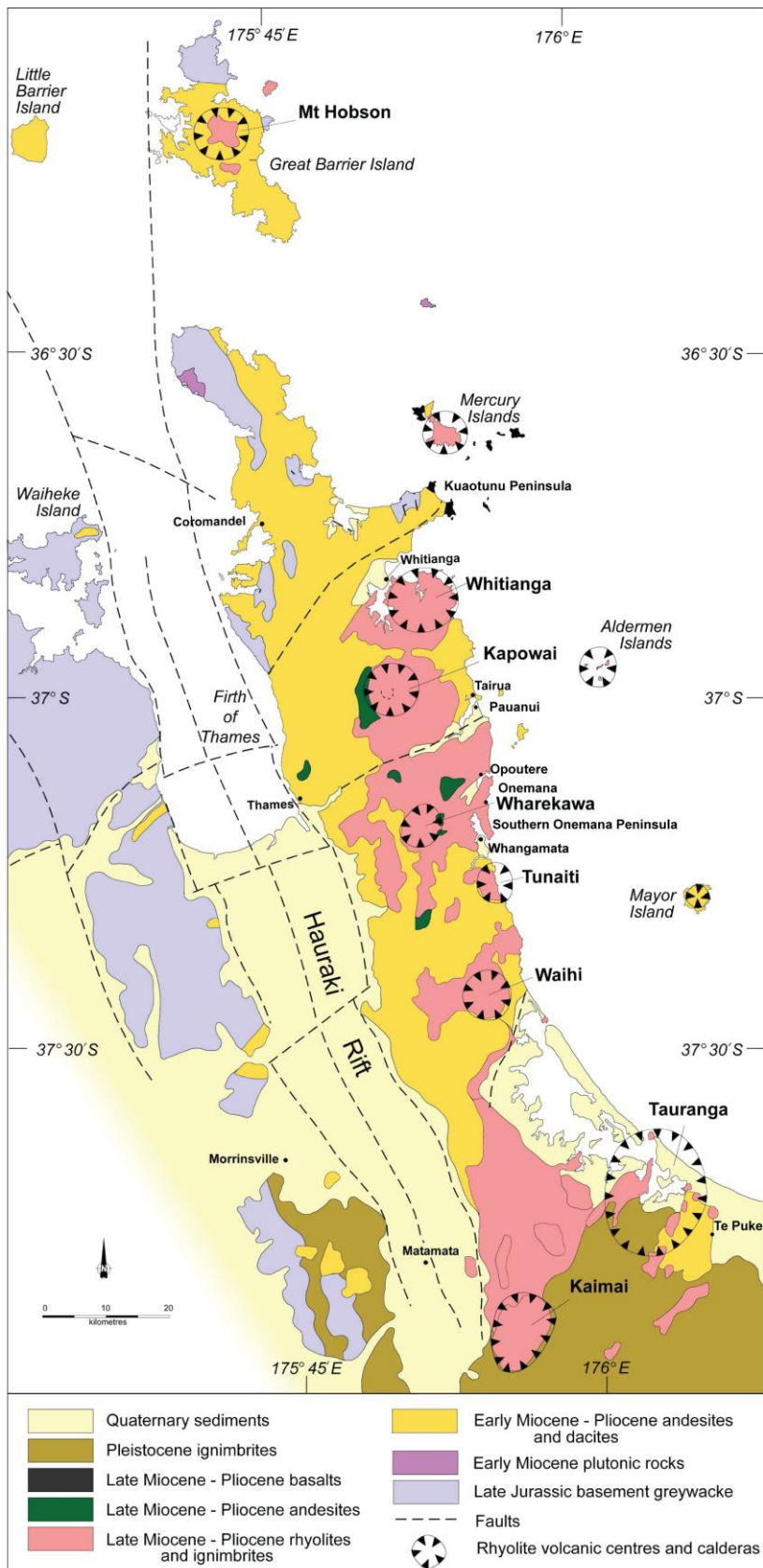


Fig. 1.2: Simplified geology of the CVZ. After Briggs & Krippner (2006).

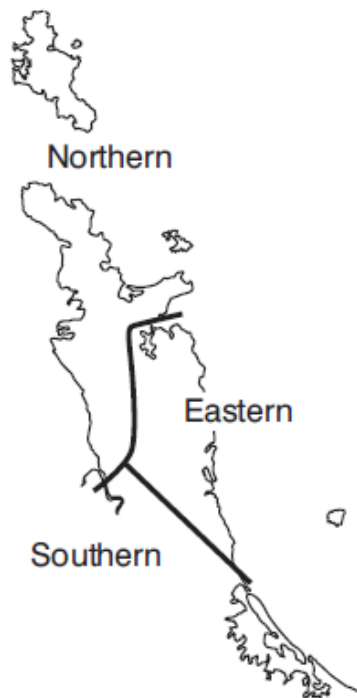


Fig. 1.3: Division of the Hauraki Goldfield into the Northern, Eastern and Southern Epithermal Provinces (Christie *et al.* 2006a).

Most faults in the Neogene rocks of the region trend NNW and NE; these structures are inherited from NNE-striking extensional rift structures, dilation jogs and pull-apart basins formed in the Early Cretaceous Rangitata Orogeny (Briggs & Krippner 2006). The block fault geometry of the basement is common throughout the North Island (Spörli *et al.* 2006). Many of the NE trending faults are downthrown to the south, creating a difference in basement elevation of over 900 m in the north of the peninsula to below sea level in the south (Spörli *et al.* 2006).

Three lithostratigraphic groups have been defined for volcanics of the CVZ: Coromandel Group (andesite/dacite/rhyodacite), Whitianga Group (rhyolite and ignimbrite) and Kerikeri Volcanic Group (basalt/basaltic andesite) (Skinner 1986) (Table 1.1). These three are further divided into subgroups; of significance to this study are the Minden, Coroglen and Ohinemuri Subgroups of the Whitianga Group (Skinner 1993; Skinner 1995; Brathwaite & Christie 1996). The Minden Subgroup includes flow and dome-building rhyolites. The Coroglen Subgroup includes ignimbrites, pumice breccias and associated sediments. The Ohinemuri Subgroup includes ignimbrites of the Waihi Basin.

Table 1.1: Summary of regional stratigraphy of the CVZ. After Skinner (1986).

Group	Subgroup	Formation	Age	Comments
Whakamaraha	Waiteariki Ignimbrite	Mid Pleistocene	Dacitic; only in Kaimai Range; young Papamoa Ignimbrite near Te Puke is also dacitic	
	Aongatei Ignimbrite informal	Plio-Pleistocene	Informal “bag” unit south of Waihi; includes andesite and ignimbrite	
Kerikeri Volcanic	Mercury Basalts	Several centres	Late Upper Miocene and/or younger	Known only in north Coromandel particularly in Mercury Islands; bimodal association with Whitianga Group; basalt and basaltic andesite
Whitianga	Minden Rhyolite Coroglen (ignimbrites)	5 formal units + many informal centres Several flow sheets + 7 formal units	Late Miocene to Pliocene Late Miocene to Early Pliocene	Group includes all pre TVZ rhyolitic rocks; Minden are rhyolite dome complexes and flows; Coroglen are ignimbrites, pumice breccias, airfall tufts and breccias, and epiclastic sediments; associated in the north with caldera formation and collapse
Coromandel	Omahine	1 formal + few informal units 3 formal units several centres 3 formal units 16 formal units Paritu and Cuvier Plutonics	Late Miocene to Pliocene Late Miocene to Pliocene Mid to Late Miocene Early late Miocene Early to Mid Miocene Late early Miocene	Group includes all predominantly “andesitic” rocks of HVR; compositions range up to dacite and even rhyodacite; Omahine includes all post Whitianga Group andesites but in Kaimai Range may be indistinguishable from Kaimai Subgroup; Kaimai Subgroup in south only; Waiawa and Kuaoitunu are central to north only, separated by regional erosional unconformity; plutonics are subvolcanic intrusive complexes in north only; Kiwitahi applies only to west of Hauraki Graben.
Waitemata	Kawau and Warkworth	Colville	Early Lower Miocene	Conformable below earliest exposed andesite
Te Kuiti		Torehina	Mid to upper Oligocene	Predates all volcanic activity
Manai Hill		Several formal units	Late Jurassic	Basement to region

1.4 Previous work

The first gold lode to be found in New Zealand was discovered in 1852 at Coromandel (Skinner 1993) and much gold and silver has been mined since then from the Hauraki Goldfield. Martha, Favona and Broken Hills Mines are still

active today and other areas are being further explored. This interest in mineral production prompted the first geological studies of the CVZ in the mid 19th century (Skinner 1986). The earliest works on CVZ geology include reports and maps by Sollas & McKay (1905; 1906), Fraser & Adams (1907), Fraser (1910), Bell & Fraser (1912), Henderson & Bartrum (1913) and Morgan (1924). Other more general works on New Zealand geology which mention the economic significance of the CVZ include von Hochstetter (1864), Park (1910) and Marshall (1912a; 1912b). Since then there has been large scale mapping and studies by students of the Universities of Waikato and Auckland, including Moore (1976), Fisher (1986), Stevenson (1986), Fulton (1988), Hunt (1991), Adams (1992), Haworth (1993), Parsons (1993), Rogers (1994), Aldrich (1995), McGunnigle (1995), Trotter (1995), Hawthorn (1996), Karl (1996), Bardebes (1997), Guay (1999), Krippner (2000), Cullingford (2003) and Fitzgerald (2004). Smaller scale geological mapping has been published of the Coromandel Harbour Area (Skinner 1993), Mercury Bay Area (Skinner 1995), Waihi Area (Brathwaite & Christie 1996) and the entire Coromandel Peninsula (Edbrooke 2001).

Previous dating work in the CVZ has been mostly on andesitic rocks. Some other volcanic and intrusive rocks have also been dated. Some previous studies are presented in Table 1.2.

Table 1.2: A selection of previous studies that have dated volcanic rocks of the CVZ. Ar-Ar = adularia (age of hydrothermal alteration), K-Ar = biotite, hornblende or plagioclase, U-Pb = zircon.

Author	Method	Rocks dated
Rutherford (1978)	Fission track	rhyolite (glass)
Seward & Moore (1987)	Fission track	rhyolite (glass)
Adams <i>et al.</i> (1994)	Fission track K-Ar	ignimbrite (zircon) basalt, dolerite, basaltic andesite, andesite, diorite, dacite, rhyolite, ignimbrite
Takagi (1995)	K-Ar	basalt, basaltic andesite, andesite, dacite, rhyolite
Brathwaite & Christie (1996)	K-Ar	andesite, dacite, rhyolite
Hoskin <i>et al.</i> (1998)	U-Pb	ignimbrite
Krippner (2000)	K-Ar	andesite, rhyolite, ignimbrite
Briggs <i>et al.</i> (2005)	Ar-Ar	dacite, rhyolite, ignimbrite
Ward <i>et al.</i> (2005)	Ar-Ar	andesite, diorite, dacite, rhyolite

1.5 Location of study area

In this study, 16 rhyolite lavas and 5 rhyolitic ignimbrites were sampled from the eastern CVZ where rhyolitic volcanism has occurred through the Late Miocene and Pliocene (Fig. 1.4). The northernmost sample is from Front Beach (Mercury Bay) and the southernmost one is from near Waikino. They are from both coastal and inland sections. This range in locations was sampled in anticipation that a range of ages would be represented as predicted by the geological history.

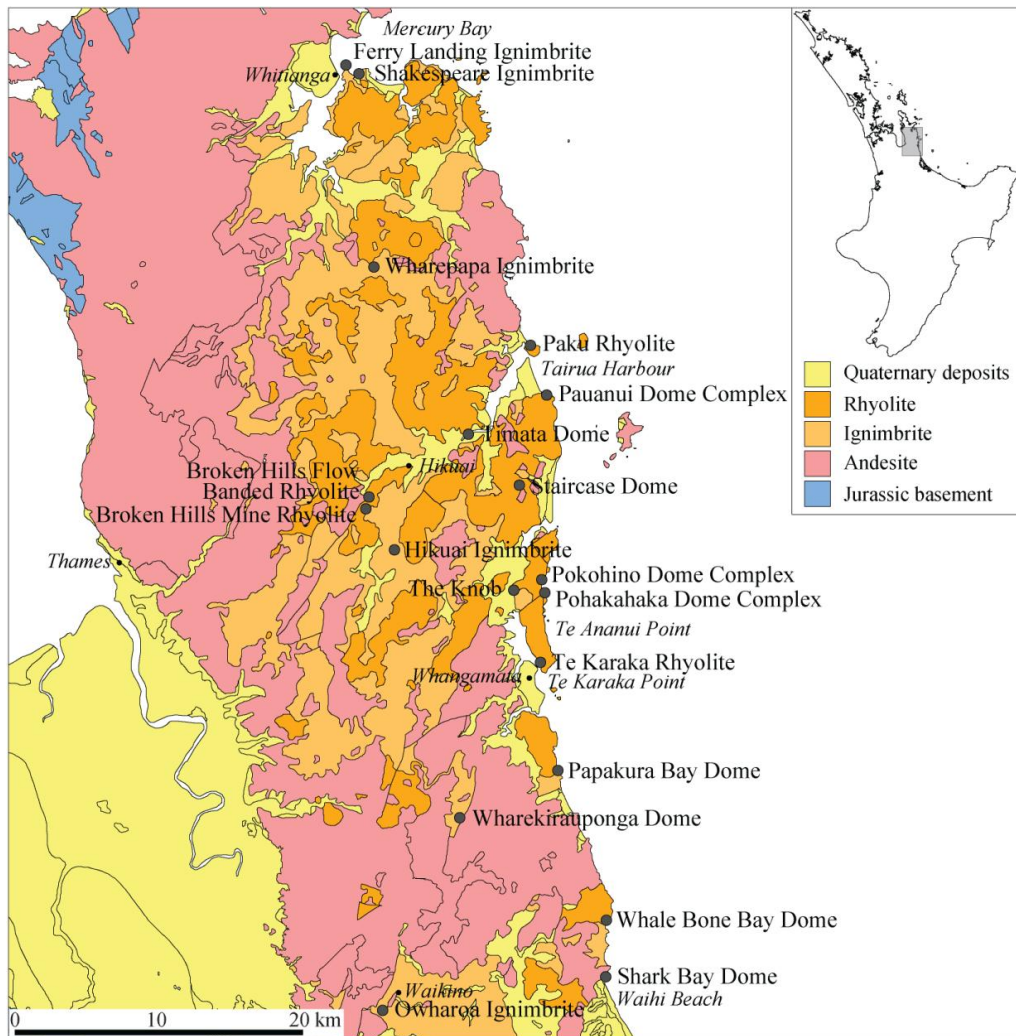


Fig. 1.4: Simplified geology of the eastern CVZ with sample sites marked.

The morphology of the eastern CVZ is dominated by the products of rhyolitic volcanism; rhyolite lavas form flows, domes and dome complexes, and ignimbrite sheets produce rolling hills, cliffs and bluffs. Some characteristic features are shown in Fig. 1.5. Many of the units are poorly exposed due to extensive vegetation coverage by native bush and exotic pine forests. The best exposures are often at the coast. There are also small areas of dairy farming. All the localities sampled are described in the following paragraphs.

Fig. 1.1: Characteristic rhyolite sections of Eastern CVZ. A) Shakespeare Ignimbrite at Shakespeare Cliff, > 60 m high. B) Steeply dipping flow banded Paku Rhyolite. C) Jointed rhyolite of Pauanui Dome Complex at Flat Rock; Paku Rhyolite Dome in background. D) Pauanui Dome Complex at Flat Rock.

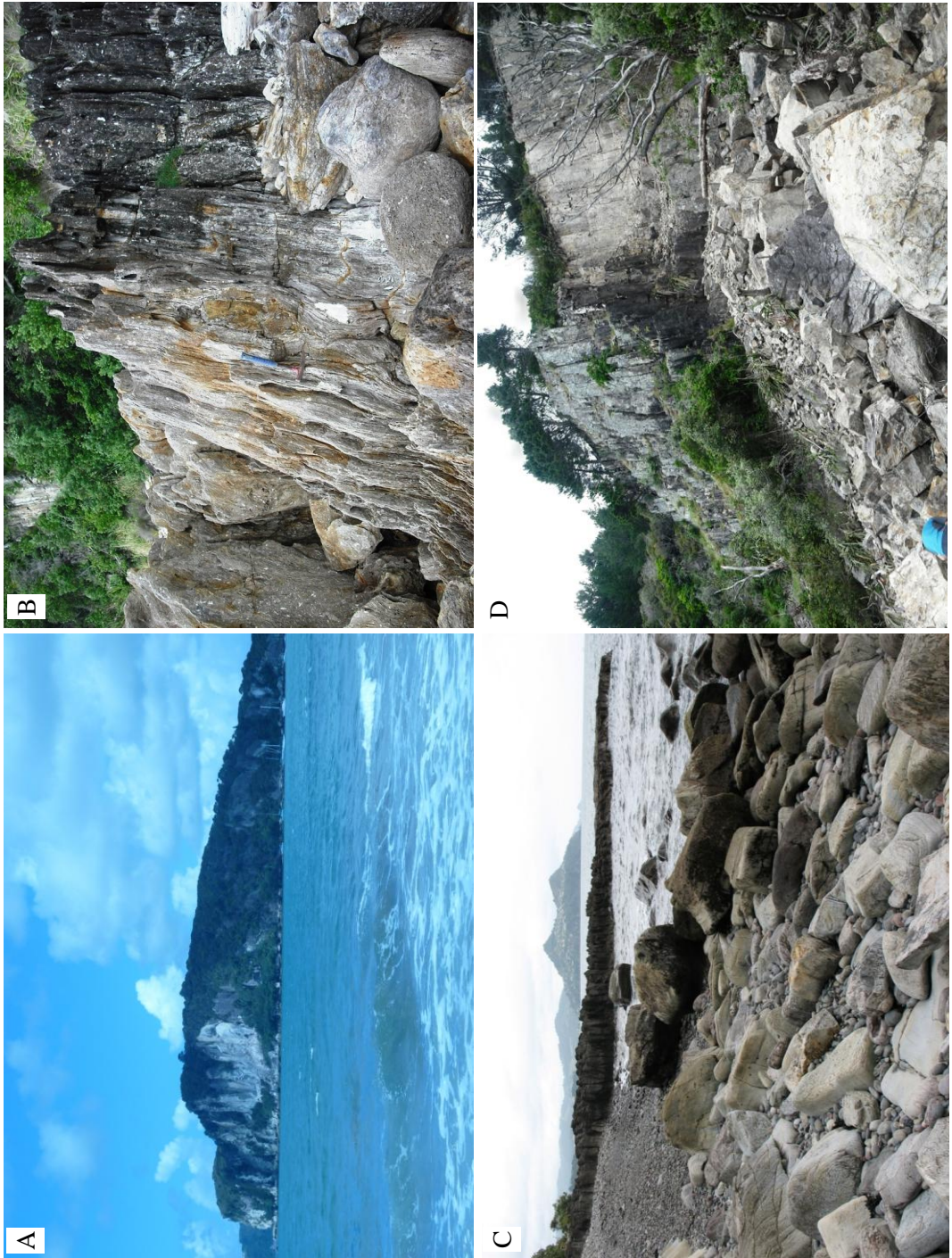
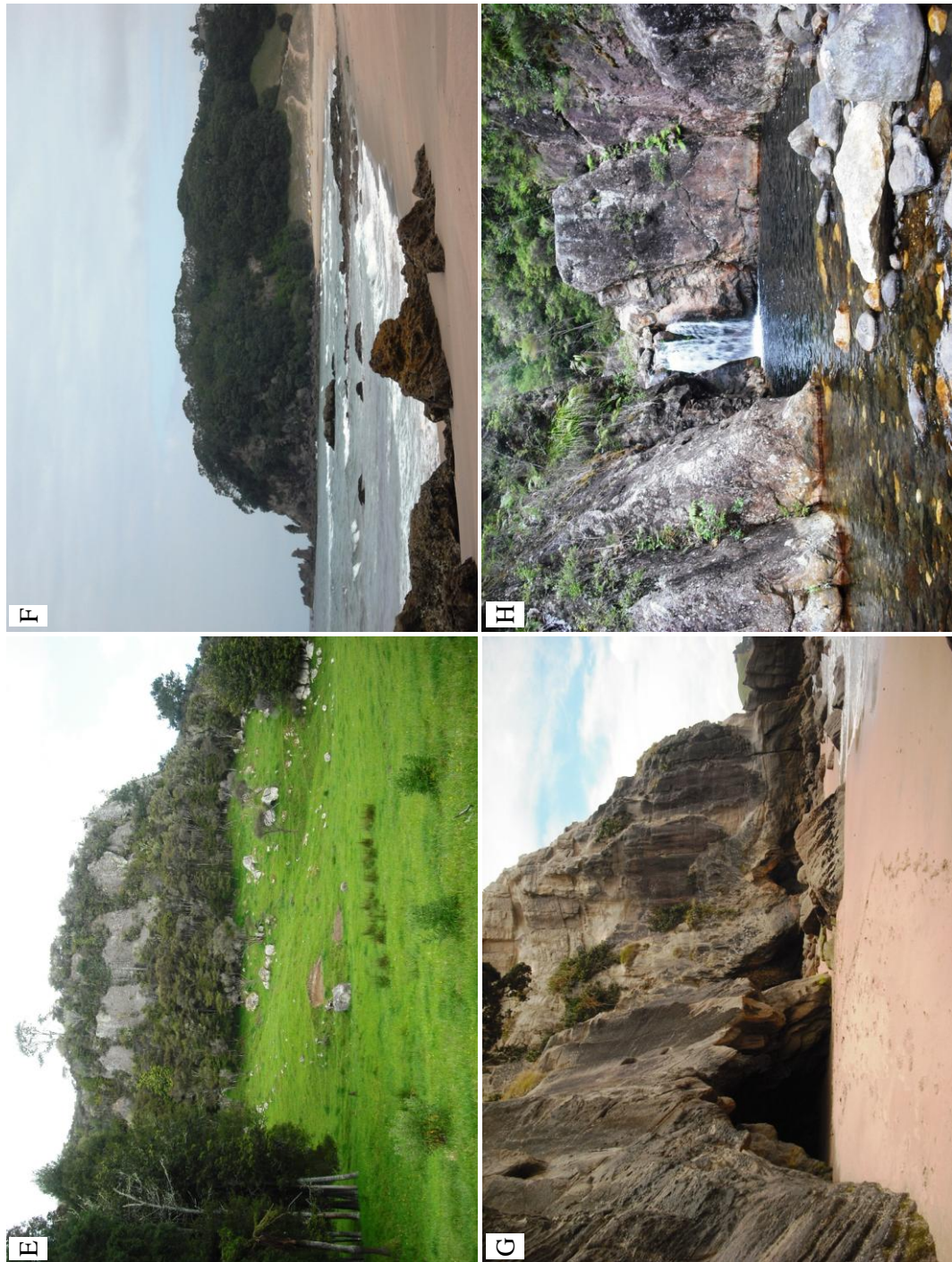


Fig. 1.5 cont.: E) Hikuai Ignimbrite bluffs. F) Pohakahaka Dome Complex at Whitipirorua Point, southern headland of Onemana Beach. G) Papakura Bay Dome. H) Wharekirauponga Dome.



Ferry Landing Ignimbrite

The Ferry Landing Ignimbrite has been mapped by Fisher (1986) and Bardebes (1997). It is only exposed at Whakapenui Point (Mercury Bay) but is inferred to cover much of the Whitianga Volcanic Centre as many of the overlying units contain lithics of Ferry Landing Ignimbrite. It consists of two main conformable flow units. It has also been mapped by Skinner (1995) as Wharepapa Ignimbrite.

Shakespeare Ignimbrite

The Shakespeare Ignimbrite has been mapped and informally named by Fisher (1986) and Bardebes (1997). It forms the Shakespeare Cliffs to the west of Cooks Beach. It has previously been included as the uppermost unit of the Pumpkin Rock Ignimbrite as described by Skinner (1995), but this subdivision is now assumed to be incorrect as there is evidence for large periods of erosion between the units of the Pumpkin Rock Ignimbrite (Bardebes 1997). It consists of three flow units which appear to have been produced in different episodes (Bardebes 1997). It contains charred logs and is occasionally cross cut by clastic dykes.

Wharepapa Ignimbrite

The Wharepapa Ignimbrite has been mapped and described by Skinner (1995) and Krippner (2000). It is part of the Wharepapa Eruptive Sequence and is the youngest explosive eruptive event from the Kapowai Caldera Complex (Krippner 2000). It forms flow sheets, breccias and associated airfall and phreatomagmatic deposits. It infilled and overflowed the Kapowai Caldera, which has an area of 110 km², and its deposits extend more than 20 km west to east. It is one of the most widespread and voluminous caldera-forming ignimbrites of the CVZ (Briggs & Krippner 2006) with a minimum calculated volume of c. 40 km³ (Krippner 2000).

Paku Rhyolite

Paku Rhyolite forms Paku “Island”, a tombolo at the entrance to Tairua Harbour. It covers an area of less than 1 km² and has a height of 179 m a.s.l.. Paku Island consists of an outer flow banded dome (bands are steeply dipping to vertical) and an inner more weakly flow banded inner spine. It has been described in Homer & Moore (1992) and mapped by Skinner (1995).

Pauanui Dome Complex

The Pauanui Dome Complex has been mapped by Trotter (1995) and described by Fitzgerald (2004) as a series of lobes to the south of Pauanui that are inferred to have originated from several vents. The complex is overall at least 4 km north to south and 3.5 km west to east and peaks at a height of 380 m a.s.l.. The lobes are likely formed from extrusive events but it is possible that endogenous activity has contributed to the height of the dome. Its geotechnical properties have been described by Stevenson (1986).

Timata Dome

This is a dome of the Ruahine Rhyolite, which consists of many flows and domes to the south and southeast of the Kapowai Caldera. It has been mapped and described by Rogers (1994) and Skinner (1995). The dome that was sampled in this study was mapped by Karl (1996); it is located on the west side of the Tairua River about 5.5 km SW of Tairua. It is intruded by the Woody Hill Basaltic Andesite. It has been named here after Timata Road which cuts through it.

Staircase Dome

The Staircase Dome Rhyolite has been mapped by Trotter (1995) as part of the Staircase Rhyolite Complex (Fitzgerald 2004). Multiple lava flows contribute to this dome. It lies to the west of Ohui and Opoutere Beach. It extends from Opoutere to about 5 km north of there, and 3 km west to east with a peak height of 303 m a.s.l..

Broken Hills Rhyolite

The Broken Hills Rhyolite has been mapped by McGunnigle (1995) and has here been divided into non-altered (Broken Hills Flow Banded Rhyolite) and hydrothermally altered (Broken Hills Mine Rhyolite). It consists of a series of lava flows in the Hikuai Region. It is bound to the west by the Tairua River and to the east by a large NNE fault and has a total length of about 7 km north to south. Its source is unknown. One sample was collected of the non-altered Broken Hills Flow Banded Rhyolite.

Broken Hills Mine Rhyolite

The Broken Hills Mine area has been mapped by Moore (1976) and has been further described by others including Moore (1979) and Rabone (2006a). There

are multiple rhyolite flows in this area and not all of them have been distinguished. The mine itself is located about 5 km SW of the Hikuai settlement, on the east side of the Tairua River. It is a Au-Ag mine and was the largest producer of Au in the Hauraki Goldfield from rhyolite hosted mineralisation (Rabone 2006a). Three samples were collected from within Broken Hills Mine for this study, and they are from the same dome as the Flow Banded Rhyolite.

Hikuai Ignimbrite

The Hikuai Ignimbrite has been mapped by McGunnigle (1995). It forms pyroclastic density currents and fall deposits with characteristic bluffs (some of which are c. 100 m high) to the east of the Tairua River. McGunnigle (1995) mapped it as covering an area around Hikuai, extending for at least 16 km to the south and an unknown distance to the north. It covers an estimated area of 50 km² with a volume of at least 7 km³; this is however a minimum estimate as much of it has been eroded or covered by younger volcanic rocks (McGunnigle 1995). Its source is unknown. Its western extent has been hydrothermally altered and silicified in the area of Broken Hills Mine.

Pokohino Dome Complex

The Pokohino Dome Complex has been mapped by Aldrich (1995) as a series of rhyolite domes and flows from multiple vents extending 2 km to the north of Onemana. The flows cover an area about 2 km wide, with a peak height of 180 m a.s.l.. It occurs within a region of hydrothermal alteration.

The Knob

This rhyolite dome forms the westernmost part of the Pokohino Dome Complex (Aldrich 1995). It has been intensively hydrothermally altered and silicified and has a peak height of 156 m a.s.l..

Pohakahaka Dome Complex

The Pohakahaka Dome Complex has been mapped by Aldrich (1995) as a series of rhyolite domes and flows from multiple vents extending about 3 km to the south of Onemana. The complex is 1.5 km wide with a peak height of 128 m a.s.l.. The southern extent of the complex is not defined but is inferred to be between Tokakahaka Island and Te Ananui Point, based on samples collected by Aldrich (1995), Takagi (1995), and in this study.

Te Karaka Rhyolite

This rhyolite has here been named after Te Karaka Point at the southern end of the Southern Onemana Peninsula. Takagi (1995) collected a sample from Te Ananui Point (on the east of the peninsula) which is a petrographic match for this sample. Cullingford (2003) mapped the entire Southern Onemana Peninsula as the Te Ananui Dome Complex, which includes Whitipirorua and Te Karaka Points. This is here assumed to be an incorrect definition as the minerals present and their abundances in the rhyolite at Whitipirorua Point are different to that which was observed in the southern part of the peninsula (see Appendix II).

Papakura Bay Dome

This is one of the intracaldera rhyolite lava domes of the Tunaiti Caldera (Briggs & Fulton 1990) and has here been named after the bay in which it is located. Such domes were referred to as Unit 10 by Fulton (1988). Aerial photographs suggest that there are up to six domes which have heights of over 100 m a.s.l. (Fulton 1988).

Maratoto Rhyolite – Wharekirauponga Dome

The Maratoto Rhyolite forms dome complexes at Maratoto, Paiakarahi, Karangahake and Wharekirauponga (Brathwaite & Christie 1996). It is variably hydrothermally altered and parts of it host gold-bearing quartz veins. It has a maximum exposed thickness of 240 m. The Wharekirauponga Dome is hydrothermally altered and occurs in the gorge section of the Wharekirauponga Stream. It was mapped in the 1980s-90s by various mining companies (Christie *et al.* 2006b).

Homunga Rhyolite – Whale Bone Bay and Shark Bay Domes

The Homunga Rhyolite includes four lava dome complexes to the east of Waihi: Whale Bone Bay, Ruahorehore, Shark Bay and Hikurangi Domes. They have been mapped by Brathwaite & Christie (1996). The Whale Bone Bay Dome forms the northern headland of Homunga Bay, 4 km north of Waihi Beach. Shark Bay Dome is the northern headland at Waihi Beach; it is silicified and hosts gold-bearing quartz veins.

Owharoa Ignimbrite

The Owharoa Ignimbrite was first mapped by Rabone (1975), having renamed it from Grange's Owharoaite (Brathwaite & Christie 1996). Its source is from within the Waihi Basin and it is distributed between Waihi and Waikino. It consists of several flow units including lenticulite and vitric-rich tuff. It is up to 80 m thick.

1.6 Thesis outline

In Chapter 2 the petrography and mineralogy of the samples is described. The petrochemistry (X-ray fluorescence results) is presented in Chapter 3. An outline of the U-Pb dating method and the age results is presented in Chapter 4. The physical properties of the zircon crystals are also described in Chapter 4. In Chapter 5 the results of this study are compared to those of previous ones and the overall geochronology of the CVZ.

Chapter 2

Petrography and Mineralogy

2.1 Introduction and methodology

The units of this study have been subdivided into three groups: slightly altered rhyolite lavas, intensively altered rhyolite lavas, and ignimbrites. An unpolished thin section of each lava and ignimbrite was used to determine its petrographic characteristics (see Appendix II).

Polished thin sections were made of samples that had fresh, unaltered phenocrysts, namely plagioclase and biotite (see Appendix III). They were analysed using the JEOL JXA-840A electron probe micro-analyser at the School of Environment, the University of Auckland. The thin sections were coated with 25 μm carbon film in an Edwards vacuum evaporator. The analysis conditions included an electron gun accelerating voltage of 15 kV, a 1000 pA beam current, and an electron spot diameter of approximately 2 μm . The X-ray analysis system used included an eumeX Si(Li) Be-window detector and Moran Scientific pulse-processor and software. Each spectrum was collected for 100 seconds of live time. A set of Astimex mineral standards was used for standardisation.

Hydrothermally altered samples and those which it was suspected contained polymorphs of SiO_2 were analysed by X-ray diffraction (XRD) in the Faculty of Science and Engineering, the University of Waikato (see Appendix IV).

The lavas were divided based on the following reasons: the hand specimen appeared altered or silicified, the sample contained quartz \pm illite veins or pyrite, and any plagioclase had been altered. XRD analysis indicated in some cases if products of alteration were present. XRF analysis (see Chapter 3) also confirmed if samples had been hydrothermally altered or silicified if samples had an SiO_2 content of at least 76-78 wt %.

2.2 Slightly altered rhyolite lavas

The slightly altered rhyolite lavas are the Paku, Pauanui Dome Complex, Timata Dome, Staircase Dome, Broken Hills Flow Banded, Pohakahaka Dome Complex, Te Karaka and Papakura Bay Dome rhyolites. These lavas are grey – pink, poorly to moderately porphyritic to vitrophyric, medium-grained phenocrysts, and have textures that vary between vesicular, flow banded, spherulitic and glassy. Mineral assemblage is variable but is generally quartz – plagioclase ± relict mafic minerals ± biotite – Fe-Ti oxides ± zircon. Groundmass is dominantly devitrified glass. Spherulites are also present in most samples.

2.2.1 Phenocrysts

Quartz

Quartz is the dominant phenocryst in the slightly altered rhyolites. Quartz occurs up to 2 mm in diameter and is typically subhedral to anhedral and irregular.

Plagioclase

Plagioclase (An_{49-23}) occurs in some of these rhyolites as tabular to irregular subhedral phenocrysts up to 3 mm long. Most display polysynthetic twinning and simple twinning is less common (Fig. 2.1 A). Plagioclase in Staircase Dome is rare and highly altered with a resorbed texture (Fig. 2.1 B). Normal, reverse and oscillatory zoning are common, with the exception of Timata Dome where zoning appears to be negligible.

The plagioclase phenocrysts have a range in compositions from oligoclase to andesine feldspars (Fig. 2.2). There appears to be a general trend towards more sodic-rich compositions from north to south. These compositions are within the range of plagioclase compositions for other Whitianga Group Rhyolites, e.g. Tunaiti rhyolite lavas (An_{50-23}) (Fulton 1988), Cooks Beach/Hahei rhyolite lavas (An_{53-22}) (Rogers 1994), Pohakahaka (An_{25-33}) and Wharekawa Dome Complexes (An_{32-45}) (Aldrich 1995), Boom Rhyolite (An_{32-29}) (McGunnigle 1995) and Flaxmill Dome rhyolite lavas (An_{47-24}) (Bardebes 1997).

Relict mafic minerals

Pseudomorphs of relict mafic minerals occur in most of these rhyolites and have been altered to chlorite-smectite (Fig. 2.1 C and D). They are anhedral and up to 1 mm in length. Relict mafic minerals have also been observed in other CVZ

rhyolites, e.g. Purangi Dome, lavas of Motueka, Centre and Poikeke Islands (Rogers 1994), and Pohakahaka Dome Complex (Aldrich 1995).

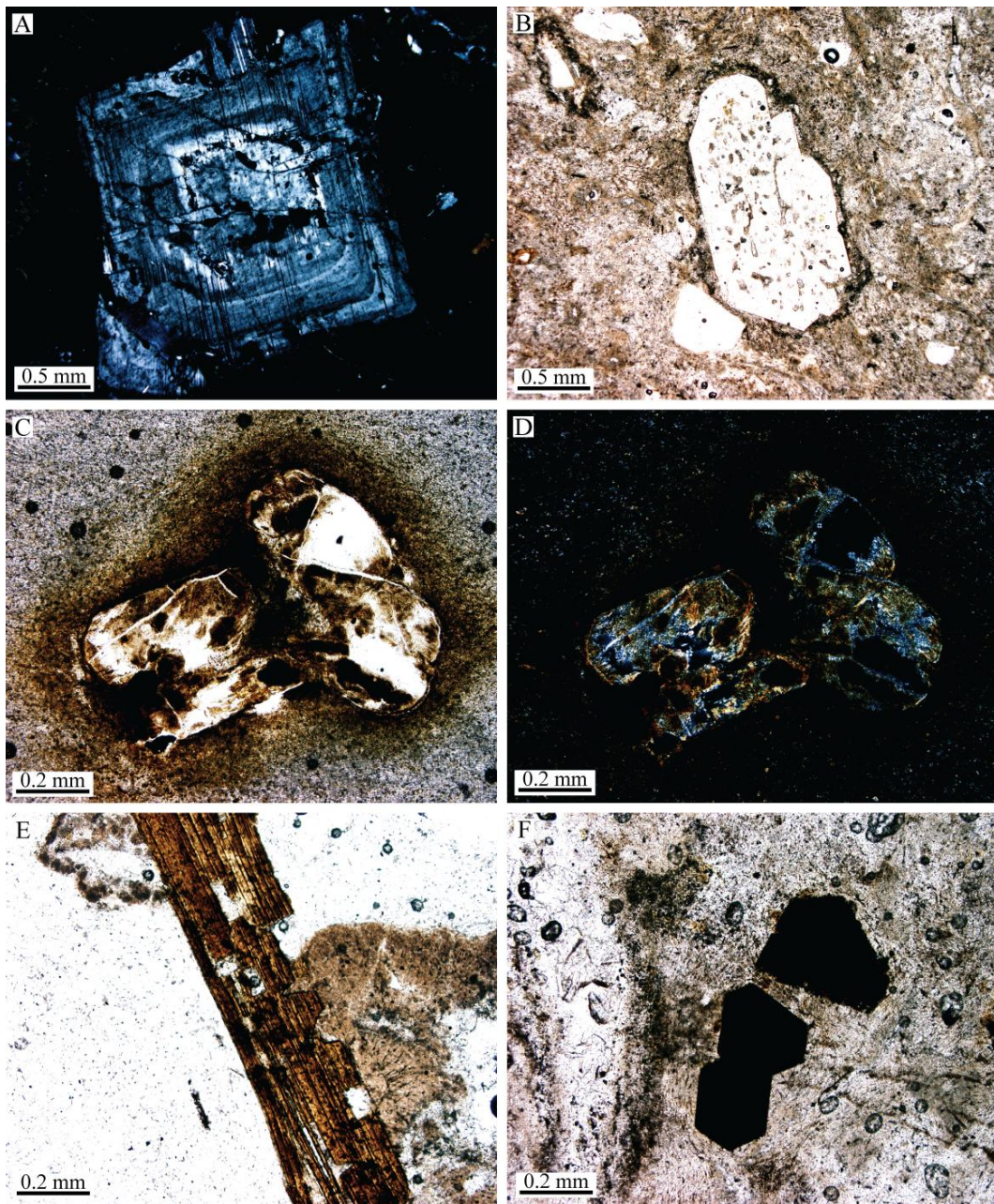


Fig. 2.1: Phenocrysts of slightly altered rhyolite lavas: A) Zoned plagioclase, Papakura Bay Dome, cross-polarised light. B) Resorbed, sieve-textured plagioclase, Staircase Dome, plane-polarised light. C) Relict mafic minerals, Pauanui Dome Complex, plane-polarised light, and D) cross-polarised light. E) Biotite with plagioclase inclusions, Papakura Bay Dome, plane-polarised light. F) Oxidised biotite in basal sections, Staircase Dome, plane-polarised light.

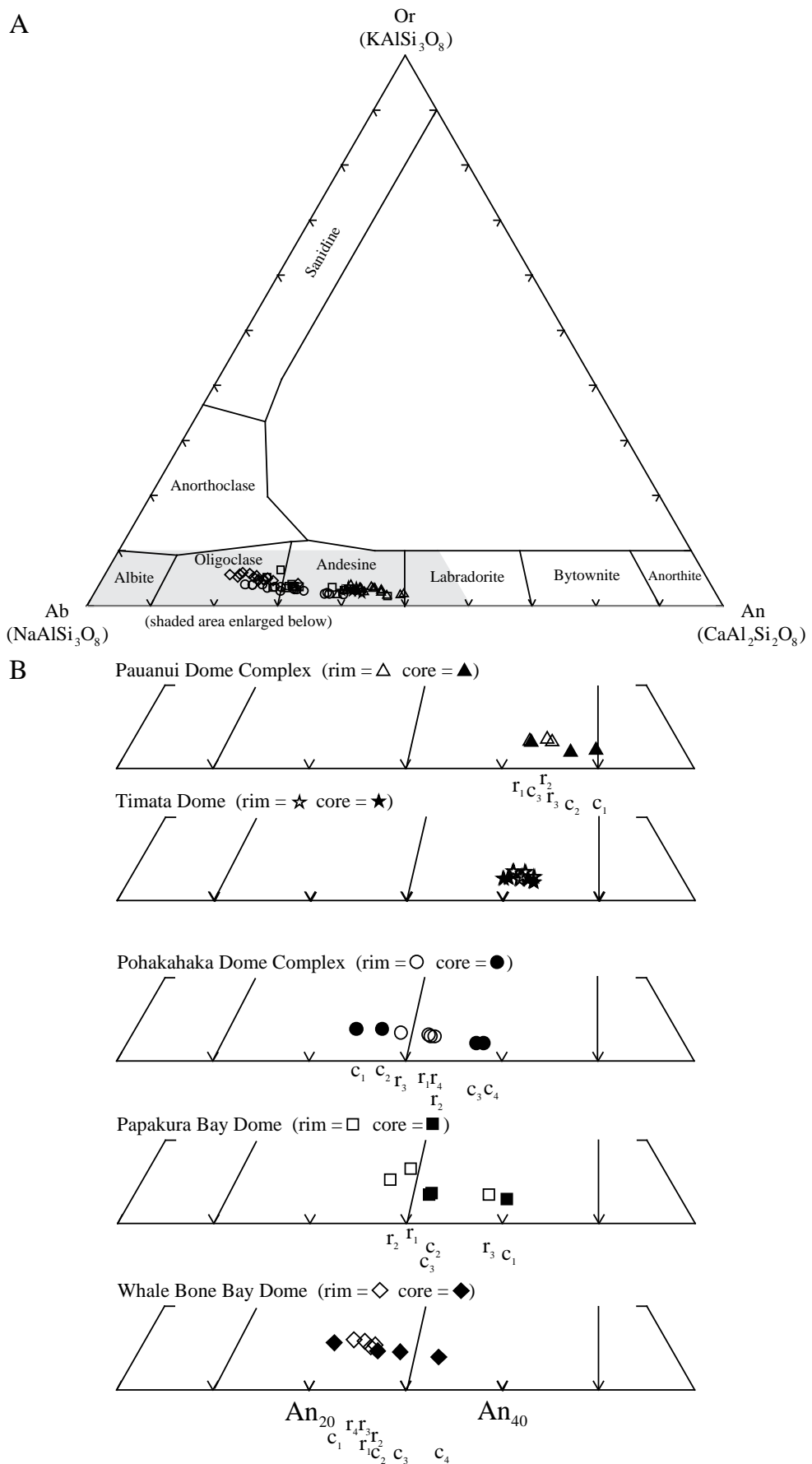


Fig. 2.2: A) Orthoclase – albite – anorthite ternary diagram for plagioclase phenocrysts of rhyolite lavas. Classification according to Deer *et al.* (1992). B) Composition of representative phenocrysts of plagioclase, ordered from north to south. Core (c) and corresponding rim (r) compositions are indicated.

Biotite

Biotite occurs as subhedral flakes up to 1.5 mm long. They may contain rare plagioclase inclusions and are sometimes oxidised (Fig. 2.1 E and F). Biotite phenocrysts from Papakura Bay Dome have a chemical composition which plots within the composition of other biotite phenocrysts from CVZ rhyolites, e.g. Tunaiti lavas (Fulton 1988), Boom Rhyolite (McGunnigle 1995) and Flaxmill Dome rhyolite lavas (Bardebes 1997) (Fig. 2.3).

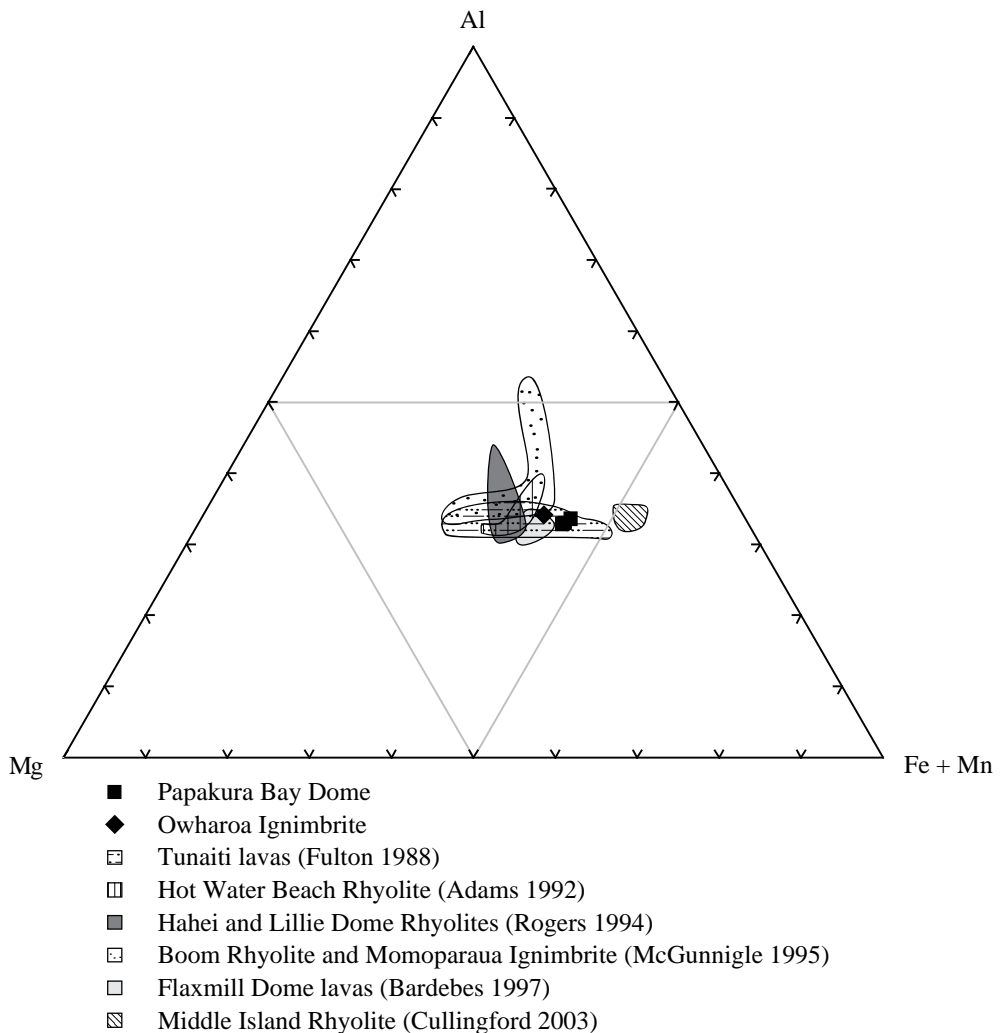


Fig. 2.3: Al – Mg – Fe+Mn ternary diagram for biotite phenocrysts of Papakura Bay Dome and Owharoa Ignimbrite, and comparisons with other CVZ rhyolites and ignimbrites.

Opaques

Fe-Ti oxides occur in variable abundances and have been identified in some samples as titanomagnetite and ilmenite. They are commonly cubic and hexagonal euhedral to anhedral phenocrysts up to 0.25 mm wide. Ilmenite is sometimes acicular.

Zircon

These rhyolites all contain zircon, with the exception of Paku Rhyolite. It was not always observed in thin section.

2.2.2 Groundmass

The groundmass is generally devitrified glass and is sometimes crystalline quartz or SiO₂ polymorphs ± feldspar. SiO₂ polymorphs are difficult to identify, and the following have been evaluated from XRD analysis: Pauanui Dome Complex contains tridymite, Staircase Dome contains cristobalite, and Paku and Timata potentially contain both.

Spherulites are common with spherical spherulites occurring up to 2.5 mm in diameter. Timata Dome contains many spherulites that can be up to 8 mm in diameter (Fig. 2.4 A and B). Flow banding is prominent in Staircase Dome and Pohakahaka Dome Complex and particularly in Paku and Broken Hills Flow Banded Rhyolites where bands can be less than 1 mm wide and very laminar (Fig. 2.4 C and D). Vesicles are also common in Pohakahaka Dome Complex and they are often lined with the same currently unidentified quartz-like mineral that is present in the Broken Hills Mine samples. Papakura Bay Dome also has some vesicles but these are unfilled. Pohakahaka Dome Complex, Te Karaka Rhyolite and Papakura Bay Dome have crystallites, which in Pohakahaka Dome Complex are aligned with the flow bands (Fig. 2.4 E).

Papakura Bay Dome is vitrophyric with phenocrysts of quartz – plagioclase – biotite set in a groundmass of non-devitrified glass with perlitic cracks (Fig. 2.4 F). The edges of the vesicles are devitrified. Pauanui and Pohakahaka Dome Complexes have quartz veins which have been oxidised in some places to limonite.

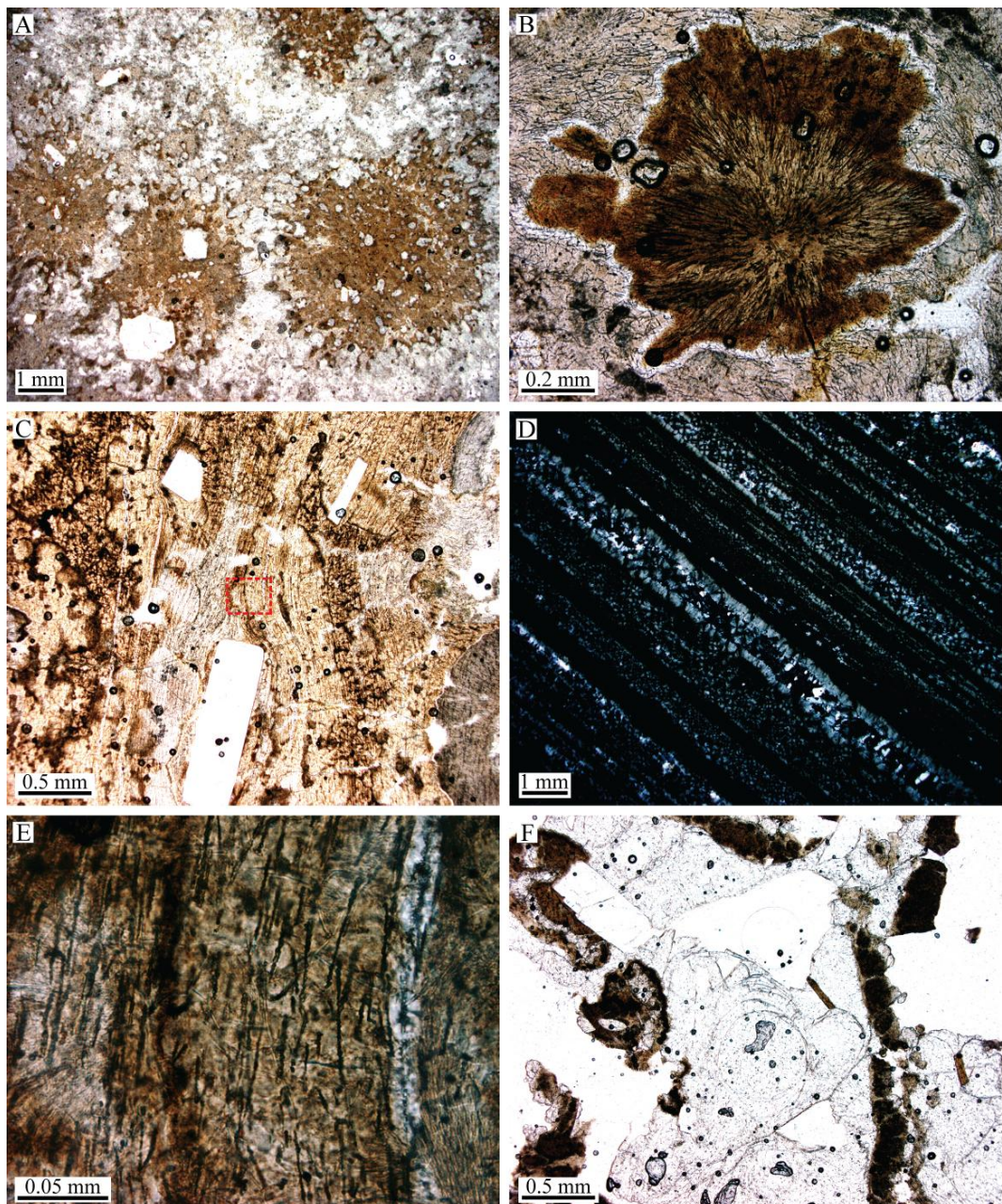


Fig. 2.4: Groundmass features of slightly altered rhyolite lavas: A) Spherulites, Timata Dome, plane-polarised light. B) Spherulite, Te Karaka Rhyolite, plane-polarised light. C) Plagioclase phenocryst and spherulites aligned with flow bands, Pohakahaka Dome Complex, plane-polarised light. D) Laminated flow bands of devitrified glass which are now polymorphs of SiO₂, Paku Rhyolite, cross-polarised light. E) Chain-like arrangements of crystallites aligned with flow bands, Pohakahaka Dome Complex, enlargement of centre of C, plane-polarised light. F) Perlitic cracks in glass and devitrified edges of vesicles, Papakura Bay Dome, plane-polarised light.

2.3 Intensively altered rhyolite lavas

The intensively altered rhyolite lavas include Broken Hills Mine (three samples), Pokohino Dome Complex, The Knob, Wharekirauponga Dome and Homunga (Whalebone Bay and Shark Bay Domes) rhyolites. These lavas are cream –

orange – pink, poorly to moderately porphyritic, have fine- to medium-grained phenocrysts, and textures that vary between flow banded, vesicular and lithophysal. Mineral assemblages are variable but are generally quartz – altered plagioclase \pm Fe-Ti oxides – zircon. Groundmass textures are dominantly granular quartz + feldspar which is sometimes devitrified glass. Spherulites are also common. Some of these lavas have been silicified.

2.3.1 Phenocrysts

Quartz

Quartz is the dominant phenocryst in the intensively altered rhyolites. Quartz is generally up to 1 mm in diameter, but can be up to 4 mm, and is typically anhedral and embayed (Fig. 2.5 A).

Altered plagioclase

Altered plagioclase occurs in most intensively altered rhyolites and has been entirely altered to quartz/adularia \pm sericite (Fig. 2.5 B). They are up to 2.5 mm in length. Only one of these samples contains relatively unaltered plagioclase: the Whale Bone Bay Dome (An_{31-20}) of the Homunga Rhyolite, where phenocrysts can occur up to 2 mm long and are often in clusters (Fig. 2.2). They are subhedral to anhedral with polysynthetic twinning, sieve textures and both normal and reverse zoning (Fig. 2.5 C). Brathwaite and Christie (1996) cite a plagioclase composition of An_{50-30} for Homunga Rhyolite.

Relict mafic minerals

Pseudomorphs of relict mafic minerals occur in some of the intensively altered rhyolites where they have been altered to chlorite-smectite. They are anhedral and up to 0.5 mm in length. They are less common here than in the slightly altered lavas.

Biotite

Biotite only occurs in one of the intensively altered rhyolites: the Pokohino Dome Complex, where it occurs as rare altered flaky phenocrysts up to 0.6 mm long.

Opaques

Fe-Ti oxides occur in variable abundances and generally only occur in the intensively altered rhyolite lavas where plagioclase or altered plagioclase is

present. They are sometimes associated with relict mafic minerals and often occur in clusters. Fe-Ti oxides have been identified in some samples as titanomagnetite and ilmenite where they occur as cubic/acyclic subhedral to anhedral crystals up to 0.25 mm.

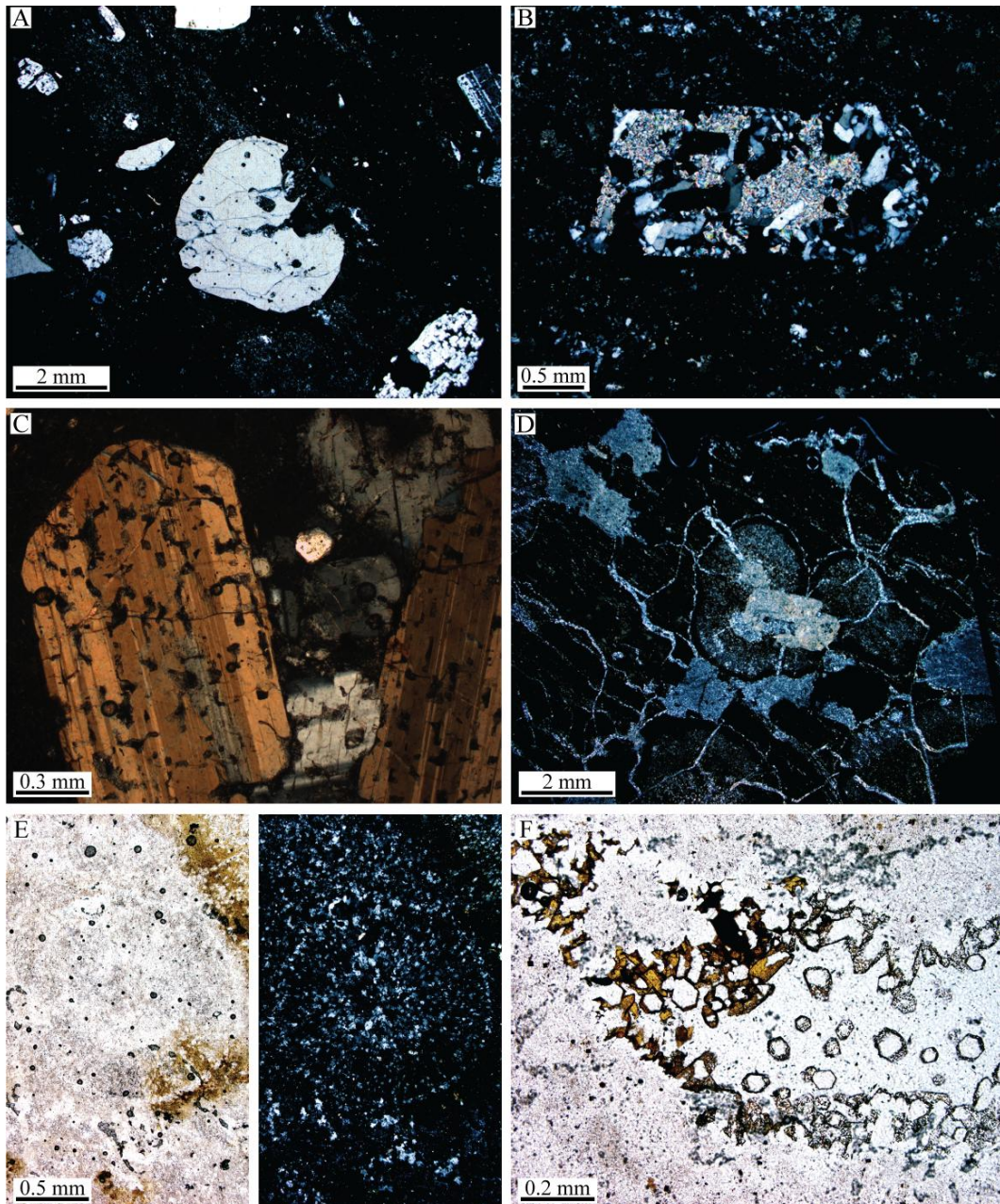


Fig. 2.5: Phenocrysts and groundmass features of intensively altered rhyolite lavas: A) Embayed, anhedral quartz, Whale Bone Bay Dome, cross-polarised light. B) Plagioclase that has been altered to quartz + adularia + sericite, Wharekirauponga Dome, cross-polarised light. C) Plagioclase, Whale Bone Bay Dome, cross-polarised light. D) Crystalline spherulites that nucleated on (now altered) plagioclase phenocrysts with quartz veins cutting through them, Broken Hills Mine, cross-polarised light. E) Crystalline spherulite, Broken Hills Mine, plane- and cross-polarised light. F) Colourless, anisotropic crystals with golden coating lining a cavity, Broken Hills Mine, plane-polarised light.

Zircon

Zircon occurs in all the intensively altered rhyolites, even though it was not always observed in thin section. It is sometimes associated with opaques and relict mafic minerals.

2.3.2 Groundmass

The groundmass commonly consists of glass that has been devitrified to polymorphs of SiO_2 . The Pokohino Dome Complex is the least devitrified and also contains crystallites. Most of the intensively altered rhyolites are spherulitic to varying degrees and most of the spherulites are now crystalline (Fig. 2.5 D and E). They are spherical (rarely fan shaped) and can be up to 5 mm in diameter but are typically less than 1 mm. The lavas from Broken Hills Mine are flow banded and lithophysal to varying degrees. The vesicles are lined with a currently unidentified quartz-like mineral (Fig. 2.5 F). These crystals are euhedral, up to 0.25 mm long and sometimes coated in an orange-brown material. Some of the samples have quartz veins, which are in parts oxidised to limonite or chlorite-illite.

2.3.3 Effects of hydrothermal alteration

Hydrothermal alteration affects the mineralogy and overall texture of a rock. Some of the minerals observed in the intensively altered rhyolite lavas only occur as a result of hydrothermal alteration. Mafic minerals, such as pyroxenes and amphiboles, are the first minerals to alter in hydrothermal alteration; they alter to chlorite-smectite. Biotite is the next mineral affected by hydrothermal alteration, however the only altered biotite observed in these samples was oxidised. Plagioclase then alters to fine-grained sericite \pm adularia. Titanomagnetite alters to pyrite, which was observed in Broken Hills Mine sample 3 and Shark Bay Dome. Finally in the intensely silicified zone SiO_2 is enhanced as other minerals are leached out.

Resulting textures and structures typical of hydrothermal alteration include recrystallised spherulites. Quartz veins are also common and are sometimes seen to be cross-cutting phenocrysts, which shows that they are a post-depositional feature. Quartz veins have sometimes been altered to chlorite-illite, which are products of hydrothermal alteration.

2.4 Ignimbrites

2.4.1 Ferry Landing Ignimbrite

The Ferry Landing Ignimbrite is a densely welded, jointed, pumice-rich, lithic-poor lenticulite. Pumice is subrounded and streaky or flattened with fiamme ends and clusters of anhedral plagioclase (An_{39-27} , Fig. 2.6) phenocrysts. There are also a few dense pumices which are obsidian-like.

The matrix contains non-devitrified glass shards which are platy and Y-shaped. Plagioclase (An_{38-27} , Fig. 2.7) crystals are mostly subhedral to anhedral, tabular to irregular, up to 1 mm long, normally zoned with polysynthetic twinning. This composition is comparable to that determined by Bardebes (1997) of An_{44-30} . Rare relict mafic minerals are altered to chlorite-smectite. Titanomagnetite and ilmenite occur in clusters as cubic and acicular anhedral crystals, up to 0.25 mm long. Zircon crystals are rare and occur as euhedral crystals up to 0.05 mm.

Lithics are angular and up to 4 mm and include the following types: trachytic rhyolite, hydrothermally altered rhyolite, plagioclase rhyolite with quartz-feldspar groundmass, and spherulitic and glassy rhyolite with many Fe-Ti oxides.

2.4.2 Shakespeare Ignimbrite

The Shakespeare Ignimbrite is a non- to partially-welded, widely jointed, pumice- and lithic-rich ignimbrite. Pumice is rounded and very vesicular. It contains some cumulophyric plagioclase (An_{29} , Fig. 2.6) which has polysynthetic twinning and normal zoning. It also contains rare cubic Fe-Ti oxides.

The matrix contains non-devitrified glass shards which are lunate, platy and Y-shaped. Plagioclase (An_{45-29} , Fig. 2.7) is the dominant crystal which is tabular, subhedral, fragmented and up to 1.75 mm long. This composition is comparable to that determined by Bardebes (1997) of An_{46-28} . It exhibits polysynthetic twinning and has normal zoning. There are also rare cubic and acicular Fe-Ti oxides, some of which were identified as ilmenite. It contains zircons, even though they were not observed in thin section.

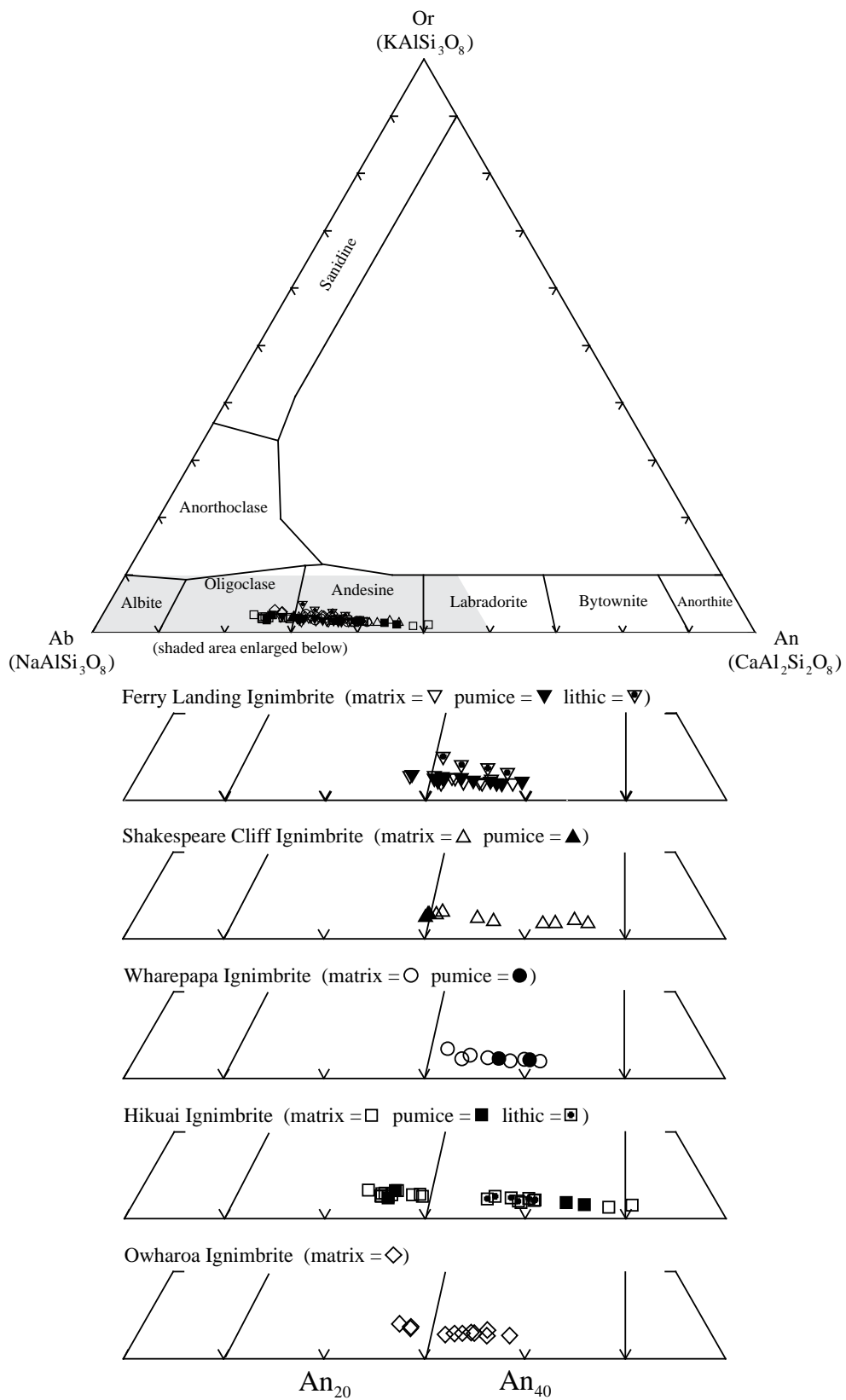


Fig. 2.6: Orthoclase – albite – anorthite ternary diagram for all plagioclase crystals (free matrix crystals, pumice phenocrysts and crystals in lithics) of ignimbrites analysed in this study, ordered from north to south. Classification according to Deer *et al.* (1992).

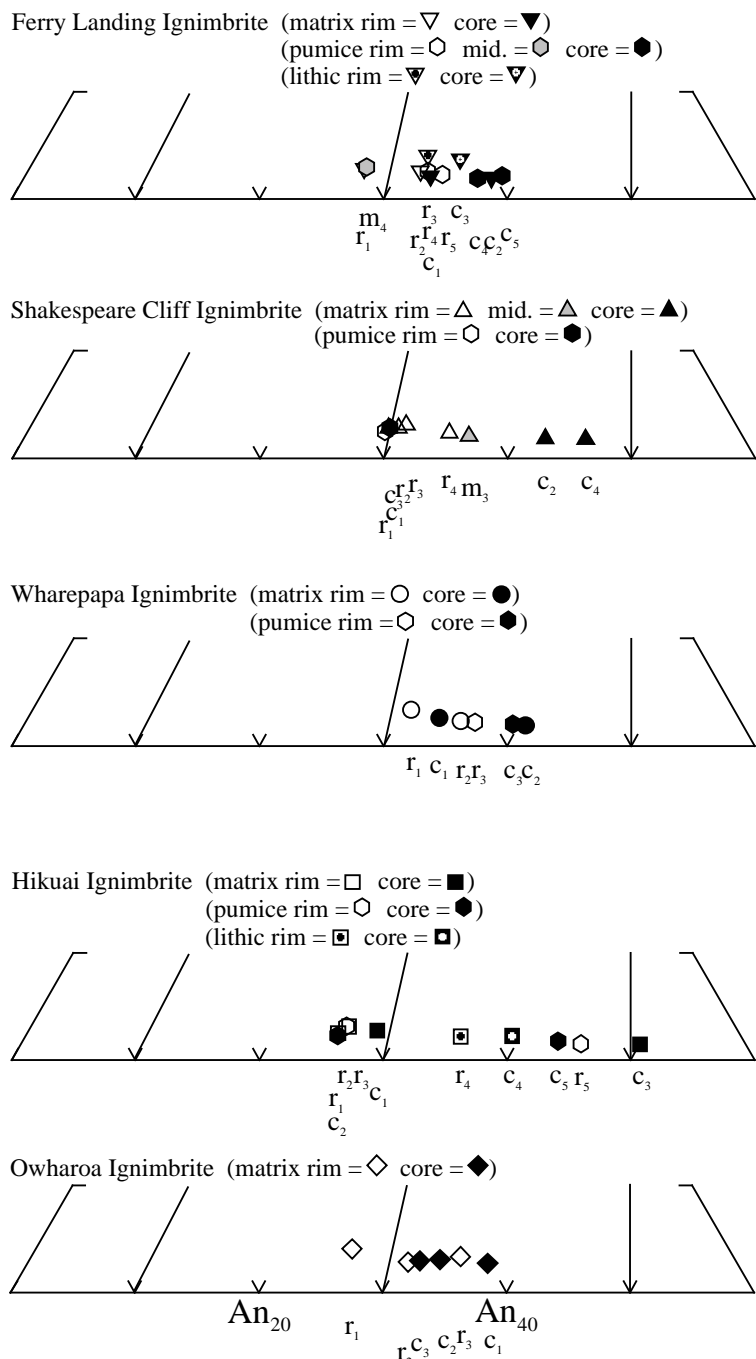


Fig. 2.7: Orthoclase – albite – anorthite ternary diagram for representative plagioclase crystals (free matrix crystals, pumice phenocrysts and crystals in lithics) of ignimbrites in this study, highlighting the variations between core (c) and rim (r) compositions. Classification according to Deer *et al.* (1992).

Lithics are subrounded to angular and up to 30 mm wide. Many varieties were observed by Fisher (1986), including grey, flow laminated non-vesicular rhyolite, light-grey-purplish finely vesicular rhyolite, mustard-coloured baked pyroclastic rock, other rhyolite and pyroclastic lithics, and rare andesite and sandstone. In this study the following types where observed: spherulitic/glassy rhyolite, rhyolite with plagioclase phenocrysts, felted feldspar rhyolite, flow banded devitrified rhyolite, vesicular rhyolite, ignimbrite, andesite and altered greywacke.

2.4.3 Wharepapa Ignimbrite

The Wharepapa Ignimbrite is a partially welded pumice-poor and lithic-rich ignimbrite. Pumice is rounded and very vesicular. Plagioclase (An_{39-36} , Fig. 2.6) phenocrysts in pumice are rare. An average composition for plagioclase phenocrysts in pumice of An_{40} is cited by Skinner (1995).

The matrix contains many non-devitrified glass shards which are lunate, cuspatate, platy and Y-shaped. Plagioclase (An_{41-31}) is the dominant crystal and is tabular, subhedral and can be greater than 2 mm long (Fig. 2.7). This composition is similar to that cited by Skinner (1995) of An_{50-36} . Some crystals have an irregular fragmented habit. Polysynthetic twinning is more common than simple. The crystals have normal zoning. Plagioclase sometimes occurs in clusters \pm orthopyroxene (Fig. 2.8 A). Orthopyroxene (En_{54}) is prismatic or sometimes irregular and can be up to 1.6 mm long (Fig. 2.9). Augite ($Wo_{42}En_{42}Fs_{15}$) is subhedral, prismatic and up to 0.5 mm wide (Fig. 2.9). These pyroxene compositions are similar to those of other CVZ ignimbrites, e.g. Hikuai and Momoparaua Ignimbrites (McGunnigle 1995). Cubic and acicular titanomagnetite and ilmenite occur up to 0.1 mm long. It contains zircons, even though they were not observed in thin section.

There are many lithics up to 4 mm wide and the following varieties were observed: felted feldspar rhyolite, some of which have oxidised rims, devitrified rhyolite rich in Fe-Ti oxides, pyroxene rhyolite in a glassy groundmass, and flow banded rhyolite rich in Fe-Ti oxides.

2.4.4 Hikuai Ignimbrite

The Hikuai Ignimbrite is a partially welded crystal-rich ignimbrite. Pumice is rounded and plagioclase (An_{45-25}) phenocrysts are rare (Fig. 2.6).

The matrix contains glass shards which are slightly devitrified and platy, lunate and Y-shaped. Plagioclase (An_{50-23}) is the dominant crystal and is tabular, sometimes fragmented, anhedral and can be greater than 2.5 mm long (Fig. 2.7). McGunnigle (1995) determined a plagioclase composition of An_{43-38} . Polysynthetic twinning is more common than simple twinning and they are normally zoned. Quartz is rare, fragmented, anhedral and up to 0.6 mm in diameter. Rare relict mafic minerals are altered to chlorite-smectite.

Titanomagnetite and ilmenite are common; they are mostly cubic, sometimes hexagonal and acicular, and up to 0.2 mm wide. They often occur in clusters and are associated with relict mafic minerals. A zircon crystal was observed in association with a cluster of Fe-Ti oxides.

Lithics are up to 60 mm in diameter and the following varieties were observed: hydrothermally altered ignimbrite with plagioclase, quartz and chlorite crystals and a hydrothermally altered andesite lithic (Fig. 2.8 B), glassy rhyolite, spherulitic rhyolite, and sandstone.

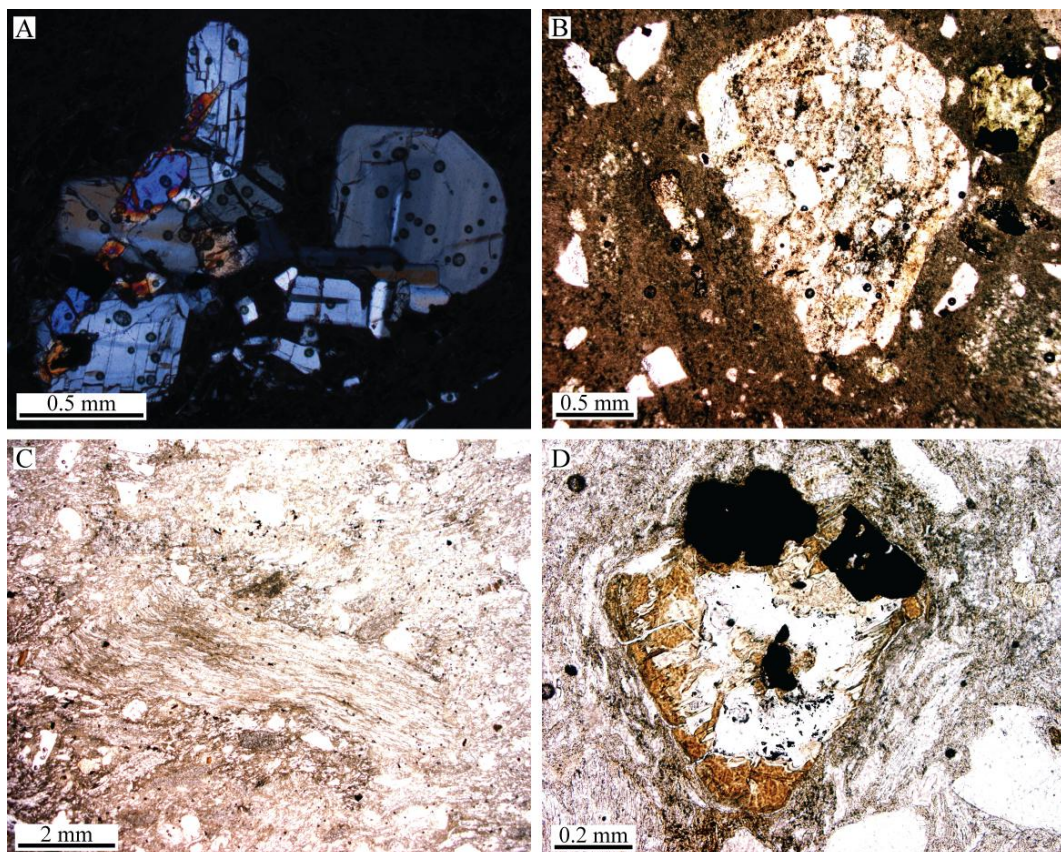


Fig. 2.8: Features of ignimbrites: A) Plagioclase + orthopyroxene cluster, Wharepapa Ignimbrite, cross-polarised light. B) Andesite lithic in an ignimbrite lithic, Hikuai Ignimbrite, plane-polarised light. C) Pumice with fiamme ends, Owharoa Ignimbrite, plane-polarised light. D) Relict mafic mineral and titanomagnetite, Owharoa Ignimbrite, plane-polarised light.

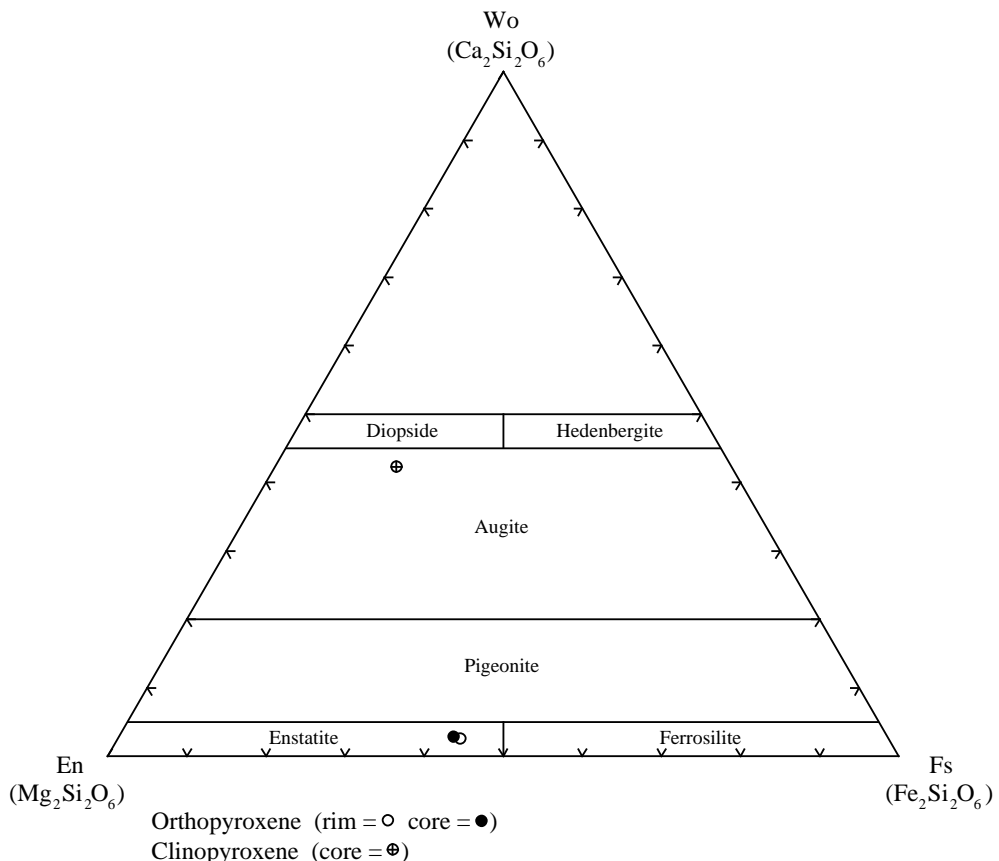


Fig. 2.9: Wollastonite – enstatite – ferrosilite ternary diagram for pyroxene crystals of the Wharepapa Ignimbrite. Classification according to Morimoto *et al.* 1988 (Deer *et al.* 1992).

2.4.5 Owharoa Ignimbrite

The Owharoa Ignimbrite is a densely welded, jointed, pumice-rich lenticulite. Most of the pumices are flattened and have fiamme ends and some of them are very dense and obsidian-like (Fig. 2.8 C). The flattened pumices are aligned which is evidence of the unit being densely welded. Some are still slightly rounded and rarely include phenocrysts of plagioclase.

The matrix is vitroclastic and contains non-devitrified glass shards which are lunate and Y-shaped. Plagioclase (An_{37-26}) is the dominant phenocryst (Fig. 2.6). It is mostly tabular, anhedral and can be irregular and fractured. It has polysynthetic twinning, normal zoning and is up to 1 mm long. It rarely occurs in clusters \pm quartz. Quartz is anhedral, almost tabular and up to 1 mm. Biotite occurs as subhedral flakes up to 0.5 mm long. Biotite has a similar composition to other CVZ rhyolites, e.g. Boom Rhyolite (McGunnigle 1995) and Flaxmill Dome rhyolite lavas (Bardebes 1997) (Fig. 2.3). There are some relict mafic minerals that have been altered to chlorite-smectite and occur either as solitary crystals up

to 1 mm long or as part of a lithic (Fig. 2.8 D). This indicates that the rock is incipiently hydrothermally altered, even though the plagioclase and biotite crystals and the glassy matrix appear fresh and unaltered. There is some titanomagnetite up to 0.25 mm wide. It contains zircons, even though they were not observed in thin section.

The following varieties of lithics were observed: spherulitic and flow banded rhyolite, and felted feldspar rhyolite.

Chapter 3

Petrochemistry

3.1 Introduction

New major and trace element analyses were determined for all 21 samples in this study. All samples (whole rock) were analysed for major element oxides and trace elements by X-ray fluorescence (XRF), using a SPECTRO X-LAB 2000 in the Faculty of Science and Engineering, University of Waikato. As these samples are from selected sites in the eastern CVZ and are only related by the tectonic setting, it is not possible to determine any genetic or chemical trends or associations. Full analytical results are given in Table 3.1. Errors are 1 % for major elements and 1-5 % for trace elements. The Whale Bone Bay Dome did not produce reliable major element data so an XRF analysis from the same site from Brathwaite & Christie (1996) has been used instead.

3.2 Methodology

Crushed powdered samples were prepared using a tungsten-carbide ring-mill. For major element analysis, glass fusion beads were made by fusing approximately 0.3 g of powdered sample with 2.50-2.55 g flux (pure 100 % Li-metaborate) and a few grains of NH₄I in Pt/Au crucibles in a furnace at progressive heating steps (650, 720, 780 and 825 °C) for 15 minutes at each stage and finally for at least 20 minutes at 1000 °C with the shaker on. The sample was then poured onto a graphite disc and pressed to make a glass disc. It was left to anneal on a hot plate at 230 °C for at least 1-2 hours, then on a cooler hot plate at 160 °C for at least 2 hours, preferably overnight. Loss on ignition was determined by calculating the per cent weight lost for 1-2 g of sample after having been in the furnace at 1100 °C for about 1 hour.

For trace element analysis, pressed pellets were made by mixing about 5 g of sample with 12-15 drops of PVA binder. This was pressed into an aluminium cap with an hydraulic press. The pressed pellet was left in an oven at 70 °C for about 2 hours to evaporate off the binder.

Table 3.1: Whole rock XRF geochemical analyses of selected rhyolite lavas and ignimbrites, eastern CVZ. Major elements normalised to 100 %, volatile free. * = Total Fe. # = Original values. - = below detectability limit.

Sample number	13 Ferry Landing Ignimbrite	14 Shakespeare Ignimbrite	21 Wharepapa Ignimbrite	01 Paku Rhyolite	03 Pauanui Dome Complex	02 Timata Dome
Major elements (wt %)						
SiO ₂	82.06	78.36	72.57	78.08	75.73	77.95
TiO ₂	0.10	0.12	0.43	0.08	0.40	0.18
Al ₂ O ₃	11.00	12.66	14.97	12.88	16.03	13.85
Fe ₂ O ₃ *	1.03	1.52	3.37	0.77	0.24	1.51
MnO	0.01	0.01	0.08	0.01	0.03	0.01
MgO	0.15	0.18	0.73	0.13	0.19	0.14
CaO	0.06	0.80	2.03	0.74	1.11	0.44
Na ₂ O	0.32	2.74	3.36	3.28	3.22	2.28
K ₂ O	5.25	3.59	2.39	3.91	2.97	3.62
P ₂ O ₅	0.01	0.04	0.04	0.11	0.09	0.02
LOI #	3.02	4.14	5.13	0.85	2.35	2.20
Total #	99.59	99.67	101.19	99.33	98.02	99.86
Trace elements (ppm)						
S	311	445	179	431	145	147
Cl	1019	1304	1437	118	40	88
V	-	3.7	21	-	6.5	-
Cr	6	4.8	-	9.9	5.6	7.7
Co	62	43	57	15	25	13
Ni	5.8	5.4	6.3	5.5	5.2	4.2
Cu	1.3	-	3.4	-	-	0.7
Zn	67	65	67	18.2	70	40
Ga	18.4	18	18	15	18.3	15.1
Ge	-	-	1.9	-	2.2	1.6
As	4.3	3.7	4	4.1	2.1	2.5
Se	1	1.1	1.5	1.6	0.5	0.8
Br	4	4.5	4.1	1.4	0.5	0.8
Rb	75	88	82	143	106	141
Sr	181	181	162	65	103	57
Y	35	42	35	22	29	24
Zr	261	257	250	112	207	184
Nb	9.7	9.7	9.3	7.6	7.8	9.3
Mo	2.3	2.4	2.4	1.8	1.5	1.7
Sn	1.8	1.4	2.4	0.8	1.7	1.2
Sb	-	-	1.8	-	-	-
Ba	591	619	644	820	526	777
La	26	38	57	35	35	33
Ce	44	71	88	59	39	50
Nd	22	38	53	29	30	28
Hf	9.9	9.8	8.2	7.5	8.9	9.2
Tl	1.8	2.2	2.5	3.2	1.4	2.2
Pb	17.1	17.9	16.3	17.1	15.8	21
Bi	1.1	1.3	2	2	0.7	1.2
Th	13.3	12.8	11.4	18.5	14.9	19.5
U	5.8	6	4.8	7.6	6.3	8

Table 3.1 cont.: Whole rock XRF geochemical analyses of selected rhyolite lavas and ignimbrites, eastern CVZ. Major elements normalised to 100 %, volatile free. * = Total Fe. # = Original values. - = below detectability limit.

Sample number	20	09	06	07	08	10	05	18
Sample name		Broken Hills Flow	Broken Hills Mine sample 1	Broken Hills Mine sample 2	Broken Hills Mine sample 3	Hikuai Ig.	Pokohi-no Dome Complex	The Knob
	Staircase Dome	Banded Rhyolite						
Major elements (wt %)								
SiO ₂	77.00	72.72	86.15	72.36	83.24	74.03	82.28	78.29
TiO ₂	0.13	0.30	0.09	0.28	0.09	0.23	0.05	0.09
Al ₂ O ₃	14.73	15.24	8.81	16.04	9.53	15.07	11.59	13.38
Fe ₂ O ₃ *	1.75	2.20	1.42	2.94	0.90	1.75	0.52	0.74
MnO	0.01	0.05	0.01	0.03	0.01	0.02	0.00	0.00
MgO	0.10	0.26	0.13	0.27	0.12	0.18	0.13	0.11
CaO	0.27	1.87	0.06	1.78	0.09	2.47	0.18	0.90
Na ₂ O	1.86	4.56	0.25	4.16	0.35	3.15	1.14	3.23
K ₂ O	3.97	2.73	3.05	2.12	5.66	2.88	4.06	3.20
P ₂ O ₅	0.18	0.08	0.02	0.03	0.02	0.22	0.04	0.05
LOI #	3.20	1.30	2.08	1.86	1.40	3.72	2.27	1.02
Total #	98.33	100.86	100.15	101.51	98.16	101.11	100.63	100.88
Trace elements (ppm)								
S	229	125	241	137	4704	257	212	145
Cl	213	46	115	106	27	192	41	5.4
V	11.2	-	-	-	-	-	-	8.5
Cr	4.3	8.6	8.1	7.2	8	12	10.1	7.8
Co	21	31	30	29	43	29	26	49
Ni	3.6	4.8	4.2	4	5.6	7.8	3	5.5
Cu	-	-	1	1.7	5.7	2.2	-	1.8
Zn	28	31	19	16.3	13.9	60	14.2	5.1
Ga	17.1	15.8	9.6	10.9	11.1	19.5	15.6	5
Ge	1.8	-	2.2	1.7	-	-	1.7	-
As	4.8	9.9	50	15.3	35	1.4	42	23
Se	0.6	1.3	1.2	1.2	2.1	1.2	1.1	2.8
Br	0.8	1.2	1.1	1	1.5	1.5	2.5	2.1
Rb	159	137	181	313	289	119	179	16
Sr	29	77	27	43	35	285	22	9
Y	33	30	24	33	26	37	30	8
Zr	126	172	142	152	142	217	102	87
Nb	8.2	8.3	6	6.9	6.5	7.9	7.1	6.9
Mo	1.4	1.2	3.2	2.2	1.8	1.1	0.7	2.3
Sn	2.4	-	-	-	2.1	-	1.3	2.1
Sb	-	1.1	5.4	2.6	3.5	-	8	28
Ba	698	767	609	801	803	480	630	99
La	56	31	22	27	34	21	24	13
Ce	61	56	43	49	58	46	47	21
Nd	52	23	23	19	38	23	22	27
Hf	6.2	6.8	6.4	6.1	5.5	8.4	6.1	3.9
Tl	2.1	2.4	2.9	3.8	4.6	1.5	2.1	3.1
Pb	18.5	18.7	11.8	5.5	9	14.7	15.9	21
Bi	0.8	1.3	1.3	1.6	3.2	1.2	0.8	3.3
Th	22	15.6	12.6	13.8	13.9	9	15.8	8.2
U	8.6	6	5.8	7.3	7.3	3.9	7.3	5.6

Table 3.1 cont.: Whole rock XRF geochemical analyses of selected rhyolite lavas and ignimbrites, eastern CVZ. Major elements normalised to 100 %, volatile free. * = Total Fe. # = Original values. - = below detectability limit. Whale Bone Bay Dome major element data is from Brathwaite & Christie (1996).

Sample number	04	19	15	11	16	17	12
Sample name	Pohaka-haka Dome Complex	Te Karaka Rhyolite	Papakura Bay Dome	Whare-kirauponga Dome	Whale Bone Bay Dome	Shark Bay Dome	Owharoa Ignimbrite
Major elements (wt %)							
SiO ₂	76.76	86.46	76.96	84.57	77.69	77.27	82.20
TiO ₂	0.13	0.12	0.10	0.08	0.12	0.07	0.06
Al ₂ O ₃	12.76	10.13	12.87	8.74	12.80	13.35	11.58
Fe ₂ O ₃ *	1.67	0.70	1.46	0.83	0.73	1.70	0.53
MnO	0.03	0.01	0.02	0.00	0.01	0.03	0.00
MgO	0.14	0.24	0.13	0.07	0.06	0.05	0.13
CaO	1.03	0.14	1.10	0.08	1.17	0.40	0.20
Na ₂ O	4.25	0.27	3.64	0.30	3.84	2.97	1.12
K ₂ O	3.23	1.86	3.67	5.19	3.55	3.98	4.09
P ₂ O ₅	0.01	0.06	0.04	0.15	0.03	0.19	0.09
LOI #	0.80	1.55	1.92	1.24	1.22	2.34	3.68
Total #	97.02	100.87	100.96	100.66		98.42	99.27
Trace elements (ppm)							
S	443	140	94	102	294	3467	179
Cl	1241	775	755	-	177	74	844
V	-	-	-	4.2	-	-	-
Cr	6.7	6.4	1.2	6.3	10.5	4	8.9
Co	41	27	38	24	28	16	26
Ni	6.3	4.7	6	3.9	4.5	3.2	4.9
Cu	2.5	1.3	1.5	0.6	1.2	-	-
Zn	61	41	42	8.6	43	15.4	46
Ga	18	18.2	17.1	9.2	18.1	11.3	17.4
Ge	2.9	2.4	2.5	-	2.1	-	2
As	8.3	11.2	12.5	96	4.5	13.8	4.9
Se	1.7	1.3	2.3	1.5	1.6	1.4	1.2
Br	4.4	2.5	3.4	1.4	2.1	1.4	3
Rb	97	147	139	242	134	121	129
Sr	71	26	81	49	76	18	86
Y	35	34	27	16	28	13	26
Zr	167	146	113	77	125	104	109
Nb	7.8	9.1	6.7	6.2	7.5	5.9	7.4
Mo	2.2	2.2	2.2	1.4	1.8	2	1.9
Sn	1.7	2.8	3.3	-	1.4	1.3	1.6
Sb	-	1	1.7	11.6	-	4.9	-
Ba	772	815	731	517	721	415	792
La	36	36	69	31	34	49	41
Ce	62	72	107	46	61	77	65
Nd	34	42	69	23	34	61	34
Hf	7	8	5.4	4.4	5.5	4.9	6.2
Tl	2.6	2.6	3.2	4.8	2.8	2.4	2.6
Pb	19.3	21	22	13.7	17.4	7.3	19.5
Bi	1.8	1.4	2.1	1.3	1.8	1.6	1.3
Th	14.7	18	17.8	13.8	16.7	17.7	18.7
U	6.3	8.4	8.2	9.4	7.8	8.7	9

3.3 Major element chemistry

SiO_2 values in this study range from 72 % in Broken Hills Mine sample 2 to 86 % in the Te Karaka Rhyolite. All the samples are therefore rhyolites. The range in SiO_2 values is comparable to other CVZ rhyolites and ignimbrites (e.g. Fulton (1988), Adams (1992), Rogers (1994), McGunnigle (1995) and Bardebes (1997)). All those that have a SiO_2 wt % value greater than 78 % have been hydrothermally altered, and possibly even those that have values of 76-78 %. The Te Karaka Rhyolite has such a high SiO_2 wt % value because it consists mostly of glass and rare quartz phenocrysts. The Ferry Landing and Owharoa Ignimbrites have rather high SiO_2 values of 82 %; however, neither of them show any evidence of hydrothermal alteration in thin section or hand specimen. Bardebes (1997) produced an average SiO_2 wt % value for Ferry Landing Ignimbrite pumices of c. 75 % and K_2O between 3 and 4 %. Bardebes (1997) also analysed pumices from the Shakespeare Ignimbrite and produced SiO_2 values between 73 and 78 % and K_2O of c. 3.3 %, which are comparable to that which was determined in this study.

Harker variation diagrams plot the weight per cent of a given oxide against the weight per cent of SiO_2 and can be used to classify volcanic rocks. The K_2O vs. SiO_2 plot is used to distinguish between high-K, medium-K and low-K rhyolites (Fig. 3.1) (Rollinson 1993). Te Karaka is the only low-K rhyolite. Ferry Landing Ignimbrite, Paku, Staircase Dome, Broken Hills Mine sample 3, Papakura Bay Dome, Wharekirauponga Dome and Shark Bay Dome Rhyolites have high-K compositions. The other 13 samples are medium-K rhyolites. CVZ rhyolites typically have high-K compositions (e.g. Adams (1992), Rogers (1994), McGunnigle (1995) and Bardebes (1997)).

Intensively hydrothermally altered rhyolites (i.e. high SiO_2) can be high-K because minerals such as plagioclase will have been altered to sericite or adularia, which are K-micas and K-feldspars respectively, in the potassic zone. After further alteration in the intensely silicified zone, K_2O is leached out and SiO_2 is further enhanced. This is shown in Fig. 3.1 where Ferry Landing Ignimbrite, Broken Hills Mine sample 3 and Wharekirauponga Dome appear to be intensively hydrothermally altered and are rich in K_2O . Sericite was observed in Wharekirauponga Dome. Broken Hills Mine sample 1 and Te Karaka Rhyolites

are very silicified and have lower K₂O; quartz and polymorphs of SiO₂ were the dominant minerals in each of these samples.

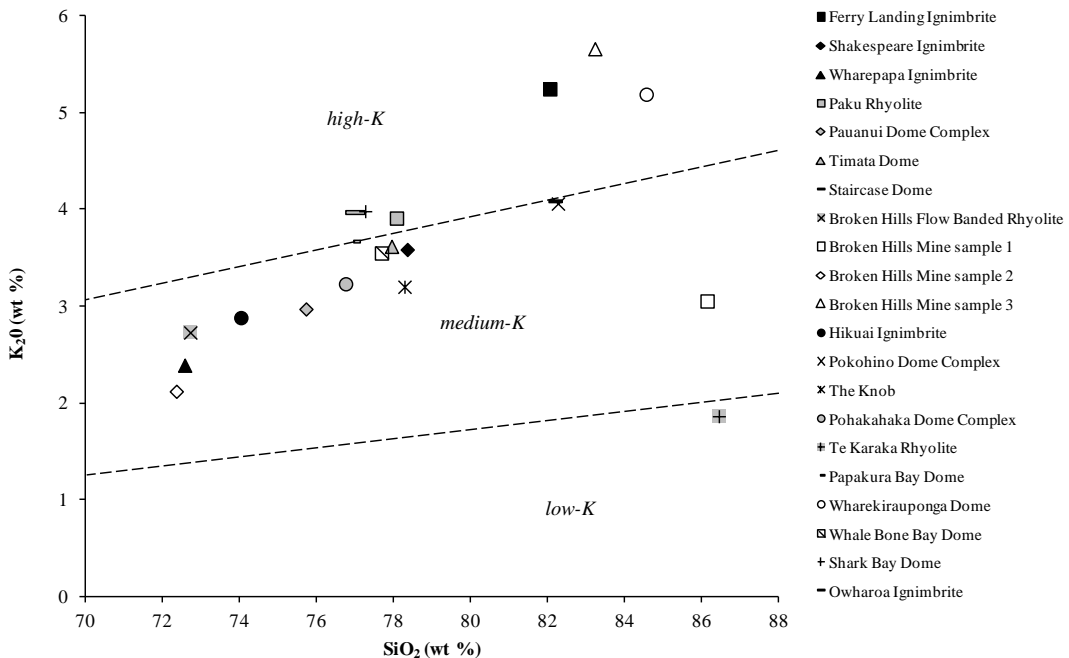


Fig. 3.1: Plot of K₂O vs. SiO₂ wt % of all samples. Divided into high-K, medium-K and low-K volcanics according to Le Maitre *et al.* (2002). Grey-filled markers = slightly hydrothermally altered rhyolite lavas. Hollow markers = intensively hydrothermally altered rhyolite lavas. Solid markers = ignimbrites.

Harker variation plots can also be used to determine the geochemical processes that may have occurred in the magma chamber (Rollinson 1993). This is only applicable however if the rocks being analysed are from the same magma chamber, and in this study they are not. Some trends can still be observed; the major elements in Fig. 3.2 all decrease with increasing SiO₂ and hydrothermal alteration (i.e. wt % SiO₂ > 76-78 %). Sodium and Ca are particularly depleted in the highly altered rocks as they are generally replaced by K. There do not appear to be any trends with location or age through the CVZ.

3.4 Trace element chemistry

As with major elements, trace element variation plots can be used to determine the geochemical processes that may have occurred in the magma chamber, but as these units are not from the same magma chamber, this is irrelevant here. Some other trends have still been observed.

Rubidium usually geochemically follows K, so the Rb vs. SiO₂ plot should be similar to the K₂O vs. SiO₂ plot; that is, Rb and K₂O increase with increasing SiO₂

(Fig. 3.1 and Fig. 3.3). Therefore, K_2O vs. Rb should plot along a straight line with a positive trend which is more or less the case (Fig. 3.4).

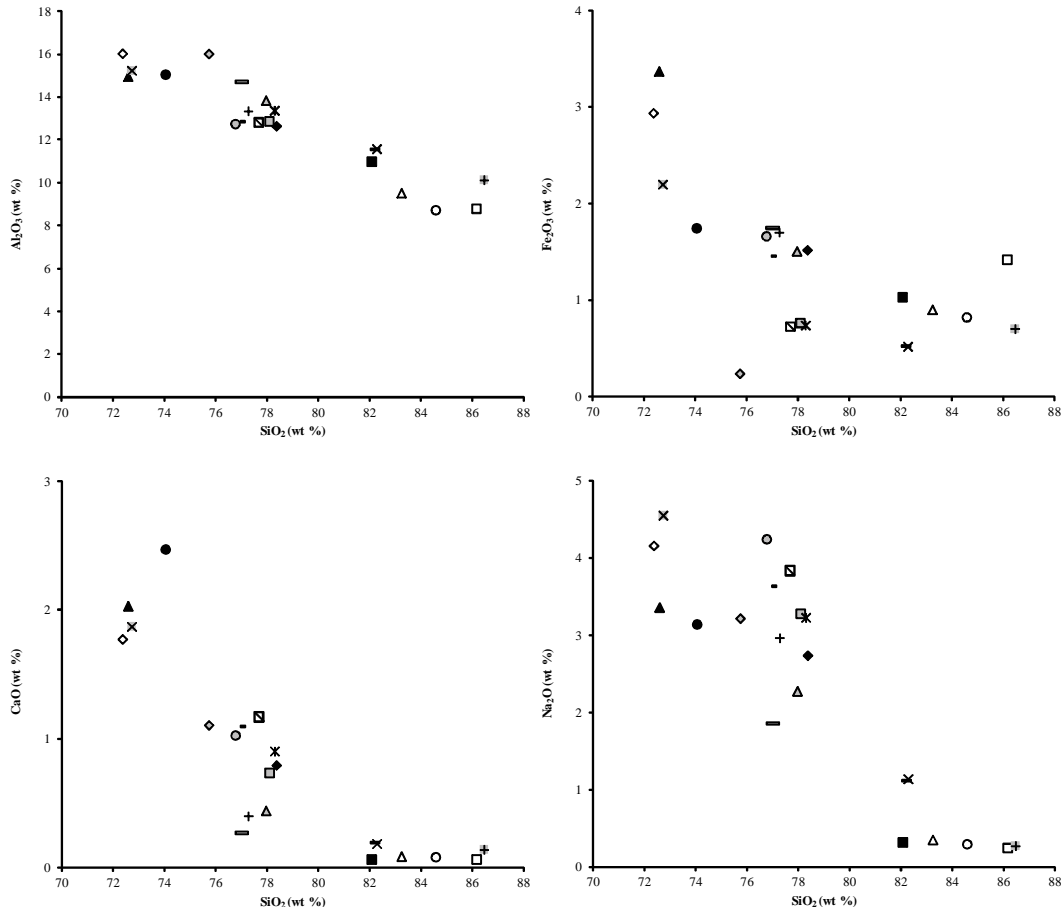


Fig. 3.2: Harker variation diagrams of selected major elements. Symbols are the same as in Fig. 3.1.

Arsenic and Sb generally increase with hydrothermal alteration; samples that have been previously defined as intensively altered plot above 13.8 ppm As and 2.6 ppm Sb (Fig. 3.3).

Major element compositions can be used to classify volcanic rocks, but this is not true for altered rocks as many major elements are mobile during alteration, as was shown in section 3.3 (Gifkins *et al.* 2005). However, immobile elements, such as Ti, Zr, Nb, Y and Th, do not change significantly with alteration so can be used to classify altered rocks. TiO_2 vs. Zr can be used to discriminate what the unaltered parent rock was. All of the samples in this study are within (or very close to) the rhyolite field (Fig. 3.4).

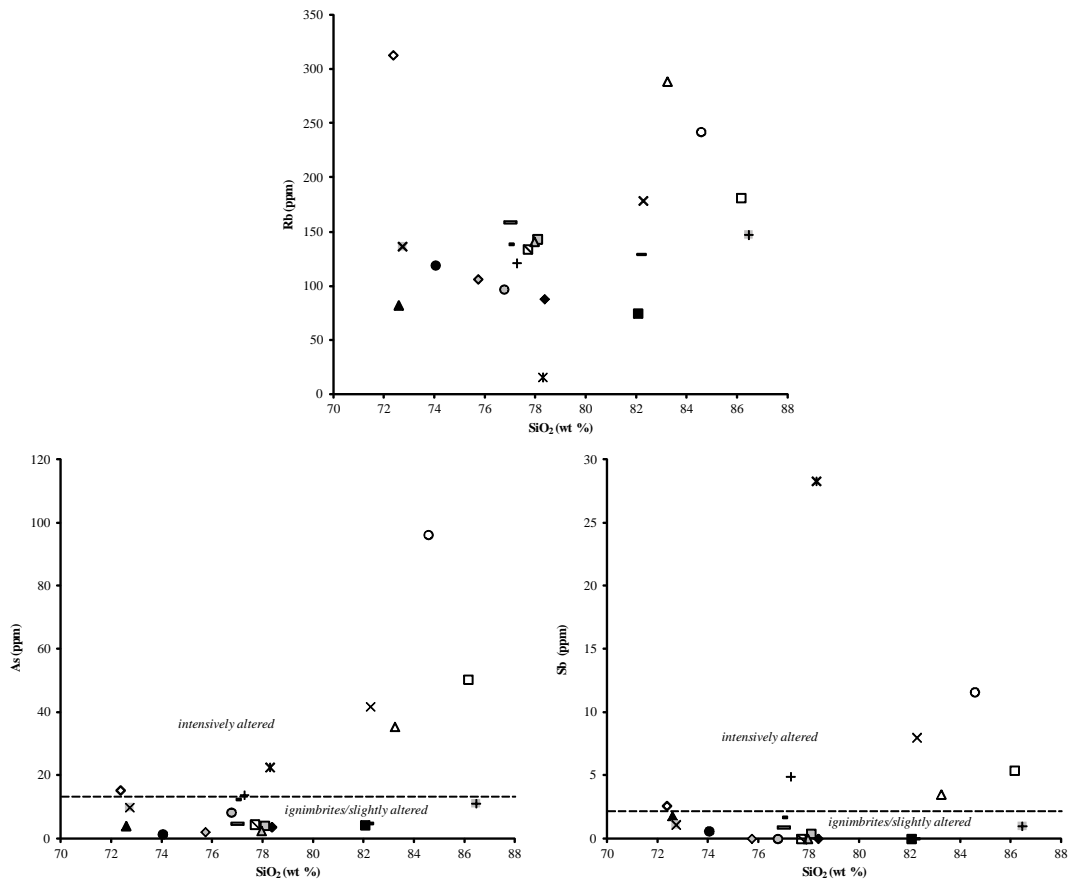


Fig. 3.3: Harker variation diagrams of selected trace elements. Any points plotted on the horizontal axis were below the limit of detection. Symbols are the same as in Fig. 3.1.

HFSE such as Zr, Y, Nb and Th do not change significantly with hydrothermal alteration because they are generally immobile, so there is no relationship between them and SiO_2 (Gifkins *et al.* 2005). When plotted as Zr vs. Y or Nb or Th, they plot along a straight line (Fig. 3.4). There do not appear to be any trends with location or age through the CVZ.

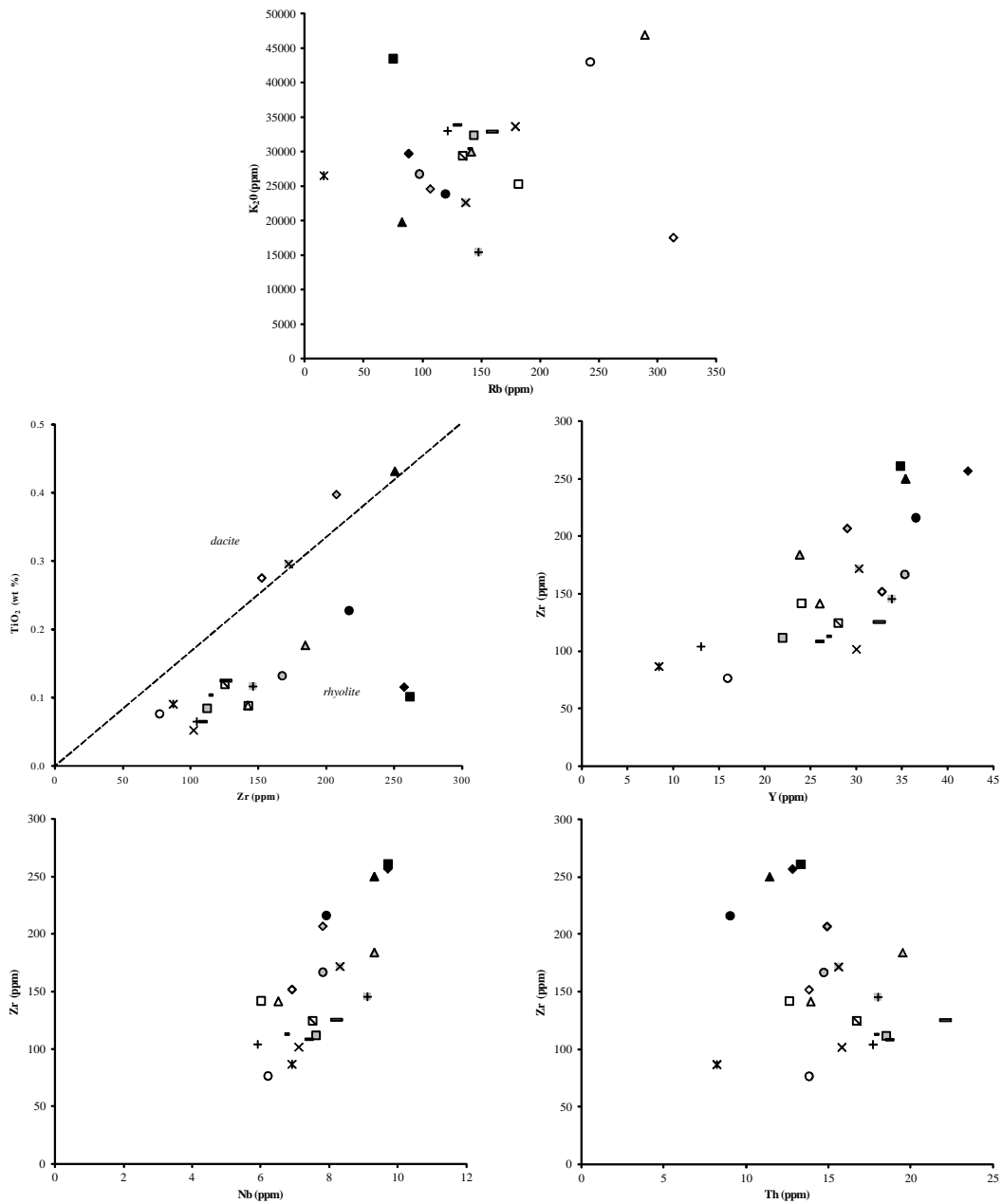


Fig. 3.4: Selected element-element plots. Symbols are the same as in Fig. 3.1. Boundary between dacite and rhyolite on TiO_2 vs. Zr plot is after Gifkins *et al.* (2005).

Chapter 4

U-Pb Dating of Zircons

4.1 Introduction

U-Pb ages are considered to be the “gold standard” in geochronology because the decay constants involved have been measured very precisely and the ages provide internal validation of the fundamental assumptions for an isotopic age determination (Ludwig 1998; Dickin 2005). U-Pb dating is theoretically similar to most isotopic dating techniques and is based on the accumulation of ^{206}Pb and ^{207}Pb over time due to the radioactive decay of ^{238}U and ^{235}U respectively (Cooper & Reid 2008). U-Pb dating, especially of zircons, has been used widely to date igneous, metamorphic and sedimentary rocks and is considered to be an accurate way of dating igneous rocks (Cooper & Reid 2008). This method has only been used for one sample in the CVZ prior to this study, the Owharoa Ignimbrite, which was dated by SIMS on SHRIMP ion microprobe (Hoskin *et al.* 1998). One of the objectives of this study was to assess whether this is an appropriate method for dating silicic volcanics of the CVZ; this will be discussed in Chapter 5 (section 5.3.3).

Zircons are ideal for U-Pb dating because they crystallise with a high concentration of uranium and no initial lead, and retain the daughter products of radioactive decay (Dickin 2005). They are a common accessory mineral in most igneous (intermediate to Si-saturated composition generally), metamorphic and sedimentary rocks (Richards 2009; Perkins 2011) and are known to occur in most CVZ rhyolites. Zircons are very hard and resistant to mechanical weathering and hydrothermal alteration (Wilson *et al.* 2008; Wilson *et al.* 2010), which is significant for geochronological studies of the CVZ as many of the units have been hydrothermally altered. Table 4.1 outlines some characteristics and properties of zircons.

Table 4.1: Optical and physical properties of zircon crystals ($\text{Zr}[\text{SiO}_4]$). Adapted from Deer *et al.* (1992) and Perkins (2011).

Optical properties	
Colour	Generally colourless under plane-polarised light, but may be yellow, grey, green, pale brown and faintly pleochroic. Very high interference colours. Colourless, yellow, pink, brown, green, blue, purple in hand specimen.
Relief	Extreme
Crystal system	Tetragonal
Cleavage	Poor to imperfect
Extinction	Straight
Physical properties	
Hardness	7.5
Specific gravity	4.68
Abundant elements	Uranium, thorium, lead and hafnium isotopes
Inclusions	Apatite, liquid or opaque

Zircon characteristics in general may be location-specific and dependent on origin (Siyambola *et al.* 2005). Zircons can occur in a variety of colours, including colourless, yellow, pink, brown, and even rare green and blue (Deer *et al.* 1992; Garver & Kamp 2002). Colour can be related to radiation damage, trace element composition and impurities (Garver & Kamp 2002). Relative colour loss may be caused because the zircon has reached a discrete temperature at some point in its history (Gastil *et al.* 1967). At near-surface temperatures, zircons will gradually become darker coloured with age as uranium and thorium decay, but significant changes may only happen after several 100 million years (Garver & Kamp 2002). If a zircon is rich in REE, or from a felsic melt (which tend to be richer in REE), colour can be acquired more quickly (Garver & Kamp 2002). However, the role of REE in colour generation is poorly understood and further studies are needed to fully understand this relationship (Garver & Kamp 2002).

There have been numerous attempts to systematically relate zircon morphology to petrogenesis (Hoskin & Schaltegger 2003). A widely used scheme was created by Pupin (1980) that relates relative development of crystal forms with temperature and host-rock type (Fig. 4.1). Zircons are of the tetragonal crystal system and can consist of zero, one or two prisms ($\{100\}$ and $\{110\}$) and pyramid forms ($\{101\}$, $\{211\}$ and $\{301\}$ most commonly) (Pupin 1980). This scheme was originally devised to classify zircons of granitic rocks, but may be applied to other studies

(e.g. detrital and volcanic). Even though this scheme is still widely used, three ongoing observations have also seen it not to be used: (1) a single rock and age population may have a variety of morphologies; (2) zircons from different rocks can have similar to identical morphologies; and (3) the external morphology of a crystal may change during a single growth event (Hoskin & Schaltegger 2003).

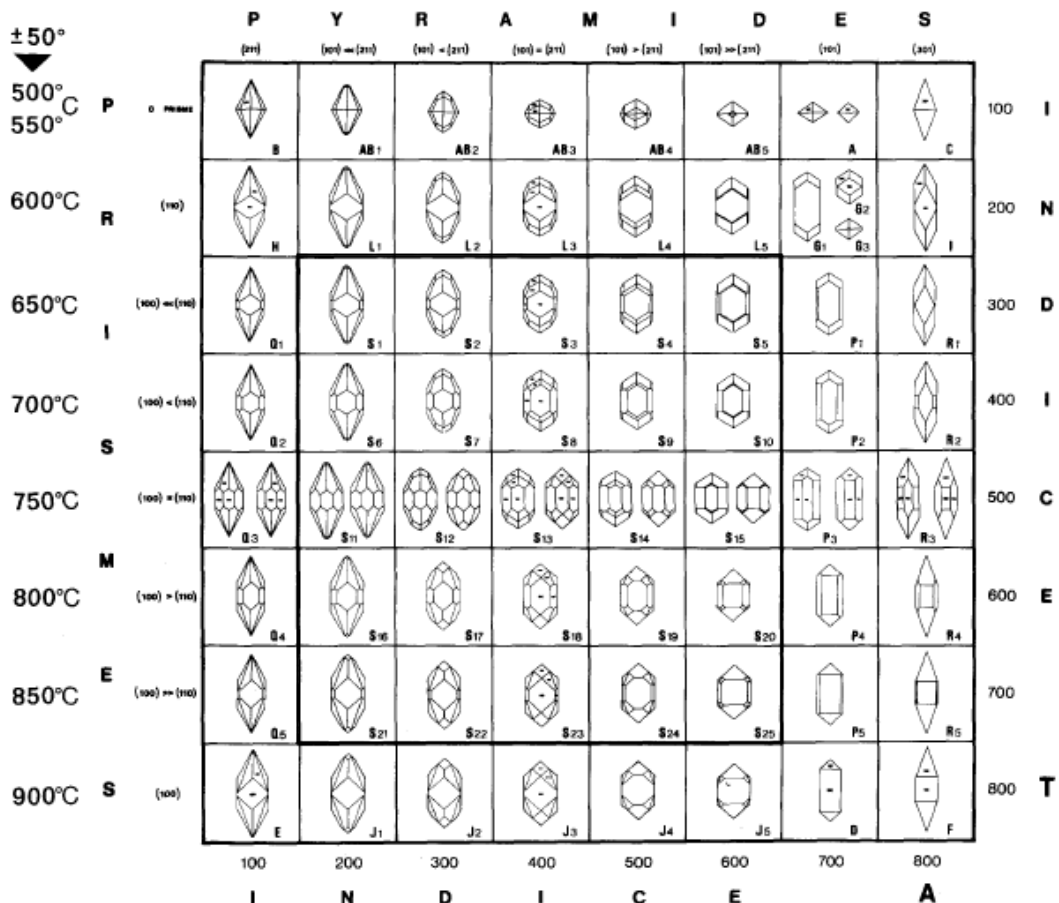


Fig. 4.1: Typological classification of zircons (Pupin 1980). Temperature is that of crystallisation. The morphologies within the bolded square are those which occur most commonly in nature.

The optical classification of zircon crystals (i.e. by colour and morphology) can be useful if undertaking a qualitative analysis (to use an unbiased representation of all colours and morphologies), but may not necessarily prove to be of any significance (Roddick & Bevier 1995; Fedo *et al.* 2003).

4.2 Methodology

The 21 samples (16 rhyolite lavas and 5 ignimbrites) used in this study were collected during 2010-2011 from rhyolites of the eastern CVZ that are known to have good outcrops. At each site 2-4 kg of rock was collected from an unweathered section. The samples were processed in the Department of Earth and

Ocean Sciences at the University of Waikato using techniques based on Richards (2009).

4.2.1 Mineral separation

The bulk rock was crushed to 500 µm using a rock crusher, jaw crusher and Bico mill. The powdered sample was separated by weight using a Gemini Table. The oven-dried heavy mineral fraction was separated using a vertical Frantz Isodynamic magnetic separator. The non-magnetic fraction was processed through sodium polytungstate (SPT) (density 3.0 g.cm³). The resultant air-dried heavy mineral fraction was processed on an inclined Frantz separator (15 ° front-to-back, 10 ° side-to-side) to produce a final non-magnetic, heavy mineral fraction. Zircons are assumed to be robust enough that they will not be broken during sample crushing, nor is any bias caused by the Gemini Table or heavy liquid separation (Fedo *et al.* 2003). For equipment settings, see Appendix V.

4.2.2 Grain selection

All equipment used in grain selection was cleaned using ethyl alcohol before picking began and between samples. A portion (approximately 150 grains) of the non-magnetic, heavy mineral fraction was poured into one of the cavities of a double cavity glass slide. The population also sometimes contained pyrite, other opaque minerals and micas. This initial population was observed through a petrographic microscope using reflected and/or transmitted light. Reflected light is useful for determining zircon colour and morphology and assessing the presence of inclusions or fractures. Transmitted light is useful for determining the morphology of grains and assessing the presence of inclusions. Zircons can readily be identified at this stage by their extreme relief and euhedral (to subhedral) tetragonal morphology. Paku Rhyolite was the only sample in which no zircons were found. Less than 10 zircons were found in both Pauanui Dome Complex and Wharepapa Ignimbrite so these samples were processed no further. Their zircons were also full of inclusions and/or too small for ablation.

A representative selection of zircons (50-70) was separated from the initial population and photographed under reflected light. The crystals needed to be at least 50 µm in width and length. Larger crystals are preferable as they produce a lower expected U-Pb age error and it is easier to ablate them (laser spot-size = 30 µm) (Richards 2009). The crystals were divided by colour into colourless, light

pink and pink, and photographed under reflected light (Fig. 4.2), so that it could later be investigated whether there is a relationship between zircon colour and age. Up to 60 crystals that were of an appropriate size (i.e. as large as possible) and whose centres were free of inclusions and fractures were mounted onto a prepared glass slide. The glass slide was cut to 25 x 25 mm (to fit in the sample chamber of the LA-ICP-MS), on top of which was attached a 10 x 10 grid on OHT paper with double-sided tape. On top of this was a square of double-sided tape, onto which the zircons were mounted. The outer squares of the grid were left empty. The colour and location on the grid of each crystal was noted on a mount map. The length and width of the crystal were estimated and the morphology was determined if possible based on Pupin's (1980) classification (see section 4.3). The sample was then ready for laser ablation.

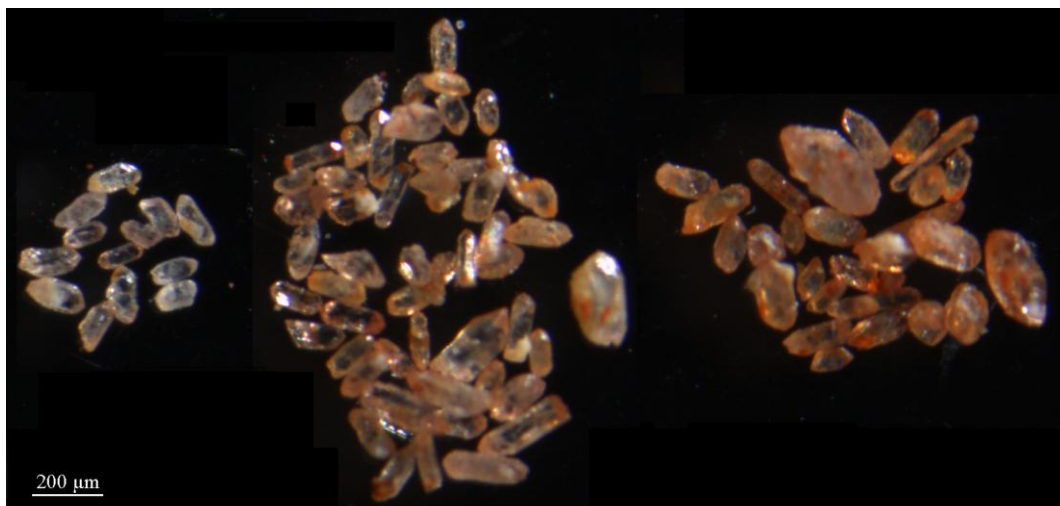


Fig. 4.2: Colourless, light pink and pink zircons, Wharekirauponga Dome, reflected light.

4.2.3 Laser Ablation Inductively Coupled Plasma Mass Spectrometry (LA-ICP-MS)

Laser ablation was carried out based on the methods of Richards (2009). U-Pb isotopes ^{238}U , ^{235}U , ^{232}Th , ^{208}Pb , ^{207}Pb and ^{206}Pb were measured using a New Wave UP-213 Deep Nd YAG (Tempest 20 Hz) Laser Ablation system and an Elan 6100 DRCII Inductively Coupled Plasma Mass Spectrometer in the Faculty of Science and Engineering, the University of Waikato. For full LA-ICP-MS specifications and settings see Appendix VI.

Two analytical standards and a zircon of known age were used as a check against the data for a sample of unknown age (i.e. the crystals being dated in this study)

(see Appendix VII for certificates of authenticity). The NIST610 is a glass standard that is completely homogeneous in 61 trace elements and was used as a base check for the concentration of elements in the unknown samples (Richards 2009). The second standard, GJ1, is a large homogenous zircon of gem quality (Jackson *et al.* 2004) obtained from the School of Earth and Planetary Sciences, Macquarie University, Australia. The GJ1 is used as a calibration to correct for any mass discrimination by the ICP-MS and has a TIMS age of 608.5 ± 0.4 My (Jackson *et al.* 2004). Temora2 zircon crystals were used as a zircon of known age (416.78 ± 0.33 My) and as a method check (Black *et al.* 2004). Temora2 zircons are from the Middledale Gabbroic Diorite of the Paleozoic Lachlan Orogen in eastern Australia (Black *et al.* 2004).

The NIST610 glass standard was run twice at the start of every ablation session, followed by four runs of the GJ1 standard, then two runs of the Temora2. After every 10-12 unknowns (or 1 hour of ablating), the GJ1 was analysed twice more to correct for any machine drift. At the end of the session, two runs were done of each: Temora2, GJ1, NIST610. A “session” is a single day of ablating, during which a single sample (i.e. one rock unit) was dated.

Laser ablation analyses were undertaken in time-resolved mode; this means that the acquisition of data is a function of time (i.e. ablation depth) (Jackson *et al.* 2004). An 80 second background signal was taken while the laser was not firing. This was followed immediately by turning on the laser and ablating the sample for 45 seconds. During data collection the laser was fired continuously with a constant power output of 60 % and 20 Hz repetition rate with a spot size of 30 μm on unknown samples. 40-60 unknown crystals were analysed per sample.

4.2.4 Data processing

Raw data was processed using GLITTER, a data reduction software which calculates the relevant isotope ratios ($^{207}\text{Pb}/^{206}\text{Pb}$, $^{208}\text{Pb}/^{206}\text{Pb}$, $^{208}\text{Pb}/^{232}\text{Th}$, $^{206}\text{Pb}/^{238}\text{U}$ and $^{207}\text{Pb}/^{235}\text{U}$) (Jackson *et al.* 2004). The most concordant, or stable, section of each ablation signal for the GJ1 standard is automatically selected (Jackson *et al.* 2004), but this can also be manually adjusted, especially if the $^{206}\text{Pb}/^{238}\text{U}$ and $^{207}\text{Pb}/^{235}\text{U}$ age estimates are far apart (more than c. 20 My in this study). Standards can also be “turned off”, and are therefore not included in the calibration, if the estimated age produced is considered too young/old (c. 600 ± 50

My). GLITTER then automatically selects an identical ablation time segment for the unknown analyses (Jackson *et al.* 2004).

Calculated ratios were then exported to Isoplot v. 3.10, an Excel add-in developed by Ken Ludwig, where concordia plots can be constructed to give age results (Ludwig 2003). Ages are calculated for each unknown in terms of concordance between the measured isotope ratios of $^{206}\text{Pb}/^{238}\text{U}$ and $^{207}\text{Pb}/^{235}\text{U}$ with 1σ internal errors (see Appendix VIII). Any discordant analyses, or analyses with a probability of concordance of $< 5.0\%$, were rejected. Crystals can give discordant ages because of lead loss (Dickin 2005; Richards 2009). Analyses that were not rejected were then plotted together on a U-Pb concordia plot, removing any outliers (i.e. potentially inherited zircons), until a concordant age was produced (see Appendix IX). Final age calculations were supported by a probability of concordance value and spot mean standard weighted deviation (MSWD) (generated within the concordia plot), and probability density plots and weighted average plots (using the estimated/calculated $^{206}\text{Pb}/^{238}\text{U}$ ages and the associated 1σ errors of concordant analyses with a probability of concordance of $> 5.0\%$, and no outliers).

No correction was made for common lead (i.e. non-radiogenic lead). Košler and Sylvester (2003) cite studies in which zircons from a wide range of rocks were sampled and were found to contain little common lead, and the correction for it always proved insignificant.

4.3 Petrography of zircons

The zircons that were prepared for U-Pb dating were classified prior to dating by colour and morphology (where possible).

All the zircon crystals observed in this study were from the common pink series (Garver & Kamp 2002). The proportion of each colour in each sample was variable (Fig. 4.3). Colourless, light pink and pink were observed. 52 % of all crystals ablated were classified as light pink, 29 % as pink and 19 % as colourless. Three particularly dark coloured ones were observed in the Owharoa Ignimbrite and were described as “rusty”.

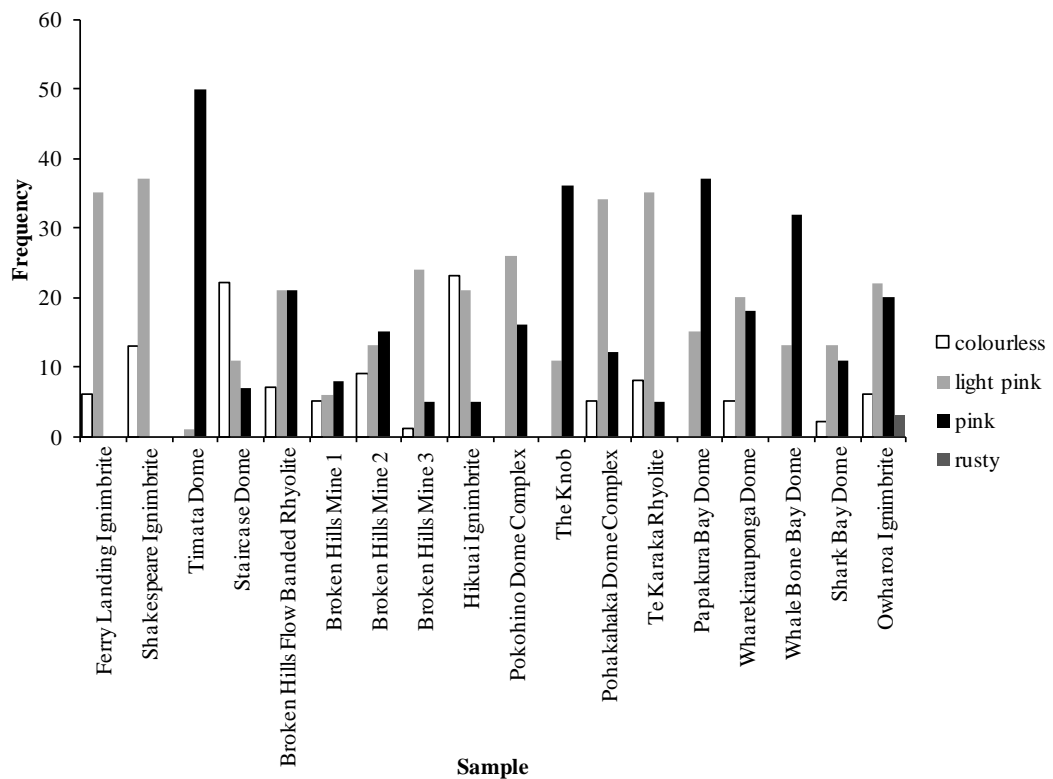


Fig. 4.3: Colour of zircon crystals that were ablated by LA-ICP-MS.

The original morphology of zircon crystals can be difficult to identify as they may be broken or rounded. In three samples, the original morphology of more than half of the crystals in each could not be documented. However, wherever possible, the primary crystal morphology was still recorded, and where this was not possible, was noted as “unidentified”. Hoskin and Schaltegger (2003) state that igneous zircon that has crystallised rapidly can have high width-to-length ratios (up to 1:12); the length of some crystals may have attributed to them breaking. Also, zircons in igneous rocks may become rounded by magmatic resorption (Deer *et al.* 1992). Fig. 4.4 shows the percentage of each morphological type that was observed in each sample. Only P and S types were observed, with P2 being the overall dominant morphology.

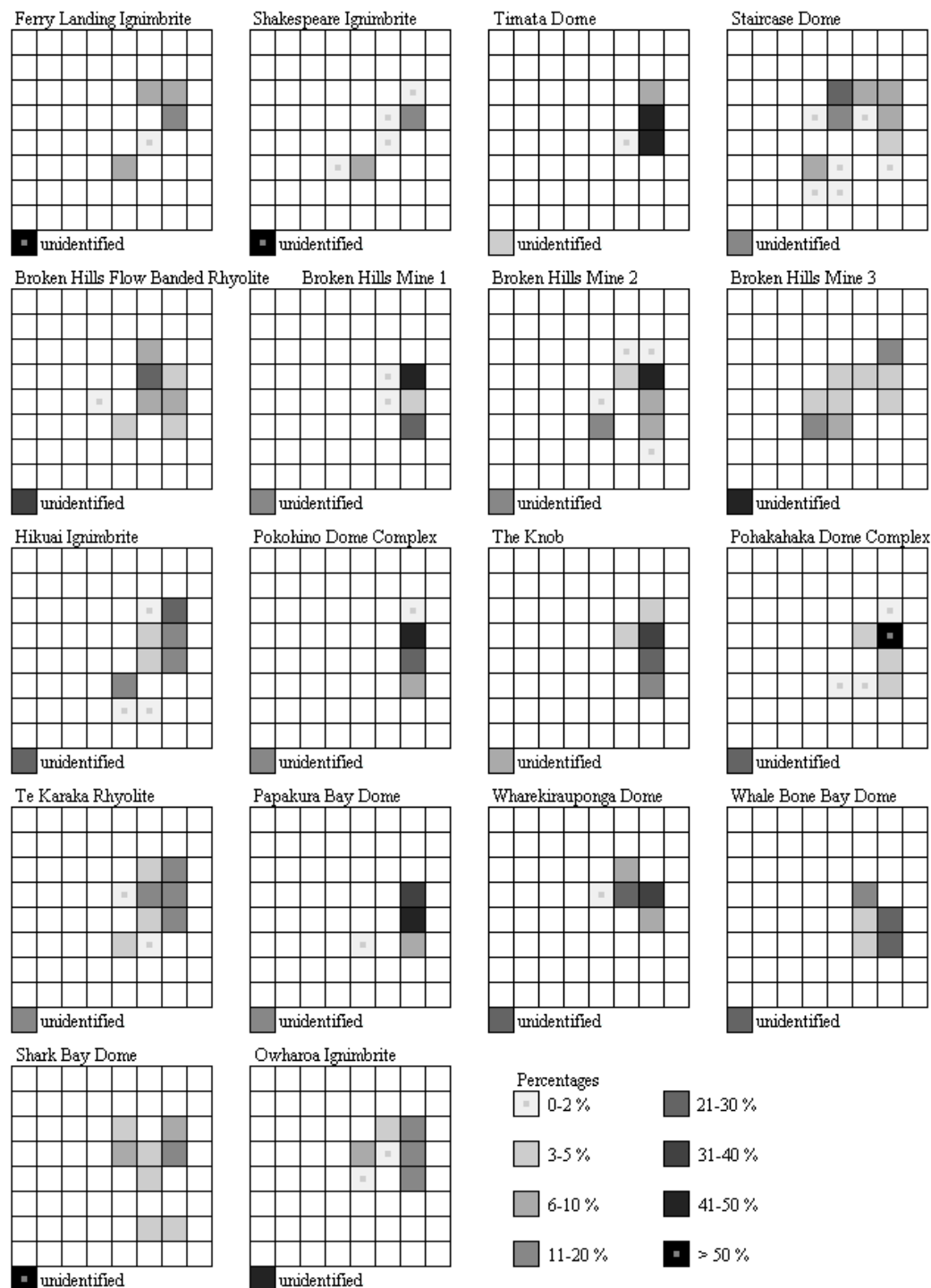


Fig. 4.4: Morphology of crystals that were ablated and the percentage of each present. Based on Pupin's (1980) classification (Fig. 4.1).

4.4 Results

4.4.1 U-Pb ages

The age of crystallisation has thus been determined for the following 18 samples (Table 4.2). This age represents the age of crystallisation for primary magmatic material and is therefore a maximum eruption age (Wilson *et al.* 2008). A

summary of the isotope ratios, age estimates, calculated ages, probability of concordance, spot MSWD and 1σ errors is in Appendix VIII.

Table 4.2: U-Pb ages (My, 1σ errors) for samples dated in this study, listed north to south.

Sample	Age (My)
Ferry Landing Ignimbrite	8.20 ± 0.25
Shakespeare Ignimbrite	5.80 ± 0.81
Timata Dome	6.75 ± 0.40
Staircase Dome	6.43 ± 0.08
Broken Hills Flow Banded Rhyolite	5.94 ± 0.21
Broken Hills Mine sample 1	5.98 ± 0.42
Broken Hills Mine sample 2	6.32 ± 0.11
Broken Hills Mine sample 3	6.61 ± 0.26
Hikuai Ignimbrite	6.80 ± 0.60
Pokohino Dome Complex	5.77 ± 0.33
The Knob	4.44 ± 0.22
Pohakahaka Dome Complex	4.71 ± 0.11
Te Karaka Rhyolite	4.10 ± 0.06
Papakura Bay Dome	5.51 ± 0.23
Maratoto Rhyolite – Wharekirauponga Dome	6.34 ± 0.27
Homunga Rhyolite – Whale Bone Bay Dome	5.58 ± 0.21
Homunga Rhyolite – Shark Bay Dome	4.85 ± 0.36
Owharoa Ignimbrite	3.76 ± 0.05

4.4.2 Inherited zircons

Most of the samples dated contained zircons that pre-date the determined age of crystallisation. These are shown as concordia and probability density plots in Appendix IX. Older zircons may be incorporated into the magma if the magma is derived by partial melting of the crust or assimilates crustal material (Dickin 2005).

Some of these zircons are within error of when rhyolitic volcanism began in the CVZ (c. 12 Ma in the Middle Miocene (Carter *et al.* 2003)) so are most likely to be antecrusts, a crystal that is derived from the same magma chamber but crystallised prior to the most recent eruption or in a previous eruption cycle (Charlier *et al.* 2005; Saunders *et al.* 2010; Folkes *et al.* 2011). The Staircase Dome appears to have had two significant crystallisation and/or eruption events. These zircons of Middle Miocene and younger age could also be derived from

rhyolite lithics within ignimbrites. It is, however, not possible to determine the exact origin of these crystals.

Some samples had zircons that gave ages that pre-date the CVZ, i.e. Late Cretaceous to Early Miocene (78.2-19.5 My). Their potential origin will be discussed in Chapter 5.

The oldest zircons in this study produced Late Jurassic to Cretaceous ages (> 93.8 My), and they are interpreted to be inherited from the Mesozoic basement. It is common for some rhyolites to contain basement-derived zircons (e.g. Unit G rhyolite from Taupo caldera (Charlier *et al.* 2005)). Fossils have been found in the sedimentary basement of the CVZ from the Puaroan Stage (Latest Jurassic, 148.5-145.5 My, Skinner 1993), but these were in clasts in conglomerate, so represent a maximum age for the enclosing sediments.

Chapter 5

Discussion

5.1 Introduction

In this chapter the results obtained in this study will be discussed and compared to previous studies, with particular reference to mineralogy, petrochemistry, U-Pb age data and the TVZ.

5.2 Mineralogy and petrochemistry

5.2.1 K₂O vs. SiO₂

The CVZ volcanic rocks, particularly dacites and rhyolites, have a high-K composition. This differs from TVZ volcanics which typically have medium-K compositions (Fig. 5.1). The rhyolites and ignimbrites in this study are all medium- and high-K rhyolites, with the exception of Te Karaka Rhyolite which is a low-K rhyolite. This range in K₂O wt % is comparable to other CVZ rhyolites.

5.2.2 Hydrothermal alteration

Hydrothermal alteration is the mineralogical, textural and chemical response of rocks in a changing thermal and chemical environment by the presence of hot water, steam or gas (Henley & Ellis 1983). Geothermal systems and fossil ore-forming hydrothermal systems are often associated with caldera structures, such as in the CVZ, TVZ and Yellowstone (U.S.A) (Henley & Ellis 1983). Hydrothermal alteration took place episodically throughout the CVZ from at least 10 Ma until the Late Pliocene/Early Pleistocene (Christie *et al.* 2006a; Rabone 2006b).

The rhyolite lava samples in this study were divided into slightly altered and intensively altered. They were initially classified based on petrographic observations and mineral assemblages. XRF analysis further confirmed if a sample had been hydrothermally altered or not. Samples with an SiO₂ content of at least 76-78 wt % are hydrothermally altered, although not all those that had previously been identified as altered had such high SiO₂. Broken Hills Mine

Sample 2 had the lowest value of all the samples in this study of 72.36 wt %. Even some samples that were not considered altered had very high SiO₂, i.e. Ferry Landing and Owharoa ignimbrites.

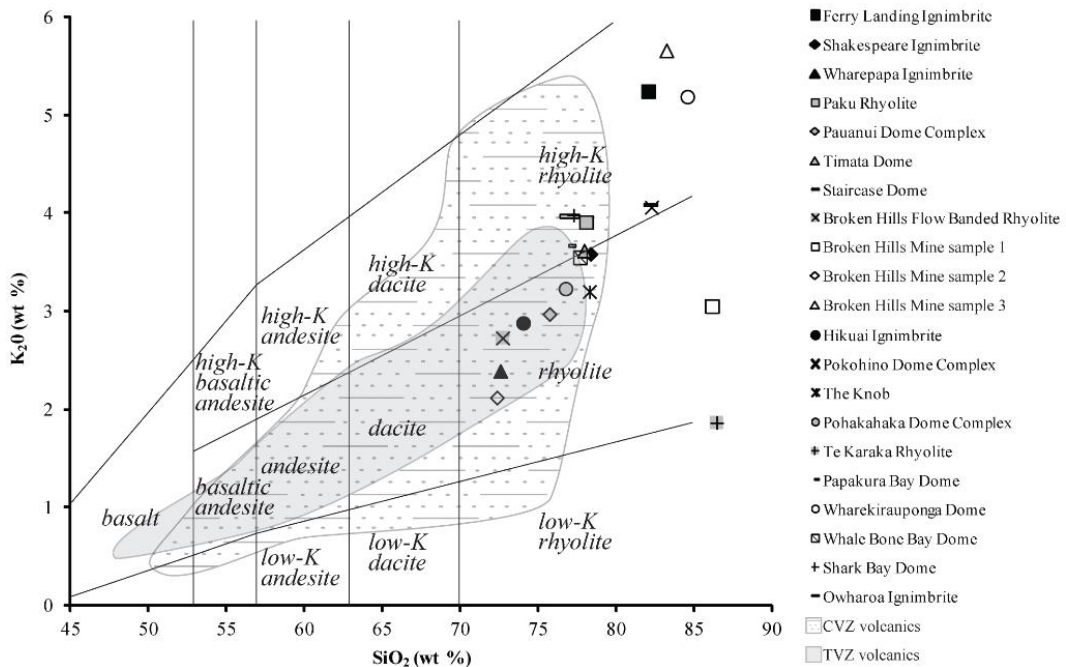


Fig. 5.1: Plot of K₂O vs. SiO₂ of all samples in this study. Shaded areas show the range of compositions of CVZ and TVZ volcanics for comparison. After Briggs (2004).

Other geochemical features indicated whether samples were altered or not. Arsenic and Sb generally increase with hydrothermal alteration and may indicate the occurrence of Au-Ag mineralisation (Henley & Ellis 1983). In this study it was found that the intensively altered lavas, except for Whale Bone Bay Dome, could be separated from those that were not altered by using As vs. SiO₂ and Sb vs. SiO₂. Aldrich (1995) and Fitzgerald (2004) also found that As increased with increasing hydrothermal alteration in the Pokohino Dome Complex and Ohui region respectively. They also noted that As was not always associated with high grade Au-Ag mineralisation and could occur in the outer weakly altered propylitic zone, and alternatively rocks could be intensely altered but have low As values.

The TVZ also has areas of hydrothermal alteration with at least 20 active systems and some relatively recent fossil systems (Grieve *et al.* 2006). It has been known since the 1930s that there is Au-Ag mineralisation in the TVZ, but exploration and detailed investigations only began in the late 1960s (Simmons *et al.* 2006). There has been no mining of precious metals in the TVZ to date (Grieve *et al.* 2006).

Studies of TVZ geothermal systems in the 1980s led to new conceptual models on epithermal mineralisation, e.g. Henley & Ellis (1983).

5.2.3 Petrography and petrochemistry of Broken Hills Rhyolite

The three samples from Broken Hills Mine are hydrothermally altered and produced very similar XRD traces indicating the presence of quartz and possibly illite, chlorite and plagioclase. Samples 1 and 2 contain an unidentified euhedral hexagonal mineral (? tridymite) that is coated in an orange-brown material of varying thickness and is assumed to be an alteration product (Fig. 2.5 F). Samples 1, 2 and 3 also contain “ghosts” of spherulites that are now mostly crystalline quartz, having been hydrothermally altered. Samples 2 and 3 contain a network of quartz veins, and also plagioclase crystals that have been entirely altered and are now fine-grained sericite. Sample 3 contains illite, as wisps and thin veins, which is evidence of hydrothermal alteration. Sample 3 contains pyrite, as observed in the heavy mineral fraction when picking for zircons and by the high S content (4704 ppm).

On the other hand, Broken Hills Flow Banded Rhyolite appears to be only slightly altered. It contains pyrite and oxidised biotite. The Broken Hills Flow Banded Rhyolite also produced a very similar XRD trace to the samples from the mine, indicating the presence of quartz, plagioclase and possibly illite.

The four samples of Broken Hills Rhyolite each have different features in hand specimen including flow banding, vesicularity and alteration. Broken Hills Flow Banded Rhyolite has laminar flow banding. Sample 1 has the finest banding of the altered samples. Sample 2 is very vesicular and is called the “bubbly” rhyolite by the miners. Sample 1 and 3 appear to be more silicified than sample 2 and the Broken Hills Flow Banded Rhyolite, based on their SiO₂ wt % (86.15, 83.24 and 72.36, 72.72 respectively).

Based on the above observations, all four samples of Broken Hills Rhyolite are considered to be the same lava, but have experienced different degrees of post-depositional alteration.

5.3 U-Pb dating of zircons

5.3.1 Results from this study

Volcanism in the CVZ has migrated southwards over time (Brothers 1984; Skinner 1986; Adams *et al.* 1994). This is also shown in the samples dated in this study but it is not a simple systematic progression. Fig. 5.2 and Fig. 5.3 show a general trend of younging from north to south throughout the study area. Shakespeare Ignimbrite, Te Karaka Rhyolite and Wharekirauponga Dome do not quite follow the systematic younging to the south. This is probably because they originated from centres that were active for a long time, e.g. the Whitianga Volcanic Centre which was active for c. 3 My (Adams *et al.* 1994), and the Kapowai Caldera Complex which was active for 3.6 My (Krippner 2000).

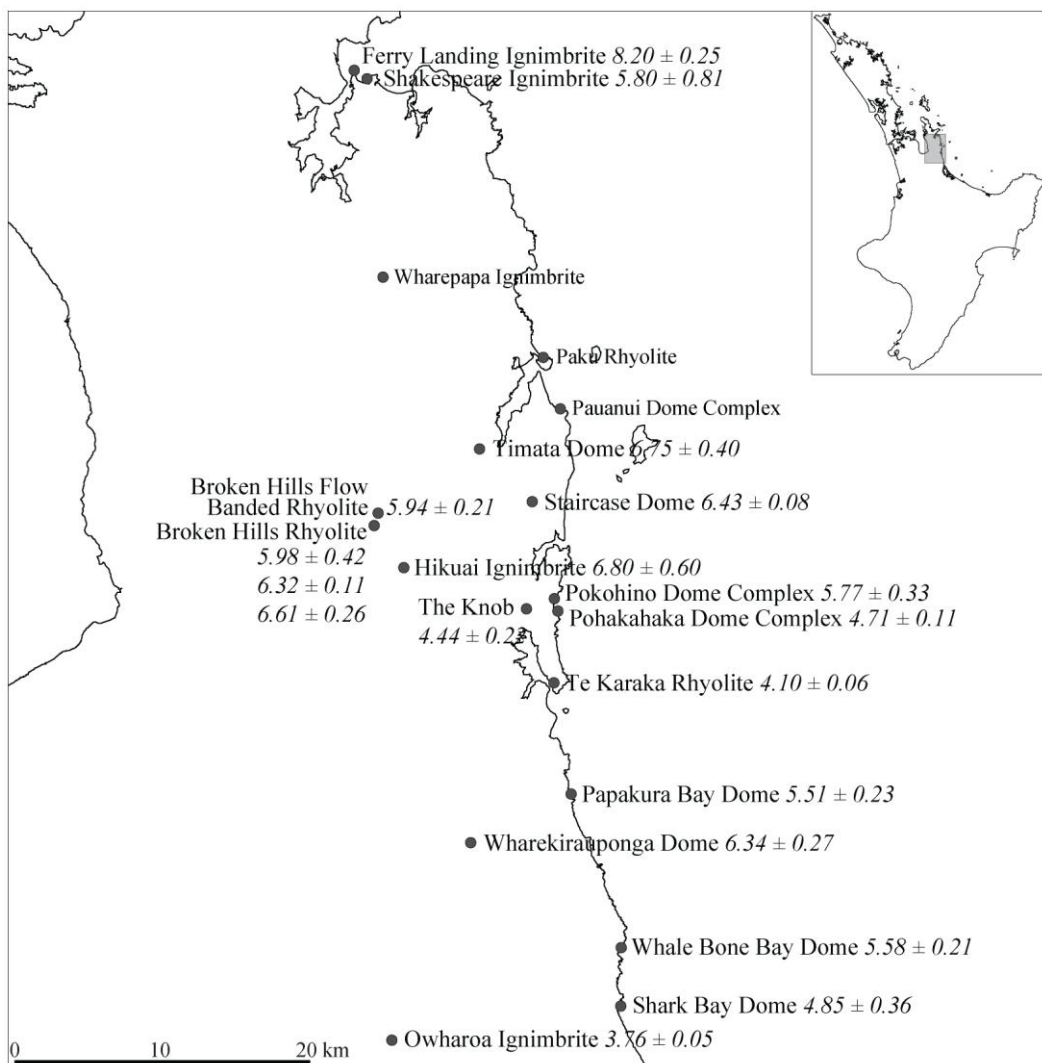


Fig. 5.2: Map of the central Eastern CVZ and the samples that were dated in this study. Ages are in millions of years, errors are 1σ . No age data was obtained in this study for Wharepapa Ignimbrite, Paku Rhyolite or Pauanui Dome Complex.

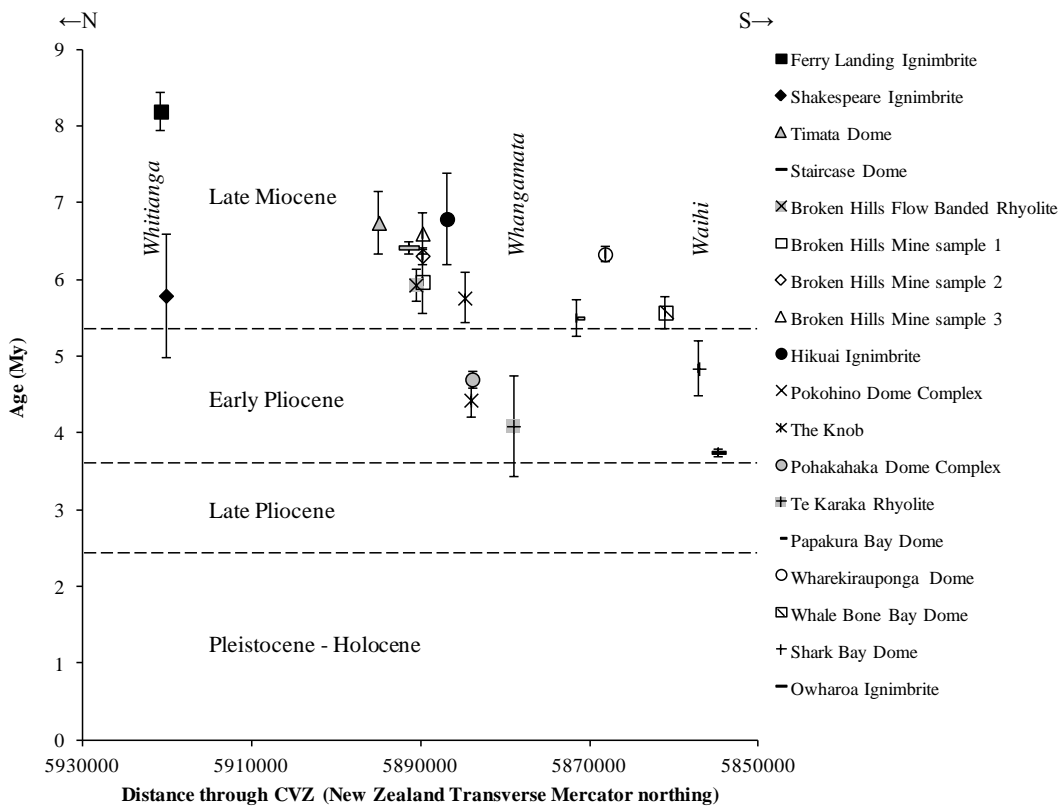


Fig. 5.3: Age of CVZ volcanics dated in this study, with respect to location from north to south. Errors are 1σ .

Hydrothermal alteration of samples in this study took place sporadically from 6.32 ± 0.06 Ma (Ward *et al.* 2005) at Wharekirauponga Dome until after the formation of The Knob (4.44 ± 0.22 Ma). This is within the age range that has previously been determined for mineralisation in the Hauraki Goldfield, i.e. from at least 10 Ma in the northern Coromandel Peninsula (Christie *et al.* 2006a) until the Late Pliocene to Early Pleistocene near Te Puke (Rabone 2006b).

5.3.2 Errors and uncertainties

It is common practice to cite 2σ errors when generating radiometric ages. However this was not done in this study. The data output from GLITTER is by default 1σ so this is the way it was treated in Isoplot.

The number of crystals that each age determination was based on varies between samples. The number of crystals used was constrained by the size of the initial population that was obtained from each sample. After ablation, some analyses were omitted because the isotope ratios were discordant, which in some cases was up to about half the ablated population. The probability of concordance of some samples (especially for inherited zircons which may only be based on one or two crystals) is very small, but the cited ages were supported by probability density

plots and weighted average plots. If a larger population had been ablated, the errors could be smaller, and the older zircons may be better represented with a greater confidence of their accuracy.

5.3.3 Comparison with previous studies

Only eight of the samples dated in this study have previously been dated. The ages from previous studies are presented in Table 5.1. They are minimum eruption age estimates, except for the Ar-Ar ages which are ages of mineralisation of adularia.

Table 5.1: Ages (My) from samples dated in this study with comparison to previous age estimates. Errors are 1σ for this study.

	This study	Previous studies	Method ¹
Ferry Landing Ignimbrite	8.20 ± 0.25		
Shakespeare Ignimbrite	5.80 ± 0.81	5.9 ± 0.7^2	FT zircon
Timata Dome	6.75 ± 0.40		
Staircase Dome	6.43 ± 0.08		
Broken Hills Flow Banded Rhyolite	5.94 ± 0.21		
Broken Hills Mine – sample 1	5.98 ± 0.42	7.12 ± 0.01^3	Ar-Ar adularia
Broken Hills Mine – sample 2	6.32 ± 0.11	“	“
Broken Hills Mine – sample 3	6.61 ± 0.26	“	“
Hikuai Ignimbrite	6.80 ± 0.60		
Pokohino Dome Complex	5.77 ± 0.33		
The Knob	4.44 ± 0.22		
Pohakahaka Dome Complex	4.71 ± 0.11	7.21 ± 0.84^4	FT obsidian
Te Karaka Rhyolite	4.10 ± 0.06	4.87 ± 0.11^5	K-Ar plagioclase
Papakura Bay Dome	5.51 ± 0.23	5.45 ± 0.15^5	K-Ar plagioclase
Wharekirauponga Dome	6.34 ± 0.27	6.32 ± 0.06^3	Ar-Ar adularia
Whale Bone Bay Dome	5.58 ± 0.21	5.51 ± 0.20^6	K-Ar
Shark Bay Dome	4.85 ± 0.36		
Owharoa Ignimbrite	3.76 ± 0.05	3.69 ± 0.07^7 2.89 ± 0.38^8	U-Pb zircon FT glass shard

¹ FT = fission track

² Weighted mean of four ages of Pumpkin Rock Ignimbrite, Adams *et al.* 1994

³ Ward *et al.* 2005

⁴ Seward & Moore 1987

⁵ Takagi 1995

⁶ Brathwaite & Christie 1996

⁷ Hoskin *et al.* 1998

⁸ Kohn 1973

The Ferry Landing Ignimbrite has not previously been dated, but was deduced by Fisher (1986) to be older than the Shakespeare Ignimbrite which overlies it. It also occurs as lithics in other younger ignimbrites which overlie it (Bardebes 1997).

The age of the Shakespeare Ignimbrite determined in this study is within error of the previous age of Adams *et al.* (1994), for the Pumpkin Rock Ignimbrite. The location that the sample in this study was taken from has been mapped by Skinner (1995) as Pumpkin Rock Ignimbrite (see section 1.5).

The Timata Dome (6.75 ± 0.40 My) is part of the Ruahine Rhyolite which has an age of 7.7-8.1 My (Adams *et al.* 1994). Given the new age determined here, the age range of the Ruahine Rhyolite is now 6.75-8.1 My.

As previously concluded (section 5.2.3), the four samples from the Broken Hills Rhyolite are considered to be the same lava. It was therefore expected that the four ages determined would be within 1σ error of each other, but they show a wider range. If, however, they had been calculated with 2σ errors, rather than 1σ , the ages probably would be within error. Ward & Wilson (1978) proposed a calculation for comparing and combining radiocarbon age determinations. This calculation assumes that the samples are from the same “object”:

$$T = 4.96; \chi^2_{3:0.05} = 7.81$$

where $3 = \text{number of samples} - 1$, and confidence interval = 95 %. To prove that the samples are statistically from the same object when the χ^2 test is applied, the result, or T-statistic, must be less than 7.81. When applied to the four ages determined here, the T-statistic is 4.96, which indicates that they are all from the same object.

When all of the concordant isotopic ratios that were used to determine the individual ages of the four samples are plotted together, they give a concordant age of 6.27 ± 0.09 My (MSWD of concordance = 0.49, probability of concordance = 48 %). This is the age that will be cited hereafter for Broken Hills Rhyolite.

In a study of mineralised deposits of the Hauraki Goldfield by Ward *et al.* (2005), an ^{40}Ar - ^{39}Ar age of adularia mineralisation of 7.12 ± 0.01 My was determined based on two adularia crystals from Night Reef, Broken Hills Mine. Adularia is a product of hydrothermal alteration and therefore should have a younger age than the age of the host rock. This is clearly not the case here with the eruption age

being 6.27 ± 0.09 My. Ward *et al.*'s (2005) age is here considered to be unreliable. Determining Ar-Ar ages by dating adularia can be difficult for a number of reasons:

- Separating pure adularia can be difficult, as it usually makes up such a small component of the sample. In this study it could not be identified by XRD analysis.
- In very young systems excess Ar can cause problems for accurate age calculations (Skinner 1986; Allègre 2008).

Mineralisation would also have to be younger than the Hikuai Ignimbrite (6.8 ± 0.60 My), as it has been hydrothermally altered in its western extent in the region of Broken Hills Mine (McGunnigle 1995), provided that this is the same hydrothermal system.

The Pohakahaka Dome Complex at Whitipirorua Point was dated by fission track on obsidian as 7.21 ± 0.84 My (Seward & Moore 1987). This is older than the age determined in this study of 4.71 ± 0.11 My. The earlier age is now considered to be unreliable because apparent fission track age can increase rapidly with temperature (Dickin 2005).

The Te Karaka Rhyolite was dated here as 4.10 ± 0.06 My. A rhyolite on the east of the peninsula was dated by K-Ar at 4.87 ± 0.11 My (Takagi 1995). Based on the similar petrography of both samples, these two rhyolites are most likely the same dome, even though the ages are not within error. The ages possibly would be within error had the age in this study been calculated to 2σ .

Papakura Bay Dome has previously been dated by K-Ar at 5.45 ± 0.15 My (Takagi 1995) which is within error of 5.51 ± 0.23 My as determined in this study.

The mineralisation of Wharekirauponga Dome was dated by Ar-Ar on adularia at 6.32 ± 0.06 My (Ward *et al.* 2005), which is appropriately younger than the age of eruption determined in this study (6.34 ± 0.27 My).

Two domes of the Homunga Rhyolite have previously been dated (Brathwaite & Christie 1996). The Ruahorehore Dome has a K-Ar age of 5.29 ± 0.14 My. The

Whale Bone Bay Dome was dated as 5.51 ± 0.20 My, which is within error of the age determined in this study (5.58 ± 0.21 My). The Shark Bay Dome has not previously been dated.

The Owharoa Ignimbrite was first dated by fission track on a glass shard with an age of 2.89 ± 0.38 My (Kohn 1973). It was next dated by U-Pb dating of zircon by SIMS on the SHRIMP ion microprobe at the Australian National University with an age of 3.69 ± 0.07 My (Hoskin *et al.* 1998). The earlier age was then disregarded because the partial fading and annealing of fission tracks in volcanic glass can give a lower apparent age (Westgate 1989; Hoskin *et al.* 1998; Briggs *et al.* 2005). Partial fading of fission tracks in natural glass can occur at surface temperatures when exposed to the sun (Wagner & van den Haute 1992). This later age is within error of that determined in this study (3.76 ± 0.05 My).

The main objective of this study was to generate new ages, while also testing the feasibility of U-Pb dating of zircon using LA-ICP-MS for CVZ rocks. The fact that the existing ages mostly agree with the new ones is supportive of the validity of the U-Pb method, and therefore supports the validity of the samples that have not previously been dated.

The Wharepapa Ignimbrite, Paku Rhyolite and Pauanui Dome Complex could not be dated in this study as an insufficient quantity of zircons was separated from each sample. The Wharepapa Ignimbrite has previously been dated by fission track of zircon as 8.2 ± 0.7 and 9.2 ± 1.9 My (Adams *et al.* 1994). It was also dated by K-Ar on plagioclase with a mean age of 5.78 ± 0.3 My (Krippner 2000). Krippner (2000) questioned whether the locations sampled by Adams *et al.* (1994) were the same unit as defined by him, and it had possibly been hydrothermally altered. Rutherford (1978) attempted to date the Paku Rhyolite by fission track on obsidian, however the obsidian was found to be of an inappropriate standard and the estimated age considered unreliable.

5.3.4 Age of CVZ volcanics

Volcanism began in the CVZ c. 18 Ma in the late-Early Miocene. The earliest recorded rhyolite volcanism of the CVZ has an age of c. 12 Ma and is from an offshore tephra layer with an indistinguishable source (Carter *et al.* 2003). This age precedes the earliest onshore record of rhyolitic volcanism by 1.6-1 My.

Rhyolitic volcanism continued into the Early Pleistocene in the Tauranga and Kaimai Volcanic Centres, terminating with the Papamoa Ignimbrite 1.9 Ma (Briggs *et al.* 2005). The earliest eruption from the TVZ was 1.55 Ma from the Mangakino Volcanic Centre (Houghton *et al.* 1995). This period of transition includes significant events in the volcano-tectonic history of New Zealand, including commencement of volcanism of the Kermadec Arc, development of the Hauraki Rift, and an increase in the frequency and volume of silicic volcanic activity in the TVZ (Briggs *et al.* 2005). Fig. 5.4 and Fig. 5.5 show how the volcanics progressively young towards the south in the CVZ.

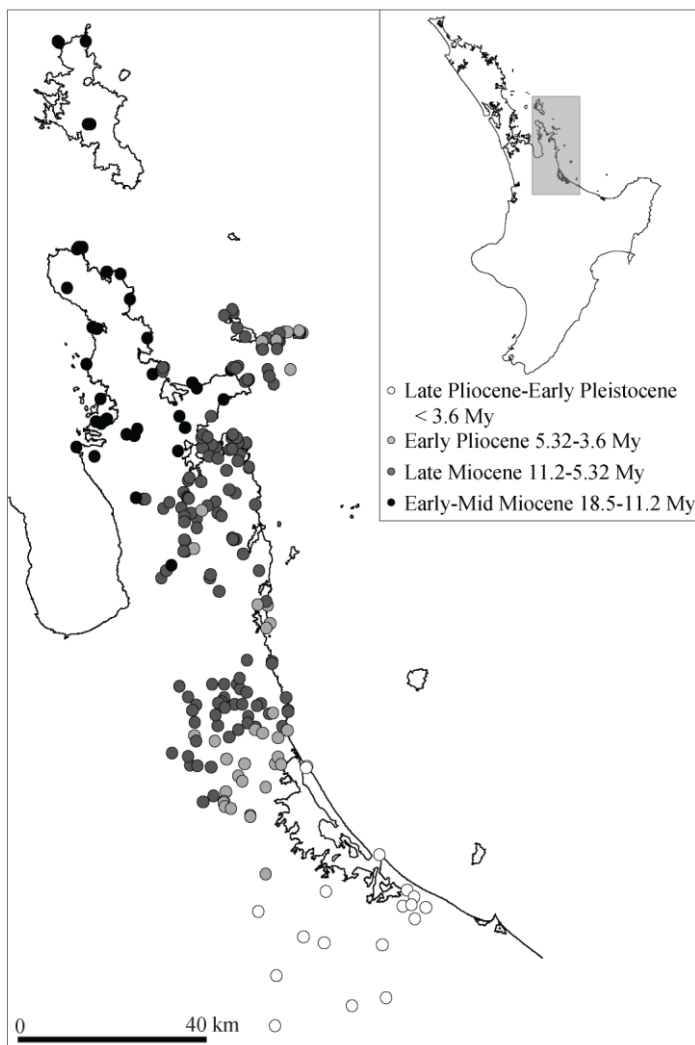


Fig. 5.4: Map of the igneous rocks of the CVZ that have been dated using all available data. Data are from Seward & Moore (1987), Adams *et al.* (1994), Takagi (1995), Brathwaite & Christie (1996), Krippner (2000), Briggs *et al.* (2005), and this study (see Appendix X).

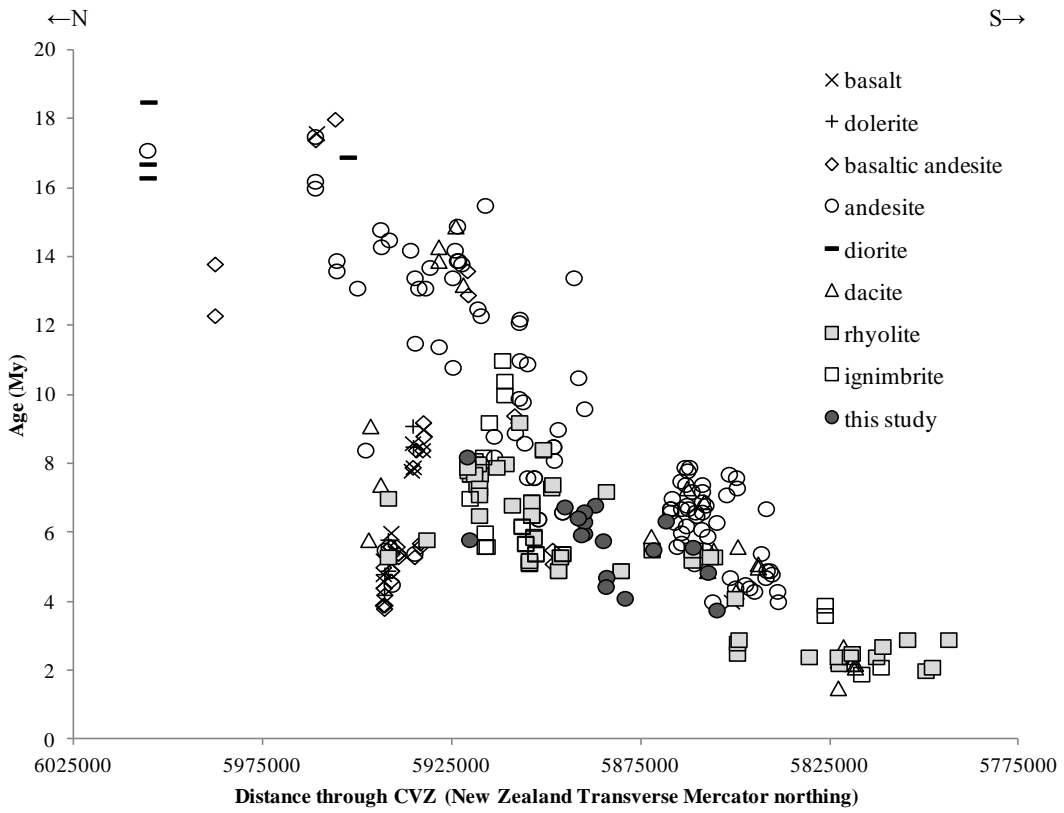


Fig. 5.5: Age versus distance through the CVZ of the igneous rocks of the CVZ that have been dated using all available data. Data are from Seward & Moore (1987), Adams *et al.* (1994), Takagi (1995), Brathwaite & Christie (1996), Krippner (2000), Briggs *et al.* (2005), and this study (see Appendix X).

5.3.5 Silicic centres of the CVZ

There are currently 10 identified silicic centres of the CVZ (Fig. 1.2). There may well be additional centres, which are perhaps buried by overlying deposits or are offshore (Briggs & Krippner 2006). Fig. 5.6 shows a summary of age data for these centres. Samples from this study fit within the ages that have already been determined, except for the Whitianga Volcanic Centre (WVC). The previous youngest age was c. 7.5 My, and after having dated the Shakespeare Ignimbrite in this study, which is assumed to originate from the WVC, the new time span of the WVC is c. 8.7-5.8 My. This time span is comparable to the Kapowai Caldera Complex (KCC, 8.5-4.9 My) (Krippner 2000). There was a marked increase in tephra thicknesses at the offshore site while the WVC and KCC were active, and even more so when the TVZ became active; the latter reflects the greater volumes of material erupted from TVZ centres.

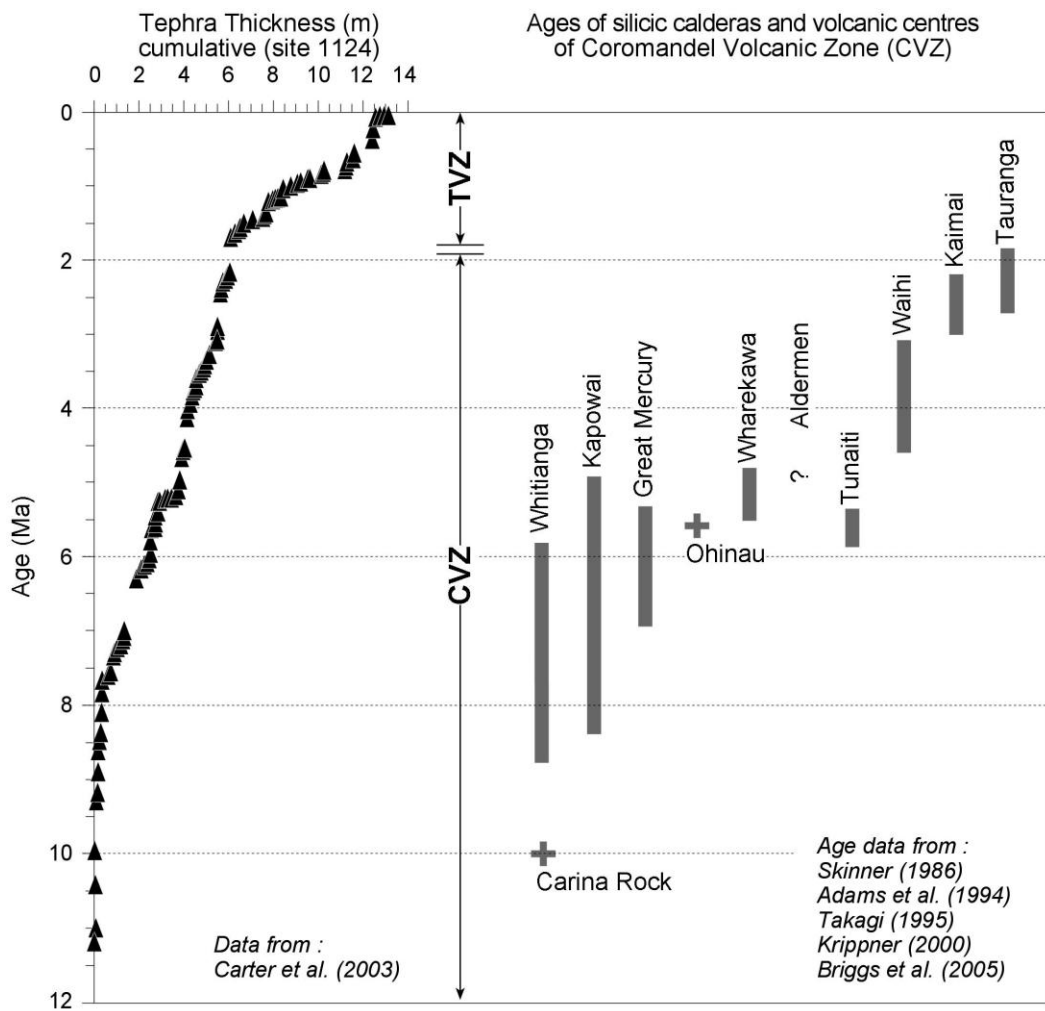


Fig. 5.6: Tephra thickness at offshore site 1124 (Carter *et al.* 2003), including tephras from both CVZ and TVZ, and age of silicic centres in the CVZ. After Briggs (2004). Note that there is currently no age data for silicic rocks of Great Barrier Island and the Aldermen Islands. Duration of Whitianga Volcanic Centre modified after this study.

5.3.6 Origin of inherited zircons

As described in section 04.4.2, most of the samples dated contained zircons that significantly predated the determined age of crystallisation. The potential origin of zircons that produced ages older than the CVZ but younger than the basement, that is Late Cretaceous to Early Miocene (78.2-19.5 My), will be discussed here.

Volcanism occurred in the South Island and offshore southern islands from c. 100 Ma (Graham 2008) (Fig. 5.7). Due to its distal location, this does not seem like a possible source for zircons. There are also only a few cases of silicic volcanism, which is where zircons are more likely to be found. The only volcanism in the North Island that pre-dates the CVZ was in the Northland Volcanic Arc, which was active from c. 23-15 Ma when the Pacific Plate began to subduct beneath the

Australian Plate (Cole *et al.* 2008). The Northland Volcanic Arc produced mainly andesite stratovolcanoes, with minor basalt and rhyolite, so this is a potential source for zircons, provided they had the means to be incorporated into the CVZ volcanics.

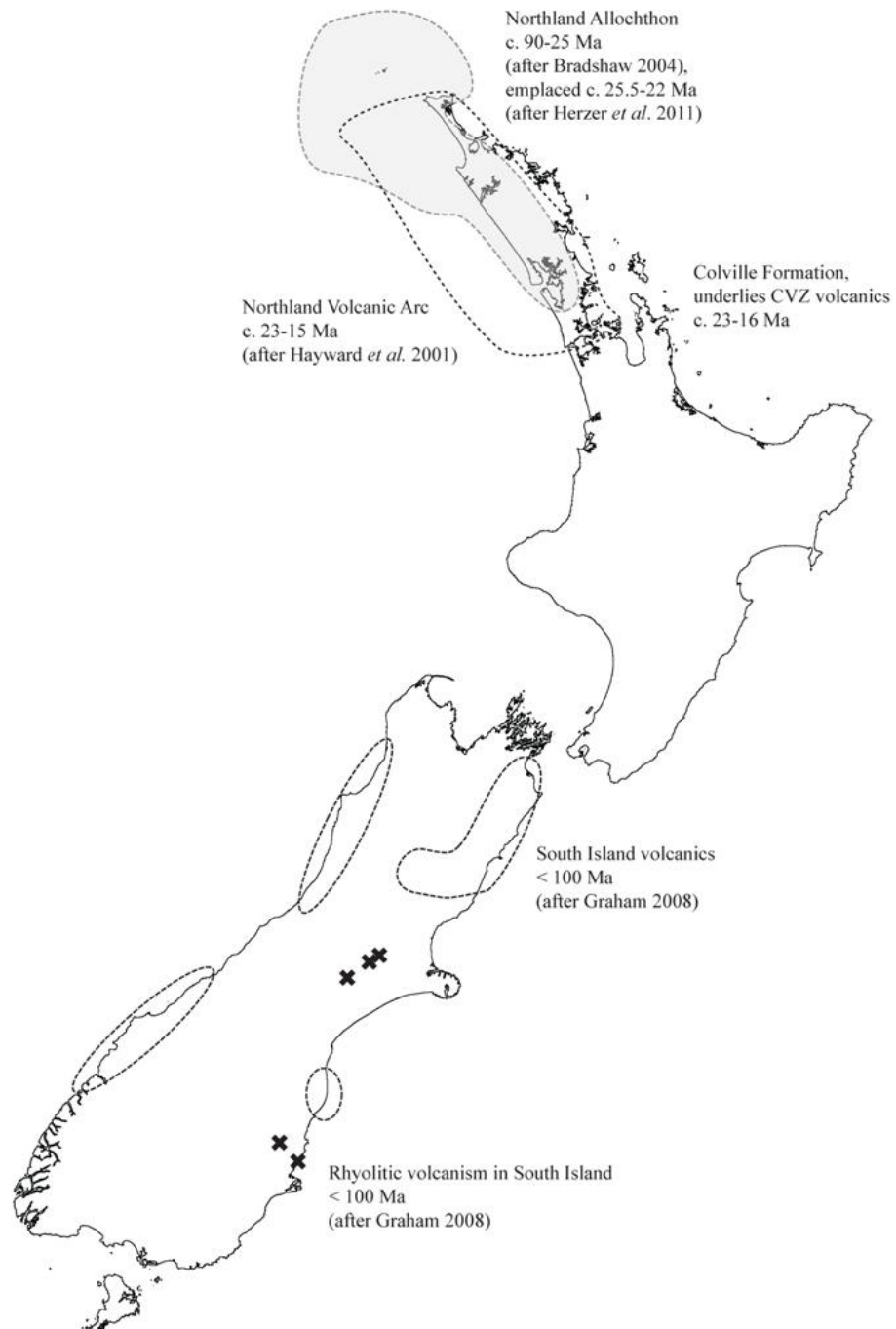


Fig. 5.7: Locations in New Zealand where inherited zircons of Late Cretaceous to Early Miocene age could have originated.

The basement of the CVZ is overlain by Oligocene and Early Miocene sediments (Skinner 1986). The Early Miocene Colville Formation (of the Waitemata Group), a volcaniclastic mass flow from the northwest of the CVZ, precedes the oldest exposed volcanic rocks of the CVZ. It contains material from the Northland Volcanic Arc, and given the direction it travelled from, is a possible mechanism for transporting zircons that gave Early Miocene ages, provided that the minor rhyolites were incorporated into the mass flow.

The Northland Allochthon, a massive gravity deposit covering much of Northland and the continental shelf, was emplaced c. 25.5-22 Ma (Herzer *et al.* 2011) prior to the commencement of the Northland Volcanic Arc. The allochthon came from an area to the north of New Zealand and includes marine sediments and the Tangihua Volcanics (Ballance & Spörli 1979). It contains fossils that indicate some of its rocks were part of the continental slope and deep-ocean floor 90-25 Ma (Herzer 2008). The allochthon may have also contained zircons, and was possibly included in the Colville Formation. This is a potential source for the zircons that gave Late Cretaceous to Early Miocene ages.

5.3.7 Physical properties of zircons

The colour of each crystal that was ablated was noted and they are plotted in Fig. 5.8 by location. There does not appear to be any relationship between colour and age or location. Crystals of all colours were generally found in all locations. Neither does there appear to be a relationship between colour and whether the host rock is unaltered, hydrothermally altered, or an ignimbrite (Fig. 4.3).

There does not appear to be any relationship between zircon morphology and age or location. For example, the similarly aged Timata Dome and Hikuai Ignimbrite have a differing range in morphological types observed (Fig. 4.4). There does not appear to be any relationship between zircon morphology and whether the host rock is unaltered, hydrothermally altered, or an ignimbrite. For example, the three samples from Broken Hills Mine all exhibit different morphological types.

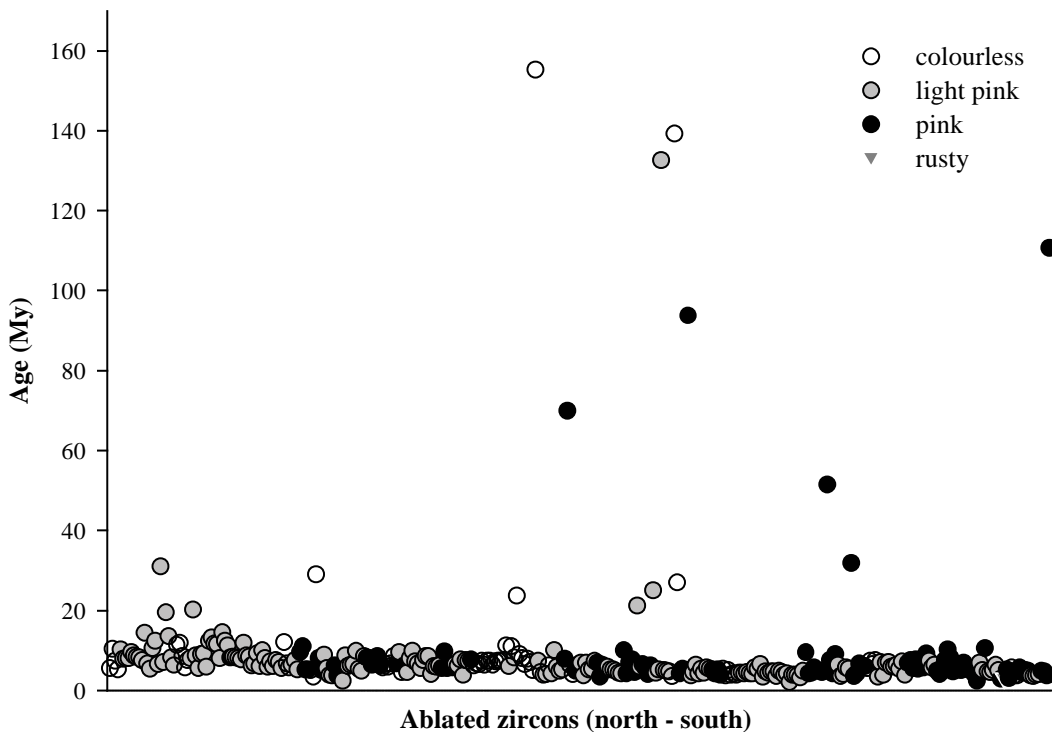


Fig. 5.8: Age of ablated zircons by location. Observed colour as indicated.

5.3.8 Comparison to the TVZ

The CVZ is considered to be the tectonic precursor to the TVZ (Adams *et al.* 1994). In this section some of the similarities and differences between the two zones will be discussed.

Major element abundances and average compositional ranges of onshore and offshore tephras of the CVZ and TVZ are very similar (Carter *et al.* 2003). Tephras from the two zones can be distinguished by dating of offshore drill-cores.

Rhyolitic volcanism in the TVZ began 1.55 Ma (Houghton *et al.* 1995). In the CVZ volcanism migrated to the southeast over time. There is no such trend in the TVZ (Fig. 5.9). TVZ volcanics are dominated by silicic volcanism. The proportion of mafic (basalt to andesite) to silicic volcanism (dacite to rhyolite) in the TVZ is about 5:95. CVZ has a greater volume of andesitic volcanism, and mafic versus silicic volcanism is approximately 40:60 (Briggs *et al.* 2005). Volcanism in the CVZ generally became more silicic with time and to the south; this has not been observed in the TVZ where the northeast and southwest ends of the zone are mostly andesitic-dacitic while the central TVZ is rhyolitic (Houghton *et al.* 1995). TVZ eruptions can be very large, producing 30 to $> 300 \text{ km}^3$ material, while CVZ eruptions were typically smaller at $< 30 \text{ km}^3$ (Briggs *et al.* 2005). This

is also reflected in the caldera sizes, which in the TVZ are typically c. 20 km diameter, and c. 8 km in the CVZ. Briggs *et al.* (2005) relate these differences to increased rates of subduction and crustal extension/thinning in the TVZ that have led to higher rates of silicic magma generation.

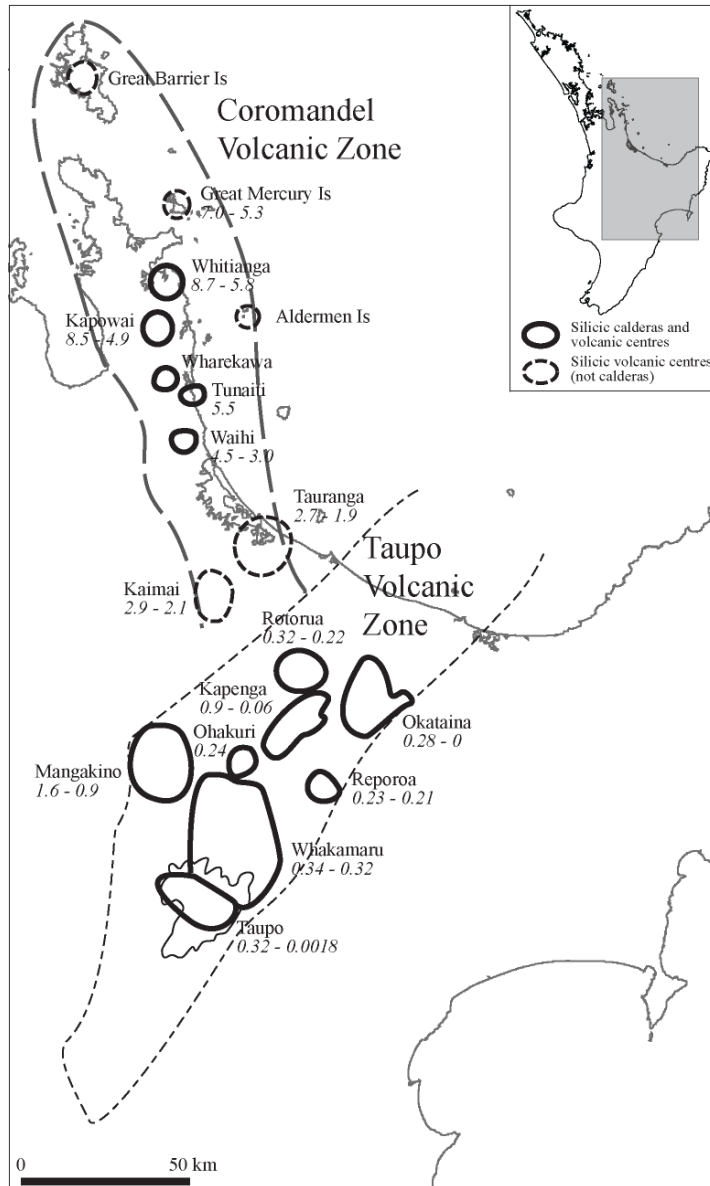


Fig. 5.9: Silicic centres and calderas of the CVZ and TVZ. The period that they were active for is indicated in millions of years where known. After Briggs *et al.* (2005) and this study.

More than one centre can be active at any given time. This is shown by the overlapping ages of the WVC and KCC in the CVZ. This is also seen today in the TVZ, where the Okataina and Taupo centres are both currently active. The length of time that centres of the CVZ were active for is contrasting to centres of the TVZ. For example, the WVC and KCC were active for c. 3 My and c. 3.6 My, respectively. The Mangakino Volcanic Centre of the TVZ was only active for 0.7

My from 1.6-0.9 Ma (Briggs *et al.* 2005) and is thought to now be extinct (Houghton *et al.* 1995). Longevity of silicic centres is thought to be related to rates of rifting and subduction, which are much higher in the TVZ than they were in the CVZ (Briggs 2004). The thickness of the crust in the TVZ is also much thinner than in the CVZ (c. 15 km vs. c. 25 km, Briggs 2004).

The Yellowstone system (U.S.A.) is often compared to the TVZ. It has been active for at least 2 My (Christiansen 2001), and possibly due to the thick, stable continental crust, will remain active for longer than the volcanic centres in TVZ. Its last eruption was c. 70 ka, and is still considered to be active (Christiansen 2001). Yellowstone has erupted a similar volume of material to the TVZ, but in only three major caldera forming events, unlike the TVZ which has had numerous, but smaller, caldera forming events from overlapping volcanic centres (Houghton *et al.* 1995).

Chapter 6

Summary and Conclusions

6.1 Introduction

The Coromandel Volcanic Zone is the easternmost part of the Hauraki Volcanic Region, New Zealand's longest lived region of andesite-dacite-rhyolite volcanism. The CVZ was active from c. 18 to 1.9 Ma, with silicic volcanism being dominant from c. 12 Ma throughout the central east and southern extent of the zone. 21 selected silicic volcanic rocks of the eastern CVZ were the subject of this study, with the presentation of new U-Pb ages being the main objective. Many of the intermediate volcanics of the CVZ have been dated (e.g. Adams *et al.* 1994, Takagi 1995, and Brathwaite & Christie 1996), but there are few ages on rhyolites. The U-Pb dating of zircon using LA-ICP-MS method has not been used for CVZ volcanics previously, so was used in this study to assess whether it is an appropriate method for dating CVZ volcanics. The physical properties of zircon, i.e. colour and morphology, were observed to see if there was any relationship between them and the age, location or host rock type. The petrographic, mineralogical and petrochemical properties of the 21 samples were also assessed in order to set the samples into a stratigraphic context.

6.2 Petrography, mineralogy and petrochemistry

The rocks of the eastern CVZ have been variably hydrothermally altered. The rhyolite lavas in this study were divided into slightly and intensively hydrothermally altered.

6.2.1 Slightly altered rhyolite lavas

Quartz is the dominant phenocryst in these lavas with common plagioclase and relict mafic minerals \pm biotite \pm Fe-Ti oxides \pm zircon. The groundmass is generally devitrified glass or crystalline SiO₂ polymorphs \pm feldspar. They are poorly to moderately porphyritic and have a range in textures that include vesicular, flow banded, spherulitic and glassy. These lavas range from low- to high-K rhyolites (72-86 wt % SiO₂), which is typical of CVZ rhyolites.

6.2.2 Intensively altered rhyolite lavas

Quartz is the dominant phenocryst in the intensively altered lavas. Altered plagioclase (now sericite-adularia) is common \pm relict mafics \pm biotite \pm Fe-Ti oxides \pm zircon. The groundmass is usually quartz + feldspar and is sometimes devitrified glass. They are poorly to moderately porphyritic and have a range in textures that include flow banded, vesicular, spherulitic and lithophysal. Some of these lavas have quartz veins which may be altered to chlorite-illite, both of which are evidence of hydrothermal alteration. They are medium- to high-K rhyolites (72-86 wt % SiO₂) and are typically enriched in As and Sb.

6.2.3 Ignimbrites

The five ignimbrites range from non- to densely-welded and jointed lenticulites. They also range in abundance of pumice, crystals and lithics. Pumice may be surrounded with clusters of phenocrysts or streaky and flattened so that it is obsidian-like. More than one pumice type may be present.

The matrices contain non-devitrified glass shards which are commonly platy and Y-shaped but also cuspatate and lunate. Plagioclase crystals are dominant in all the ignimbrites, with some having rare quartz \pm rare relict mafics \pm titanomagnetite/ilmenite \pm zircon. The Wharepapa Ignimbrite has minor orthopyroxene \pm augite, and the Owharoa Ignimbrite has biotite.

Lithics are sub-rounded to angular, 4 to 60 mm in diameter and a variety of types were observed, including: andesite, hydrothermally altered andesite, crystalline rhyolite, glassy/spherulitic/flow banded rhyolite, hydrothermally altered rhyolite and ignimbrite.

6.3 U-Pb dating

18 new U-Pb ages were generated by U-Pb dating of zircons by LA-ICP-MS. The zircons were assumed to be primary or magmatic zircons and represent the age of crystallisation of the zircon and are therefore a maximum eruption age. Three samples did not have sufficient zircons to be dated. The new ages from this study generally agree with any existing age estimates, so this supports the validity of the method and also supports the samples that do not have existing age estimates. These samples generally young north to south, which is consistent with what is already known about the geochronological evolution of the CVZ. They also fit

within the temporal evolution of silicic centres/calderas that they occur in, except for the Whitianga Volcanic Centre, the time span of which has here been extended.

Some samples contained zircons that were older than the age of eruption. These were inferred to be inherited from a range of sources given their different ages. The zircons that were of Middle Miocene and younger age are inferred to be antecrysts, crystals that crystallised in an earlier eruption or crystallisation event. They could also be from lithics in ignimbrites. Some zircons gave Late Cretaceous to Early Miocene ages which pre-date the CVZ and could possibly be from the Northland Volcanic Arc or the Northland Allochthon, both of which could have been transported by the Colville Formation, a volcaniclastic mass flow from the northwest of the CVZ. The oldest zircons found in this study were Late Jurassic to early-Late Cretaceous and are interpreted to be inherited from the Mesozoic basement. No relationship was found between zircon colour or morphology and age, location or host rock type.

References

- Adams, C. J., Graham, I. J., Seward, D. & Skinner, D. N. B. 1994, 'Geochronological and geochemical evolution of late Cenozoic volcanism in the Coromandel Peninsula, New Zealand', *New Zealand Journal of Geology and Geophysics*, vol. 37, no. 3, pp. 359-379.
- Adams, J. C. 1992, A Facies Approach to the Geology of the Hot Water Beach - Whenuakite Region, Coromandel Volcanic Zone, MSc Thesis, University of Waikato.
- Aldrich, S. M. 1995, Volcanic Geology and Hydrothermal Alteration of the Onemana Area, Eastern Coromandel Peninsula, MSc Thesis, University of Waikato.
- Allègre, C. J. 2008, *Isotope Geology*, Cambridge University Press, New York.
- Ballance, P. F. & Spörli, K. B. 1979, 'Northland Allochthon', *Journal of the Royal Society of New Zealand*, vol. 9, no. 2, pp. 259-275.
- Bardebes, P. A. 1997, Volcanic Geology of the Rhyolitic Rocks of the Cooks Beach-Whitianga Harbour Region, Coromandel Volcanic Zone, MSc Thesis, University of Waikato.
- Bell, J. M. & Fraser, C. 1912, *The geology of the Waihi-Tairua subdivision: Hauraki, Auckland*, New Zealand Geological Survey Bulletin no. 15, Wellington.
- Black, L. P., Kamo, S. L., Allen, C. M., Davis, D. W., Aleinikoff, J. N., Valley, J. W., Mundil, R., Campbell, I. H., Korsch, R. J., Williams, I. S. & Foudoulis, C. 2004, 'Improved $^{206}\text{Pb}/^{238}\text{U}$ microprobe geochronology by the monitoring of a trace-element-related matrix effect; SHRIMP, ID-TIMS, ELA-ICP-MS and oxygen isotope documentation for a series of zircon standards', *Chemical Geology*, vol. 205, no. pp. 115-140.
- Bradshaw, J. D. 2004, 'Northland Allochthon: An alternative hypothesis of origin', *New Zealand Journal of Geology and Geophysics*, vol. 47, no. 3, pp. 375-382.
- Brathwaite, R. L. & Christie, A. B. 1996, *Geology of the Waihi Area 1:50 000. Institute of Geological & Nuclear Sciences geological map 21. 1 sheet + 64 p*, Institute of Geological & Nuclear Sciences Limited, Lower Hutt.
- Brathwaite, R. L., Christie, A. B. & Skinner, D. N. B. 1989, 'The Hauraki Goldfield - Regional setting, mineralisation and recent exploration', in D. Kear (ed.), *Mineral Deposits of New Zealand*, Australasian Institute of Mining and Metallurgy, Parkville, pp. 45-56.
- Briggs, R. M. 2004, 'Silicic volcanism in Coromandel Volcanic Zone: precursor to Taupo Volcanic Zone activity in the North Island, New Zealand',

Proceedings of the IAVCEI General Assembly 2004, International Association of Volcanology and Chemistry of the Earth's Interior, Pucon, Chile, pp. 147.

- Briggs, R. M. & Fulton, B. W. J. 1990, 'Volcanism, structure, and petrology of the Whiritoa-Whangamata coastal section, Coromandel Volcanic Zone, New Zealand: facies model evidence for the Tunaiti Caldera', *New Zealand Journal of Geology and Geophysics*, vol. 33, no. 4, pp. 623-633.
- Briggs, R. M., Houghton, B. F., McWilliams, M. & Wilson, C. J. N. 2005, ' $^{40}\text{Ar}/^{39}\text{Ar}$ ages of silicic volcanic rocks in the Tauranga-Kaimai area, New Zealand: dating the transition between volcanism in the Coromandel Arc and the Taupo Volcanic Zone', *New Zealand Journal of Geology and Geophysics*, vol. 48, no. 3, pp. 459-469.
- Briggs, R. M. & Krippner, S. J. P. 2006, 'The Control by Caldera Structures on Epithermal Au-Ag Mineralisation and Hydrothermal Alteration at Kapowai, Central Coromandel Volcanic Zone', in A. B. Christie & R. L. Brathwaite (ed.), *Geology and Exploration of New Zealand Mineral Deposits*, Australasian Institute of Mining and Metallurgy, Carlton, pp. 101-107.
- Brothers, R. N. 1984, 'Subduction regression and oceanward migration of volcanism, North Island, New Zealand', *Nature*, vol. 309, no. 5970, pp. 698-700.
- Carter, L., Shane, P., Alloway, B., Hall, I. R., Harris, S. E. & Westgate, J. A. 2003, 'Demise of one volcanic zone and birth of another - A 12 m.y. marine record of major rhyolitic eruptions from New Zealand', *Geology*, vol. 31, no. 6, pp. 493-496.
- Charlier, B. L. A., Wilson, C. J. N., Lowenstern, J. B., Blake, S., van Calsteren, P. W. & Davidson, J. P. 2005, 'Magma Generation at a Large, Hyperactive Silicic Volcano (Taupo, New Zealand) Revealed by U-Th and U-Pb Systematics in Zircons', *Journal of Petrology*, vol. 46, no. 1, pp. 3-32.
- Christiansen, R. L. 2001, *The Quaternary and Pliocene Yellowstone Plateau Volcanic Field of Wyoming, Idaho, and Montana* U. S. Geological Survey Professional Paper, U. S. Geological Survey, Reston, VA.
- Christie, A. B., Brathwaite, R. L., Mauk, J. L. & Simpson, M. P. 2006a, 'Hauraki Goldfield - Regional Exploration Databases and Prospectivity Studies', in A. B. Christie & R. L. Brathwaite (ed.), *Geology and Exploration of New Zealand Mineral Deposits*, Australasian Institute of Mining and Metallurgy, Carlton, pp. 73-84.
- Christie, A. B., Rabone, S. D. C., Barker, R. G. & Merchant, R. J. 2006b, 'Exploration of the Wharekirauponga Epithermal Au-Ag Deposit, Hauraki Goldfield', in A. B. Christie & R. L. Brathwaite (ed.), *Geology and Exploration of New Zealand Mineral Deposits*, Australasian Institute of Mining and Metallurgy, Carlton, pp. 137-144.

- Cole, J. W., Briggs, R. M. & Smith, I. E. M. 2008, 'Progression', in I. J. Graham (ed.), *A Continent on the Move: New Zealand Geoscience into the 21st Century*, Geological Society of New Zealand in association with GNS Science, Wellington, pp. 154-157.
- Cole, J. W., Hochstein, M. P., Skinner, D. N. B. & Briggs, R. M. 1987, *Tectonic setting of North Island Cenozoic volcanism*, New Zealand Geological Survey, Record 21, New Zealand Geological Survey, Wellington.
- Cooper, K. M. & Reid, M. R. 2008, 'Uranium-series Crystal Ages', *Reviews in Mineralogy & Geochemistry*, vol. 69, no. pp. 479–544.
- Cullingford, M. D. 2003, The volcanism of the Alderman Islands, Ohinau Island, and Southern Onemana Peninsula, Eastern Coromandel Volcanic Zone, New Zealand, MSc Thesis, University of Waikato.
- Deer, W. A., Howie, R. A. & Zussman, J. 1992, *An Introduction to the Rock-Forming Minerals* (2nd ed.), Longman Scientific & Technical, Harlow.
- Dickin, A. P. 2005, *Radiogenic Isotope geology* (2nd ed.), Cambridge University Press, Cambridge.
- Edbrooke, S. W. (compiler) 2001, *Geology of the Auckland Area. Institute of Geological & Nuclear Sciences 1:250 000 geological map 3. 1 sheet + 74 p*, Institute of Geological & Nuclear Sciences Limited, Lower Hutt.
- Fedo, C. M., Sircombe, K. N. & Rainbird, R. H. 2003, 'Detrital zircon analysis of the sedimentary record', *Reviews in Mineralogy & Geochemistry*, vol. 53, no. pp. 277-303.
- Fisher, G. D. 1986, Geological aspects of an area near Whitianga, Coromandel Peninsula, MSc Thesis, University of Auckland.
- Fitzgerald, M. J. 2004, Gold Mineralisation at Ohui, Eastern Coromandel, MSc Thesis, University of Waikato.
- Folkes, C. B., de Silva, S. L., Schmitt, A. K. & Cas, R. A. F. 2011, 'A reconnaissance of U-Pb zircon ages in the Cerro Galán system, NW Argentina: Prolonged magma residence, crystal recycling, and crustal assimilation', *Journal of Volcanology and Geothermal Research*, vol. 206, no. 3-4, pp. 136-147.
- Fraser, C. 1910, *The geology of the Thames subdivision: Hauraki, Auckland*, New Zealand Geological Survey Bulletin no. 10, Wellington.
- Fraser, C. & Adams, J. H. 1907, *The geology of the Coromandel subdivision : Hauraki, Auckland*, New Zealand Geological Survey Bulletin no. 4, Wellington.
- Fulton, B. W. J. 1988, The Volcanic Geology of the Whiritoa-Whangamata Area, MSc Thesis, University of Waikato.
- Furlong, K. P. & Kamp, P. J. J. 2009, 'The lithospheric geodynamics of plate boundary transpression in New Zealand: Initiating and emplacing

- subduction along the Hikurangi margin, and the tectonic evolution of the Alpine Fault system', *Tectonophysics*, vol. 474, no. 3-4, pp. 449-462.
- Garver, J. I. & Kamp, P. J. J. 2002, 'Integration of zircon color and zircon fission-track zonation patterns in orogenic belts: application to the Southern Alps, New Zealand', *Tectonophysics*, vol. 349, no. 1-4, pp. 203-219.
- Gastil, R. G., DeLisle, M. & Morgan, J. R. 1967, 'Some Effects of Progressive Metamorphism on Zircons', *Geological Society of America Bulletin*, vol. 78, no. 7, pp. 879-906.
- Gifkins, C., Herrmann, W. & Large, R. 2005, *Altered Volcanic Rocks: a guide to description and interpretation*, Centre for Ore Deposit Research, Tasmania.
- Graham, I. J. 2008, 'Relicts of a Fiery Past', in I. J. Graham (ed.), *A Continent on the Move: New Zealand Geoscience into the 21st Century*, Geological Society of New Zealand in association with GNS Science, Wellington, pp. 150-153.
- Grieve, P. L., Corbett, G. J. & Leach, T. M. 2006, 'Exploration at Ohakuri North Epithermal Au-Ag Prospect, Taupo Volcanic Zone', in A. B. Christie & R. L. Brathwaite (ed.), *Geology and Exploration of New Zealand Mineral Deposits*, Australasian Institute of Mining and Metallurgy, Carlton, pp. 197-202.
- Guay, C. M. Y. 1999, Volcanic Geology and Geochemistry of the Coroglen-Whenuakite Area, Eastern Coromandel Peninsula, New Zealand, MSc Thesis, University of Waikato.
- Haworth, A. V. 1993, Volcanic Geology and Hydrothermal Alteration of the Lower Waitekauri Valley, Waihi, New Zealand, MSc Thesis, University of Waikato.
- Hawthorn, B. M. 1996, Volcanic Geology of the Opito Bay Region, Northern Coromandel Peninsula, MSc Thesis, University of Waikato.
- Hayward, B. W., Black, P. M., Smith, I. E. M., Ballance, P. F., Itaya, T., Doi, M., Takagi, M., Bergman, S., Adams, C. J., Herzer, R. H. & Robertson, D. J. 2001, 'K-Ar ages of early Miocene arc-type volcanoes in northern New Zealand', *New Zealand Journal of Geology and Geophysics*, vol. 44, no. 2, pp. 285-311.
- Henderson, J. & Bartrum, J. A. 1913, *The geology of the Aroha subdivision : Hauraki, Auckland*, New Zealand Geological Survey Bulletin no. 16, Wellington.
- Henley, R. W. & Ellis, A. J. 1983, 'Geothermal Systems Ancient and Modern: A Geochemical Review', *Earth-Science Reviews*, vol. 19, no. 1, pp. 1-50.
- Herzer, R. 2008, 'Unrest in the North', in I. J. Graham (ed.), *A Continent on the Move: New Zealand Geoscience into the 21st Century*, Geological Society of New Zealand in association with GNS Science, Wellington, pp. 136-137.

- Herzer, R. H., Barker, D. H. N., Roest, W. R. & Mortimer, N. 2011, 'Oligocene-Miocene spreading history of the northern South Fiji Basin and implications for the evolution of the New Zealand plate boundary', *Geochemistry Geophysics Geosystems*, vol. 12, no. 2, pp. 20.
- Homer, L. & Moore, P. 1992, *Vanishing Volcanoes: A guide to the landforms and rock formations of Coromandel Peninsula*, Landscape Publications, Wellington.
- Hoskin, P. W. O. & Schaltegger, U. 2003, 'The Composition of Zircon and Igneous and Metamorphic Petrogenesis', *Reviews in Mineralogy & Geochemistry*, vol. 53, no. pp. 27-62.
- Hoskin, P. W. O., Wysoczanski, R. J. & Briggs, R. M. 1998, 'U-Pb age determination of 'lenticulite' (Owharoa Ignimbrite) at Waikino, Waihi Area, Coromandel Peninsula, and implications', *Geological Society of New Zealand & New Zealand Geophysical Society Joint Annual Conference*, University of Canterbury, Christchurch, pp. 123.
- Houghton, B. F., Wilson, C. J. N., McWilliams, M. O., Lanphere, M. A., Weaver, S. D., Briggs, R. M. & Pringle, M. S. 1995, 'Chronology and dynamics of a large silicic magmatic system: Central Taupo Volcanic Zone, New Zealand', *Geology*, vol. 23, no. 1, pp. 13-16.
- Hunt, P. 1991, The Volcanic Geology of the Whiritoa Hill Area, MSc Thesis, University of Waikato.
- Jackson, S. E., Pearson, N. J., Griffin, W. L. & Belousova, E. A. 2004, 'The application of laser ablation-inductively coupled plasma-mass spectrometry to in situ U-Pb zircon geochronology', *Chemical Geology*, vol. 211, no. pp. 47-69.
- Karl, M. L. 1996, Volcanic Geology of the Tairua Region, Eastern Coromandel Peninsula, MSc Thesis, University of Waikato.
- King, P. R. 2000, 'Tectonic reconstructions of New Zealand: 40 Ma to the Present', *New Zealand Journal of Geology and Geophysics*, vol. 43, no. 4, pp. 611-638.
- Kohn, B. P. 1973, Some studies of New Zealand Quaternary pyroclastic rocks, PhD Thesis, Victoria University of Wellington.
- Košler, J. & Sylvester, P. J. 2003, 'Present Trends and the Future of Zircon in Geochronology: Laser Ablation ICPMS', *Reviews in Mineralogy & Geochemistry*, vol. 53, no. pp. 243-275.
- Krippner, S. J. P. 2000, Volcanic geology, geochemistry and geochronology of the Kapowai Caldera Complex, Coromandel Volcanic Zone, New Zealand, PhD Thesis, University of Waikato.
- Le Maitre, R. W., Streckeisen, A., Zanettin, B., Le Bas, M. J., Bonin, B., Bateman, P., Bellieni, G., Dudek, A., Efremova, S., Keller, J., Lameyre, J., Sabine, P. A., Schmid, R., Sørensen, H. & Woolley, A. R. 2002, *Igneous rocks: a*

classification and glossary of terms (2nd ed.), Cambridge University Press, West Nyack, NY.

Ludwig, K., R. 1998, 'On the treatment of concordant uranium-lead ages', *Geochimica et Cosmochimica Acta*, vol. 62, no. 4, pp. 665-676.

Ludwig, K., R. 2003, *User's Manual for Isoplot 3.00: A Geochronological Toolkit for Microsoft Excel*, Special Publication No. 4, Special Publication No. 4, Berkeley Geochronology Center, Berkeley.

Marshall, P. 1912a, *Geology of New Zealand*, Government Printer, Wellington.

Marshall, P. 1912b, *New Zealand and adjacent islands*, Winter, Heidelberg.

McGunnigle, N. K. 1995, Volcanic Geology of the Hikuai Region, Eastern Coromandel Peninsula, MSc Thesis, University of Waikato.

Moore, C. R. 1976, Gold-silver mineralisation of the Broken Hills area, Hikuai, MSc Thesis, University of Auckland.

Moore, C. R. 1979, 'Geology and mineralisation of the former Broken Hills gold mine, Hikuai, Coromandel, New Zealand', *New Zealand Journal of Geology and Geophysics*, vol. 22, no. 3, pp. 339-351.

Morgan, P. G. 1924, *The geology and mines of the Waihi district, Hauraki Goldfield, New Zealand*, New Zealand Geological Survey Bulletin no. 26, Wellington.

Park, J. 1910, *The Geology of New Zealand*, Whitcombe and Tombs, Christchurch.

Parsons, S. L. 1993, The Volcanic Geology of Great Mercury Island, MSc Thesis, University of Waikato.

Perkins, D. 2011, *Mineralogy (3rd ed.)*, Prentice Hall, Upper Saddle River, NJ.

Pupin, J. P. 1980, 'Zircon and Granite Petrology', *Contributions to Mineralogy and Petrology*, vol. 73, no. 3, pp. 207-220.

Rabone, S. D. C. 1975, 'Petrography and hydrothermal alteration of Tertiary andesite-rhyolite volcanics in the Waitekauri Valley, Ohinemuri, New Zealand', *New Zealand Journal of Geology and Geophysics*, vol. 18, no. 2, pp. 239-258.

Rabone, S. D. C. 2006a, 'Broken Hills Rhyolite-Hosted High Level Epithermal Vein System, Hauraki Goldfield — 100 Years On', in A. B. Christie & R. L. Brathwaite (ed.), *Geology and Exploration of New Zealand Mineral Deposits*, Australasian Institute of Mining and Metallurgy, Carlton, pp. 117-122.

Rabone, S. D. C. 2006b, 'Exploration at Te Puke, Hauraki Goldfield - The last 30 years', in A. B. Christie & R. L. Brathwaite (ed.), *Geology and Exploration of New Zealand Mineral Deposits*, Australasian Institute of Mining and Metallurgy, Carlton, pp. 191-194.

- Richards, R. E. 2009, U-Pb geochronology of detrital zircon from Eocene - Oligocene sediments in the Te Anau Basin (New Zealand) and inferred provenance, MSc Thesis, University of Waikato.
- Roddick, J. C. & Bevier, M. L. 1995, 'U-Pb dating of granites with inherited zircon: Conventional and ion microprobe results from two Paleozoic plutons, Canadian Appalachians', *Chemical Geology*, vol. 119, no. 1-4, pp. 307-329.
- Rogers, J. 1994, Rhyolitic volcanics of the Cooks Beach/Hahei Region, Eastern Coromandel Peninsula, MSc Thesis, University of Waikato.
- Rollinson, H. R. 1993, *Using Geochemical Data: Evaluation, Presentation, Interpretation*, Longman Scientific & Technical, Harlow, Essex.
- Rutherford, N. F. 1978, 'Fission-track age and trace element geochemistry of some Minden Rhyolite obsidians', *New Zealand Journal of Geology and Geophysics*, vol. 21, no. 4, pp. 443-448.
- Saunders, K. E., Morgan, D. J., Baker, J. A. & Wysoczanski, R. J. 2010, 'The Magmatic Evolution of the Whakamaru Supereruption, New Zealand, Constrained by a Microanalytical Study of Plagioclase and Quartz', *Journal of Petrology*, vol. 51, no. 12, pp. 2465-2488.
- Seward, D. & Moore, P. R. 1987, *New fission track ages for some Minden Rhyolites (Whitianga Group), eastern Coromandel Peninsula*, New Zealand Geological Survey, Record 20, New Zealand Geological Survey, Wellington.
- Simmons, S. F., Brown, K. L. & Browne, P. R. L. 2006, 'Precious Metals in Hydrothermal Systems of the Taupo Volcanic Zone', in A. B. Christie & R. L. Brathwaite (ed.), *Geology and Exploration of New Zealand Mineral Deposits*, Australasian Institute of Mining and Metallurgy, Carlton, pp. 203-210.
- Siyambola, W. O., Fasasi, A. Y., Funtua, I. I., Fasasi, M. K., Tubosun, I. A., Pelemo, D. A. & Adesinan, T. A. 2005, 'Energy dispersive Z-ray fluorescence analysis of samples of the Nigerian Zircons', *Nuclear Instruments and Methods in Physics Research B*, vol. 239, no. pp. 426-432.
- Skinner, D. N. B. 1986, 'Neogene Volcanism of the Hauraki Volcanic Region', in I. E. M. Smith (ed.), *Late Cenozoic Volcanism in New Zealand*, The Royal Society of New Zealand, Wellington, pp. 21-47.
- Skinner, D. N. B. 1993, *Geology of the Coromandel Harbour Area, scale 1:50 000. Institute of Geological & Nuclear Sciences geological map 4. 1 sheet + 44 p*, Institute of Geological & Nuclear Sciences Limited, Lower Hutt.
- Skinner, D. N. B. 1995, *Geology of the Mercury Bay Area, scale 1:50 000. Institute of Geological & Nuclear Sciences geological map 17. 1 sheet + 56 p*, Institute of Geological & Nuclear Sciences Limited, Lower Hutt.

- Sollas, W. J. & McKay, A. 1905, *Rocks of Cape Colville Peninsula, Auckland, New Zealand*, Government Printer, Wellington.
- Sollas, W. J. & McKay, A. 1906, *Rocks of Cape Colville Peninsula, Auckland, New Zealand*, Government Printer, Wellington.
- Spörli, K. B., Begbie, M. J., Irwin, M. R. & Rowland, J. V. 2006, 'Structural processes and tectonic controls on the epithermal Au-Ag deposits of the Hauraki Goldfield', in A. B. Christie & R. L. Brathwaite (ed.), *Geology and Exploration of New Zealand Mineral Deposits*, Australasian Institute of Mining and Metallurgy, Carlton, pp. 85-94.
- Stevenson, R. J. 1986, The Geotechnical Properties of Minden Rhyolite at Pauanui and Onemana, Eastern Coromandel, MSc Thesis, University of Waikato.
- Takagi, M. 1995, Miocene-Pliocene arc volcanism of the Hauraki region in North Island, New Zealand, MSc Thesis, Okayama University of Science.
- Trotter, W. M. 1995, The Volcanic Geology of the Pauanui-Opoutere Beach Region, Eastern Coromandel Volcanic Zone, MSc Thesis, University of Waikato.
- von Hochstetter, F. 1864, *Geology of New Zealand*, translated from German by C.A. Fleming 1959, Government Printer, Wellington.
- Wagner, G. & van den Haute, P. 1992, *Fission-Track Dating*, Kluwer Academic Publishers, Dordrecht.
- Ward, G. K. & Wilson, S. R. 1978, 'Procedures for comparing and combining radiocarbon age determinations: a critique', *Archaeometry*, vol. 20, no. 1, pp. 19-31.
- Ward, K. T., Mauk, J. L. & Hall, C. 2005, 'New $^{40}\text{Ar}/^{39}\text{Ar}$ dates of adularia from epithermal deposits in the Hauraki Goldfield, New Zealand', *New Zealand Minerals Conference*, Crown Minerals and Australasian Institute of Mining and Metallurgy, Auckland, pp. 426-433.
- Westgate, J. A. 1989, 'Isothermal plateau fission-track ages of hydrated glass shards from silicic tephra beds', *Earth and Planetary Science Letters*, vol. 95, no. 3-4, pp. 226-234.
- Wilson, C. J. N., Charlier, B. L. A., Fagan, C. J., Spinks, K. D., Gravley, D. M., Simmons, S. F. & Browne, P. R. L. 2008, 'U-Pb dating of zircon in hydrothermally altered rocks as a correlation tool: Application to the Mangakino geothermal field, New Zealand', *Journal of Volcanology and Geothermal Research*, vol. 176, no. 2, pp. 191-198.
- Wilson, C. J. N., Charlier, B. L. A., Rowland, J. V. & Browne, P. R. L. 2010, 'U-Pb dating of zircon in subsurface, hydrothermally altered pyroclastic deposits and implications for subsidence in a magmatically active rift: Taupo Volcanic Zone, New Zealand', *Journal of Volcanology and Geothermal Research*, vol. 191, no. 1-2, pp. 69-78.

Wright, I. 2008, 'Rumbles from the Deep', in I. J. Graham (ed.), *A Continent on the Move: New Zealand Geoscience into the 21st Century*, Geological Society of New Zealand in association with GNS Science, Wellington, pp. 174-175.

Appendix I: Sample catalogue

Table I.1: Sample catalogue listing samples collected, field and University of Waikato rock store numbers, and sample locations.

Sample no.	University of Waikato no.	Rock name	Grid reference (error and elevation) (New Zealand Transverse Mercator Projection)	Location
01	W110850	Paku Rhyolite	1854982 5901277 (± 7 m, 10 m)	Paku Island, Tairua, outcrops on the coast of flow banded rhyolite, boulders of spherulitic rhyolite.
01 B	W110851	Paku Rhyolite - spherulites	1854982 5901277 (± 7 m, 10 m)	Paku Island, Tairua, outcrops on the coast of flow banded rhyolite, boulders of spherulitic rhyolite.
02	W110852	Timata Dome	1850618 5895060 (± 6 m, 16 m)	Outcrop on the northern side of State Highway 25 in a corner beside the Tairua River, south of Timata Road.
03	W110853	Pauanui Dome Complex	1856115 5897832 (± 6 m, 5 m)	Flat Rock, Pauanui. From a rock fall on the coast. Abundant cobbles: white-cream-grey-pink-red, autobreccia, some flow banded.
04	W110854	Pohakahaka Dome Complex	1855987 5884002 (± 9 m, 6 m)	Whitipirorua Point, southern headland of Onemana Beach, outcrop on coast.
05	W110855	Pokohino Dome Complex	1855733 5884890 (± 6 m, 10 m)	Northern headland of Onemana Beach, from a boulder of a rock fall.
06	W110856	Broken Hills Mine sample 1	1843457 5889883 (± 66 m)	From inside Broken Hills Mine, in “the chamber”.
07	W110857	Broken Hills Mine sample 2	1843457 5889883 (± 66 m)	From inside Broken Hills Mine. Known as “bubbly rhyolite”.
08	W110858	Broken Hills Mine sample 3	1843457 5889883 (± 66 m)	From inside Broken Hills Mine.
09	W110859	Broken Hills Flow Banded Rhyolite	1843683 5890681 (± 11 m, 24 m)	Outcrop on eastern side of Puketui Valley Rd (off Morrisons Rd) beside swimming hole in Tairua River. Outcrop c. 15 m high.

10 W110860	Hikuai Ignimbrite	1845442 5886990 (± 6 m, 77 m)	From a boulder off the bluffs, on the northern side of Kitahi Road, Yule's Farm.
11 W110861	Wharekirauponga Dome	1850018 5868269 (± 25 m, 48 m)	Outcrop by waterfall under swing bridge at southern end of walking track.
12 W110862	Owharoa Ignimbrite	1844618 5854813 (± 10 m, 70 m)	Outcrop on eastern side of road to Owharoa Falls, close to intersection with State Highway 2.
13 W110863	Ferry Landing Ignimbrite	1842074 5920879	From a cove at Whakapenui Point, northern end of Front Beach (Maramaratotara Bay). Section c. 20 m thick.
14 W110864	Shakespeare Ignimbrite	1842976 5920281	Base of cliffs at eastern end of Maramaratotara Bay. Section > 70 m thick.
15 W110865	Papakura Bay Dome	1856873 5871562 (± 9 m, 7 m)	From a cave at the northern end of Papakura Bay (Whiritoa).
16 W110866	Whale Bone Bay Dome	1860278 5861103 (± 8 m)	Outcrop at northern headland of Homunga Bay, c. 5 m back from water. Bay consists of dm size boulders: andesite to rhyolite, south to north.
17 W110867	Shark Bay Dome	1860216 5857130 (± 30 m)	South side of northern headland at Waihi Beach.
18 W110868	The Knob	1853816 5884163 (± 5 m, 106 m)	Outcrop on western side of The Knob, off Pokohino Road in forestry on the way to Onemana.
19 W110869	Te Karaka Rhyolite	1855671 5879125 (± 20 m)	Outcrop to the west of Te Karaka Point, Whangamata Harbour.
20 W110870	Staircase Dome	1854184 5891525 (± 7 m, 56 m)	Outcrop at the intersection of two tracks in forestry near Ohui.
21 W110871	Wharepapa Ignimbrite	1844005 5906778	Outcrop at a waterhole in Kapowai River 100 m upstream of ford at beginning of Parakau Rd (off McGoram Rd-Kapowai Rd).

Table I.2: Sample catalogue listing analytical procedures performed on each sample and the nature of remaining samples held in the University of Waikato rock store.

Sample no.	University of Waikato no.	Rock name	Analysis performed	Stored sample
01	Paku Rhyolite	HS TS XRD XRF	R T P V	
W110850				
01 B	Paku Rhyolite - spherulites	HS TS	R T	
W110851				
02	Timata Dome	HS TS M XRD XRF U-Pb	R T pT P V Z	
W110852				
03	Pauanui Dome Complex	HS TS M XRD XRF	R T pT P V	
W110853				
04	Pohakahaka Dome Complex	HS TS M XRF U-Pb	R T pT P V Z	
W110854				
05	Pokohino Dome Complex	HS TS XRF U-Pb	R T P V Z	
W110855				
06	Broken Hills Mine sample 1	HS TS XRD XRF U-Pb	R T P V Z	
W110856				
07	Broken Hills Mine sample 2	HS TS XRD XRF U-Pb	R T P V Z	
W110857				
08	Broken Hills Mine sample 3	HS TS XRD XRF U-Pb	R T P V Z	
W110858				
09	Broken Hills Flow Banded Rhyolite	HS TS XRD XRF U-Pb	R T P V Z	
W110859				
10	Hikuai Ignimbrite	HS TS M XRF U-Pb	R T pT P V Z	
W110860				
11	Wharekirauponga Dome	HS TS XRD XRF U-Pb	R T P V Z	
W110861				
12	Owharoa Ignimbrite	HS TS M XRF U-Pb	R T pT P V Z	
W110862				
13	Ferry Landing Ignimbrite	HS TS M XRF U-Pb	R T pT P V Z	
W110863				
14	Shakespeare Ignimbrite	HS TS M XRF U-Pb	R T pT P V Z	
W110864				

15 W110865	Papakura Bay Dome	HS TS M XRF U-Pb	R T pT P V Z
16 W110866	Whale Bone Bay Dome	HS TS M XRF U-Pb	R T pT P V Z
17 W110867	Shark Bay Dome	HS TS XRD XRF U-Pb	R T P V Z
18 W110868	The Knob	HS TS XRD XRF U-Pb	R T P V Z
19 W110869	Te Karaka Rhyolite	HS TS XRF U-Pb	R T P V Z
20 W110870	Staircase Dome	HS TS XRD XRF U-Pb	R T P V Z
21 W110871	Wharepapa Ignimbrite	HS TS M XRF	R T pT P V

HS, TS Hand specimen and thin section characteristics have been documented (Appendix II)
 M Phenocrysts have been analysed by electron probe micro-analyser (Appendix III)
 XRD Whole rock has been analysed by X-ray diffraction (Appendix IV)
 XRF Whole rock has been analysed by X-ray fluorescence (Chapter 3)
 U-Pb Sample has been dated by U-Pb dating of zircons

Stored sample Stored sample in the University of Waikato rock store as rock (R), unpolished thin section (T), polished thin section (pT), powder (P), zircon separates in vial (V) and mounted zircon on glass slide (Z)

Appendix II: Hand specimen and thin section descriptions

Table II.1: Hand specimen and thin section descriptions of samples collected.

Sample no.	Rock name	Hand specimen	Thin section
01	Paku Rhyolite	White-grey-pink-red laminar flow banded (< 2 mm) devitrified rhyolite. Very hard and splintery.	Highly devitrified, flow banded (< 2 mm) fine-grained quartz/tridymite/cristobalite rhyolite. Some spherulites, < 0.3 mm. Biotite: subhedral flakes, < 0.2 mm. Rare pyrite: cubic crystals << 0.05 mm.
01B	Paku Rhyolite - spherulites	White-grey-pink spherulites, < 15 mm diameter. Very hard.	Devitrified spherulites. Quartz, tridymite(?): subhedral, < 0.2 mm. Some spherulites < 0.3 mm. Veins of the macro-spherulites are devitrified glass. Rare biotite: flakes, < 0.1 mm.
02	Timata Dome	Pink rhyolite, c. 30 % spherulites, modal size 6-8 mm. Quite unaltered, hard.	Devitrified, spherulitic rhyolite. Quartz: irregular, ~0.2 mm. Rare plagioclase: tabular, < 3 mm, sometimes in clusters with quartz. Rare altered mafics – cannot determine what they were: golden-dark brown, no pleochroism, yellow-brown interference colours, < 1 mm. Chlorite/illite alteration: occurs as small flecks < 0.04 mm and thin veins. Groundmass is devitrified glass. Fe-Ti oxides: ilmenite, titanomagnetite.
03	Pauanui Dome Complex	Light grey rhyolite with quartz and plagioclase crystals, fresh (but looks weathered with orange patches/veins). Columnar jointed, c. 5 % phenocrysts.	Grey, porphyritic rhyolite. Plagioclase: tabular, subhedral, easily pluck out, < 2 mm. Altered mafics – now chlorite-smectite: rounded to anhedral, 0.25 - > 1.25 mm. Groundmass: fine-grained quartz. Quartz veins: < 0.15 mm wide, often lined with illite. Also orange-brown veins that can be seen in hand specimen: appear to be a result of weathering. Cubic Fe-Ti oxides: titanomagnetite, < 0.25 mm.

04	Pohakahaka Dome Complex	Dark grey-red, very vesicular, flow banded, crystal poor rhyolite. Some lithophysae (some > 20 mm diameter) have abundant pale secondary minerals infilling them.	Vesicular, flow banded, devitrified rhyolite. Plagioclase: multiple twinning, tabular to irregular, cumulophyric, < 3 mm. Quartz: irregular, some embayed, < 2 mm. Altered mafics – now chlorite-smectite: rounded to anhedral. Unidentified mineral lining some vesicles: orangey-brown outline, colourless non-pleochroic interior, fractured, high relief, interference colours are quartz-like, but entire crystal does not go into extinction at once, anhedral, rounded to hexagonal and elongated, < 0.1 mm. Groundmass: glassy, flow banded, vesicles (some > 2.5 mm) irregular and rounded. Spherulites max ~0.5 mm. Microlites: aligned within bands. Fe-Ti oxides: titanomagnetite and ilmenite, < 0.3 mm.
05	Pokohino Dome Complex	Pale cream, soft, crystal rich, hydrothermally altered rhyolite. Some lithophysae (< few mm diameter), but others in local rocks are > 15 mm. Weathered to light yellow-brown.	Porphyritic, devitrified quartz rhyolite. Quartz: irregular, anhedral, prismatic, some have an altered rim, < 1 mm. Biotite: rare, highly altered. Groundmass: devitrified (now quartz, < 0.05 mm), microlites, rare spherulites < 0.5 mm. Almost veiny texture.
06	Broken Hills Mine sample 1	White and orange, banded (> 3 mm) hydrothermally altered rhyolite. Some lithophysae, < 6 mm diameter, some are infilled or lined with crystals. Orange staining might be from weathering?	Broadly flow banded, fine-grained rhyolite. Only phenocrysts are those lining cavities: unidentified crystal with orange coating/replacement (similar to unidentified mineral in 04). Groundmass: Quartz + tridymite(?), some lithophysae, some spherulites < 1 mm, ghosts of spherulites crystallised to SiO ₂ .
07	Broken Hills Mine sample 2	White and orange “bubbly” banded hydrothermally altered rhyolite. Many lithophysae, < 10 mm diameter, some are infilled or lined with crystals. Some spherulites. Orange staining might be from weathering? Crumbly.	Similar to 06. Vesicular, spherulitic rhyolite. Altered plagioclase: now sericite/adularia/quartz, sub-tabular. Quartz: veins (which contain the largest crystals < 0.15 mm), and groundmass. Some crystals around vesicles are coated with orange mineral as in 06. Rare Fe-Ti oxides < 0.2 mm. Ghosts of spherulites (< 2.5 mm) crystallised to quartz, glass absent.

08	Broken Hills Mine sample 3	White-pink-grey broadly banded hydrothermally altered rhyolite. Some spherulites. Few open lithophysae, most are infilled. A little crumbly.	Banded, devitrified, spherulitic, hydrothermally altered rhyolite. Altered plagioclase: now sericite + adularia, tabular, 2 mm. Quartz: very fine grained (< 0.1 mm), mostly forms bands and veins, devitrified glass in some places, crystals in veins can be bigger (> 0.1 mm). Thickest vein ~ 0.5 mm wide. Illite: thin veiny wisps. Spherulites, some ~ 5 mm, veins cut through them. Many Fe-Ti oxides: mostly pyrite, few elongated hexagonal.
09	Broken Hills Flow Banded Rhyolite	Pink-grey-white laminar flow banded (< 2 mm) rhyolite. Some lenses of grey crystals. Very hard and splintery. (Overall, slightly less laminar and paler than Paku Rhyolite.)	Flow banded (< 2 mm) slightly devitrified rhyolite. Quartz: mostly very fine grained (< 0.1 mm), some in thickest bands ~0.25 mm, rarely ~1 mm, anhedral, and irregular. Biotite: altered/oxidised, flaky, < 0.5 mm, many tiny flakes < 0.1 mm relatively unaltered. Many Fe-Ti oxides: pyrite?
10	Hikuai Ignimbrite	Pale cream, crystal-rich partially welded, jointed ignimbrite. Pale grey/white and altered yellow pumices (modal size c. 10 mm). Variety of lithics < 1 mm to > 60 mm diameter. Very light weight.	See section 2.4.4
11	Wharekirauponga Dome	Cream-orange flow banded, silicified, hydrothermally altered rhyolite with quartz veins. Some vugs with crystals growing on their edges. Some brecciated bits. Still evidence of porphyritic texture - can see crystals.	Porphyritic flow banded rhyolite. Quartz: subhedral to anhedral and irregular, some are embayed or slightly prismatic, 2 mm. Altered plagioclase: now sericite ± adularia, subhedral, tabular, < 2.5 mm. Groundmass: fine-grained quartz, devitrified glass. Quartz veins (<0.5 mm wide). Illite-sericite veins (<0.01 mm wide). Some Fe-Ti oxides: pyrite?
12	Owharoa Ignimbrite	Creamy-grey densely welded and jointed lenticulite, flattened dense pumice (< 20 mm) some are still whitish, some almost like obsidian. Some lithics.	See section 2.4.5

13	Ferry Landing Ignimbrite	Greyish-brown, densely welded, jointed pumice-rich, lithic-poor lenticulite. Yellow-peachy pumice (wide range of sizes, > 50 mm). Some crystals. Some pumices have clusters of crystals in them.	See section 2.4.1
14	Shakespeare Ignimbrite	Light grey, pumice-rich, crystal-rich, lithic-poor, un- to partially welded, widely jointed ignimbrite. Pale creamy-white pumices (modal size 12 mm, max > 30 mm). Variety of lithics.	See section 2.4.2
15	Papakura Bay Dome	Black to greeny-black glassy broadly flow banded (mm to cm) rhyolite. Many small vesicles (< 4 mm, most c. 1-2 mm), most are infilled (at least partially) with secondary minerals (grey-green). Small clusters of quartz and plagioclase crystals and solitary biotite flakes.	Vitrophyric, spherulitic rhyolite. Quartz: irregular, anhedral, some embayed, < 2 mm, sometimes in clusters with plagioclase. Plagioclase: multiple twinning, anhedral, irregular, some tabular, most are fractured, < 2.5 mm. Biotite: flaky, rare plagioclase inclusions, < 1.5 mm. Rare relict mafics. Groundmass: non-devitrified glass, perlitic cracks, edges of vesicles are devitrified. Rare Fe-Ti oxides: titanomagnetite. Microlites.
16	Whale Bone Bay Dome	Dark reddish grey devitrified, slightly vesicular, broadly banded, hydrothermally altered, jointed rhyolite. Phenocrysts of quartz and plagioclase. Few lithophysae, some are > 20 mm and infilled or lined with secondary minerals. Rare spherulites. Very hard.	Porphyritic banded rhyolite. Quartz: embayed, anhedral, some are almost hexagonal, mostly irregular, < 4 mm, occurs in clusters ± plagioclase. Plagioclase: sieve-texture (resorbed), multiple twinning, anhedral, irregular – tabular, < 2 mm. Groundmass: devitrified glass, few spherulites: < 0.8 mm, fan-shaped, a few smaller ones (0.15 mm) are whole and not devitrified. Fe-Ti oxides: titanomagnetite, ilmenite, pyrite.

17	Shark Bay Dome	Light creamy-grey hydrothermally altered, silicified, weathered (probably from sea water) rhyolite. Quartz phenocrysts.	Porphyritic altered rhyolite. Quartz: anhedral, rounded, embayed, < 1.5 mm. Rare altered plagioclase. Tridymite(?) lining cavities. Groundmass: fine-grained (< 0.05 mm) quartz. Clusters of pyrite.
18	The Knob	Grey-cream-pink highly silicified and hydrothermally altered broadly flow banded rhyolite. Very hard. Almost a sinter in places. Some cracks that have rusty looking coating. Patches of quartz infilling vugs.	Porphyritic silicified rhyolite. Quartz: subhedral to anhedral, irregular, embayed, prismatic, < 2 mm. Altered plagioclase: now fine-grained SiO ₂ , subhedral and tabular. Groundmass: fine-grained quartz, noticeable absence of veins, quartz structures that are crystallised remains of spherulites. Rare Fe-Ti oxides: pyrite?
19	Te Karaka Rhyolite	Creamy pinkish grey vesicular spherulitic (< 2 mm diameter) rhyolite with abundant lithophysae, most of which are infilled. The spherulites are > 15 % of the rock.	Devitrified, spherulitic, crystal-poor rhyolite. Quartz: rare phenocrysts, subhedral, 1 mm. Altered glass and spherulites – look like they have been altered, rough outlines. No opaques.
20	Staircase Dome	Pinkish light grey crystal-rich (c. 25 %) broadly flow banded quartz-biotite rhyolite.	Medium-grained, porphyritic, flow banded rhyolite. Quartz: subhedral and irregular, some are embayed or display sub-conchoidal fractures, < 1.25 mm, also tridymite(?). Biotite: subhedral flakes, some are hexagonal and almost opaque, oxidised, < 1.25 mm. Rare plagioclase: subhedral and tabular to irregular, multiple twinning, often resorbed textures, < 2 mm. Groundmass: fine-grained quartz, variably devitrified glass. Rare spherulites < 0.7 mm. No opaques.
21	Wharepapa Ignimbrite	Light grey soft ignimbrite. White pumices (modal size < 15 mm, some are > 40 mm), a couple of yellowish pumices (which are very soft). Abundant dark lithics (< 4 mm).	See section 2.4.3

Appendix III: Microprobe analyses

Table III.1: Plagioclase phenocrysts. Plagioclase in ignimbrites are free crystals in the matrix unless otherwise stated (r = rim, c = core, m = mid-way). Total iron is expressed as FeO*.

Ferry Landing Ignimbrite W110863																				
analysis number	2 c	2 r	3 r	3 c	3b r	3b c	4 r	4 c	5 r	5 c	6 r	6 c	7 r	7 c	8 r	8 c	9 r	9 c	10 r	10 c
Major oxide			lithic		lithic		pumice													
SiO ₂	57.97	60.10	60.48	59.35	60.97	58.98	60.26	58.92	59.80	59.42	60.95	59.08	59.60	58.29	60.83	59.87	60.25	59.23	61.48	59.91
TiO ₂	-0.02	0.05	-0.04	0.07	-0.02	-0.01	-0.06	0.13	-0.03	0.03	0.08	0.04	-0.03	0.01	0.07	-0.09	-0.03	0.10	0.12	0.04
Al ₂ O ₃	25.70	24.65	24.36	25.07	24.09	25.64	24.28	25.24	24.44	25.16	24.46	25.46	25.16	26.14	24.35	24.81	24.59	25.29	23.76	24.84
FeO*	0.18	0.16	0.22	0.31	0.22	0.20	0.15	0.05	0.33	0.23	0.36	0.25	0.28	0.28	0.14	0.25	0.31	0.17	0.23	0.24
MnO	0.04	0.02	0.02	-0.03	0.03	-0.05	0.04	0.10	0.13	0.06	-0.07	0.12	0.04	0.02	0.07	-0.11	-0.05	0.03	-0.02	0.00
MgO	-0.06	-0.13	-0.07	-0.04	-0.05	-0.11	-0.04	-0.08	-0.10	-0.07	-0.04	-0.09	-0.08	-0.07	-0.01	-0.12	-0.10	-0.05	-0.10	-0.08
CaO	7.75	6.55	6.48	7.18	5.94	7.66	6.23	7.35	6.30	7.14	6.26	7.14	6.92	7.93	6.08	6.38	6.32	7.13	5.60	6.77
Na ₂ O	6.84	7.50	7.30	7.15	7.37	6.97	7.60	6.96	7.81	6.96	7.93	6.94	7.29	6.74	7.68	7.70	7.71	7.29	8.02	7.44
K ₂ O	0.34	0.45	0.70	0.65	0.86	0.56	0.47	0.34	0.39	0.37	0.50	0.41	0.39	0.37	0.44	0.42	0.35	0.36	0.49	0.37
Total	98.74	99.35	99.45	99.71	99.41	99.84	98.93	99.01	99.07	99.30	100.43	99.35	99.57	99.71	99.65	99.11	99.35	99.55	99.58	99.53
Normalised values																				
Ca	37.74	31.71	31.57	34.37	29.26	36.58	30.33	36.12	30.15	35.39	29.52	35.37	33.63	38.56	29.66	30.65	30.55	34.36	27.06	32.75
Na	60.28	65.70	64.37	61.93	65.70	60.23	66.95	61.89	67.63	62.43	67.67	62.21	64.11	59.30	67.79	66.95	67.44	63.57	70.12	65.12
K	1.97	2.59	4.06	3.70	5.04	3.18	2.72	1.99	2.22	2.18	2.81	2.42	2.26	2.14	2.56	2.40	2.01	2.07	2.82	2.13

100

Shakespeare Ignimbrite W110864															Wharepapa Ignimbrite W110871					
analysis number	11 r	11 m	11 c	12 r	12 c	2 r	2 m	2 c	3 r	3 m	3 c	4 r	4 c	5 r	5 c	5 m	1 r	1 c	2 c	2 r
Major oxide												pumice		pumice						
SiO ₂	59.98	61.04	58.52	60.22	59.49	59.82	56.62	56.67	60.35	59.22	61.10	60.99	61.39	61.08	57.94	57.49	58.83	57.37	57.73	56.79
TiO ₂	-0.05	0.05	0.06	0.01	0.10	0.12	0.00	-0.03	0.02	0.16	0.02	0.06	0.00	0.07	0.12	0.05	0.13	0.08	-0.04	-0.01
Al ₂ O ₃	24.79	23.89	25.84	24.69	25.33	25.03	26.85	26.89	24.47	25.55	24.18	24.15	24.46	24.46	26.54	26.79	25.09	26.19	25.62	24.59
FeO*	0.30	0.18	0.31	0.36	0.38	0.25	0.36	0.43	0.34	0.35	0.17	0.25	0.17	0.31	0.25	0.35	0.10	0.37	0.18	0.29
MnO	-0.04	0.06	0.08	-0.09	0.10	-0.07	0.07	-0.03	-0.07	-0.04	-0.02	0.07	0.05	-0.08	0.01	0.08	0.01	-0.07	0.03	0.13
MgO	-0.07	-0.11	-0.07	-0.04	-0.04	-0.04	0.00	-0.01	0.00	0.03	0.07	0.09	0.16	-0.03	-0.08	0.04	-0.11	-0.16	-0.06	-0.18
CaO	6.60	5.54	7.65	6.44	7.18	7.05	9.22	9.31	6.40	7.36	6.00	6.09	6.13	6.32	8.66	8.39	7.24	8.30	8.00	7.53
Na ₂ O	7.35	7.87	7.08	7.49	7.25	7.25	6.27	5.98	7.78	7.04	7.80	8.00	7.93	7.90	6.36	6.49	7.13	6.51	6.71	6.70
K ₂ O	0.44	0.51	0.34	0.45	0.34	0.41	0.38	0.30	0.55	0.35	0.49	0.44	0.50	0.50	0.31	0.30	0.39	0.32	0.36	0.32
Total	99.30	99.03	99.81	99.53	100.13	99.82	99.77	99.51	99.84	100.02	99.81	100.14	100.79	100.53	100.11	99.98	98.81	98.91	98.53	96.16
Normalised values																				
Ca	32.31	27.17	36.66	31.37	34.68	34.13	43.87	45.44	30.28	35.87	28.99	28.88	29.09	29.80	42.17	40.94	35.13	40.56	38.89	37.58
Na	65.12	69.85	61.40	66.02	63.37	63.51	53.98	52.82	66.62	62.10	68.19	68.64	68.09	67.40	56.04	57.31	62.61	57.57	59.03	60.51
K	2.56	2.98	1.94	2.61	1.96	2.36	2.15	1.74	3.10	2.03	2.82	2.48	2.82	1.80	1.74	2.25	1.86	2.08	1.90	

		Pauanui Dome Complex W110853																			
analysis number		5 r	5 c	6 c	7 r	7 c	1 r	1 m	1 m	1 c	2 r	2 c	3 r	3 c	4 r	4 c	4 m	5 r	5 c	6 r	6 m
Major oxide		pumice	pumice																		
SiO ₂		58.90	57.44	59.73	61.93	59.71	56.81	57.85	57.10	56.78	57.30	55.78	58.49	58.67	56.37	57.55	57.66	56.88	55.61	57.62	57.12
TiO ₂		0.01	-0.06	0.01	0.05	0.11	0.13	0.08	0.09	0.18	0.03	0.00	0.01	-0.02	0.05	-0.06	-0.03	0.05	0.12	0.01	0.05
Al ₂ O ₃		25.25	26.02	24.34	24.04	24.70	26.37	26.27	26.41	26.90	26.98	27.42	26.09	25.76	26.72	26.20	26.14	26.09	27.13	26.27	26.80
FeO*		0.17	0.22	0.25	0.48	0.29	0.59	0.29	0.13	0.22	0.48	0.26	0.44	0.12	0.48	0.48	0.30	0.36	0.35	0.50	0.32
MnO		-0.02	0.09	0.04	0.04	0.05	-0.04	-0.07	-0.03	-0.01	0.03	0.12	-0.09	0.00	-0.09	-0.03	0.04	-0.05	-0.08	-0.16	0.00
MgO		-0.07	-0.09	-0.04	-0.01	-0.09	0.01	0.00	-0.04	-0.07	-0.02	0.05	-0.02	0.01	0.05	-0.05	-0.04	0.01	0.09	0.06	0.08
CaO		7.39	8.10	6.66	6.19	6.94	9.01	8.20	8.67	9.17	9.40	9.91	8.01	7.98	8.86	8.62	8.39	8.79	9.61	8.56	9.14
Na ₂ O		6.92	6.64	7.36	7.38	7.41	6.12	6.35	6.24	5.91	6.05	5.64	6.33	6.85	5.96	6.35	6.37	6.05	5.96	6.36	5.89
K ₂ O		0.37	0.35	0.37	0.56	0.45	0.56	0.48	0.44	0.42	0.52	0.34	0.65	0.36	0.54	0.55	0.47	0.60	0.34	0.57	0.48
Total		98.92	98.71	98.72	100.66	99.57	99.56	99.45	99.01	99.50	100.77	99.52	99.91	99.73	98.94	99.61	99.30	98.78	99.13	99.79	99.88
Normalised values																					
Ca		36.31	39.45	32.62	30.63	33.23	43.42	40.47	42.32	45.03	44.83	48.29	39.58	38.36	43.67	41.51	40.97	42.98	46.20	41.26	44.87
Na		61.53	58.52	65.23	66.08	64.21	53.37	56.71	55.12	52.52	52.22	49.74	56.60	59.58	53.16	55.34	56.29	53.53	51.85	55.47	52.32
K		2.16	2.03	2.16	3.30	2.57	3.21	2.82	2.56	2.46	2.95	1.97	3.82	2.06	3.17	3.15	2.73	3.49	1.95	3.27	2.81

		Timata Dome W110852									Hikurangi Ignimbrite W110860										
analysis number	6 c	3 r	3 m	3 c	4 r	4 c	5 r	5 c	6 r	6 c	11 r	11 c	10 r	10 m	10 c	7 r	7 c	8 r	8 c	9 r	
Major oxide											pumice	pumice									
SiO ₂		55.85	57.77	57.30	58.01	57.80	58.44	58.42	58.41	57.40	57.11	62.07	61.92	62.04	62.04	61.23	57.92	55.90	56.20	56.55	61.70
TiO ₂		-0.03	0.08	0.03	-0.04	0.23	0.09	-0.03	-0.04	0.16	0.00	0.07	0.19	0.00	0.11	0.08	0.06	0.18	0.06	0.08	0.07
Al ₂ O ₃		27.78	25.92	26.06	26.14	25.94	25.68	25.87	25.59	26.00	26.27	23.77	23.74	23.63	23.70	23.95	26.09	27.64	27.66	26.69	23.69
FeO*		0.37	0.31	0.34	0.25	0.34	0.15	0.28	0.22	0.41	0.24	0.32	0.15	0.25	0.29	0.12	0.22	0.25	0.18	0.27	0.21
MnO		0.08	-0.05	0.09	-0.02	-0.10	-0.03	0.23	0.05	-0.06	-0.05	-0.08	-0.06	0.08	-0.14	0.04	0.09	0.00	-0.01	0.02	0.11
MgO		0.07	0.06	0.10	0.07	0.05	-0.05	-0.04	0.06	-0.01	-0.03	-0.06	-0.08	-0.10	-0.08	-0.06	-0.08	-0.07	0.00	-0.08	-0.11
CaO		9.87	8.27	8.29	8.27	8.41	7.97	8.02	7.97	8.53	8.62	5.11	5.25	5.05	5.16	5.59	8.05	9.76	9.46	9.01	5.37
Na ₂ O		5.50	6.41	6.46	6.21	6.40	6.66	6.44	6.52	6.24	6.30	7.91	8.35	8.23	8.54	7.86	6.83	5.75	6.16	6.33	8.22
K ₂ O		0.37	0.50	0.44	0.43	0.60	0.46	0.61	0.46	0.49	0.38	0.53	0.40	0.49	0.50	0.45	0.31	0.21	0.26	0.31	0.55
Total		99.86	99.27	99.11	99.32	99.67	99.37	99.80	99.24	99.16	98.84	99.64	99.86	99.67	100.12	99.26	99.49	99.62	99.97	99.18	99.81
Normalised values																					
Ca		48.71	40.41	40.43	41.31	40.62	38.75	39.31	39.23	41.80	42.10	25.48	25.20	24.60	24.33	27.47	38.74	47.81	45.23	43.25	25.69
Na		49.12	56.68	57.01	56.13	55.93	58.59	57.13	58.07	55.34	55.69	71.37	72.52	72.56	72.86	69.90	59.48	50.97	53.29	54.98	71.17
K		2.17	2.91	2.56	2.56	3.45	2.66	3.56	2.70	2.86	2.21	3.15	2.29	2.84	2.81	2.63	1.78	1.22	1.48	1.77	3.13

analysis number															Pohakahaka Dome Complex W110854					
	9 c	6 r	6 c	5 r	5 m	4 c	3 r lithic	3 c lithic	3b c lithic	3b r lithic	4 c	4 r	2 r lithic	2 c lithic	1 r lithic	1 c	1 r	2 r	2 m	2 c
SiO ₂	55.82	62.08	62.80	62.19	61.09	61.33	59.66	59.04	58.21	58.17	62.27	62.72	58.80	58.39	59.80	61.92	60.64	60.68	58.58	61.51
TiO ₂	0.00	0.00	-0.01	0.13	0.02	0.14	0.06	0.01	0.03	0.08	0.07	0.01	0.13	0.01	0.05	-0.01	0.03	0.00	0.12	-0.04
Al ₂ O ₃	27.86	23.66	23.33	23.75	24.23	24.37	25.13	26.21	25.60	25.71	23.92	23.52	26.07	25.86	25.34	22.75	24.55	23.89	25.68	23.44
FeO*	0.46	0.40	0.26	0.17	0.17	0.16	0.35	0.25	0.52	0.34	0.27	0.27	0.22	0.47	0.36	0.20	0.21	0.35	0.16	0.16
MnO	-0.06	-0.08	-0.12	-0.03	0.03	0.02	0.06	0.09	-0.08	0.06	0.15	0.07	-0.07	0.00	-0.10	-0.05	-0.04	-0.03	0.10	0.01
MgO	-0.09	0.15	-0.13	0.00	-0.06	-0.10	-0.10	-0.01	-0.03	0.01	0.01	-0.06	-0.10	-0.04	-0.03	-0.04	-0.07	-0.09	-0.03	-0.07
CaO	10.22	5.05	4.67	5.27	5.91	6.03	7.43	7.94	7.72	7.86	5.32	5.02	8.11	8.24	7.25	4.75	6.47	5.85	7.58	5.48
Na ₂ O	5.48	8.34	8.38	8.39	7.90	8.17	7.31	6.53	6.85	6.75	8.34	8.34	6.52	6.59	6.90	8.35	7.65	7.61	6.98	7.93
K ₂ O	0.25	0.43	0.55	0.44	0.43	0.49	0.39	0.38	0.40	0.33	0.47	0.44	0.34	0.36	0.42	0.66	0.55	0.58	0.40	0.56
Total	99.94	100.03	99.73	100.31	99.72	100.61	100.29	100.44	99.22	99.31	100.82	100.33	100.02	99.88	99.99	98.53	99.99	98.84	99.57	98.98
Normalised values																				
Ca	50.01	24.45	22.79	25.12	28.53	28.18	35.18	39.29	37.49	38.40	25.37	24.33	39.92	40.01	35.83	23.01	30.86	28.80	36.64	26.74
Na	48.53	73.07	74.01	72.38	69.00	69.09	62.63	58.47	60.20	59.68	71.96	73.13	58.08	57.91	61.70	73.19	66.02	67.80	61.06	70.01
K	1.46	2.48	3.20	2.50	2.47	2.73	2.20	2.24	2.31	1.92	2.67	2.54	1.99	2.08	2.47	3.81	3.12	3.40	2.30	3.25

analysis number											Papakura Bay Dome W110865									
	3 r	3 c	3b r	3b m	3b c	4 r	4 m	4 c	6 r	6 c	2 r	2 c	2b r	2b c	3 c	3 m	3 r	4 r	4 c	5 r
SiO ₂	60.00	61.05	59.94	57.77	56.56	60.88	62.24	58.96	61.01	59.95	60.27	59.53	61.60	60.05	60.22	55.87	58.48	61.26	60.05	63.93
TiO ₂	0.14	0.13	-0.04	0.05	-0.08	0.09	0.14	0.11	0.16	0.12	0.15	0.00	0.04	0.07	-0.02	0.00	0.07	0.07	0.07	-0.03
Al ₂ O ₃	24.37	23.54	24.69	26.23	25.21	23.71	23.34	25.54	24.07	25.20	24.19	24.61	23.55	24.68	24.37	27.28	25.42	24.23	24.26	21.28
FeO*	0.20	0.34	0.24	0.20	0.15	0.30	0.26	0.16	0.18	0.17	0.12	0.17	0.08	0.29	0.16	0.25	0.14	0.13	0.23	0.17
MnO	0.04	0.00	0.07	0.01	0.10	0.10	0.14	-0.07	0.00	-0.04	-0.16	-0.01	0.11	-0.03	0.10	-0.14	0.03	-0.04	-0.01	-0.01
MgO	0.06	-0.01	-0.08	-0.06	-0.11	-0.09	-0.04	-0.06	0.05	-0.07	0.00	0.00	-0.10	-0.01	0.03	0.06	-0.08	-0.05	-0.06	-0.03
CaO	6.31	5.38	6.53	8.18	7.36	5.61	5.04	7.51	5.93	6.80	6.06	6.61	5.33	6.35	6.29	9.56	7.65	5.79	6.39	4.92
Na ₂ O	7.23	8.16	7.63	6.74	6.67	7.65	8.31	7.04	7.68	7.40	7.44	7.48	7.92	7.47	7.47	5.90	6.85	8.03	7.69	6.63
K ₂ O	0.49	0.67	0.52	0.35	0.35	0.57	0.66	0.37	0.45	0.47	0.62	0.62	0.92	0.63	0.60	0.32	0.60	0.60	0.71	1.00
Total	98.84	99.26	99.50	99.47	96.21	98.82	100.09	99.56	99.53	100.00	98.69	99.01	99.45	99.50	99.22	99.10	99.16	100.02	99.33	97.86
Normalised values																				
Ca	31.59	25.69	31.16	39.34	37.08	27.87	24.16	36.30	29.12	32.77	29.91	31.65	25.68	30.80	30.65	46.37	36.85	27.52	30.21	27.17
Na	65.49	70.50	65.89	58.66	60.82	68.76	72.08	61.57	68.25	64.53	66.45	64.81	69.05	65.56	65.87	51.78	59.71	69.08	65.79	66.26
K	2.92	3.81	2.95	2.00	2.10	3.37	3.77	2.13	2.63	2.70	3.64	3.53	5.28	3.64	3.48	1.85	3.44	3.40	4.00	6.58

analysis number	Whale Bone Bay Dome W110866														Owharoa Ignimbrite W110862					
	5 m	5 c	1 r	1 c	2 r	2 c	3 r	4 r	4 c	3 c	5 r	5 c	6 r	6 c	8 r	8 c	2 r	2 c	3 r	3 m
	Major oxide																			
SiO ₂	60.90	58.17	62.52	60.15	62.26	61.11	62.04	61.84	63.14	60.81	63.11	61.87	61.87	63.17	61.99	61.73	59.38	59.91	60.54	60.22
TiO ₂	0.07	-0.09	0.18	0.10	0.05	0.06	0.06	0.08	0.00	0.15	-0.02	-0.02	0.21	0.07	0.09	0.05	0.07	-0.01	0.03	-0.02
Al ₂ O ₃	24.70	26.14	22.85	24.85	23.29	23.75	23.96	23.77	23.10	23.87	22.72	23.88	23.10	22.70	23.28	23.33	25.23	24.78	24.82	25.31
FeO*	0.19	0.17	0.37	0.17	0.22	0.13	0.19	0.03	0.16	0.13	0.11	0.13	0.15	0.25	0.27	0.16	0.12	0.03	0.26	0.14
MnO	0.16	-0.03	-0.09	-0.03	0.07	-0.04	-0.02	-0.01	0.09	0.15	-0.10	-0.02	-0.03	0.03	0.18	-0.01	0.02	-0.05	-0.07	-0.02
MgO	-0.12	0.09	-0.16	-0.05	-0.04	-0.04	-0.03	-0.17	-0.02	0.00	-0.04	-0.12	-0.09	0.01	-0.06	-0.07	-0.06	-0.10	-0.05	-0.06
CaO	6.21	8.08	4.45	6.54	4.76	5.60	5.35	5.14	4.47	5.35	4.35	5.22	4.80	4.24	4.99	5.16	7.29	6.52	6.44	7.00
Na ₂ O	7.77	6.65	8.22	7.43	8.21	7.79	8.09	8.11	8.57	7.82	8.26	7.82	7.91	8.83	8.05	8.13	7.21	7.48	7.71	7.43
K ₂ O	0.58	0.51	1.04	0.69	1.02	0.79	0.83	0.80	0.92	0.87	0.99	0.80	0.87	1.02	0.94	0.82	0.59	0.51	0.50	0.53
Total	100.46	99.69	99.38	99.85	99.84	99.15	100.47	99.59	100.43	99.15	99.38	99.56	98.79	100.32	99.73	99.30	99.85	99.07	100.18	100.62
Normalised values																				
Ca	29.63	38.99	21.64	31.43	22.85	27.14	25.50	24.75	21.21	26.05	21.24	25.68	23.82	19.78	24.13	24.75	34.65	31.55	30.68	33.50
Na	67.08	58.08	72.34	64.62	71.32	68.31	69.79	70.66	73.59	68.91	73.00	69.63	71.04	74.55	70.45	70.57	62.01	65.51	66.48	63.52
K	3.29	2.93	6.02	3.95	5.83	4.56	4.71	4.59	5.20	5.04	5.76	4.69	5.14	5.67	5.41	4.68	3.34	2.94	2.84	2.98

analysis number	3 c	4 r	4 c	5 c	5 r	6 r	6 c
Major oxide							
SiO ₂	59.82	61.49	59.06	61.81	61.28	59.89	59.66
TiO ₂	0.06	0.10	0.11	0.06	0.02	0.08	0.16
Al ₂ O ₃	24.97	23.86	25.85	23.78	23.95	24.87	25.61
FeO*	0.23	0.20	0.06	0.21	0.22	0.16	0.32
MnO	0.07	-0.06	0.06	0.07	0.07	0.00	-0.02
MgO	-0.15	-0.07	-0.05	-0.08	-0.04	-0.07	-0.04
CaO	6.81	5.30	7.67	5.65	5.48	6.61	7.28
Na ₂ O	7.25	8.08	6.86	8.09	7.85	7.31	7.19
K ₂ O	0.53	0.71	0.47	0.63	0.64	0.51	0.47
Total	99.59	99.61	100.09	100.22	99.47	99.36	100.63
Normalised values							
Ca	33.12	25.52	37.15	26.85	26.80	32.33	34.91
Na	63.81	70.41	60.13	69.58	69.47	64.70	62.40
K	3.07	4.07	2.71	3.57	3.73	2.97	2.68

Table III.2: Mafic minerals. Minerals in ignimbrites are free crystals in the matrix (r = rim, c = core, m = mid-way). Total iron is expressed as FeO*.

Pyroxenes

Wharepapa Ignimbrite W110871			
analysis number	3 r orthopyroxene	3 c orthopyroxene	4 c augite
Major oxide			
SiO ₂	51.85	52.41	52.38
TiO ₂	0.11	0.34	0.32
Al ₂ O ₃	0.45	0.74	1.31
FeO*	25.91	26.12	9.42
MnO	1.53	1.08	0.30
MgO	18.20	19.02	14.60
CaO	1.21	1.37	20.27
Na ₂ O	-0.05	-0.11	0.19
K ₂ O	0.08	0.09	0.05
Total	99.29	101.06	98.84
Normalised values			
Ca	2.59	2.84	42.29
Fe	43.26	42.29	15.34
Mg	54.15	54.87	42.37

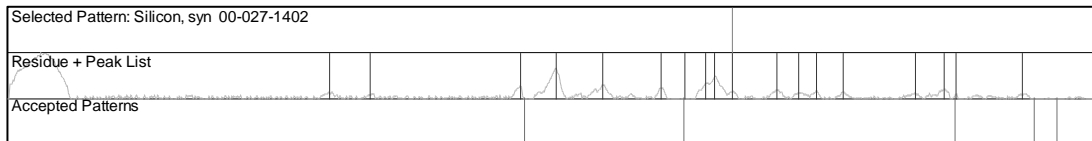
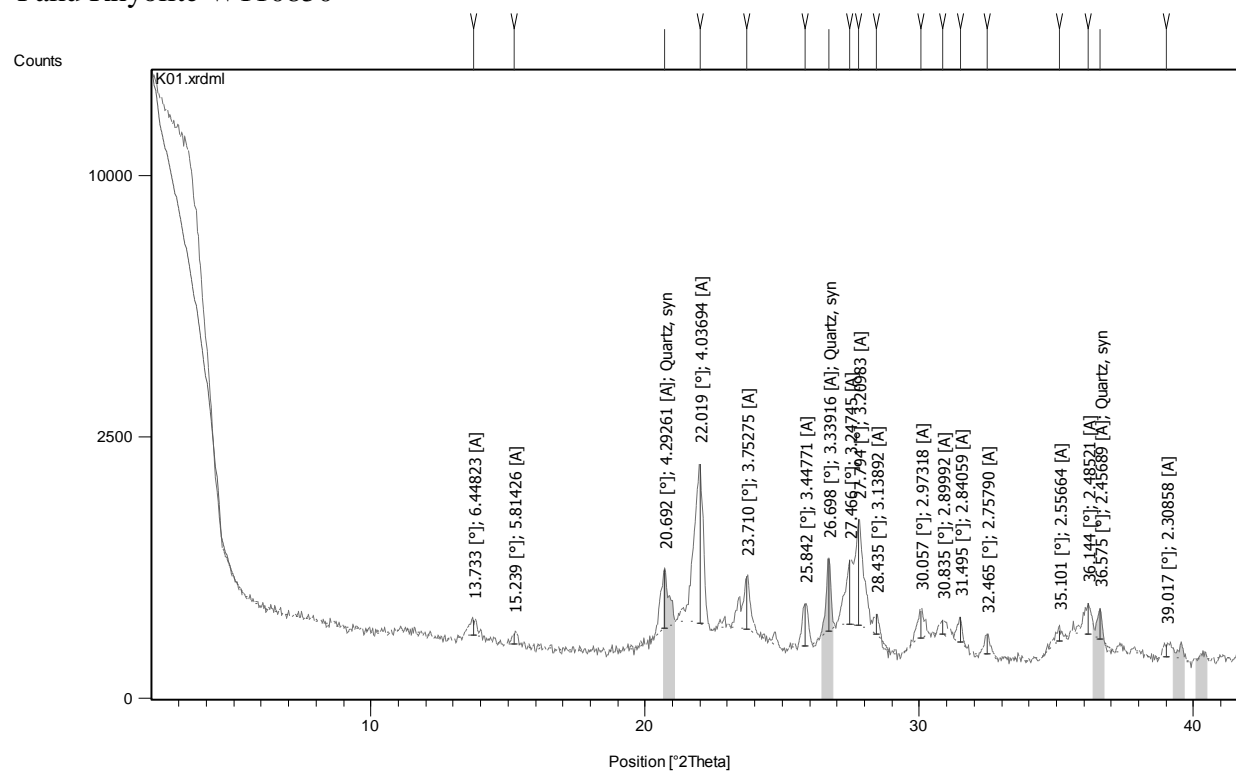
Biotite

Papakura Bay Dome W110865								Owharoa Ignimbrite W110862			
analysis number	1	1 c	6 r	6 c	7 r	7 c	8 r	8 c	1 r	1 c	7 r
Major oxide											
SiO ₂	35.01	35.41	35.43	35.53	35.42	35.23	35.09	35.23	35.13	35.91	38.24
TiO ₂	4.88	4.54	5.02	5.37	5.04	5.20	5.06	5.04	4.94	4.92	3.79
Al ₂ O ₃	13.69	13.68	13.79	13.81	13.82	13.80	13.54	13.56	14.19	14.31	16.45
FeO*	25.31	25.85	25.82	25.78	26.20	26.00	25.33	25.72	23.57	24.42	19.34
MnO	0.09	0.12	0.09	0.45	0.00	0.00	0.17	0.09	0.13	0.05	0.03
MgO	7.10	7.45	7.26	7.37	7.19	6.93	7.28	7.42	7.99	8.05	6.51
CaO	-0.01	0.02	0.02	0.07	0.05	0.02	0.05	0.10	0.11	0.04	0.13
Na ₂ O	0.53	0.39	0.36	0.58	0.48	0.57	0.38	0.31	0.60	0.42	0.47
K ₂ O	8.36	8.64	8.61	8.50	8.48	8.27	8.27	8.52	8.25	8.45	6.86
Total	94.96	96.10	96.40	97.46	96.68	96.02	95.17	95.99	94.91	96.57	91.82
Normalised values											
Al	34.52	34.19	42.81	33.64	32.94	33.35	33.08	33.30	33.65	33.15	32.87
Mg	24.57	24.32	21.42	22.06	22.68	22.20	22.32	21.91	21.37	22.54	22.74
Fe+Mn	40.91	41.49	35.77	44.29	44.37	44.46	44.59	44.79	44.98	44.31	44.39

Appendix IV: XRD traces

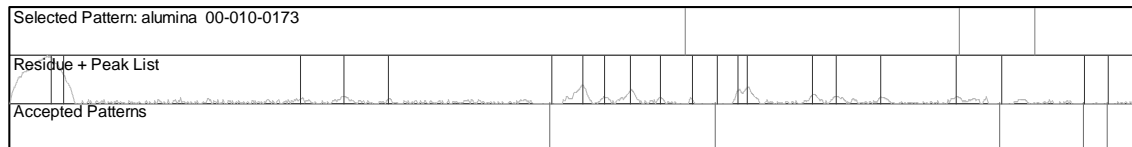
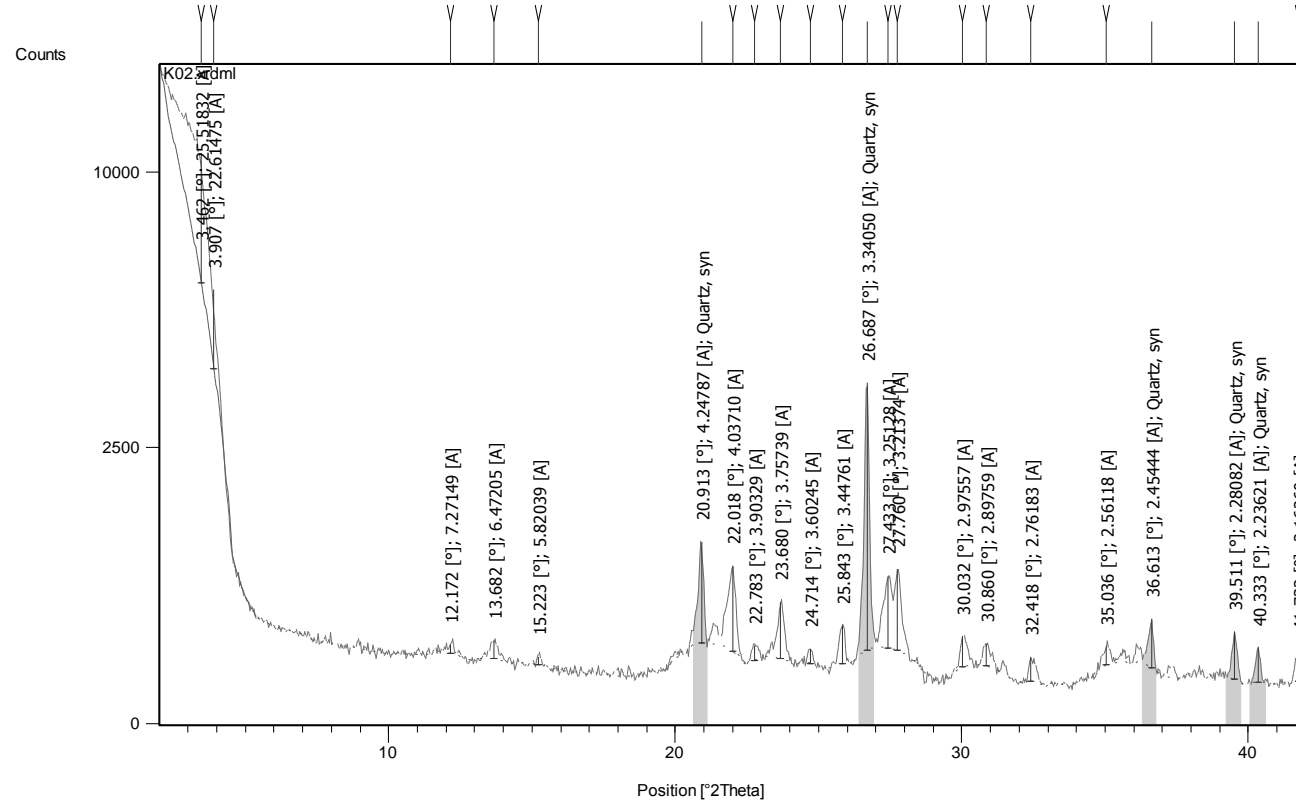
Paku Rhyolite W110850

90I

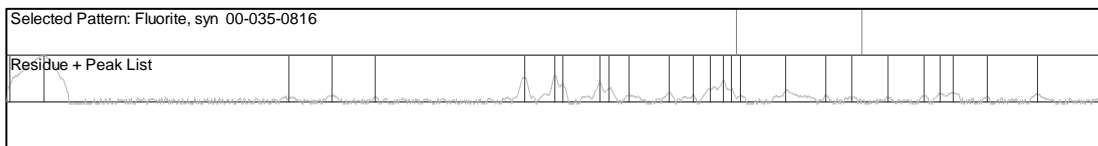
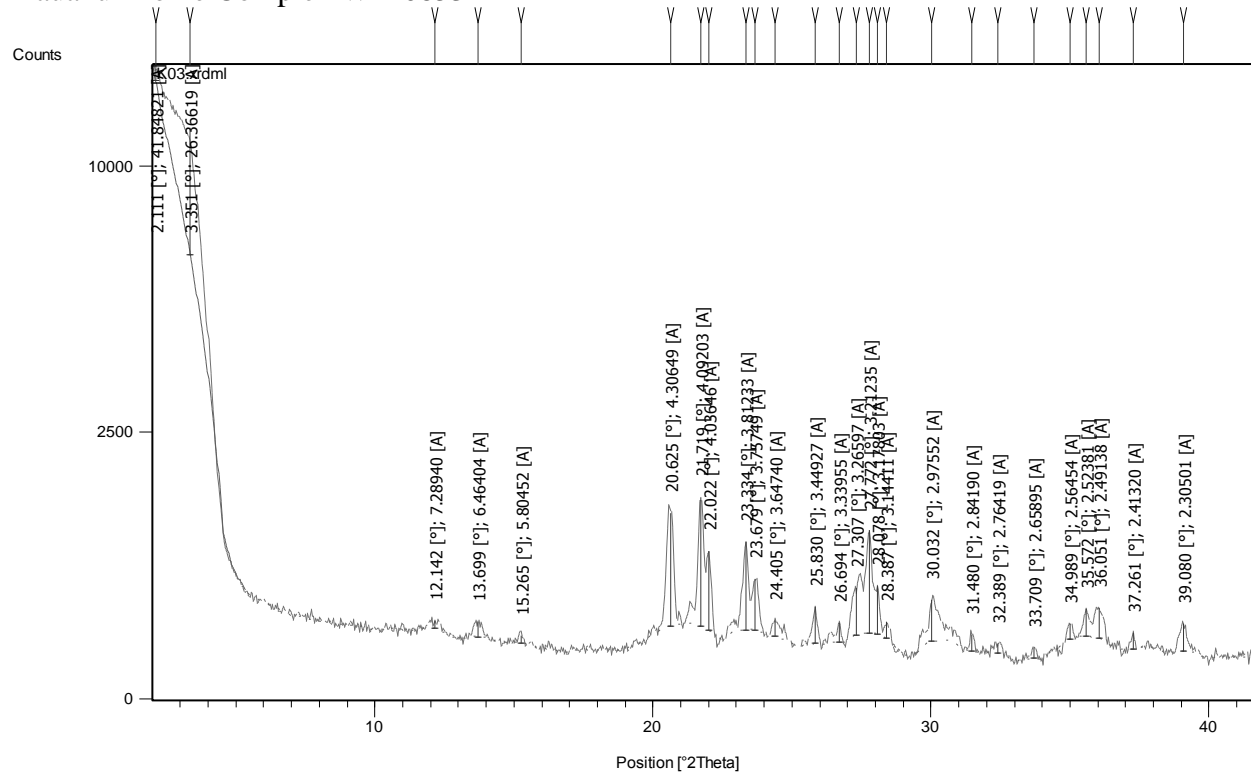


L0I

Timata Dome W110852

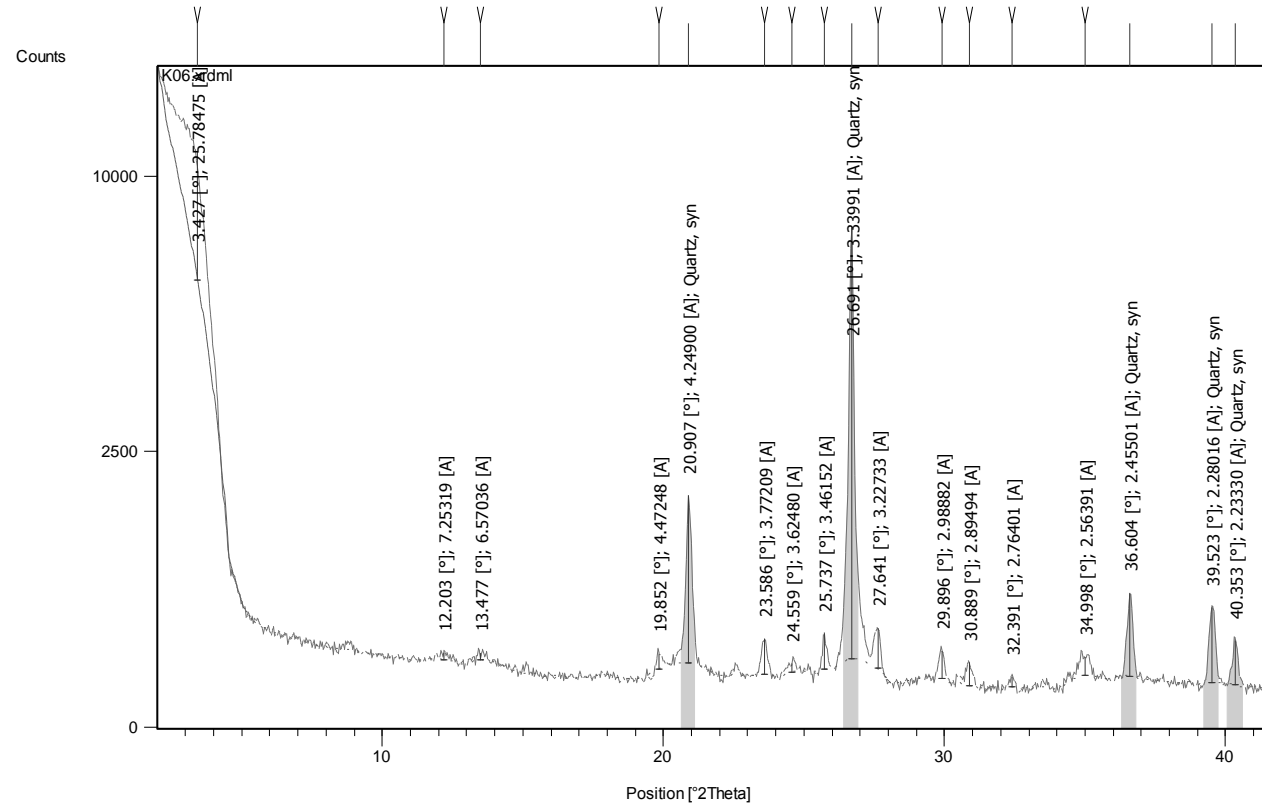


Pauanui Dome Complex W110853



109

Broken Hills Mine sample 1 W110856

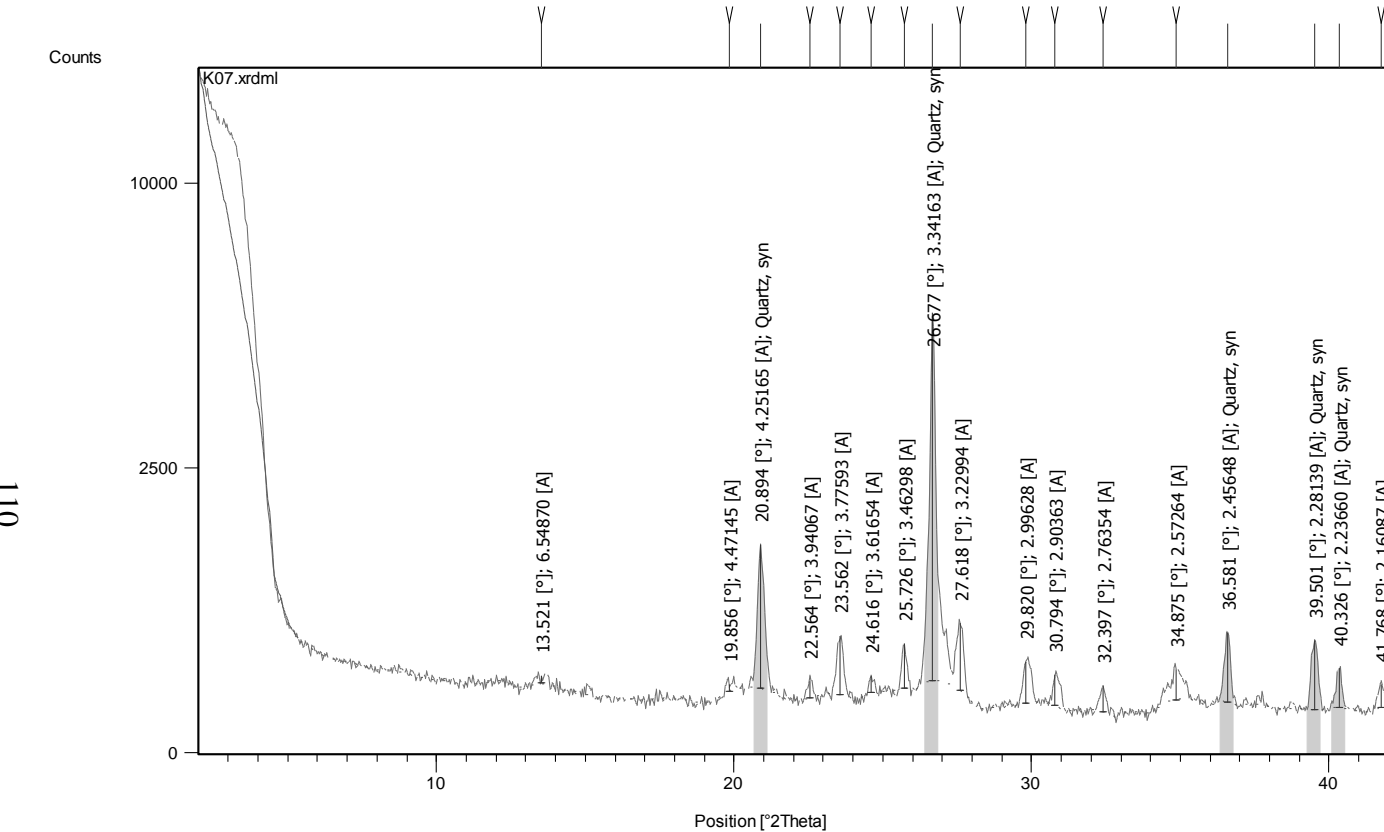


Selected Pattern: alumina 00-010-0173

Residue + Peak List

Accepted Patterns

Broken Hills Mine sample 2 W110857

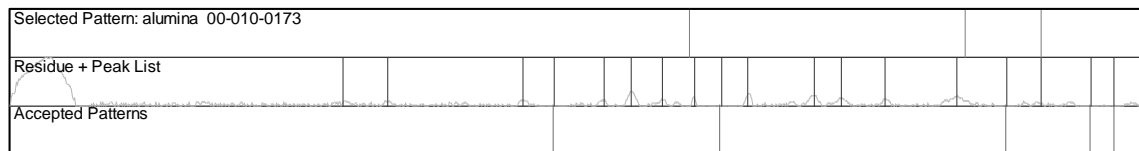
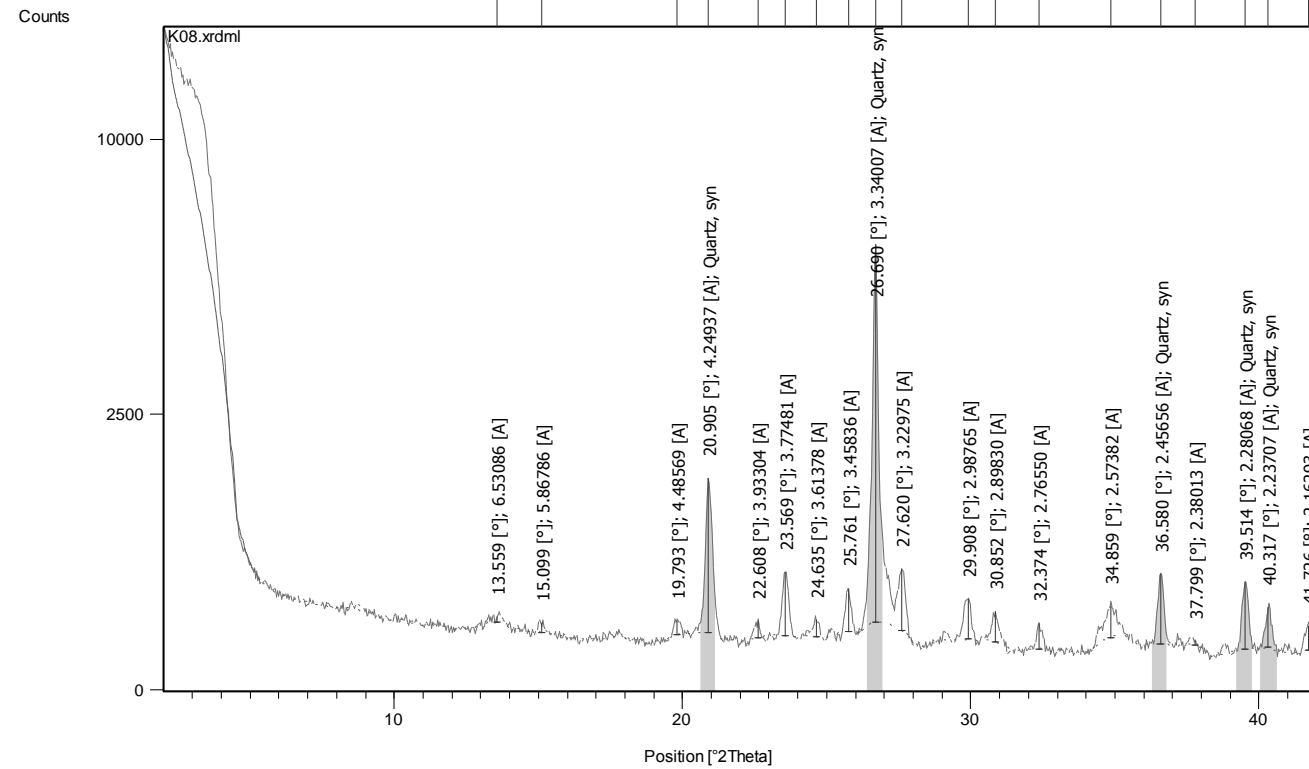


Selected Pattern: alumina 00-010-0173

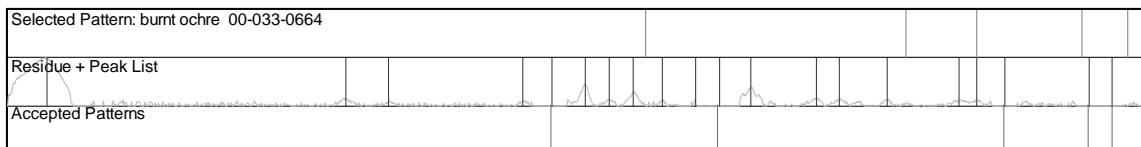
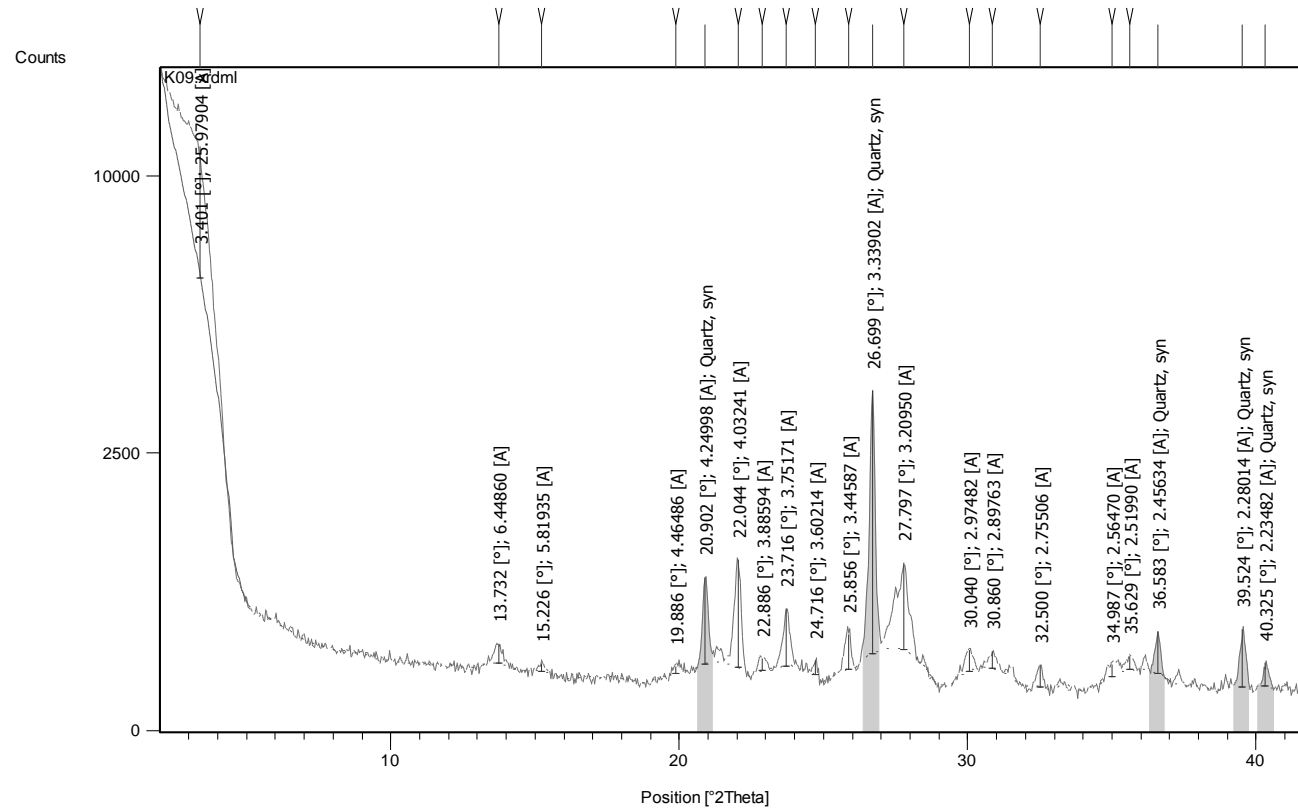
Residue + Peak List

Accepted Patterns

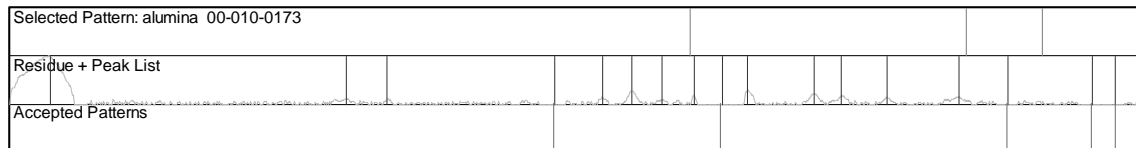
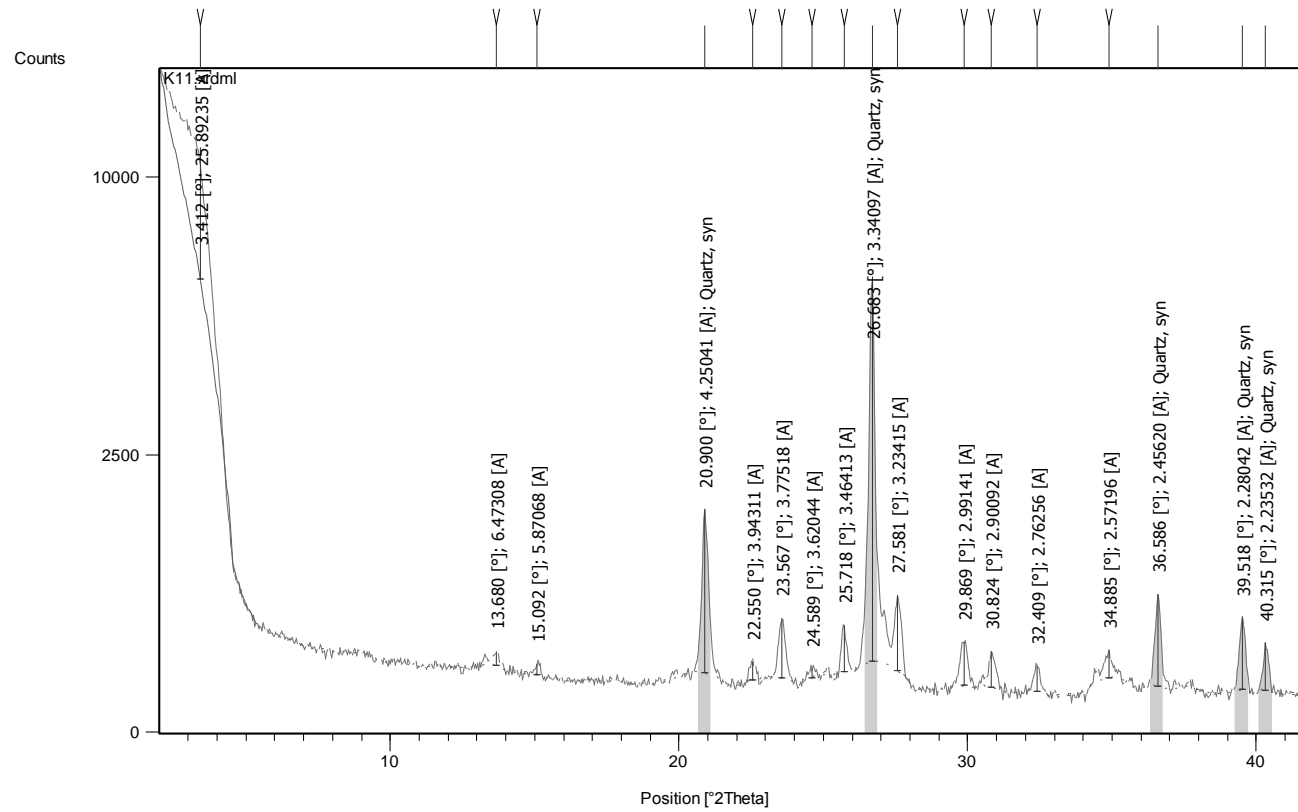
Broken Hills Mine sample 3 W110858



Broken Hills Flow Banded Rhyolite W110859

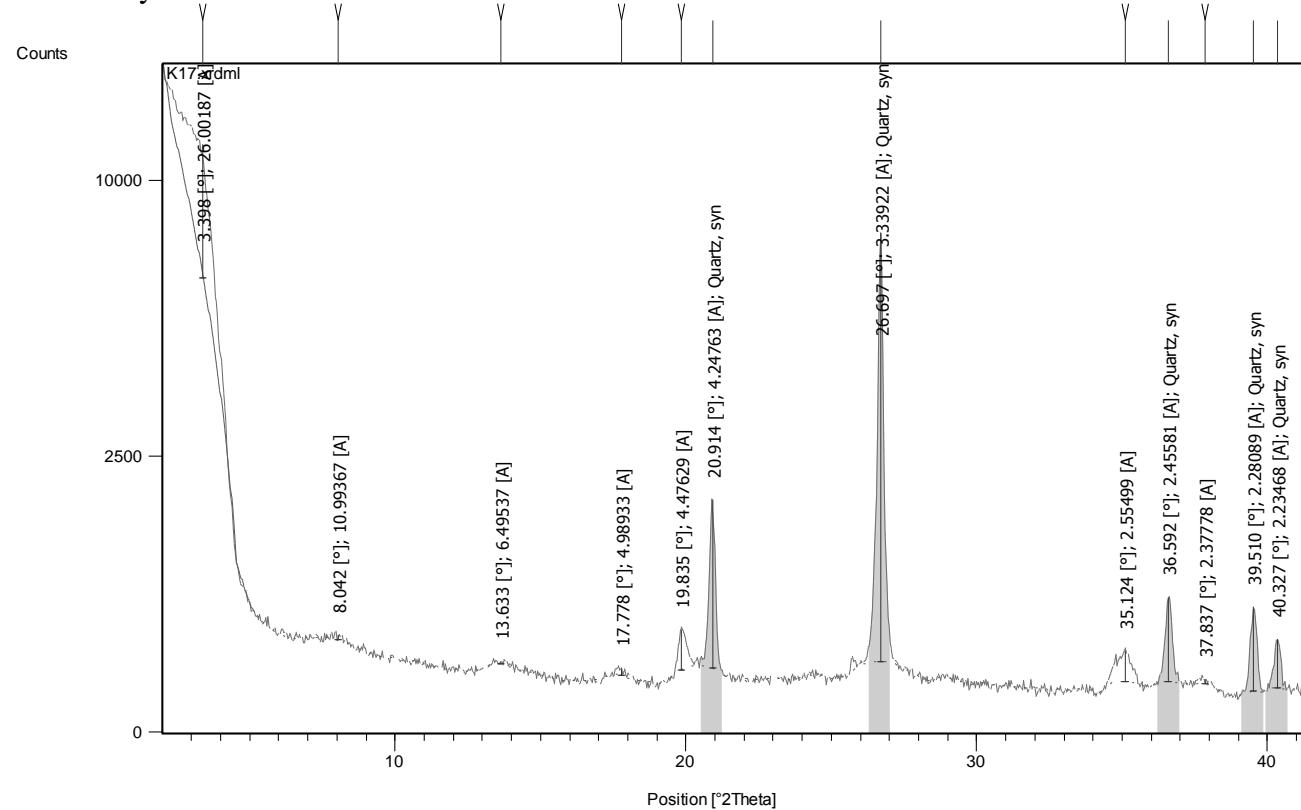


Wharekirauponga Dome W110861



14

Shark Bay Dome W110867



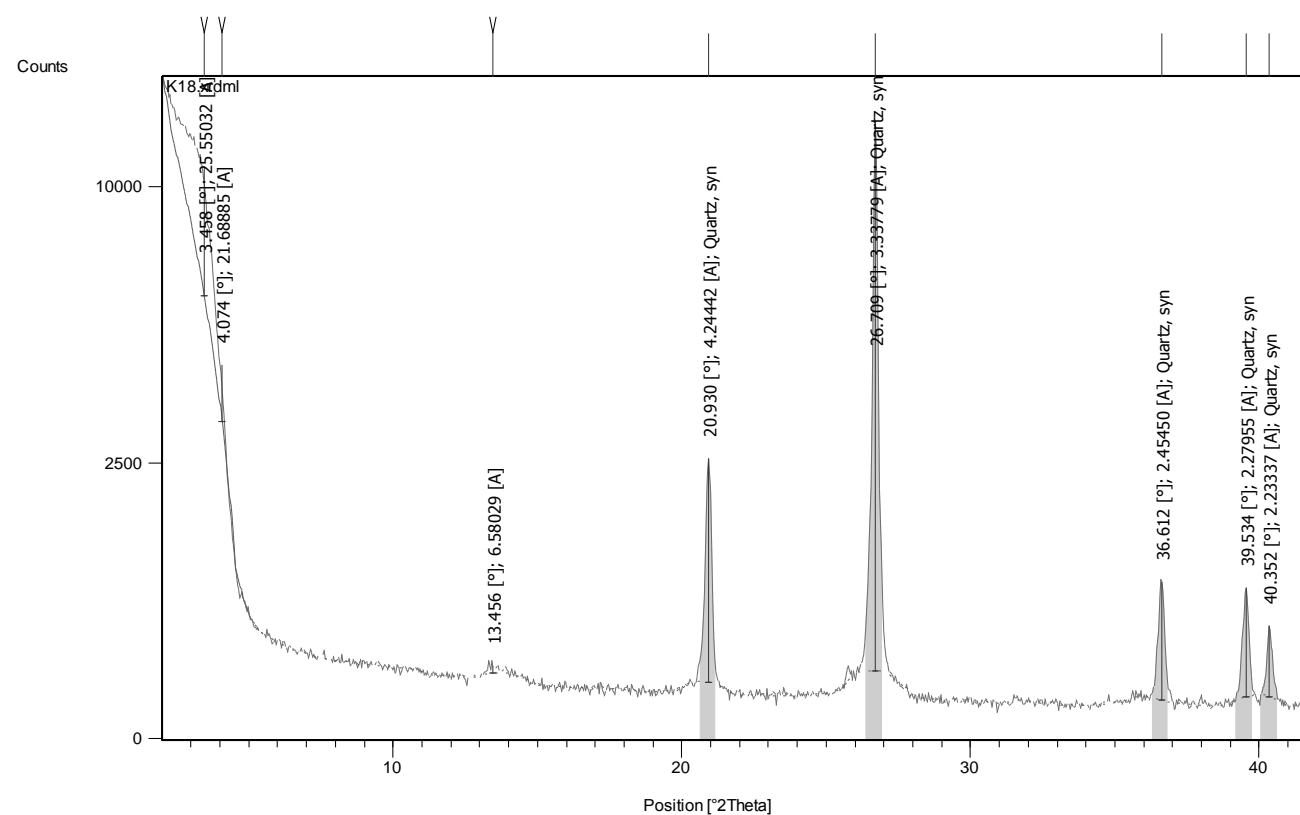
Selected Pattern: alumina 00-010-0173

Residue + Peak List

Accepted Patterns

The Knob W110868

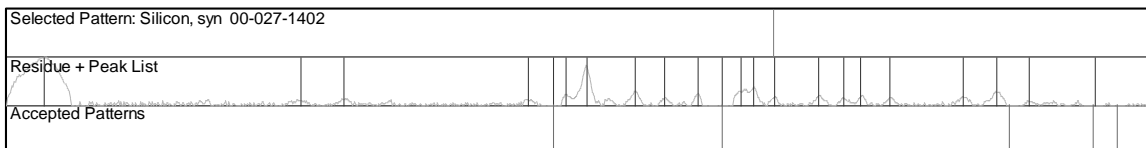
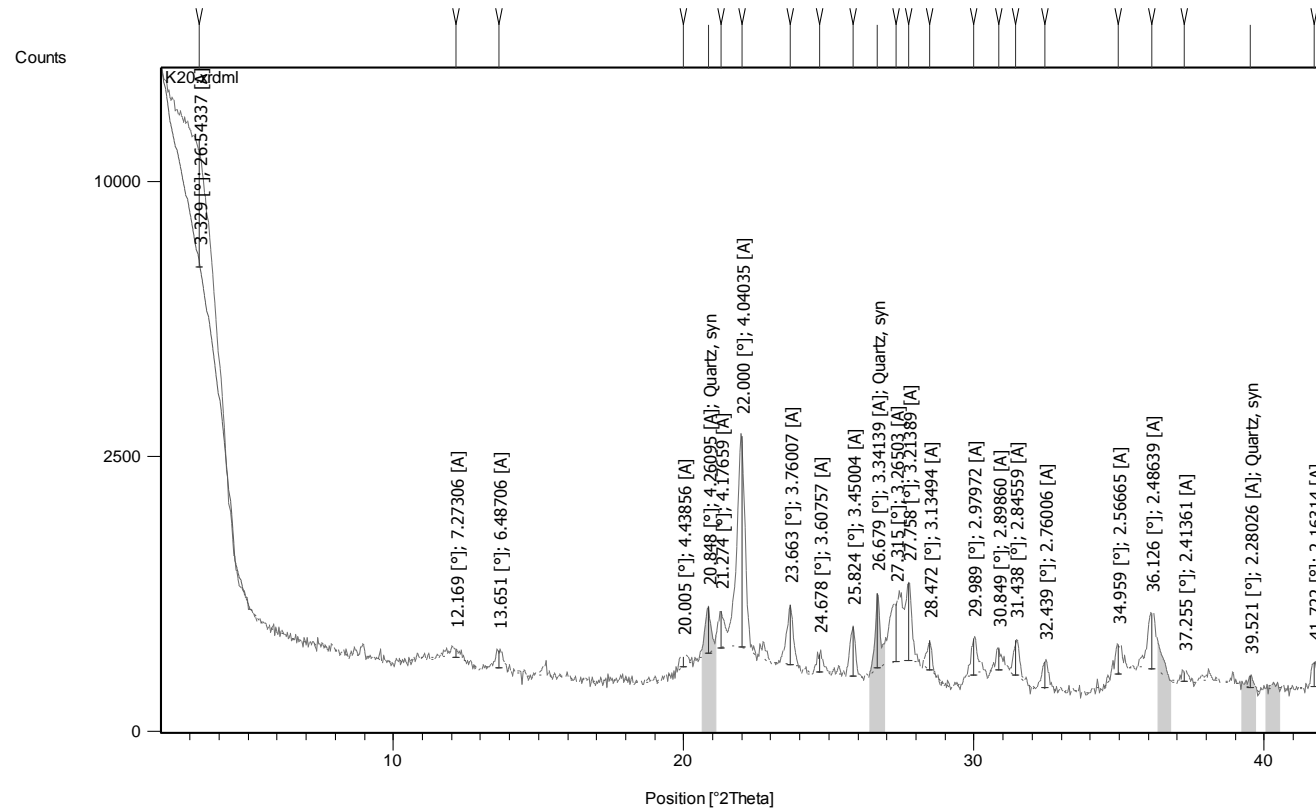
SII



Selected Pattern: alumina 00-010-0173	
Residue + Peak List	
Accepted Patterns	

911

Staircase Dome W110870



Appendix V: Equipment settings

Table V.1: Equipment settings for sample preparation.

Gemini table		
Sample tray	55 Hz	
Table	19.9 Hz	
Vertical magnetic separator		
Current	1.0 Am	
Horizontal magnetic separator		
Tilt	front to back side to side	15 ° 10 °
Current	0.5 Am	
Chute	2	

Appendix VI: LA-ICP-MS specifications

Table VI.1: Operating conditions and data acquisition parameters used for U-Pb dating using LA-ICP-MS.

ICP-MS	
Model	Elan 6100 DRCII ICP-MS (Perkin Elmer Sciex)
Gas flows	Plasma (Ar) 15 L.min Auxiliary (Ar) 1.2 L.min Carrier (He) 1.0 L.min Nebuliser 0.63 L.min
Shield torch	Used for most analyses
Vacuum pressure	1×10^{-5} Torr
Software	Elan 3.4
LA	
Model	New Wave UP-213 Deep Nd YAG – Tempest 20 Hz
Wavelength	5 th Harmonic @ 213 nm
Repetition rate	20 Hz
Pre-ablation laser warm-up	Laser fired continuously
Pulse duration (FWHM)	< 4 ns (stability 3 %)
Beam – expander setting	0
Focussing objective	5X, f.l. = 40 mm
Degree of defocusing	Not known
Spot size	30-60 μm
Incident pulse energy	c. > 1 mJ per pulse
Energy density on sample	c. > 3 mJ
Software	New Wave Research (Merchantek) Laser Ablation System 1.8.13.1
Data Acquisition Parameters	
Data acquisition protocol	Time resolved analyses
Scanning mode	Peak hopping, 1 point per peak
Detector mode	Pulse counting, dead time correction applied
Isotopes determined	^{206}Pb , ^{207}Pb , ^{208}Pb , ^{232}Th , ^{238}U , ^{29}Si , ^{87}Sr , ^{89}Y , ^{91}Zr , ^{177}Hf
Dwell time per isotope	15, 30, 10, 10, 15, 5, 5, 5, 5 ms respectively
Quadrupole settling time	c. 2 ms
Time/scan	c. 89 ms
Data acquisition	180 s (60 s gas blank, up to 120 s ablation)
Software	GLITTER (version 4.4.1). Gemoc Laser ICP-MS.

Table VI.2: Specific information regarding standards used during LA-ICP-MS sessions.

Standards	
Concentration	NIST610 – doped glass standard
Isotope ratio	Gem zircon “GJ1”, 608.5 My
Known/Unknown	Gem zircon “Temora2”, 416.78 My

Table VI.3: Laser parameters as used per standard and unknown sample.

Laser parameters	NIST610	GJ1	Temora2	Unknown
Power output (%)	60	60	60	60
Repetition rate (Hz)	20	20	20	20
Spot size (μm)	60	30	30	30
Dwell time per spot (s)	60	60	45	45
Warm up time (s)	60	60	80	80

Appendix VII: Certificates of authenticity



National Institute of Standards & Technology

Certificate of Analysis

Standard Reference Materials

610, Trace Elements in a Glass Matrix (3 mm Wafer)
611, Trace Elements in a Glass Matrix (1 mm Wafer)

(Nominal Trace Element Concentration 500 mg/kg (ppm))

These Standard Reference Materials (SRMs) were produced and certified to facilitate the development of chemical methods of analysis for trace elements and are one of a series of four pairs of SRMs. For both SRMs, 610 and 611, the nominal trace element concentration is 500 mg/kg for each of the sixty-one elements that have been added to the glass support matrix. The two SRMs differ only in the thickness of the glass wafer. Units of SRMs 610 and 611 are issued as sets of six wafers.

(Certified Values are Listed on Page 2)

These materials were prepared in rod form and have been sliced into wafers. The rods were hand-pulled, and therefore are not uniform over their length. Each wafer is oval to circular in cross-section, with a nominal diameter of 12-14 mm. The certified values are for an entire wafer (no fragment thereof). The debris from wafering has been only partially removed and each wafer should be surface cleaned before use. The first step in preparing the wafer for analysis is to wipe it clean with alcohol, and then to give it a mild surface cleaning (not etch) in dilute (1:10) nitric acid. The wafers were cut with a copper-bonded diamond wheel and the nitric acid step is included to remove any possible copper contamination.

Considerable care and effort have gone into the manufacturing of these SRMs to ensure homogeneity. The target level of precision and accuracy for certification of these materials was 2 percent or better. To date no element has been proven to be heterogeneous outside this limit for the SRM wafer used in its entirety. However, spatial inhomogeneity does exist within each wafer. For certification, two or more methods or laboratories must agree to at least the target level.

The overall direction and coordination of the technical measurements leading to certification were performed under the chairmanship of W.R. Shields.

The technical and support aspects involved in the original preparation, certification, and issuance of these Standard Reference Materials were coordinated through the Standard Reference Materials Program by J.L. Hague. Revision of this certificate was coordinated through the Standard Reference Materials Program by J.S. Kane.

This Certificate of Analysis has undergone editorial revision to reflect program and organizational changes at NIST and at the Department of Commerce. No attempt was made to reevaluate the certificate values or any technical data presented in this certificate.

Gaithersburg, MD 20899
January 27, 1992
(Revision of certificate dated 1-4-82)

William P. Reed, Chief
Standard Reference Materials Program

(over)

Fig. VII.1: Certificate of authenticity, NIST610 glass standard reference material.

A listing of the 61 elements added and the present status of the analytical certification are given in the following table. An asterisk before the element indicates a certified concentration for that element. The indicated limits on the concentration are equal to the entire range of observed results among sample points and/or the 95 percent confidence interval, whichever is larger. Values in parentheses are information values and are not certified, for the reasons given in the footnotes. Nominal composition of the support matrix is 72% SiO₂, 12% CaO, 14% Na₂O, and 2% Al₂O₃.

<u>Element</u>	<u>Value</u>	<u>Notes</u>	<u>Element</u>	<u>Value</u>	<u>Notes</u>
Antimony	--		Boron	(351)	1,a
Arsenic	--		Cadmium	--	
Barium	--		Cerium	--	
Beryllium	--		Cesium	--	
Bismuth	--		Chlorine	--	
Chromium	--		Europium	--	
Cobalt	(390)	2,b,c	Fluorine	--	
Copper	(444±4)	3,a	Gadolinium	--	
Dysprosium	--		Gallium	--	
Erbium	--		Germanium	--	
Gold	(25)	4,b,d	Lanthanum	--	
Hafnium	--		*Lead	426±1	6,a,f
Holmium	--		Lithium	--	
Indium	--		Lutetium	--	
*Iron	458±9	5,d,e	Magnesium	--	
*Manganese	485±10	7,d,g	Phosphorus	--	
Molybdenum	--		Potassium	(461)	1,a
Neodymium	--		Praseodymium	--	
*Nickel	458.7±4	8,a,d,e	Rhenium	--	
Niobium	--		*Rubidium	425.7±0.8	9,a,h,j
Samarium	--		Sulfur	--	
Scandium	--		Tantalum	--	
Selenium	--		Tellurium	--	
Silver	(254±10)	10,a,b	Terbium	--	
*Strontium	515.5±0.5	11,a,h,j	Thallium	(61.8±2.5)	12,a
*Thorium	457.2±1.2	13,a,f	*Uranium	461.5±1.1	15,a,f
Thulium	--		Vanadium	--	
Tin	--		Ytterbium	--	
Titanium	(437)	14,e	Yttrium	--	
Tungsten	--		Zinc	(433)	16,k
			Zirconium	--	

(All values given in table are in mg/kg (ppm) by weight.)

-2-

Fig. VII.1 cont.: Certificate of authenticity, NIST610 glass standard reference material.

DEPT. OF EARTH & PLANETARY SCIENCES,
MACQUARIE UNIVERSITY
SYDNEY, NSW, AUSTRALIA 2109
Telephone: (02) 9850 6126
(ISD): 61 2 9850 6126
Fax: (02) 9850 6904
(ISD): 61 2 9850 6904
Email: ebelouso@cls.mq.edu.au



Australian Research Council
NATIONAL KEY CENTRE
GEOCHEMICAL EVOLUTION AND METALLOGENY OF CONTINENTS

5 November, 2007

Amber Whittaker
Dept Earth and Ocean Sciences
University of Waikato
Hamilton
New Zealand

Re: GJ1 zircon standard

Dear Amber,

Please find enclosed a piece of the GEMOC GJ1 zircon standard.
Please notice that this pieces number is GJ1/50. The table with TIMS data for the GJ1 standard is attached. We suggest that you obtain a TIMS age on the individual fragment to see that it does not deviate from what we already know, and we ask that you send us these data.

Please e-mail me when you receive the standard and I will organize an invoice for it.

Best wishes,

Elena Belousova

Fig. VII.1: Certificate of authenticity, gem zircon GJ1.

TIMS Data: GJ Zircon Standard									
Fraction	Weight [ug]	PbI [ppm]	U [ppm]	Th/U	PbC [ppm]	PbCom [ppm]	206/204	207/235	2 sigma [abs]
(1)	(2)	(2)	(2)	(3)	(4)	(5)	(6)	(7)	(7)
GJ4 019/51	2949	19.5	215	0.06	0.00	9	420650	0.8125	0.0022
GJ4 019/52	1519	19.3	212	0.06	0.01	14	146133	0.8126	0.0018
GJ3 019/53A	6119	27.9	313	0.02	0.00	26	452072	0.8067	0.0034
GJ3 019/53B	6119	27.9	313	0.02	0.00	22	533252	0.8064	0.0030
GJ2 019/56	3144	37.4	422	0.02	0.00	13	612660	0.8034	0.0035
GJ2 019/59	2876	33.3	373	0.02	0.00	11	610787	0.8058	0.0027
GJ1 019/61A	4800	20.2	224	0.03	0.01	39	170396	0.8119	0.0033
GJ1 019/61B	4800	20.1	224	0.03	0.00	12	543384	0.8074	0.0027
91500 019/58A	738	14.1	77	0.35	0.05	55	11494	1.8476	0.0100
91500 019/58B	738	14.0	77	0.34	0.01	10	62869	1.8543	0.0037

(1) one zircon fragment in each fraction; A and B denote fractions split after spiking, dissolution, and HCl re-equilibration, but before chemical separation.
(2,4) weights better than 0.5%; U and Pb concentrations probably +/- 10% (spike concentration uncertainty)
(3) Th/U model ratio inferred from 206/204 ratio and age of sample
(4) PbC=initial common Pb
(5) Total common Pb in sample (initial +blank)
(6) raw data corrected for fractionation and blank
(7) corrected for fractionation, spike, blank and initial common Pb (estimated from Stacey and Kramers (1975) model); error calculated by propagating the main sources of uncertainty; error does not include uncertainty of U-Pb ratio in spike, about 0.1% based on spike calibration results.
(8) degree of discordance (in percent).

Fraction	208/206	208/232	232/208	MODEL	MODEL	sample
(1)	(7)	(9)	(9)			
GJ4 019/51	0.01945	0.0303	33.04	GJ4	019/51	
GJ4 019/52	0.01991	0.0302	33.06	GJ4	019/52	
GJ3 019/53A	0.00654	0.03	33.28	GJ3	019/53	
GJ3 019/53B	0.00654	0.03	33.29	GJ3	019/53B	
GJ2 019/56	0.00619	0.0299	33.41	GJ2	019/56	
GJ2 019/59	0.00584	0.03	33.28	GJ2	019/59	
GJ1 019/61A	0.01079	0.0302	33.07	GJ1	019/61A	
GJ1 019/61B	0.01079	0.0301	33.25	GJ1	019/61B	
91500 019/58A	0.10745	0.0539	18.56	91500	019/58A	
91500 019/58B	0.10750	0.0541	18.50	91500	019/58B	

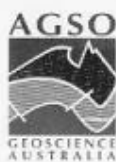
(9) model 208Pb/232Th ratio, calculated from 206/204 ratio assuming same degree of discordance as U-Pb ratios

Fig. VII.3: Relative element concentrations of the key U-Pb isotopes and the known TIMS age of the GJ1 crystal.

WITH COMPLIMENTS

Page 1 of 1

02/08/2006



<@ga.gov.au>

Temora 2
Zircon Standard
0.01g minor impurities present

S Ridgway
for Lance Black

L NAME

Telephone: (02) 6249 9111
Facsimile: (02) 6249 9999
website: www.agso.gov.au
ABN 60 001 780 039

Cnr Jerrabomberra Avenue & Hindmarsh Drive,
Symonston ACT 2609
GPO Box 378, Canberra,
ACT, 2601, Australia

Dear Peter,

Following a request from Keith Sircombe after he visited you, our Minsep team sent 0.01 grams of the TEMORA standard to you last week. The supply you receive will be about 95% pure, and there will also be some inferior grains of zircon present, some of which will contain inclusions of iron oxide. It will be up to you to handpick the grains to the calibre you need. Unfortunately, we do not have the resources to do this, particularly as the standard is now being used in more than 70 different laboratories. What you will be receiving, in common with those other laboratories, is the TEMORA 2 standard. I presume you are fully aware that the latest reference to the standard is in Black et al (Chemical Geology 205, 115-140), which also lists the earlier references.

Please advise me when the standard arrives, or let me know if it has not arrived by this time next week. We have been finding that it is commonly delayed in the mail for "security reasons". I guess it might be confused with anthrax or cocaine, or something similar.

Best wishes,

Lance

Middledale Gabbroic Diorite Paleozoic Lachlan Orogen
Eastern Australia

$^{206}\text{Pb}/^{238}\text{U}$ age 416.5 ± 0.22 Ma
 416.78 ± 0.33 Ma best estimate

11/08/2006

Fig. VII.4: Certificate of authenticity, Temora2.

Appendix VIII: Isotope ratios

The following tables summarise the colour, $^{206}\text{Pb}/^{238}\text{U}$ and $^{207}\text{Pb}/^{235}\text{U}$ isotope ratio, age estimate data and associated 1σ age errors for the 18 samples that were dated in this study. Zircon crystals that are discordant, have low probability of concordance (< 5 %), have large errors (> 50 %), or display negative values are displayed with a strike through the data. These crystals have not been included in any subsequent age data analysis.

Table VIII.1: Timata Dome W110852

Spot No.	Colour	Measured isotope ratios and 1σ (%) internal errors						Estimated ages and 1σ absolute internal errors (My)				$^{206}\text{Pb}/^{238}\text{U}$ & $^{207}\text{Pb}/^{235}\text{U}$ Concordance (%)	Spot MSWD	Selected age and 1σ absolute external error (My)			
		$^{207}\text{Pb}/^{206}\text{Pb}$	\pm	$^{206}\text{Pb}/^{238}\text{U}$	\pm	$^{207}\text{Pb}/^{235}\text{U}$	\pm	$^{208}\text{Pb}/^{232}\text{Th}$	\pm	$^{206}\text{Pb}/^{238}\text{U}$	\pm	$^{207}\text{Pb}/^{235}\text{U}$	\pm				
K02-1	pink	0.07767	0.03357	0.00142	0.00014	0.01716	0.00728	0.0003	0.00013	9.2	0.87	17.3	7.27	21	1.6	8.16	0.44
K02-2	light pink	0.20423	0.05208	0.00121	0.00013	0.03644	0.00854	0.00055	0.00015	7.8	0.86	36.3	8.37	DISCORDANT			
K02-3	light pink	0.10164	0.06408	0.0015	0.00023	0.02106	0.01295	0.00148	0.00032	9.7	1.47	21.2	12.88	32	0.98	8.4	0.72
K02-4	light pink	0.065	0.04701	0.00136	0.00017	0.01268	0.00905	0.00127	0.00022	8.7	1.1	12.8	9.08	62	0.25	8.3	0.53
K02-5	light pink	0.12619	0.03151	0.00144	0.00012	0.0235	0.0056	0.00056	0.0001	9.3	0.8	23.6	5.55	0.4	8.5	7.32	14
K02-6	light pink	0.20715	0.02706	0.0013	0.00009	0.03838	0.00454	0.00063	0.00008	8.4	0.55	38.2	4.44	DISCORDANT			
K02-7	light pink	0.05295	0.02444	0.00129	0.00011	0.00944	0.0043	0.0004	0.00009	8.3	0.73	9.5	4.32	74	0.11	8.11	0.36
K02-8	light pink	0.04839	0.01055	0.00123	0.00006	0.00837	0.0018	0.00049	0.00006	7.9	0.39	8.5	1.81	71	0.13	7.8	0.21
K02-9	light pink	0.20783	0.07518	0.00122	0.0002	0.03709	0.01224	0.00093	0.00022	7.8	1.26	37	11.99	0.8	7	4.9	24
K02-11	light pink	0.15626	0.06055	0.00165	0.00023	0.03744	0.01372	0.00002	0.00028	10.6	1.54	37.3	13.42	3	4.7	7.8	20
K02-12	light pink	0.06982	0.01279	0.00119	0.00006	0.01183	0.00211	0.00042	0.00004	7.7	0.4	11.9	2.12	4.7	5.7	6.87	6.4
K02-13	light pink	0.06455	0.03426	0.00195	0.0002	0.01715	0.00898	0.00068	0.00019	12.5	1.26	17.3	8.97	55	0.36	11.9	0.64
K02-15	light pink	0.51664	0.11399	0.00115	0.00018	0.08795	0.0149	0.00096	0.00023	7.4	1.14	85.6	13.94	DISCORDANT			
K02-16	light pink	0.05097	0.01693	0.00138	0.00009	0.01	0.00328	0.00067	0.00011	8.9	0.58	10.1	3.29	66	0.19	8.67	0.3
K02-17	light pink	0.05039	0.03498	0.0013	0.00014	0.00866	0.00596	0.00112	0.00024	8.4	0.88	8.8	6	94	0.0053	8.32	0.45
K02-18	light pink	0.08864	0.02085	0.00122	0.00009	0.0152	0.00345	0.00093	0.00006	7.8	0.57	15.3	3.45	1.2	6.4	6.6	9.5
K02-19	light pink	0.11069	0.05443	0.00116	0.00016	0.01785	0.00849	0.00059	0.00017	7.5	1.02	18	8.47	17	1.9	6.2	0.5
K02-20	light pink	0.36064	0.05805	0.00158	0.00016	0.07599	0.01035	0.00218	0.00038	10.2	1.01	74.4	9.76	DISCORDANT			
K02-21	light pink	0.14765	0.0462	0.00128	0.00015	0.02754	0.00814	0.00064	0.00014	8.3	0.96	27.6	8.04	0.8	7.1	6	16
K02-22	light pink	0.09283	0.01479	0.00134	0.00007	0.01751	0.00269	0.0004	0.00006	8.7	0.48	17.6	2.68	DISCORDANT			
K02-23	light pink	0.23868	0.05243	0.00173	0.00018	0.05602	0.01124	0.00144	0.00025	11.1	1.18	55.3	10.81	DISCORDANT			
K02-24	light pink	0.14654	0.02867	0.00163	0.00012	0.03652	0.0068	0.00075	0.00011	10.5	0.8	36.4	6.66	DISCORDANT			
K02-25	light pink	0.116	0.03196	0.00144	0.00013	0.0237	0.00628	0.00056	0.00017	9.3	0.83	23.8	6.23	0.9	6.9	7.37	14
K02-26	light pink	0.13443	0.04619	0.00168	0.0002	0.03112	0.01022	0.00062	0.00018	10.8	1.27	31.1	10.06	2.5	5	8.3	18
K02-27	light pink	0.09844	0.03331	0.00123	0.00012	0.01654	0.00542	0.00059	0.00012	7.9	0.77	16.7	5.41	6.6	3.4	6.69	0.39
K02-28	light pink	0.10934	0.01947	0.00736	0.00048	0.10525	0.0189	0.00173	0.0004	47.3	3.05	101.6	17.37	DISCORDANT			
K02-29	light pink	0.30146	0.06303	0.00138	0.00016	0.05896	0.01075	0.00094	0.00018	8.9	1.03	58.2	10.34	DISCORDANT			
K02-30	light pink	0.06329	0.00966	0.00121	0.00005	0.01051	0.00158	0.00051	0.00006	7.8	0.34	10.6	1.59	3.4	4.6	7.21	4.7
K02-31	light pink	0.0884	0.00948	0.00127	0.00005	0.01545	0.00163	0.00061	0.00008	8.2	0.32	15.6	1.63	DISCORDANT			
K02-32	light pink	0.15849	0.03915	0.00104	0.00011	0.02339	0.00538	0.00046	0.00008	6.7	0.69	23.5	5.34	DISCORDANT			
K02-33	light pink	0.08867	0.04176	0.00166	0.00019	0.02218	0.01023	0.00066	0.00019	10.7	1.21	22.3	10.16	21	1.6	9.3	0.6
K02-34	light pink	0.36136	0.06268	0.00215	0.00022	0.10653	0.01618	0.00144	0.00034	13.8	1.44	102.8	14.84	DISCORDANT			
K02-35	light pink	0.51666	0.05495	0.00526	0.00038	0.36111	0.03704	0.01439	0.00182	33.8	2.46	313	27.63	DISCORDANT			
K02-36	light pink	0.16729	0.05914	0.00147	0.0002	0.03708	0.01237	0.00084	0.00026	9.4	1.29	37	12.11	1.4	6.1	6.7	19
K02-37	light pink	0.17532	0.03476	0.00132	0.00012	0.03109	0.00569	0.00064	0.00013	8.5	0.77	31.1	5.56	DISCORDANT			
K02-38	light pink	0.54273	0.23013	0.0012	0.00036	0.09871	0.03118	0.0011	0.00057	7.7	2.31	95.6	28.81	0.2	9.8	1.3	43

K02-39	light pink	0.17915	0.03108	0.00137	0.00011	0.03444	0.00557	0.00044	0.00008	8.8	0.7	34.4	5.47	DISCORDANT
K02-40	light pink	0.28837	0.0695	0.00172	0.00022	0.06751	0.01445	0.00237	0.00049	11.1	1.43	66.3	13.74	DISCORDANT
K02-42	light pink	0.2666	0.09366	0.00101	0.00018	0.03504	0.01085	0.00096	0.00026	6.5	1.16	35	10.65	0.4
K02-43	light pink	0.12449	0.0554	0.00118	0.00016	0.02364	0.01015	0.00071	0.0002	7.6	1.02	23.7	10.07	8.1
K02-44	light pink	0.04755	0.03132	0.00155	0.00016	0.01009	0.00659	0.00048	0.00013	10	1.03	10.2	6.63	97
K02-45	light pink	0.09246	0.04381	0.00144	0.00017	0.01836	0.00851	0.00085	0.00018	9.3	1.07	18.5	8.49	22
K02-46	light pink	0.16876	0.06085	0.00154	0.00021	0.03779	0.01285	0.00083	0.00024	9.9	1.37	37.7	12.57	1.6
K02-47	light pink	0.06205	0.05283	0.00096	0.00014	0.00847	0.00713	0.00042	0.00013	6.2	0.88	8.6	7.18	71
K02-48	light pink	0.19701	0.06828	0.00134	0.00021	0.03774	0.01293	0.00066	0.00022	8.6	1.33	37.6	11.77	0.7
K02-49	light pink	0.2008	0.07573	0.00105	0.00017	0.02932	0.01019	0.00064	0.00018	6.8	1.09	29.3	10.05	1.4
K02-50	light pink	0.05175	0.00927	0.00115	0.00005	0.0081	0.00145	0.00037	0.00006	7.4	0.34	8.2	1.46	51
K02-51	light pink	0.06127	0.0579	0.00098	0.00015	0.00837	0.00782	0.00038	0.00014	6.3	0.96	8.5	7.88	76
K02-52	light pink	0.07261	0.04274	0.00126	0.00015	0.01181	0.00685	0.00068	0.00018	8.1	0.96	11.9	6.88	53
K02-53	light pink	0.07067	0.03642	0.0012	0.00013	0.01214	0.00615	0.00053	0.00012	7.7	0.86	12.3	6.17	41
K02-54	light pink	0.12403	0.05228	0.00109	0.00015	0.01739	0.00703	0.00028	0.00018	7	0.95	17.5	7.02	9.1
														2.9
														5.6
														0.48

Table VIII.2: Pohakahaka Dome Complex W110854

Spot No.	Colour	Measured isotope ratios and 1 σ (%) internal errors					Estimated ages and 1 σ absolute internal errors (My)			$^{206}\text{Pb}/^{238}\text{U}$ & $^{207}\text{Pb}/^{235}\text{U}$		Concordance (%)	Spot MSWD	Selected age and 1 σ absolute external error (My)			
		$^{207}\text{Pb}/^{206}\text{Pb}$	\pm	$^{206}\text{Pb}/^{238}\text{U}$	\pm	$^{207}\text{Pb}/^{235}\text{U}$	\pm	$^{208}\text{Pb}/^{232}\text{Th}$	\pm	$^{206}\text{Pb}/^{238}\text{U}$	\pm	$^{207}\text{Pb}/^{235}\text{U}$	\pm				
K04-1	light pink	0.19096	0.04098	0.00079	0.00008	0.02004	0.00391	0.00054	0.00008	5.1	0.5	20.1	3.89	DISCORDANT			
K04-2	light pink	0.20966	0.0707	0.00124	0.00018	0.03622	0.01123	0.00215	0.00045	8	1.17	36.1	11.01	0.6	7.7	5.2	20
K04-3	pink	0.31759	0.15791	0.00082	0.00019	0.03611	0.01623	0.00101	0.00046	5.3	1.19	36	15.9	4.1	4.2	3.1	15
K04-4	light pink	0.27782	0.09359	0.00099	0.00016	0.03787	0.01145	0.00113	0.00032	6.4	1.03	37.7	11.2	0.3	9	3.66	19
K04-6	light pink	0.21341	0.25292	0.00035	0.00016	0.01113	0.01242	0.00045	0.00032	2.3	1.02	11.4	12.47	43	0.62	1.54	0.48
K04-7	pink	0.13098	0.03395	0.00113	0.0001	0.02061	0.00507	0.00074	0.00021	7.3	0.68	20.7	5.04	0.3	8.9	5.61	12
K04-8	pink	0.33878	0.0644	0.00129	0.00014	0.06714	0.01103	0.0019	0.00029	8.3	0.91	66	10.49	DISCORDANT			
K04-9	pink	0.05023	0.08336	0.00099	0.00022	0.00708	0.01166	0.00046	0.00029	6.4	1.43	7.2	11.76	94	0.0056	6.3	0.69
K04-10	light pink	0.11086	0.03509	0.00082	0.00008	0.01299	0.00393	0.00044	0.0001	5.3	0.54	13.1	3.94	2.5	5	4.28	7.2
K04-11	light pink	0.07597	0.04011	0.00431	0.00052	0.04926	0.02581	0.00263	0.00081	27.7	3.36	48.8	24.97	34	0.89	25	1.6
K04-12	light pink	0.40816	0.08863	0.00132	0.00018	0.078	0.01404	0.00273	0.00047	8.5	1.18	76.3	13.23	DISCORDANT			
K04-13	light pink	0.05593	0.03888	0.0007	0.00009	0.0052	0.00356	0.00047	0.00011	4.5	0.57	5.3	3.6	81	0.06	4.39	0.29
K04-14	light pink	0.07528	0.0486	0.00089	0.00012	0.00974	0.00618	0.00026	0.00014	5.8	0.76	9.8	6.21	46	0.55	5.24	0.38
K04-15	light pink	0.13929	0.04414	0.00086	0.0001	0.01564	0.00468	0.00046	0.00015	5.5	0.64	15.8	4.68	1.3	6.1	4.16	10
K04-17	light pink	0.05072	0.00559	0.02099	0.00068	0.14585	0.01779	0.0056	0.0008	133.9	4.31	138.2	15.76	72	0.13	132.6	2.4
K04-18	light pink	0.09615	0.04919	0.00091	0.00012	0.01227	0.0061	0.00074	0.00018	5.8	0.78	12.4	6.12	23	1.4	5.06	0.38
K04-19	light pink	0.16447	0.07891	0.00166	0.0003	0.03483	0.01571	0.00046	0.00057	10.7	1.95	34.8	15.42	8.3	3	7.8	0.94
K04-20	light pink	0.27296	0.11808	0.00067	0.00014	0.02661	0.01018	0.00078	0.00023	4.3	0.91	26.7	10.07	1.7	5.7	2.42	13

K04-21	light pink	0.12404	0.04352	0.00084	0.00009	0.0138	0.00464	0.00027	0.00009	5.4	0.61	13.9	4.64	4.1	4.2	4.38	7.4
K04-22	light pink	0.08341	0.06666	0.00083	0.00014	0.01023	0.00802	0.00024	0.00022	5.4	0.9	10.3	8.06	49	0.47	4.81	0.44
K04-23	light pink	0.48436	0.46215	0.00026	0.00015	0.02012	0.01502	0.001	0.00041	1.7	4	20.2	14.95	19	1.7	0.56	0.45
K04-24	light pink	0.18515	0.07162	0.00125	0.00019	0.03044	0.011	0.00094	0.00024	8	1.24	30.4	10.84	2.3	5.1	5.6	17
K04-25	colourless	0.1298	0.05245	0.00095	0.00013	0.01614	0.00622	0	0.00017	6.1	0.82	16.3	6.21	6.6	3.4	4.78	0.41
K04-28	colourless	0.07946	0.03215	0.00062	0.00007	0.00643	0.00251	0.00019	0.00005	4	0.47	6.5	2.53	24	1.4	3.54	0.23
K04-29	colourless	0.05125	0.00952	0.02259	0.00118	0.17472	0.03642	0.01043	0.00171	144	7.41	163.5	31.48	44	0.59	139.2	4.1
K04-30	colourless	0.08457	0.03897	0.00467	0.00054	0.0501	0.02289	0.00139	0.00073	30	3.47	49.6	22.14	31	1.03	27	1.7
K04-31	colourless	0.10258	0.05018	0.00054	0.00008	0.00744	0.00351	0.00061	0.00013	3.5	0.49	7.5	3.53	49	1.7	2.9	0.26
K04-32	pink	0.21297	0.04576	0.00081	0.00009	0.02252	0.00435	0.00047	0.00012	5.2	0.56	22.6	4.34	DISCORDANT			
K04-33	pink	0.09546	0.05729	0.00076	0.00011	0.01021	0.00598	0.00026	0.00014	4.9	0.7	10.3	6.01	32	1.01	4.28	0.34
K04-34	pink	0.18623	0.06211	0.00192	0.00027	0.05365	0.01682	0.00244	0.00061	12.4	1.74	53.4	16.21	0.7	7.3	8.2	29
K04-35	pink	0.1459	0.06584	0.00107	0.00016	0.01927	0.00831	0.00068	0.00022	6.9	1.02	19.4	8.28	9.2	2.8	5.4	0.5
K04-36	pink	0.53187	0.11233	0.00198	0.00029	0.14529	0.02527	0.00434	0.00089	12.7	1.85	137.7	22.41	DISCORDANT			
K04-37	pink	0.06441	0.03971	0.00084	0.0001	0.00782	0.00474	0.00033	0.00011	5.4	0.67	7.9	4.78	55	0.35	5.08	0.32
K04-38	pink	0.05252	0.0093	0.01503	0.00072	0.10929	0.02063	0.00546	0.00105	96.2	4.56	105.3	18.88	54	0.37	93.8	2.5
K04-39	pink	0.47225	0.1682	0.00116	0.00028	0.07507	0.02118	0.00202	0.00063	7.5	1.78	73.5	20	DISCORDANT			
K04-40	pink	0.57721	0.13764	0.0014	0.00024	0.13473	0.02532	0.00245	0.00059	9	1.57	128.3	22.66	DISCORDANT			
K04-41	light pink	0.09139	0.03944	0.00067	0.00008	0.00804	0.00334	0.00044	0.00014	4.3	0.52	8.4	3.37	49	1.7	3.74	0.26
K04-42	light pink	0.23389	0.07763	0.00078	0.00013	0.02408	0.0071	0.00042	0.00014	5	0.84	24.2	7.04	0.3	9	2.83	46
K04-43	light pink	0.0537	0.02954	0.00072	0.00007	0.00503	0.00273	0.00031	0.00008	4.6	0.46	5.1	2.76	85	0.037	4.56	0.23
K04-44	light pink	0.17674	0.12479	0.00128	0.00028	0.03141	0.02128	0.00119	0.00066	8.3	1.83	31.4	20.95	24	1.4	6.4	0.85
K04-45	light pink	0.08943	0.07634	0.00072	0.00014	0.00766	0.00639	0.0003	0.00019	4.7	0.91	7.7	6.43	58	0.3	4.21	0.45
K04-46	light pink	0.3659	0.05683	0.00139	0.00013	0.07004	0.0095	0.00174	0.00032	8.9	0.87	68.7	9.01	DISCORDANT			
K04-47	light pink	0.38949	0.16639	0.00102	0.00026	0.05801	0.02078	0.00607	0.00128	6.6	1.65	57.3	19.95	0.8	7.1	2.6	27
K04-48	light pink	0.07672	0.18612	0.00089	0.00029	0.01139	0.02742	0.00224	0.00088	5.7	1.86	11.5	27.53	82	0.049	5.4	0.87
K04-50	light pink	0.15311	0.06863	0.00224	0.00038	0.04401	0.01878	0.00054	0.0005	14.4	2.46	43.7	18.27	7.4	3.2	10.6	1.2
K04-51	light pink	0.06526	0.12693	0.00071	0.00019	0.00628	0.01211	0.00045	0.00034	4.6	1.23	6.4	12.22	87	0.026	4.4	0.59
K04-52	light pink	0.80512	0.04489	0.01731	0.00062	1.8959	0.15623	0.12233	0.02024	110.7	3.95	1079.7	54.78	DISCORDANT			
K04-53	light pink	0.73904	0.26498	0.00157	0.00042	0.16154	0.04371	0.01603	0.00328	10.1	2.7	152	38.24	DISCORDANT			
K04-54	light pink	0.77032	0.38982	0.00055	0.00021	0.05919	0.02089	0.00075	0.00044	3.6	1.34	58.4	20.02	0.5	8	0.2	22
K04-56	light pink	0.66953	0.15899	0.00229	0.00041	0.17633	0.03281	0.00519	0.00125	14.7	2.61	164.9	28.32	DISCORDANT			
K04-58	light pink	0.08836	0.17537	0.00098	0.00036	0.01055	0.02061	0.00099	0.00072	6.3	2.32	10.7	20.71	82	0.54	5.8	1.1
K04-59	light pink	0.1155	0.07576	0.00101	0.00018	0.0166	0.01058	0.0008	0.00028	6.5	1.14	16.7	10.56	29	1.13	5.4	0.56

Table VIII.3: Pokohino Dome Complex W110855

Spot No.	Colour	Measured isotope ratios and 1σ (%) internal errors						Estimated ages and 1σ absolute internal errors (My)						$^{206}\text{Pb}/^{238}\text{U}$ & $^{207}\text{Pb}/^{235}\text{U}$	Concordance (%)	Selected age and 1σ absolute external error (My)		
		$^{207}\text{Pb}/^{206}\text{Pb}$	\pm	$^{206}\text{Pb}/^{238}\text{U}$	\pm	$^{207}\text{Pb}/^{235}\text{U}$	\pm	$^{208}\text{Pb}/^{232}\text{Th}$	\pm	$^{206}\text{Pb}/^{238}\text{U}$	\pm	$^{207}\text{Pb}/^{235}\text{U}$	\pm			Spot MSWD	Selected age	1σ absolute external error (My)
K05-1	pink	0.78456	0.0406	0.01864	0.00068	1.8556	0.13834	0.04912	0.00904	119	4.31	1065.4	49.19	DISCORDANT		6	3.88	13
K05-2	pink	0.1761	0.06374	0.00088	0.00013	0.02099	0.00704	0.00038	0.00022	5.7	0.83	21.1	7	DISCORDANT				
K05-3	pink	0.56335	0.13214	0.00117	0.00023	0.0881	0.01307	0.0013	0.00059	7.5	1.46	85.7	12.2	DISCORDANT				
K05-5	pink	0.12132	0.05677	0.0009	0.0001	0.01554	0.00712	0.00075	0.00019	5.8	0.62	15.7	7.12	13	2.2	4.95	0.31	
K05-6	pink	0.27171	0.0701	0.00134	0.00014	0.04899	0.01184	0.00132	0.0004	8.6	0.92	48.6	11.46	DISCORDANT				
K05-7	pink	0.0636	0.02383	0.00104	0.00007	0.00873	0.00324	0.0003	0.00013	6.7	0.47	8.8	3.26	46	0.55	6.41	0.22	
K05-9	light pink	0.48577	0.03555	0.0016	0.00008	0.10678	0.00735	0.00165	0.00033	10.3	0.49	103	6.74	DISCORDANT				
K05-10	light pink	0.62459	0.03896	0.00607	0.00026	0.55919	0.03916	0.0141	0.00284	39	1.67	451	25.5	DISCORDANT				
K05-11	light pink	0.1846	0.20268	0.00131	0.00036	0.03512	0.03748	0.00187	0.00056	8.4	2.33	35	36.77	45	0.57	6.9	1.1	
K05-12	light pink	0.12175	0.05085	0.00072	0.00009	0.01145	0.00459	0.00034	0.00009	4.7	0.59	11.6	4.61	9.2	2.8	3.79	0.28	
K05-13	pink	0.13527	0.0318	0.02172	0.00164	0.40711	0.10649	0.03565	0.00778	138.5	10.34	346.8	76.84	0.7	7.4	114	170	
K05-14	light pink	0.21796	0.05202	0.00117	0.0001	0.03647	0.00838	0.00138	0.00033	7.5	0.62	36.4	8.21	DISCORDANT				
K05-15	light pink	0.5629	0.07798	0.00209	0.0002	0.15517	0.0182	0.0025	0.00067	13.5	1.28	146.5	16	DISCORDANT				
K05-16	light pink	0.18928	0.04128	0.00099	0.00008	0.0263	0.00551	0.00065	0.00018	6.4	0.49	26.4	5.45	DISCORDANT				
K05-17	light pink	0.12649	0.07629	0.00121	0.00013	0.02363	0.0141	0.0031	0.00076	7.8	0.85	23.7	13.99	23	1.4	6.91	0.39	
K05-18	light pink	0.17872	0.10595	0.00096	0.00013	0.02353	0.01365	0.00104	0.00038	6.2	0.85	23.6	13.54	18	1.8	5.18	0.39	
K05-19	light pink	0.26741	0.03775	0.00149	0.00012	0.05297	0.00678	0.00123	0.00034	9.6	0.76	52.4	6.53	DISCORDANT				
K05-20	light pink	0.12094	0.04979	0.00098	0.00009	0.01687	0.00682	0.00055	0.00021	6.3	0.6	17	6.81	9.2	2.8	5.45	0.27	
K05-21	light pink	0.2184	0.05605	0.00101	0.00013	0.02856	0.00663	0.00068	0.00022	6.5	0.81	28.6	6.54	DISCORDANT				
K05-22	light pink	0.16775	0.06385	0.00103	0.00013	0.0231	0.00841	0.00074	0.00023	6.6	0.84	23.2	8.35	3.4	4.6	5.05	11	
K05-23	light pink	0.07072	0.09413	0.00118	0.00024	0.0107	0.01409	0.00048	0.00036	7.6	1.52	10.8	14.16	80	0.063	7.3	0.75	
K05-24	pink	0.11342	0.07388	0.0012	0.00014	0.01839	0.01183	0.00135	0.00039	7.8	0.93	18.5	11.79	33	0.95	6.95	0.42	
K05-25	pink	0.25636	0.26189	0.00072	0.00023	0.0248	0.0242	0.00102	0.00044	4.6	1.45	24.9	23.97	38	0.78	3.5	0.68	
K05-26	pink	0.23194	0.12523	0.00128	0.0002	0.04487	0.02348	0.0008	0.0003	8.3	1.29	44.6	22.82	10	2.7	6.4	0.59	
K05-27	pink	0.0871	0.12272	0.00096	0.00019	0.01042	0.01455	0.00052	0.00034	6.2	1.22	10.5	14.63	75	0.102	5.8	0.58	
K05-28	light pink	0.53111	0.10935	0.00069	0.0001	0.0469	0.00714	0.00113	0.00033	4.4	0.67	46.5	6.93	DISCORDANT				
K05-29	pink	0.28689	0.05373	0.00116	0.00014	0.06223	0.01098	0.00157	0.00045	10.3	0.93	61.3	10.49	DISCORDANT				
K05-30	light pink	0.67137	0.11938	0.00237	0.0003	0.22142	0.03309	0.00371	0.0011	15.3	1.93	203.1	27.51	DISCORDANT				
K05-31	light pink	0.65048	0.08949	0.00171	0.00017	0.13451	0.01563	0.00387	0.0011	11	1.07	128.1	13.99	DISCORDANT				
K05-32	light pink	0.25372	0.11098	0.0009	0.00019	0.02877	0.01126	0.00046	0.00018	5.8	1.21	28.8	11.11	2.4	5.1	3.4	17	
K05-33	light pink	0.31206	0.10891	0.00122	0.00022	0.05203	0.01617	0.00138	0.00064	7.8	1.39	51.5	15.61	0.3	8.8	4.2	25	
K05-34	light pink	0.05107	0.07406	0.00092	0.00013	0.00591	0.00854	0.00046	0.00016	6	0.86	6	8.62	99.4	0	5.92	0.4	
K05-35	pink	0.67853	0.101	0.00234	0.00024	0.22854	0.03094	0.00604	0.00192	15.1	1.53	209	25.57	DISCORDANT				
K05-36	light pink	0.53684	0.06127	0.00383	0.00027	0.2568	0.02994	0.00582	0.00177	24.7	1.7	232.1	24.19	DISCORDANT				
K05-37	light pink	0.11772	0.07146	0.00094	0.00012	0.0156	0.00933	0.00011	0.00012	6	0.75	15.7	9.33	27	1.2	5.3	0.36	
K05-38	pink	0.41184	0.07119	0.00212	0.00021	0.11401	0.01846	0.00268	0.00086	13.7	1.32	109.6	16.82	DISCORDANT				

Geochronology of Broken Hills Mine samples

K05-39	light pink	0.1164	0.07086	0.00091	0.00011	0.01403	0.00843	0.00056	0.00026	5.9	0.7	14.1	8.44	29	1.11	5.2	0.33
K05-40	pink	0.52794	0.12333	0.00094	0.00017	0.0715	0.01171	0.00105	0.00042	6	1.1	70.1	11.09	DISCORDANT			
K05-41	light pink	0.32536	0.07036	0.00119	0.00011	0.04731	0.00987	0.00092	0.00034	7.7	0.69	46.9	9.57	DISCORDANT			
K05-42	light pink	0.07508	0.04437	0.0008	0.00008	0.00847	0.00496	0.00025	0.00012	5.2	0.55	8.6	4.99	45	0.56	4.82	0.25
K05-43	light pink	0.17639	0.07786	0.00085	0.00011	0.02052	0.0088	0.00024	0.00015	5.5	0.69	20.6	8.76	6.5	3.4	4.32	0.33
K05-44	pink	0.94097	0.12767	0.00265	0.00028	0.33983	0.04068	0.00867	0.00288	17.1	1.78	297	30.83	DISCORDANT			

Table VIII.4: Broken Hills Mine sample 1 W110856

Spot No.	Colour	Measured isotope ratios and 1 σ (%) internal errors						Estimated ages and 1 σ absolute internal errors (My)				$^{206}\text{Pb}/^{238}\text{U}$ & $^{207}\text{Pb}/^{235}\text{U}$		Concordance (%)	Selected age and 1 σ absolute external error (My)		
		$^{207}\text{Pb}/^{206}\text{Pb}$	\pm	$^{206}\text{Pb}/^{238}\text{U}$	\pm	$^{207}\text{Pb}/^{235}\text{U}$	\pm	$^{208}\text{Pb}/^{232}\text{Th}$	\pm	$^{206}\text{Pb}/^{238}\text{U}$	\pm	$^{207}\text{Pb}/^{235}\text{U}$	\pm	Spot MSWD			
K06-1.1	colourless	0.06889	0.25586	0.00083	0.00041	0.00843	0.03106	-0.00008	0.00043	5.4	2.66	8.5	31.28	91	0.012	5.1	1.2
K06-3	colourless	0.41562	0.4571	0.00132	0.00085	0.07416	0.06794	0.00232	0.00177	8.5	5.45	72.6	64.23	30	1.09	3.5	2.6
K06-8	colourless	2.15648	1.39471	0.00161	0.00094	0.41607	0.15313	0.00706	0.00294	10.3	6.05	353.2	109.8	0.6	7.5	4.5	96
K06-9	colourless	4.00431	11.50541	0.48182	1.58045	1.19808	1.33657	0.3079	0.37864	2535.2	6875.5	799.7	617.41	DISCORDANT			
K06-10	colourless	0.15925	0.20153	0.00582	0.00243	0.13882	0.17702	0.03961	0.01359	37.4	15.56	132	157.83	53	0.39	29	7.4
K06-16	pink	0.16033	0.13275	0.00168	0.00048	0.04083	0.03233	0.00044	0.00035	10.8	3.12	40.6	31.54	31	1.04	8.1	1.5
K06-17	pink	0.06129	0.19872	0.00081	0.00031	0.00688	0.02217	0.00097	0.00047	5.2	2.01	7	22.35	93	0.0072	5.1	0.95
K06-18	light pink	0.19416	0.16219	0.00187	0.00056	0.04294	0.03403	0.00198	0.00115	12	3.57	42.7	33.14	31	1.01	8.9	1.7
K06-19	light pink	0.05108	0.32302	0.00087	0.0005	0.00673	0.04241	0.00148	0.00099	5.6	3.2	6.8	42.77	98	0.00091	5.5	1.5
K06-23	light pink	0.35958	0.2009	0.00118	0.00035	0.05811	0.02867	0.00186	0.00074	7.6	2.22	57.3	27.51	5.8	3.6	3.8	1.1
K06-25	light pink	0.31639	0.24413	0.0011	0.00044	0.05059	0.03445	0.00024	0.00031	7.4	2.85	50.4	33.29	17	1.9	3.7	4.3
K06-26	pink	0.23466	0.08363	0.00113	0.0002	0.04531	0.0149	0.00084	0.00029	7.3	1.26	45	14.48	0.6	7.7	4.1	21
K06-27	pink	0.72837	0.1964	0.0062	0.00125	0.57711	0.16044	0.00944	0.00338	39.8	7.98	462.6	103.29	DISCORDANT			
K06-28	pink	0.11153	0.07987	0.00116	0.00022	0.01872	0.01308	0.00097	0.00038	7.5	1.42	18.8	13.04	34	0.92	6.3	0.68
K06-29	pink	0.25995	0.17615	0.00085	0.00025	0.02953	0.0183	0.00018	0.00021	5.5	1.64	29.6	18.05	45	2	3.7	0.76
K06-33	pink	0.43747	0.18941	0.00191	0.00053	0.10019	0.03697	0.00336	0.00133	42.3	3.42	97	34.12	4	6.7	4.5	53
K06-34	pink	0.05304	0.15778	0.00099	0.00038	0.00791	0.02337	0.00049	0.00037	6.4	2.44	8	23.55	94	0.0057	6.2	1.2
K06-37	light pink	0.2012	0.29538	0.0005	0.00024	0.01322	0.01839	0.00123	0.00056	3.2	1.57	13.3	18.43	56	0.35	2.4	0.73
K06-38	light pink	0.06432	0.17907	0.0014	0.00047	0.0123	0.03407	0.00074	0.00067	9	3.03	12.4	34.17	91	0.0116	8.7	1.4

Table VIII.5: Broken Hills Mine sample 2 W110857

Spot No.	Colour	Measured isotope ratios and 1σ (%) internal errors						Estimated ages and 1σ absolute internal errors (My)				$^{206}\text{Pb}/^{238}\text{U}$ & $^{207}\text{Pb}/^{235}\text{U}$		Selected age and 1σ absolute external error (My)			
		$^{207}\text{Pb}/^{206}\text{Pb}$	\pm	$^{206}\text{Pb}/^{238}\text{U}$	\pm	$^{207}\text{Pb}/^{235}\text{U}$	\pm	$^{208}\text{Pb}/^{232}\text{Th}$	\pm	$^{206}\text{Pb}/^{238}\text{U}$	\pm	$^{207}\text{Pb}/^{235}\text{U}$	\pm	Concordance (%)	Spot MSWD		
K07-1	light pink	0.08726	0.02438	0.0011	0.00009	0.01286	0.00349	0.00043	0.00007	7.4	0.58	43	3.5	5	3.9	6.11	7.4
K07-2	light pink	0.10383	0.05504	0.00119	0.00019	0.01671	0.00854	0.00031	0.00013	7.7	1.22	16.8	8.53	22	1.5	6.4	0.61
K07-3	light pink	0.05164	0.04186	0.00102	0.00015	0.00667	0.00534	0.00052	0.00012	6.6	0.96	6.8	5.38	97	0.0015	6.5	0.5
K07-4	light pink	0.0956	0.04294	0.00177	0.00021	0.02318	0.01015	0.00076	0.00018	11.4	1.37	23.3	10.07	18	1.8	9.8	0.67
K07-8	light pink	0.35955	0.09739	0.0017	0.00027	0.08342	0.01953	0.00093	0.00028	44	1.73	81.4	48.3	DISCORDANT			
K07-9	light pink	0.05562	0.06095	0.00087	0.00014	0.00723	0.00786	0.00037	0.00011	5.6	0.87	7.3	7.92	81	0.057	5.42	0.44
K07-10	light pink	0.07567	0.01372	0.00129	0.00007	0.01375	0.00244	0.00044	0.00006	8.3	0.46	43.9	2.45	0.7	7.3	7.27	8
K07-11	light pink	0.13955	0.09737	0.00099	0.00022	0.02079	0.01386	0.00117	0.00038	6.4	1.44	20.9	13.79	25	1.3	4.9	0.68
K07-13	light pink	0.3302	0.08945	0.00244	0.00037	0.10515	0.02559	0.00282	0.00064	15.7	2.37	101.5	23.51	DISCORDANT			
K07-14	light pink	0.28931	0.07033	0.00166	0.00022	0.07972	0.01745	0.00198	0.00024	10.7	1.42	77.9	16.41	DISCORDANT			
K07-16	light pink	0.06222	0.05617	0.00139	0.00022	0.01181	0.01054	0.00064	0.00022	9	1.44	11.9	10.57	75	0.101	8.6	0.7
K07-17	pink	0.08824	0.03833	0.00145	0.00016	0.01841	0.00781	0.00058	0.00014	9.3	1.06	18.5	7.79	18	1.8	8.2	0.51
K07-18	pink	0.91834	0.23778	0.00168	0.00036	0.25274	0.04677	0.00303	0.0007	10.8	2.3	228.8	37.91	DISCORDANT			
K07-19	pink	0.19078	0.06661	0.00132	0.00018	0.04035	0.01326	0.00045	0.00016	8.5	1.18	40.2	12.94	0.9	6.8	5.8	48
K07-20	pink	0.04991	0.02208	0.00128	0.00011	0.00876	0.00383	0.00027	0.00008	8.2	0.69	8.9	3.86	85	0.036	8.13	0.37
K07-22	pink	0.22174	0.07034	0.00104	0.00015	0.03196	0.00933	0.00081	0.0002	6.7	0.94	31.9	9.18	0.3	8.9	4.17	48
K07-23	pink	0.19442	0.07185	0.00137	0.00021	0.03572	0.01233	0.00046	0.00018	8.8	1.35	35.6	12.09	1.5	5.9	6	20
K07-24	pink	0.25894	0.0828	0.00128	0.0002	0.04337	0.01247	0.00081	0.00022	8.3	1.31	43.4	12.13	0.2	9.7	4.7	24
K07-25	pink	0.14709	0.0415	0.00114	0.00014	0.02327	0.00614	0.0005	0.00012	7.4	0.87	23.4	6.09	0.3	9	5.01	17
K07-26	pink	0.15306	0.0712	0.00126	0.00019	0.02527	0.01125	0.00044	0.00018	8.1	1.24	25.3	11.15	9	2.9	6.3	0.59
K07-27	pink	0.12495	0.04128	0.00138	0.00016	0.02534	0.00804	0.00097	0.00023	8.9	1.02	25.4	7.96	2	5.4	6.8	15
K07-28	pink	0.11988	0.11858	0.00147	0.0005	0.02278	0.02145	0.00007	0.00041	9.4	3.2	22.9	21.3	47	0.52	7.5	4.6
K07-29	pink	0.37052	0.086	0.00173	0.00024	0.09183	0.01867	0.00205	0.00046	11.1	4.56	89.2	47.36	DISCORDANT			
K07-30	pink	0.10852	0.04252	0.00161	0.00019	0.02359	0.00899	0.00094	0.00022	10.4	1.2	23.7	8.92	9.2	2.8	8.6	0.61
K07-31	pink	0.08614	0.05165	0.00109	0.00016	0.01363	0.00799	0.00041	0.00014	7	1.02	13.7	8	35	0.89	6.2	0.51
K07-32	colourless	0.07467	0.02362	0.00102	0.00009	0.01113	0.00345	0.0004	0.00008	6.6	0.55	11.2	3.47	12	2.5	5.79	0.3
K07-33	colourless	0.29571	0.03014	0.00171	0.0001	0.0672	0.00676	0.00129	0.00022	11	0.63	66	6.43	DISCORDANT			
K07-36	colourless	0.32522	0.07846	0.0014	0.00018	0.06523	0.01412	0.00163	0.00036	9	1.19	64.2	13.46	DISCORDANT			
K07-37	colourless	0.29685	0.13778	0.00152	0.00039	0.05704	0.02322	0.00111	0.00048	9.8	2.5	56.3	22.34	2.4	5.1	4.8	35
K07-39	colourless	0.38782	0.34232	0.00097	0.00048	0.05504	0.04118	0.00137	0.00107	6.2	3.1	54.4	39.64	20	1.6	2.8	44
K07-40	colourless	0.06951	0.03332	0.00116	0.00016	0.01204	0.00562	0.00075	0.00037	7.5	1.01	12.2	5.64	32	0.97	6.6	0.53
K07-41	colourless	0.06952	0.02435	0.00101	0.0001	0.00913	0.00313	0.00035	0.00009	6.5	0.63	9.2	3.15	29	1.1	5.93	0.34
K07-42	colourless	0.04893	0.00922	0.00106	0.00005	0.00694	0.00132	0.00034	0.00007	6.8	0.34	7	1.33	85	0.034	6.78	0.18
K07-43	colourless	0.06433	0.04707	0.0014	0.0002	0.01196	0.00863	0.00083	0.00031	9	1.31	12.1	8.66	69	0.16	8.6	0.65
K07-45	pink	0.1097	0.06473	0.00128	0.00022	0.02116	0.01211	0.0002	0.00015	8.2	1.41	21.3	12.05	23	1.4	6.8	0.69
K07-47	light pink	0.24846	0.09776	0.00118	0.00023	0.03588	0.01273	0.00111	0.00039	7.6	1.46	35.8	42.47	4.3	6.2	4.4	23
K07-48	light pink	0.11812	0.04827	0.00187	0.00024	0.03311	0.0132	0.0008	0.0003	12.1	1.52	33.1	12.98	7.4	3.2	9.6	0.75

Table VIII.6: Broken Hills Mine sample 3 W110858

Spot No.	Colour	Measured isotope ratios and 1σ (%) internal errors						Estimated ages and 1σ absolute internal errors (My)				$^{206}\text{Pb}/^{238}\text{U}$ & $^{207}\text{Pb}/^{235}\text{U}$		Concordance (%)	Spot MSWD	Selected age and 1σ absolute external error (My)	
		$^{207}\text{Pb}/^{206}\text{Pb}$	\pm	$^{206}\text{Pb}/^{238}\text{U}$	\pm	$^{207}\text{Pb}/^{235}\text{U}$	\pm	$^{208}\text{Pb}/^{232}\text{Th}$	\pm	$^{206}\text{Pb}/^{238}\text{U}$	\pm	$^{207}\text{Pb}/^{235}\text{U}$	\pm				
K08-1	colourless	0.17107	0.18444	0.00091	0.00029	0.02651	0.02747	0.00055	0.00036	5.9	1.84	26.6	27.17	42	0.64	4.5	0.87
K08-2	pink	0.37674	0.08298	0.00473	0.00022	0.08693	0.01664	0.00242	0.00049	11.2	1.4	84.6	45.55	DISCORDANT			
K08-3	pink	0.13404	0.06173	0.00124	0.00019	0.02181	0.0096	0.00052	0.00018	8	1.2	21.9	9.54	10	2.7	6.2	0.6
K08-4	pink	0.16707	0.07258	0.00436	0.00021	0.03594	0.01482	0.00072	0.00024	8.8	1.36	35.8	44.53	4.5	4	6.4	46
K08-5	pink	0.21524	0.0884	0.00121	0.0002	0.03469	0.0133	0.00089	0.00026	7.8	1.26	34.6	43.05	2.7	4.9	5.3	47
K08-6	pink	0.40441	0.10231	0.00224	0.00033	0.12209	0.02693	0.0023	0.00064	14.4	2.14	117	24.37	DISCORDANT			
K08-7	light pink	0.20504	0.15753	0.00097	0.00026	0.02831	0.02052	0.00049	0.00028	6.3	1.68	28.4	20.27	25	1.4	4.5	0.79
K08-8	light pink	0.09539	0.08734	0.00137	0.00022	0.0184	0.01663	0.0006	0.00027	8.8	1.44	18.5	16.58	53	0.4	8	0.67
K08-9	light pink	0.08456	0.0369	0.0017	0.00015	0.02046	0.00881	0.00125	0.00046	11	0.99	20.6	8.77	23	1.5	9.93	0.47
K08-10	light pink	0.35671	0.22733	0.00082	0.00026	0.04336	0.02431	0.00004	0.00037	5.3	1.65	43.1	23.66	9.5	2.8	2.8	0.78
K08-11	light pink	0.07459	0.05053	0.0012	0.00017	0.01083	0.00721	0.00063	0.00016	7.7	1.1	10.9	7.24	61	0.26	7.2	0.55
K08-12	light pink	0.08971	0.10516	0.00114	0.00024	0.01423	0.01644	0.00096	0.00032	7.4	1.57	14.3	16.46	64	0.21	6.7	0.73
K08-13	light pink	0.19131	0.06975	0.00479	0.00023	0.04748	0.01654	0.00129	0.00038	11.6	1.48	47.1	46.03	4.8	5.6	8.4	24
K08-14	light pink	0.12839	0.06693	0.00106	0.00015	0.01907	0.00964	0.00038	0.00014	6.8	0.98	49.2	9.6	46	2	5.64	0.46
K08-15	light pink	0.23549	0.1061	0.00121	0.00023	0.03952	0.01645	0.00065	0.00031	7.8	1.47	39.4	16.06	3.6	4.4	5.1	49
K08-16	light pink	0.23877	0.09667	0.00272	0.00046	0.09537	0.03646	0.0014	0.00065	17.5	2.98	92.5	33.8	2.1	5.3	11.5	44
K08-17	light pink	0.05583	0.08766	0.00122	0.00024	0.01029	0.01605	0.0004	0.00023	7.8	1.53	10.4	16.13	86	0.029	7.6	0.74
K08-18	light pink	0.05931	0.10272	0.00137	0.00028	0.01069	0.0184	0.00086	0.00041	8.8	1.83	10.8	18.48	91	0.014	8.6	0.86
K08-19	light pink	0.06425	0.06158	0.00136	0.00018	0.01137	0.01081	0.00047	0.0002	8.8	1.19	11.5	10.86	78	0.076	8.5	0.56
K08-20	light pink	0.24511	0.09058	0.00096	0.00016	0.03009	0.01012	0.00055	0.00019	6.2	1.04	30.1	9.98	0.9	6.8	3.83	46
K08-21	light pink	0.15056	0.11253	0.00082	0.00021	0.01519	0.01074	0.00051	0.00019	5.3	1.38	15.3	10.74	30	1.09	4.1	0.66
K08-22	light pink	0.17345	0.1102	0.00236	0.00054	0.05042	0.03048	0.00112	0.00057	15.2	3.48	50	29.46	20	1.7	11.3	4.7
K08-23	light pink	0.53032	0.16614	0.00155	0.00032	0.11317	0.0288	0.00245	0.00074	10	2.07	108.9	26.27	DISCORDANT			
K08-26	light pink	0.08912	0.0808	0.00102	0.00017	0.01228	0.01099	0.00022	0.00014	6.5	1.08	12.4	11.02	56	0.33	6	0.52
K08-27	light pink	0.15206	0.12925	0.00113	0.00027	0.02237	0.01833	0.00054	0.00035	7.3	1.77	22.5	18.21	37	0.82	5.9	0.83
K08-28	light pink	0.35467	0.1364	0.00148	0.00031	0.06694	0.02257	0.00123	0.0005	9.5	1.98	65.8	21.48	0.6	7.6	4.7	33
K08-30	light pink	0.1182	0.042	0.00114	0.00011	0.01772	0.00618	0.0004	0.00011	7.3	0.72	17.8	6.16	6	3.5	6.18	0.34
K08-31	light pink	0.2923	0.14509	0.00115	0.00027	0.04687	0.02111	0.00054	0.00033	7.4	1.71	46.5	20.48	4.3	4.1	4.3	24
K08-32	light pink	0.32729	0.14441	0.00133	0.00029	0.07168	0.02862	0.00072	0.00045	8.6	1.85	70.3	27.12	4.9	5.5	4.7	26
K08-33	light pink	0.18991	0.08086	0.00092	0.00015	0.02342	0.00939	0.00055	0.00018	5.9	0.96	23.5	9.32	4	4.2	4.18	12

Table VIII.7: Broken Hills Flow Banded Rhyolite W110859

Spot No.	Colour	Measured isotope ratios and 1 σ (%) internal errors						Estimated ages and 1 σ absolute internal errors (My)				$^{206}\text{Pb}/^{238}\text{U}$ & $^{207}\text{Pb}/^{235}\text{U}$		Selected age and 1 σ absolute external error (My)			
		$^{207}\text{Pb}/^{206}\text{Pb}$	\pm	$^{206}\text{Pb}/^{238}\text{U}$	\pm	$^{207}\text{Pb}/^{235}\text{U}$	\pm	$^{208}\text{Pb}/^{232}\text{Th}$	\pm	$^{206}\text{Pb}/^{238}\text{U}$	\pm	$^{207}\text{Pb}/^{235}\text{U}$	\pm	Concordance (%)	Spot MSWD		
K09-1	colourless	0.3494	0.1036	0.00148	0.00026	0.07377	0.01869	0.00171	0.00046	9.6	1.64	72.3	17.67	DISCORDANT			
K09-2	colourless	0.06955	0.0762	0.00197	0.00031	0.01962	0.02133	0.0018	0.00051	12.7	2	19.7	21.24	72	0.13	12.1	0.95
K09-3	colourless	0.31609	0.12492	0.00178	0.00037	0.06472	0.02252	0.00143	0.00108	11.4	2.35	63.7	21.48	0.9	6.8	6	38
K09-4	colourless	0.23312	0.10189	0.00161	0.0003	0.05423	0.02189	0.00106	0.0004	10.4	1.94	53.6	21.09	2.9	4.7	6.7	25
K09-5	colourless	0.49725	0.11878	0.00201	0.00032	0.13361	0.02627	0.00477	0.0009	13	2.03	127.3	23.53	DISCORDANT			
K09-6	colourless	0.1659	0.09707	0.00135	0.00025	0.02919	0.01631	0.001	0.00036	8.7	1.63	29.2	16.09	17	1.9	6.7	0.77
K09-7	colourless	0.14493	0.07777	0.00113	0.00017	0.02581	0.01339	0.00092	0.00024	7.3	1.12	25.9	13.25	13	2.2	5.8	0.51
K09-8	light pink	0.36045	0.1033	0.00182	0.0003	0.08132	0.02	0.00193	0.00049	11.7	1.95	79.4	18.78	DISCORDANT			
K09-9	light pink	0.24429	0.04598	0.00116	0.00011	0.03959	0.00672	0.00132	0.00023	7.5	0.7	39.4	6.56	DISCORDANT			
K09-10	light pink	0.30844	0.15224	0.00134	0.00032	0.05557	0.02451	0.00138	0.00049	8.6	2.07	54.9	23.58	3.8	4.3	4.9	26
K09-11	light pink	0.18291	0.05538	0.00115	0.00014	0.03168	0.00899	0.00078	0.0002	7.4	0.89	31.7	8.85	0.3	8.8	5.06	16
K09-12	light pink	0.72717	0.13794	0.0032	0.00046	0.32125	0.04972	0.00845	0.00141	20.6	2.98	282.9	38.24	DISCORDANT			
K09-13	light pink	0.48484	0.10206	0.00547	0.00077	0.37958	0.07639	0.01403	0.00243	35.1	4.93	326.7	56.23	DISCORDANT			
K09-14	light pink	0.27082	0.08422	0.00217	0.00034	0.0803	0.02266	0.00223	0.00071	14	2.16	78.4	21.3	0.1	10.3	7.8	43
K09-15	light pink	0.10955	0.01589	0.00112	0.00006	0.0169	0.00238	0.00044	0.00006	7.2	0.38	17	2.38	DISCORDANT			
K09-16	light pink	0.4473	0.13498	0.00249	0.00046	0.14984	0.03882	0.00345	0.00095	16	2.99	141.8	34.28	DISCORDANT			
K09-17	light pink	0.06265	0.03185	0.00106	0.0001	0.00961	0.00482	0.00032	0.00011	6.9	0.66	9.7	4.85	50	0.45	6.45	0.32
K09-18	light pink	0.1023	0.02293	0.00126	0.00009	0.01776	0.00386	0.00044	0.00008	8.1	0.58	17.9	3.85	0.4	8.4	6.66	11
K09-19	light pink	0.50823	0.10056	0.0021	0.00027	0.15481	0.0261	0.0025	0.00056	13.6	1.75	146.1	22.95	DISCORDANT			
K09-20	light pink	0.09856	0.06182	0.00133	0.00021	0.01733	0.0106	0.00058	0.00024	8.5	1.32	17.4	10.58	35	0.89	7.5	0.66
K09-21	light pink	0.20475	0.12662	0.00116	0.00027	0.03599	0.02085	0.00169	0.00058	7.5	1.75	35.9	20.43	14	2.2	5.2	0.82
K09-22	light pink	1.01754	0.37164	0.00094	0.00029	0.14265	0.03123	0.00203	0.00052	6.1	1.87	135.4	27.76	DISCORDANT			
K09-23	light pink	0.51883	0.14312	0.00221	0.0004	0.18335	0.04269	0.00224	0.00061	14.2	2.57	170.9	36.63	DISCORDANT			
K09-24	pink	0.05658	0.14759	0.00151	0.0004	0.01101	0.0286	0.00049	0.0006	9.7	2.58	11.1	28.73	96	0.0028	9.6	1.2
K09-25	pink	0.38294	0.12533	0.00115	0.00022	0.06471	0.01783	0.00085	0.00031	7.4	1.43	63.7	17.04	DISCORDANT			
K09-26	pink	0.24477	0.05862	0.00106	0.00012	0.03754	0.00818	0.00048	0.00011	6.8	0.79	37.4	8.04	DISCORDANT			
K09-27	pink	0.09858	0.07122	0.00191	0.00028	0.02564	0.01826	0.00098	0.00031	12.3	1.8	25.7	18.08	42	0.65	11	0.86
K09-28	pink	0.37451	0.11803	0.00297	0.0005	0.14443	0.04147	0.00536	0.00139	19.1	3.21	137	36.8	0.1	10.6	9.9	62
K09-29	pink	0.19319	0.10421	0.00112	0.00022	0.03173	0.01612	0.00051	0.00028	7.2	1.42	31.7	15.86	9.8	2.7	5.2	0.67
K09-30	pink	0.42442	0.10387	0.00154	0.00024	0.09867	0.02017	0.00194	0.00045	9.9	1.55	95.5	18.64	DISCORDANT			
K09-31	pink	0.27794	0.09571	0.00149	0.00026	0.05698	0.0175	0.00068	0.00032	9.6	1.69	56.3	16.84	0.3	8.8	5.2	30
K09-32	pink	0.50146	0.08314	0.00151	0.00017	0.10289	0.01442	0.00231	0.00044	9.7	1.06	99.4	13.28	DISCORDANT			
K09-33	pink	0.44209	0.12411	0.00199	0.00034	0.13799	0.03413	0.0023	0.00065	12.8	2.16	131.3	30.45	DISCORDANT			
K09-34	pink	0.26659	0.09955	0.00178	0.00029	0.06576	0.02281	0.00137	0.00045	11.5	1.88	64.7	21.73	4	6.6	7.2	29
K09-35	pink	0.11456	0.06923	0.00096	0.00015	0.01445	0.00849	0.00071	0.00018	6.2	0.97	14.6	8.5	28	1.19	5.26	0.47
K09-36	pink	0.27184	0.1064	0.0018	0.00035	0.06974	0.02461	0.0011	0.00044	11.6	2.27	68.5	23.36	4	6.6	6.5	35
K09-37	pink	0.59855	0.08559	0.00217	0.00022	0.19999	0.02534	0.00366	0.00073	14	1.39	185.1	21.44	DISCORDANT			

K09-38	pink	0.5014	0.08272	0.00239	0.00027	0.16405	0.02372	0.00264	0.00057	15.4	1.71	154.2	20.69	DISCORDANT			
K09-40	pink	0.18239	0.07664	0.00127	0.00019	0.03145	0.01256	0.00045	0.0002	8.2	1.24	31.4	12.36	4.2	4.1	6	45
K09-41	pink	0.24447	0.06937	0.000212	0.00027	0.06753	0.0179	0.00221	0.00056	13.6	1.77	66.4	17.03	DISCORDANT			
K09-42	pink	0.79121	0.04785	0.06537	0.00252	7.52441	1.10467	0.36531	0.06596	408.2	15.26	2175.9	131.58	DISCORDANT			
K09-43	pink	0.49867	0.15299	0.00204	0.0004	0.16284	0.04277	0.00757	0.00161	13.1	2.56	153.2	37.35	DISCORDANT			
K09-44	pink	0.36925	0.11772	0.00184	0.00034	0.08112	0.02236	0.00161	0.00057	11.9	2.19	79.2	21.04	DISCORDANT			
K09-45	pink	0.26998	0.04986	0.0017	0.00016	0.06827	0.01188	0.00124	0.00027	10.9	1.03	67.1	11.29	DISCORDANT			
K09-46	light pink	0.58867	0.22546	0.00082	0.00022	0.0643	0.01854	0.00087	0.0003	5.3	1.41	63.3	17.69	DISCORDANT			
K09-47	light pink	0.45904	0.08659	0.00199	0.00024	0.12631	0.02098	0.00167	0.00042	12.8	1.57	120.8	18.94	DISCORDANT			
K09-48	light pink	0.78129	0.16304	0.00408	0.00064	0.39585	0.07191	0.01099	0.00246	26.3	4.14	338.6	52.31	DISCORDANT			
K09-49	light pink	0.41631	0.13483	0.00129	0.00024	0.07643	0.02157	0.00138	0.00046	8.3	1.52	74.8	20.35	DISCORDANT			
K09-50	light pink	0.18719	0.07181	0.00146	0.00022	0.03708	0.0134	0.00086	0.0003	9.4	1.44	37	13.12	2.2	5.2	6.6	20

Table VIII.8: Hikuai Ignimbrite W110860

Spot No.	Colour	Measured isotope ratios and 1 σ (%) internal errors						Estimated ages and 1 σ absolute internal errors (My)						$^{206}\text{Pb}/^{238}\text{U}$ & $^{207}\text{Pb}/^{235}\text{U}$		Selected age and 1 σ absolute external error (My)	
		$^{207}\text{Pb}/^{206}\text{Pb}$	\pm	$^{206}\text{Pb}/^{238}\text{U}$	\pm	$^{207}\text{Pb}/^{235}\text{U}$	\pm	$^{208}\text{Pb}/^{232}\text{Th}$	\pm	$^{206}\text{Pb}/^{238}\text{U}$	\pm	$^{207}\text{Pb}/^{235}\text{U}$	\pm	Concordance (%)	Spot MSWD		
K10-1	light pink	0.23575	0.23228	0.00136	0.00051	0.04259	0.03912	0.00184	0.0016	8.8	3.3	42.3	38.1	35	0.88	6	1.5
K10-2	colourless	0.07853	0.12107	0.00182	0.00046	0.01914	0.02919	0.00168	0.00107	11.7	2.95	19.2	29.08	78	0.08	11	1.4
K10-3	colourless	0.04713	0.05595	0.00128	0.00021	0.00956	0.01127	0.00061	0.00019	8.2	1.33	9.7	11.33	89	0.019	8.16	0.66
K10-4	colourless	0.05992	0.11023	0.00367	0.00088	0.02273	0.04159	0.00094	0.00107	23.6	5.64	22.8	41.29	98	0.00048	23.7	2.8
K10-6	light pink	0.19582	0.0789	0.00124	0.00024	0.03818	0.01428	0.00043	0.0003	8	1.36	38	43.96	24	5.4	5.2	49
K10-7	colourless	0.43711	0.48303	0.00053	0.00036	0.03153	0.02782	-0.00007	0.00097	3.4	2.32	31.5	27.39	27	1.19	1.2	1.1
K10-9	colourless	0.05124	0.17364	0.00143	0.00045	0.00993	0.03354	0.00196	0.00093	9.2	2.89	10	33.72	98	0.00069	9.1	1.4
K10-10	colourless	0.17124	0.10228	0.00169	0.00036	0.03863	0.02184	0.00101	0.00045	10.9	2.35	38.5	21.35	16	2	8	1.1
K10-11	colourless	0.43908	0.46411	0.00059	0.00035	0.03266	0.02872	0.00144	0.00082	3.8	2.27	32.6	28.24	28	1.17	1.6	1.1
K10-12	colourless	0.10055	0.08531	0.00118	0.00026	0.01612	0.0133	0.00062	0.00028	7.6	1.66	16.2	13.29	47	0.53	6.5	0.82
K10-13	light pink	0.35895	0.14543	0.00169	0.00041	0.06499	0.02214	0.00215	0.00076	10.9	2.63	63.9	21.1	0.6	7.5	4.6	45
K10-14	colourless	0.51857	0.28829	0.00079	0.00028	0.06412	0.02867	0.00093	0.00055	5.1	1.78	63.1	27.36	2.9	4.8	1.6	23
K10-15	colourless	0.22098	0.12638	0.00192	0.00048	0.06417	0.03402	0.00104	0.00091	12.4	3.11	63.1	32.46	9.7	2.8	7.9	1.5
K10-16	colourless	0.06665	0.04207	0.00119	0.00016	0.01133	0.00703	0.00033	0.00011	7.7	1.01	11.4	7.06	54	0.37	7.1	0.52
K10-17	colourless	0.22606	0.24288	0.00106	0.00039	0.03222	0.03273	0.0023	0.00097	6.8	2.52	32.2	32.2	40	0.7	5	1.2
K10-18	light pink	0.64448	0.08177	0.0035	0.00032	0.32931	0.03931	0.01694	0.00333	22.5	2.07	289	30.03	DISCORDANT			
K10-19	colourless	0.05515	0.00799	0.02528	0.00107	0.19744	0.03246	0.0129	0.00269	161	6.74	183	27.52	32	1	155.3	3.7
K10-20	light pink	0.85349	0.16882	0.00158	0.00024	0.19072	0.02915	0.00351	0.00082	10.2	1.58	177.2	24.86	DISCORDANT			
K10-21	colourless	0.30097	0.06136	0.0009	0.0001	0.03853	0.00693	0.00053	0.00012	5.8	0.65	38.4	6.78	DISCORDANT			
K10-22	pink	0.23549	0.10298	0.00308	0.0006	0.09394	0.03868	0.00772	0.0024	19.8	3.83	91.2	35.91	3.5	4.4	12.7	49
K10-23	colourless	0.39801	0.15087	0.00214	0.00049	0.13859	0.04608	0.00337	0.00123	13.8	3.13	131.8	41.09	0.4	8.3	5.7	54
K10-24	light pink	0.04996	0.02822	0.00116	0.00011	0.00802	0.00449	0.00053	0.00017	7.5	0.74	8.1	4.52	87	0.027	7.37	0.36

K10-25	colourless	0.29306	0.16728	0.00128	0.00036	0.04585	0.02333	0.00062	0.00047	8.2	2.32	45.5	22.65	7.7	3.1	4.6	1.1
K10-27	colourless	0.11261	0.01337	0.00149	0.00007	0.02292	0.00274	0.00071	0.00013	9.6	0.46	23	2.72	DISCORDANT			
K10-28	light pink	0.40832	0.16795	0.00113	0.00026	0.06019	0.02123	0.00118	0.0005	7.3	1.7	59.3	20.34	0.7	7.2	3.3	27
K10-29	colourless	0.2503	0.11643	0.00251	0.00058	0.08898	0.0384	0.00722	0.00228	16.1	3.71	86.6	35.52	3.6	4.4	9.3	47
K10-30	light pink	0.06991	0.00911	0.02088	0.0009	0.20958	0.03186	0.00852	0.00194	133.2	5.71	193.2	26.74	0.8	7	120.5	400
K10-31	light pink	0.28265	0.25184	0.001	0.0004	0.03633	0.02925	0.0051	0.00171	6.4	2.6	36.2	28.66	27	1.2	3.9	1.2
K10-32	colourless	0.5081	0.14953	0.00197	0.00039	0.15912	0.03916	0.00348	0.00102	12.7	2.52	149.9	34.3	DISCORDANT			
K10-34	light pink	1.12764	0.45467	0.00166	0.00056	0.21705	0.05541	0.00673	0.00222	10.7	3.63	199.5	46.23	DISCORDANT			
K10-35	light pink	0.2936	0.19521	0.00115	0.00038	0.04586	0.02707	0.00067	0.00067	7.4	2.45	45.5	26.28	12	2.4	4.1	1.2
K10-36	light pink	0.16073	0.05979	0.00119	0.00018	0.02821	0.00986	0.00049	0.00017	7.7	1.14	28.2	9.74	2	5.4	5.3	47
K10-37	pink	0.70597	0.14577	0.00316	0.00049	0.31778	0.05747	0.00935	0.00253	20.3	3.16	280.2	44.28	DISCORDANT			
K10-38	colourless	0.11721	0.12288	0.00113	0.00029	0.01728	0.01766	0.00057	0.0004	7.3	1.86	17.4	17.63	53	0.4	6.2	0.9
K10-39	light pink	0.24906	0.1999	0.00099	0.00031	0.04025	0.03021	0.00113	0.00061	6.4	1.98	40.1	29.49	23	1.4	4.3	0.92
K10-40	light pink	0.07789	0.13517	0.00166	0.00049	0.01609	0.02759	0.0008	0.00082	10.7	3.14	16.2	27.58	82	0.049	10.1	1.5
K10-41	light pink	0.09042	0.09388	0.00106	0.00027	0.01511	0.01531	0.00076	0.00039	6.8	1.75	15.2	15.31	54	0.37	5.9	0.84
K10-42	light pink	0.36023	0.57373	0.00043	0.00037	0.01742	0.02338	-0.00111	0.00066	2.7	2.38	17.5	23.33	49	0.48	1.3	1.1
K10-43	light pink	0.1937	0.19042	0.00097	0.0003	0.02532	0.02382	0.00028	0.00043	6.3	1.93	25.4	23.59	39	0.75	4.8	0.91
K10-44	light pink	0.06984	0.15116	0.00088	0.0003	0.01003	0.02148	0.00048	0.00043	5.7	1.91	10.1	21.6	82	0.05	5.3	0.91
K10-45	light pink	0.84325	0.47376	0.00073	0.00032	0.06913	0.02616	0.00168	0.00084	4.7	2.04	67.9	24.84	0.8	7	0.1	33
K10-47	light pink	0.26905	0.09293	0.00055	0.0001	0.01911	0.00584	0.00033	0.00013	3.6	0.64	19.2	5.82	0.3	8.8	1.87	42
K10-48	light pink	0.10032	0.02379	0.00124	0.0001	0.01736	0.00407	0.0004	0.00012	8	0.63	17.5	4.06	0.7	7.3	6.49	44
K10-49	pink	0.24623	0.12642	0.00201	0.00047	0.08147	0.03888	0.00222	0.00105	12.9	3.05	79.5	36.5	5.8	3.6	7.9	1.4
K10-50	pink	0.10284	0.04988	0.01285	0.00176	0.21968	0.11449	0.00435	0.00273	82.3	11.18	201.6	95.32	19	1.7	70	5.4
K10-51	pink	0.57831	0.23352	0.0043	0.00122	0.27948	0.10399	0.01865	0.01821	27.7	7.83	250.2	82.53	0.9	6.7	9.7	120
K10-52	colourless	0.22775	0.17794	0.00148	0.00048	0.04753	0.03453	0.00274	0.00128	9.6	3.07	47.1	33.47	23	1.4	6.3	1.5
K10-53	colourless	0.34825	0.14757	0.00085	0.00021	0.04458	0.01601	0.00113	0.00041	5.5	1.34	44.3	15.56	0.8	7	2.3	24
K10-54	colourless	0.39405	0.19517	0.00136	0.00038	0.07089	0.03039	0.0017	0.00085	8.8	2.42	69.5	28.81	2.7	4.9	4	32

Table VIII.9: Wharekirauponga Dome W110861

Spot No.	Colour	Measured isotope ratios and 1 σ (%) internal errors						Estimated ages and 1 σ absolute internal errors (My)						$^{206}\text{Pb}/^{238}\text{U}$ & $^{207}\text{Pb}/^{235}\text{U}$ Concordance (%)	Selected age and 1 σ absolute external error (My)		
		$^{207}\text{Pb}/^{206}\text{Pb}$	\pm	$^{206}\text{Pb}/^{238}\text{U}$	\pm	$^{207}\text{Pb}/^{235}\text{U}$	\pm	$^{208}\text{Pb}/^{232}\text{Th}$	\pm	$^{206}\text{Pb}/^{238}\text{U}$	\pm	$^{207}\text{Pb}/^{235}\text{U}$	\pm				
K11-1	colourless	0.07095	0.00977	0.00103	0.00004	0.00961	0.00132	0.00028	0.00004	6.7	0.27	9.7	1.33	0.5	7.8	6.03	4.8
K11-3	colourless	0.08317	0.04022	0.00095	0.0001	0.01093	0.0052	0.00021	0.00007	6.1	0.62	11	5.22	29	1.11	5.53	0.32
K11-4	colourless	0.07866	0.03173	0.00123	0.0001	0.01269	0.00505	0.00009	0.00007	8	0.66	12.8	5.06	28	1.17	7.32	0.32
K11-6	colourless	0.04914	0.01801	0.00102	0.00006	0.00709	0.00258	0.00018	0.00006	6.6	0.4	7.2	2.6	79	0.071	6.48	0.19
K11-7	colourless	0.11423	0.05227	0.00136	0.00016	0.02083	0.0093	0.0004	0.00015	8.8	1.01	20.9	9.25	15	2.1	7.5	0.5
K11-8	light pink	0.19811	0.22719	0.00072	0.00026	0.02042	0.02229	0.00049	0.00024	4.7	1.68	20.5	22.18	45	0.58	3.5	0.78
K11-9	light pink	0.52944	0.24105	0.00163	0.00049	0.11832	0.04223	0.00165	0.00055	10.5	3.17	113.6	38.34	0.6	7.5	2.9	54

K11-10	light pink	0.07049	0.02511	0.00117	0.00008	0.01146	0.00404	0.0003	0.00006	7.6	0.53	11.6	4.05	26	1.2	7.04	0.25
K11-11	light pink	0.30292	0.17494	0.00098	0.00025	0.04209	0.02195	0.00054	0.00039	6.3	1.63	41.9	21.39	8.4	3.4	3.8	0.75
K11-12	light pink	0.10074	0.02673	0.00117	0.00008	0.01624	0.00423	0.00042	0.00011	7.5	0.54	16.4	4.22	2	5.4	6.49	7.4
K11-14	light pink	0.08579	0.04846	0.00117	0.00013	0.01379	0.00767	0.00021	0.0001	7.6	0.85	13.9	7.68	36	0.84	6.87	0.4
K11-15	light pink	0.05995	0.01215	0.00116	0.00005	0.00948	0.00192	0.00024	0.00005	7.4	0.34	9.6	1.94	20	1.6	7.12	0.16
K11-17	light pink	0.06562	0.04566	0.00097	0.00011	0.00921	0.00635	0.00049	0.00013	6.3	0.71	9.3	6.39	60	0.28	5.92	0.34
K11-18	light pink	0.11533	0.11925	0.00105	0.00023	0.01532	0.01554	0.00021	0.00021	6.8	1.45	15.4	15.54	54	0.37	6	0.7
K11-19	light pink	0.06475	0.04509	0.00105	0.00011	0.00983	0.00679	0.0003	0.00008	6.8	0.71	9.9	6.83	61	0.26	6.45	0.34
K11-20	light pink	0.10494	0.02418	0.00118	0.00008	0.01709	0.00388	0.00044	0.00013	7.6	0.5	47.2	3.88	0.5	7.8	6.35	9
K11-21	light pink	0.30794	0.07326	0.00123	0.00016	0.05645	0.01184	0.00033	0.0002	7.9	1.04	55.8	11.38	DISCORDANT			
K11-23	light pink	0.20942	0.11608	0.00117	0.00024	0.03208	0.01672	0.00149	0.00047	7.5	1.54	32.1	16.45	11	2.6	5.4	0.73
K11-24	light pink	0.68729	0.04628	0.00732	0.00032	0.70649	0.05895	0.01607	0.00341	47	2.06	542.7	35.08	DISCORDANT			
K11-26	light pink	0.3835	0.15808	0.00127	0.0003	0.07307	0.02571	0.00054	0.00041	8.2	1.9	71.6	24.32	0.7	7.3	3.6	34
K11-28	light pink	0.15043	0.0443	0.00118	0.00012	0.0241	0.00686	0.00067	0.00018	7.6	0.76	24.2	6.8	0.7	7.2	5.79	13
K11-29	light pink	0.05414	0.0492	0.00114	0.00013	0.00905	0.00818	0.00036	0.00014	7.3	0.85	9.1	8.23	81	0.058	7.17	0.4
K11-30	light pink	0.26425	0.12241	0.00119	0.00024	0.04835	0.02054	0.00226	0.00073	7.7	1.56	47.9	19.9	3.3	4.5	4.8	20
K11-31	light pink	0.44469	0.29211	0.00133	0.00049	0.07971	0.0444	0.0026	0.00099	8.5	3.14	77.9	41.75	8.7	2.9	3.8	1.5
K11-32	light pink	0.29535	0.12443	0.00137	0.00027	0.06242	0.02385	0.00053	0.00032	8.9	1.76	61.5	22.8	1.6	5.8	5.1	25
K11-33	pink	0.06473	0.03799	0.00113	0.00013	0.01045	0.00606	0.0003	0.00013	7.3	0.86	10.6	6.09	54	0.37	6.84	0.42
K11-34	pink	0.09596	0.18828	0.00128	0.00046	0.01617	0.03125	0.00275	0.00108	8.2	2.93	16.3	31.22	78	0.078	7.5	1.4
K11-35	pink	0.37053	0.15282	0.00388	0.00091	0.18723	0.06994	0.00619	0.00244	24.9	5.84	174.3	59.82	1.2	6.3	42	88
K11-36	pink	0.12391	0.06359	0.00104	0.00014	0.01954	0.00979	0.00106	0.00038	6.7	0.9	19.6	9.75	15	2.1	5.56	0.43
K11-37	pink	0.06604	0.02217	0.00128	0.00008	0.01201	0.00404	0.00038	0.00013	8.2	0.54	12.1	4.05	28	1.16	7.75	0.25
K11-39	pink	0.11906	0.20693	0.00096	0.00034	0.01714	0.02921	0.00214	0.00099	6.2	2.19	17.3	29.16	69	0.16	5.4	1
K11-40	pink	0.49137	0.55119	0.00099	0.00069	0.05589	0.04966	0.00042	0.00088	6.4	4.45	55.2	47.76	28	1.18	2.4	2.4
K11-41	pink	0.35269	0.09159	0.00173	0.00024	0.08556	0.02023	0.00233	0.0009	11.1	1.55	83.4	18.92	DISCORDANT			
K11-42	pink	0.66858	0.4452	0.00127	0.00061	0.12404	0.05988	0.0032	0.00186	8.2	3.9	118.7	54.1	4	4.2	4	47
K11-44	pink	0.10602	0.03242	0.00138	0.00012	0.0219	0.00669	0.00064	0.00029	8.9	0.74	22	6.65	2.9	4.8	7.42	10
K11-46	pink	0.04698	0.05064	0.00123	0.00015	0.00894	0.00961	0.00085	0.00041	7.9	0.95	9	9.68	90	0.016	7.82	0.46
K11-47	pink	0.09335	0.07982	0.00099	0.00017	0.01353	0.01141	0.00154	0.0007	6.3	1.06	13.6	11.43	49	0.48	5.7	0.52
K11-48	pink	0.32704	0.09416	0.00122	0.00019	0.06102	0.01595	0.00087	0.00043	7.8	1.21	60.1	15.26	DISCORDANT			
K11-49	pink	0.72004	0.71489	0.00105	0.00079	0.08795	0.05916	0.00068	0.00191	6.8	5.07	85.6	55.21	14	2.2	0.1	2.4
K11-50	pink	0.1119	0.06248	0.0017	0.00023	0.03026	0.01668	0.00069	0.00045	10.9	1.48	30.3	16.44	21	1.6	9.3	0.7
K11-51	pink	0.08016	0.01678	0.00112	0.00006	0.01368	0.00301	0.00053	0.00025	7.2	0.39	13.8	3.01	1.4	6	6.39	5.9
K11-52	pink	0.43259	0.18528	0.00133	0.00033	0.08697	0.03204	0.00187	0.0011	8.5	2.12	84.7	29.93	0.9	6.8	3.7	33
K11-53	pink	0.1474	0.03382	0.00488	0.00039	0.10905	0.02614	0.00149	0.0009	31.4	2.51	105.1	23.93	0.1	10.6	24.2	49

Table VIII.10: Owharoa Ignimbrite W110862

Spot No.	Colour	Measured isotope ratios and 1σ (%) internal errors						Estimated ages and 1σ absolute internal errors (My)			$^{206}\text{Pb}/^{238}\text{U}$ & $^{207}\text{Pb}/^{235}\text{U}$	Concordance (%)	Selected age and 1σ absolute external error (My)				
		$^{207}\text{Pb}/^{206}\text{Pb}$	\pm	$^{206}\text{Pb}/^{238}\text{U}$	\pm	$^{207}\text{Pb}/^{235}\text{U}$	\pm	$^{208}\text{Pb}/^{232}\text{Th}$	\pm	$^{206}\text{Pb}/^{238}\text{U}$	\pm	$^{207}\text{Pb}/^{235}\text{U}$	\pm	Spot MSWD	1σ absolute external error (My)		
K12-1	rusty	0.13816	0.07684	0.00057	0.00008	0.01134	0.00613	0.00032	0.00019	3.7	0.51	11.4	6.15	17	1.8	3.06	0.24
K12-2	rusty	0.52087	0.10546	0.00101	0.00013	0.07147	0.01151	0.00116	0.00029	6.5	0.85	70.1	10.91	DISCORDANT			
K12-3	rusty	0.38569	0.08063	0.00123	0.00015	0.06874	0.01219	0.00158	0.0003	7.9	0.95	67.5	11.58	DISCORDANT			
K12-4	pink	0.11676	0.03795	0.00195	0.00017	0.03445	0.0109	0.00179	0.00045	12.6	1.12	34.4	10.7	2.7	4.9	10.4	15
K12-5	pink	0.06806	0.11657	0.00083	0.00017	0.00754	0.01282	0.00072	0.0003	5.4	1.11	7.6	12.92	85	0.036	5.2	0.52
K12-6	pink	0.72271	0.15323	0.00154	0.00024	0.15761	0.02469	0.00466	0.00074	9.9	1.54	148.6	21.65	DISCORDANT			
K12-7	pink	0.23235	0.14875	0.00068	0.00016	0.02241	0.01341	0.00138	0.0005	4.4	1.03	22.5	13.32	15	2.1	3.06	0.48
K12-9	colourless	0.18845	0.07455	0.00107	0.00014	0.02894	0.01089	0.00095	0.00028	6.9	0.91	29	10.75	2.8	4.8	5.15	12
K12-11	colourless	0.28393	0.19172	0.00132	0.00034	0.05782	0.03638	0.00006	0.0006	8.5	2.21	57.1	34.92	45	2.1	5.7	4
K12-12	colourless	0.0507	0.01502	0.00059	0.00003	0.00404	0.00119	0.00021	0.00003	3.8	0.19	4.1	1.2	78	0.08	3.76	0.098
K12-13	colourless	0.1491	0.08336	0.00069	0.0001	0.01448	0.00785	0.0005	0.00017	4.4	0.64	14.6	7.86	17	1.9	3.66	0.3
K12-14	colourless	0.27148	0.13042	0.00115	0.00003	0.05438	0.02413	0.00218	0.00051	9.7	1.9	53.8	23.24	4.6	4	6.3	23
K12-15	colourless	0.19423	0.05495	0.00089	0.00009	0.02387	0.00635	0.00115	0.00022	5.7	0.6	24	6.3	0.2	9.7	4.14	11
K12-16	pink	0.22384	0.10494	0.00126	0.00022	0.04047	0.01784	0.00204	0.00067	8.1	1.39	40.3	17.44	5	3.8	5.7	0.66
K12-17	pink	0.24905	0.1705	0.00095	0.00023	0.03068	0.01971	0.00366	0.00098	6.1	1.5	30.7	19.41	18	1.8	4.4	0.69
K12-18	pink	0.45967	0.13492	0.00082	0.00015	0.05313	0.01271	0.00066	0.00036	5.3	0.94	52.6	12.25	DISCORDANT			
K12-19	pink	0.39555	0.15271	0.00082	0.00017	0.04428	0.01462	0.00132	0.00055	5.3	1.1	44	14.22	0.4	8.2	2.5	19
K12-20	pink	0.19726	0.03752	0.00068	0.00005	0.01897	0.00337	0.00027	0.00004	4.4	0.34	19.1	3.35	DISCORDANT			
K12-21	pink	0.72427	0.1747	0.0014	0.00025	0.14594	0.02522	0.00289	0.00053	9	1.63	138.3	22.35	DISCORDANT			
K12-22	pink	0.19092	0.10045	0.00103	0.00018	0.02693	0.01343	0.00184	0.00051	6.6	1.17	27	13.27	10	2.7	5	0.55
K12-23	pink	0.09488	0.09723	0.00084	0.00014	0.01074	0.01087	0.0006	0.00025	5.4	0.93	10.8	10.92	59	0.29	4.99	0.42
K12-24	light pink	0.12536	0.1045	0.00066	0.00012	0.01129	0.00919	0.00013	0.00022	4.2	0.79	11.4	9.23	40	0.69	3.68	0.36
K12-25	light pink	0.43591	0.14748	0.00092	0.00018	0.05422	0.01521	0.00073	0.00038	5.9	1.18	53.6	14.65	DISCORDANT			
K12-26	light pink	0.38906	0.13696	0.00097	0.00018	0.05221	0.01591	0.00245	0.00053	6.3	1.16	51.7	15.36	0.2	9.6	3.1	21
K12-27	light pink	0.31495	0.15839	0.00082	0.0002	0.03569	0.01595	0.00111	0.0004	5.3	1.27	35.6	15.63	4	4.2	2.9	16
K12-28	light pink	0.48014	0.15859	0.00063	0.00013	0.03954	0.01049	0.00083	0.00027	4.1	0.83	39.4	10.25	DISCORDANT			
K12-29	light pink	0.99757	0.31515	0.00085	0.00022	0.12041	0.02308	0.00185	0.00056	5.5	1.42	115.4	20.92	DISCORDANT			
K12-30	light pink	0.4683	0.107	0.0015	0.00021	0.09279	0.01765	0.00256	0.00048	9.6	1.34	90.1	16.4	DISCORDANT			
K12-31	light pink	0.17294	0.06612	0.00081	0.00011	0.01908	0.00693	0.00085	0.00018	5.2	0.68	19.2	6.9	2.7	4.9	3.85	9.5
K12-32	light pink	0.54292	0.12939	0.0009	0.00015	0.07193	0.01321	0.00094	0.00028	5.8	0.94	70.5	12.51	DISCORDANT			
K12-33	light pink	0.64132	0.13589	0.00092	0.00014	0.08062	0.01279	0.00152	0.00034	6	0.9	78.7	12.02	DISCORDANT			
K12-34	light pink	0.10061	0.0249	0.00064	0.00004	0.00911	0.00221	0.00022	0.00004	4.1	0.27	9.2	2.22	4.1	6.5	3.55	4
K12-35	light pink	0.59733	0.09412	0.00155	0.00017	0.12242	0.01539	0.00176	0.00039	10	1.1	117.3	13.92	DISCORDANT			
K12-36	light pink	0.21278	0.10926	0.0008	0.00015	0.02482	0.01194	0.00083	0.00028	5.2	0.98	24.9	11.83	7.5	3.2	3.64	0.45
K12-37	light pink	0.05023	0.00782	0.0006	0.00002	0.00406	0.00064	0.00021	0.00003	3.9	0.14	4.1	0.64	64	0.21	3.82	0.068
K12-38	light pink	0.22374	0.07372	0.0007	0.00009	0.02193	0.0067	0.00047	0.00016	4.5	0.61	22	6.65	0.5	8	3.07	9.8
K12-39	light pink	0.12439	0.06747	0.00074	0.0001	0.01335	0.00705	0.00089	0.0002	4.8	0.64	13.5	7.06	18	1.8	4.01	0.31

Table VIII.11: Ferry Landing Ignimbrite W110863

K12-40	light pink	0.55113	0.07555	0.00219	0.0002	0.15234	0.01783	0.00336	0.00057	+4.1	+2.9	+44	+5.74	DISCORDANT
K12-41	light pink	0.66122	0.23796	0.00066	0.00016	0.06254	0.01666	0.00018	0.00036	-4.2	-1.06	-61.6	+5.92	DISCORDANT
K12-42	light pink	0.3533	0.06367	0.00091	0.00009	0.04512	0.00718	0.00066	0.00013	-5.8	-0.57	-44.8	6.98	DISCORDANT
K12-43	light pink	0.40819	0.17131	0.00052	0.00013	0.02827	0.00977	0.00041	0.00021	-3.3	0.82	-28.3	9.65	0.6
K12-44	light pink	0.09629	0.02611	0.00057	0.00004	0.00726	0.00193	0.00015	0.00003	-3.7	0.26	-7.3	+1.94	3.3
K12-45	light pink	0.31789	0.16956	0.0005	0.00012	0.02241	0.01072	0.00093	0.00021	-3.2	0.78	-22.5	+0.64	5.5
K12-46	pink	0.5819	0.24892	0.0017	0.00051	0.14615	0.04693	0.00282	0.00119	+0.9	3.25	+138.5	41.58	0.2
K12-47	pink	0.84597	0.41922	0.00106	0.0004	0.12143	0.04122	0.00213	0.00093	-6.9	2.56	+16.4	37.33	0.3
K12-48	pink	0.14777	0.07024	0.00092	0.00012	0.01982	0.00912	0.00032	0.00014	-5.9	0.78	-19.9	9.09	9.8
K12-49	pink	0.14486	0.05978	0.00092	0.00011	0.01847	0.00737	0.00031	0.00016	-6	0.71	-18.6	7.35	6.1
K12-50	pink	0.46429	0.20562	0.00048	0.00013	0.02936	0.01024	0.00031	0.00023	-3.4	0.86	-29.4	10.1	0.6
K12-51	pink	0.24329	0.21058	0.00043	0.00014	0.01425	0.0114	0.00148	0.0004	-2.8	0.93	-14.4	+1.41	28
K12-52	pink	0.21511	0.11191	0.00081	0.00016	0.02422	0.01266	0.00078	0.00031	-5.2	1.01	-24.3	12.55	10
K12-53	pink	0.05598	0.00525	0.01777	0.00049	0.13037	0.01387	0.00496	0.00087	-113.5	3.12	-124.4	12.46	27

Spot No.	Colour	Measured isotope ratios and 1 σ (%) internal errors				Estimated ages and 1 σ absolute internal errors (My)				$^{206}\text{Pb}/^{238}\text{U}$ & $^{207}\text{Pb}/^{235}\text{U}$		Concordance (%)	Spot MSWD	Selected age and 1 σ absolute external error (My)			
		$^{207}\text{Pb}/^{206}\text{Pb}$	\pm	$^{206}\text{Pb}/^{238}\text{U}$	\pm	$^{207}\text{Pb}/^{235}\text{U}$	\pm	$^{208}\text{Pb}/^{232}\text{Th}$	\pm	$^{206}\text{Pb}/^{238}\text{U}$	\pm	$^{207}\text{Pb}/^{235}\text{U}$	\pm				
K13-2	colourless	0.27832	0.15014	0.00131	0.00029	0.0547	0.02731	0.00069	0.00026	8.4	+1.84	+54.1	26.3	7.4	3.3	5.5	0.87
K13-3	colourless	0.17703	0.1782	0.002	0.00053	0.05014	0.04902	0.00085	0.00058	12.9	3.4	49.7	47.4	42	0.66	10.4	1.6
K13-4	colourless	0.19912	0.14085	0.00149	0.00031	0.04633	0.03155	0.00089	0.00034	9.6	2.02	46	30.61	22	1.5	7.4	0.92
K13-5	colourless	0.42042	0.25918	0.0018	0.00061	0.10969	0.05818	0.00248	0.00085	11.6	3.92	105.7	53.24	7.3	3.2	5.3	1.8
K13-6	light pink	0.36354	0.2491	0.00117	0.0004	0.05122	0.03064	0.00035	0.00046	-7.5	2.59	50.7	29.59	12	2.4	4	1.2
K13-7	light pink	0.30495	0.34182	0.00246	0.0011	0.12824	0.1352	0.00094	0.00146	15.9	7.1	122.5	121.68	38	0.76	10.3	3.2
K13-8	light pink	0.20961	2.14933	0.00054	0.00163	0.01208	0.011842	0.00142	0.00169	-3.5	10.5	+12.2	+18.8	94	0.0063	2.7	5
K13-9	light pink	0.05528	0.28473	0.00125	0.00056	0.0107	0.0549	0.0016	0.00079	8.1	3.6	10.8	55.15	96	0.0028	7.9	1.7
K13-10	light pink	1.60712	5.60288	0.00042	0.00133	0.07558	0.10717	0.0009	0.00145	-2.7	8.57	74	+101.17	46	0.54	-2.8	4
K13-11	light pink	0.08209	0.23184	0.00132	0.00045	0.01719	0.04823	0.00053	0.00065	8.5	2.93	17.3	48.15	85	0.037	8	1.3
K13-13	light pink	0.30909	0.17348	0.00196	0.00046	0.10565	0.05536	0.00042	0.00066	12.6	2.96	102	50.84	7.7	3.1	8	1.4
K13-15	light pink	0.40779	0.2085	0.00174	0.00048	0.08413	0.03682	0.00072	0.00066	-14	3.08	82	34.49	32	4.6	5.2	40
K13-19	light pink	0.17666	0.07557	0.00165	0.00023	0.04132	0.01696	0.00033	0.00021	+10.6	1.46	+41.1	+16.53	4.9	3.9	8.1	47
K13-20	light pink	0.09066	0.14849	0.0016	0.00041	0.0198	0.03208	-0.00008	0.00065	10.3	2.67	19.9	31.95	75	0.104	9.6	1.2
K13-21	light pink	0.13652	0.08669	0.00163	0.00026	0.0341	0.02111	0.00066	0.00026	10.5	1.68	34.1	20.73	23	1.5	8.7	0.78
K13-22	light pink	0.23135	0.2122	0.00084	0.00029	0.02698	0.02302	0.00065	0.00026	-5.4	1.88	27	22.76	34	4.02	3.7	0.88
K13-23	light pink	0.05842	0.04004	0.00133	0.00012	0.01073	0.00731	0.0004	0.00011	8.6	0.8	10.8	7.34	73	0.116	8.34	0.37
K13-24	light pink	0.12656	0.10494	0.00149	0.00027	0.0253	0.02054	0.00053	0.00027	9.6	1.77	25.4	20.34	41	0.69	8.3	0.82
K13-26	light pink	0.14383	0.12591	0.00139	0.00029	0.02817	0.02405	0.00051	0.00037	9	1.88	28.2	23.75	39	0.74	7.5	0.87
K13-27	light pink	0.05278	0.10337	0.00224	0.0004	0.01447	0.02824	0.00108	0.0004	14.4	2.6	14.6	28.27	99.5	0	14.4	1.2

K13-28	light pink	0.17664	0.20661	0.00131	0.00043	0.03512	0.03961	0.00101	0.00042	8.4	2.75	35	38.86	47	0.52	6.7	1.3
K13-29	light pink	5.57674	45.19504	0.00009	0.00075	0.07737	0.07549	0.00098	0.00096	0.6	4.86	75.7	71.15	28	1.16	4	2.2
K13-30	light pink	0.22153	0.14783	0.00118	0.00028	0.03624	0.02274	0.00077	0.00033	7.6	1.83	36.1	22.25	47	1.8	5.4	0.85
K13-32	light pink	1.78432	1.60685	0.00105	0.00088	0.23024	0.08466	0.00228	0.00146	6.8	5.66	210.4	69.88	0.5	7.9	-7.3	94
K13-33	light pink	0.22963	0.28961	0.00231	0.00101	0.08915	0.1071	0.00139	0.00128	14.9	6.52	86.7	99.84	46	0.54	10.6	3
K13-35	light pink	0.0728	0.16567	0.002	0.00056	0.01848	0.04179	0.00087	0.00061	12.9	3.61	18.6	41.66	88	0.022	12.4	1.7
K13-36	light pink	0.31157	0.25304	0.00172	0.00064	0.06447	0.04717	-0.0014	0.00097	11.1	4.11	63.4	44.99	22	1.5	6.6	1.9
K13-37	light pink	0.26961	0.19839	0.00679	0.0019	0.20944	0.15197	0.00927	0.00304	43.7	12.18	193.1	127.58	24	1.4	31	5.7
K13-38	light pink	0.34366	0.16977	0.00247	0.0006	0.10247	0.04561	0.00094	0.00078	15.9	3.86	99.4	42.04	4	4.2	8.9	48
K13-39	light pink	0.24782	0.1746	0.0016	0.00043	0.04891	0.03222	0.00062	0.00044	10.3	2.76	48.5	31.19	19	1.7	7.1	1.3
K13-40	light pink	0.31382	0.74044	0.0007	0.00074	0.02938	0.06269	-0.00104	0.00093	4.5	4.57	29.4	61.84	67	0.18	2.8	2.4
K13-41	light pink	0.31288	0.11607	0.00199	0.00036	0.09441	0.03186	0.00089	0.00029	12.8	2.3	91.3	29.57	0.6	7.5	7.2	37
K13-42	light pink	0.40539	0.1253	0.00233	0.00042	0.13209	0.03554	0.00123	0.0004	4.5	2.72	426	31.88	DISCORDANT			
K13-43	light pink	0.15071	0.17204	0.00372	0.0011	0.09492	0.10638	0.00112	0.00111	23.9	7.09	92.1	98.66	48	0.5	19.5	3.3
K13-44	light pink	0.19549	0.18555	0.00274	0.00081	0.06713	0.0613	0.00119	0.00104	17.7	5.19	66	58.33	38	0.77	13.6	2.5
K13-45	light pink	0.61163	0.13105	0.00437	0.00066	0.39843	0.07953	0.00544	0.00164	28.1	4.23	340.5	57.75	DISCORDANT			
K13-46	light pink	0.1716	0.15428	0.00161	0.00042	0.03432	0.02973	0.00115	0.00043	10.3	2.69	34.3	29.18	38	0.77	8.3	1.3
K13-47	light pink	0.14487	0.0583	0.00124	0.00015	0.02663	0.01043	0.0004	0.00015	8	0.94	26.7	10.32	5	3.8	6.33	0.46
K13-48	light pink	0.64281	0.18669	0.00253	0.00053	0.23929	0.05599	0.00299	0.0009	16.3	3.39	217.8	45.88	DISCORDANT			
K13-49	colourless	0.50568	0.48201	0.00182	0.00104	0.09474	0.07394	0.00044	0.00186	11.7	6.67	91.9	68.58	22	4.5	4.5	3.2
K13-51	colourless	0.20542	0.16766	0.00241	0.00067	0.07325	0.05714	0.00122	0.00092	15.5	4.34	71.8	54.06	28	1.18	11.4	2

142

Table VIII.12: Shakespeare Cliff Ignimbrite W110864

Spot No.	Colour	Measured isotope ratios and 1 σ (%) internal errors						Estimated ages and 1 σ absolute internal errors (My)				$^{206}\text{Pb}/^{238}\text{U}$ & $^{207}\text{Pb}/^{235}\text{U}$		Concordance (%)	Spot MSWD	Selected age and 1 σ absolute external error (My)	
		$^{207}\text{Pb}/^{206}\text{Pb}$	\pm	$^{206}\text{Pb}/^{238}\text{U}$	\pm	$^{207}\text{Pb}/^{235}\text{U}$	\pm	$^{208}\text{Pb}/^{232}\text{Th}$	\pm	$^{206}\text{Pb}/^{238}\text{U}$	\pm	$^{207}\text{Pb}/^{235}\text{U}$	\pm				
K14-1	colourless	0.54117	0.30209	0.00304	0.00107	0.23785	0.1097	0.00403	0.00184	49.4	6.88	216.7	89.98	3.5	4.5	6.5	85
K14-2	colourless	0.38491	0.28769	0.00343	0.00129	0.20502	0.14001	0.00307	0.00281	22.1	8.29	189.4	117.98	17	1.9	11.9	3.8
K14-3	colourless	0.47899	0.13811	0.00153	0.00028	0.10116	0.02382	0.00131	0.00034	9.8	1.78	98.3	21.95	DISCORDANT			
K14-4	colourless	0.29869	0.24248	0.00225	0.00084	0.0937	0.06881	0.00071	0.00135	14.5	5.39	90.9	63.88	22	1.5	8.6	2.5
K14-5	colourless	0.38137	0.16759	0.00239	0.00055	0.12567	0.04875	0.00275	0.00079	45.4	3.54	120.2	43.98	4.5	5.9	7.8	54
K14-6	colourless	0.35457	0.26231	0.00159	0.00057	0.06997	0.04591	0.0022	0.0008	10.2	3.64	68.7	43.57	16	2	5.7	1.7
K14-7	colourless	0.53998	0.31966	0.00165	0.0006	0.12261	0.05881	0.00362	0.00109	40.6	3.87	117.4	53.19	4.3	4.1	3.7	46
K14-8	colourless	0.32132	0.22443	0.00194	0.00061	0.0876	0.05553	0.00346	0.00111	12.5	3.91	85.3	51.84	15	2.1	7.5	1.8
K14-9	colourless	0.65636	0.40722	0.00162	0.00073	0.14431	0.06461	0.00234	0.00129	40.4	4.67	136.9	57.33	2.7	4.9	4.2	62
K14-10	colourless	0.43344	0.11336	0.00178	0.00027	0.11228	0.0251	0.0013	0.0003	11.5	1.75	108	22.92	DISCORDANT			
K14-11	colourless	0.36927	0.12724	0.00169	0.00031	0.0927	0.02796	0.00214	0.00045	40.9	4.99	90	25.98	0.2	9.8	5.4	37
K14-12	colourless	1.50892	2.49276	0.00051	0.00078	0.12589	0.08575	0.00161	0.00091	3.3	5	120.4	77.34	43	2.3	-3.4	2.3
K14-13	colourless	0.40792	0.15672	0.007	0.00144	0.42705	0.16777	0.01088	0.00352	44.9	9.23	361.1	119.37	4.7	5.7	25.3	130

K14-14	light pink	0.44006	0.37194	0.0024	0.00103	0.14798	0.11089	0.00115	0.00261	15.5	6.64	140.1	98.08	21	1.6	8	3.1
K14-15	light pink	0.19667	0.06837	0.00136	0.00016	0.03855	0.01275	0.00102	0.00025	8.8	4.05	38.4	12.47	4.2	6.4	6.46	46
K14-16	light pink	0.73072	0.41309	0.00227	0.00096	0.29882	0.12603	0.00188	0.00181	44.6	6.16	265.5	98.52	1.8	5.6	4.6	84
K14-17	light pink	0.10753	0.14198	0.00346	0.00086	0.04394	0.05722	0.00586	0.00208	22.3	5.53	43.7	55.66	68	0.17	20.2	2.6
K14-18	light pink	0.5795	0.25242	0.00258	0.00072	0.18656	0.06596	0.00184	0.00109	46.6	4.66	173.7	56.44	0.6	7.6	5.3	75
K14-19	light pink	0.08972	0.03019	0.01345	0.00097	0.162	0.05586	0.00616	0.0013	86.1	6.18	152.5	48.81	14	2.2	78.2	3
K14-20	light pink	0.10133	0.34954	0.00145	0.00075	0.01852	0.06321	0.00164	0.00107	9.3	4.82	18.6	63.01	87	0.025	8.7	2.3
K14-21	light pink	0.24996	0.25896	0.00125	0.00048	0.04294	0.04153	0.00084	0.00059	8	3.08	42.7	40.44	37	0.81	5.6	1.4
K14-22	light pink	0.4009	0.16873	0.00546	0.00123	0.33218	0.13201	0.00585	0.00216	35.4	7.94	291.2	100.62	4.7	5.7	18.4	110
K14-23	light pink	0.67412	0.40418	0.00486	0.00206	0.46201	0.23822	0.01584	0.00487	31.3	13.24	385.7	165.45	5.7	3.6	9	6.1
K14-24	light pink	0.28026	0.11017	0.00182	0.00034	0.06679	0.02415	0.00186	0.00059	44.7	2	65.6	22.98	4.4	6.1	7.4	29
K14-25	light pink	0.28543	0.19419	0.00221	0.00061	0.09477	0.06	0.00085	0.00097	14.2	3.9	91.9	55.65	15	2	9.3	1.8
K14-27	light pink	0.24497	0.1758	0.0014	0.0004	0.05978	0.03983	0.0005	0.0005	9	2.56	59	38.17	18	1.8	5.9	1.2
K14-28	light pink	2.56718	0.83481	0.00245	0.00075	0.82478	0.13254	0.00717	0.00206	45.8	4.85	610.7	73.75	DISCORDANT			
K14-29	light pink	0.61687	0.13748	0.0025	0.0004	0.22264	0.03935	0.00378	0.00096	46.1	2.56	204.1	32.68	DISCORDANT			
K14-30	light pink	0.17043	0.15948	0.0024	0.00061	0.06471	0.05876	0.00273	0.00116	15.5	3.91	63.7	56.04	37	0.8	12.3	1.8
K14-32	light pink	0.24798	0.12276	0.00296	0.00055	0.11283	0.05328	0.00313	0.00098	19	3.54	108.6	48.61	6.1	3.5	13.2	1.6
K14-33	light pink	0.3614	0.10119	0.00233	0.00034	0.12307	0.03106	0.00099	0.00038	45	2.19	117.9	28.08	DISCORDANT			
K14-34	light pink	0.88537	0.1697	0.00522	0.00079	0.60317	0.09827	0.00701	0.00172	33.6	5.05	479.2	62.24	DISCORDANT			
K14-35	light pink	0.23277	0.14388	0.00255	0.00055	0.09722	0.05751	0.00192	0.00084	16.4	3.53	94.2	53.22	14	2.2	11.7	1.6
K14-36	light pink	0.23224	0.09492	0.00279	0.00044	0.09373	0.03633	0.003	0.00089	48	2.85	94	33.73	2.5	5	12.3	38
K14-37	light pink	0.45559	0.2038	0.0028	0.00071	0.18704	0.07299	0.00296	0.00116	48.1	4.57	174.1	62.44	4.4	6	8.1	66
K14-38	light pink	0.50092	0.34125	0.0014	0.00053	0.14396	0.06363	0.00064	0.00069	9	3.42	136.6	56.48	2.6	5	2.3	44
K14-39	light pink	0.44394	0.10129	0.00181	0.00024	0.12423	0.02487	0.00126	0.0004	11.6	1.56	118.9	22.46	DISCORDANT			
K14-40	light pink	3.10823	7.91913	0.00019	0.00047	0.09104	0.05401	0.00161	0.00093	4.2	3.04	88.5	50.27	8	3.1	3.5	4.4
K14-41	light pink	0.48246	0.20243	0.00318	0.0008	0.27513	0.10213	0.0043	0.00148	20.5	5.12	246.8	81.33	0.9	6.8	8.5	78
K14-42	light pink	0.37254	0.16174	0.00213	0.00044	0.11324	0.04462	0.00138	0.00075	43.7	2.84	108.9	40.7	4.8	5.6	7.8	39
K14-43	light pink	0.70149	0.31832	0.00262	0.00085	0.24148	0.08283	0.00593	0.00239	16.9	5.47	219.6	67.74	0.4	8.3	2.9	93
K14-44	light pink	0.31513	0.20879	0.00286	0.00082	0.12162	0.07453	0.00388	0.00171	18.4	5.27	116.5	67.47	14	2.2	11.5	2.5
K14-45	light pink	0.223	0.14756	0.00172	0.00039	0.05649	0.03549	0.00005	0.00005	11.1	2.54	55.8	34.11	17	1.9	8	1.2
K14-46	light pink	0.33779	0.07892	0.00179	0.00022	0.09629	0.02065	0.00187	0.00055	44.5	4.44	93.3	19.13	DISCORDANT			
K14-48	light pink	0.79024	0.12755	0.00523	0.00062	0.57284	0.08737	0.0073	0.00212	33.6	3.98	459.9	56.4	DISCORDANT			
K14-49	light pink	0.78394	0.06367	0.00272	0.00117	2.71788	0.35323	0.04324	0.01186	144.8	7.38	1333.4	96.47	DISCORDANT			
K14-50	light pink	0.0935	0.08411	0.00247	0.00037	0.03486	0.03108	0.00181	0.00064	15.9	2.41	34.8	30.5	51	0.43	14.5	1.1
K14-51	light pink	0.26136	0.13262	0.00374	0.00071	0.16439	0.08083	0.00251	0.00113	24.1	4.57	154.5	70.48	6.7	3.3	16.6	2.1
K14-52	light pink	0.30004	0.19092	0.00309	0.00085	0.14865	0.08832	0.00337	0.00169	19.9	5.47	140.7	78.08	12	2.4	12.4	2.5
K14-53	light pink	0.11157	0.19403	0.00197	0.00062	0.03302	0.05661	0.0005	0.00096	12.7	4.01	33	55.64	70	0.15	11.3	1.9

Table VIII.13: Papakura Bay Dome W110865

Spot No.	Colour	Measured isotope ratios and 1σ (%) internal errors						Estimated ages and 1σ absolute internal errors (My)				$^{206}\text{Pb}/^{238}\text{U}$ & $^{207}\text{Pb}/^{235}\text{U}$		Selected age and 1σ absolute external error (My)			
		$^{207}\text{Pb}/^{206}\text{Pb}$	\pm	$^{206}\text{Pb}/^{238}\text{U}$	\pm	$^{207}\text{Pb}/^{235}\text{U}$	\pm	$^{208}\text{Pb}/^{222}\text{Th}$	\pm	$^{206}\text{Pb}/^{238}\text{U}$	\pm	$^{207}\text{Pb}/^{235}\text{U}$	\pm	Concordance	Spot MSWD		
K15-1	pink	0.14872	0.0854	0.00202	0.00042	0.0498	0.02724	0.00335	0.00155	13	2.71	49.3	26.34	14	2.2	9.5	1.3
K15-2	pink	0.369	0.1376	0.00092	0.0002	0.04333	0.01353	0.0041	0.004	5.9	1.29	43.1	13.16	0.3	9.4	2.5	24
K15-3	pink	0.09681	0.10173	0.00077	0.0002	0.01072	0.01097	0.00022	0.00025	5	1.27	10.8	11.02	55	0.35	4.3	0.63
K15-4	pink	0.42323	0.15976	0.001	0.00024	0.06479	0.01956	0.00265	0.00068	6.4	1.56	63.7	18.66	0.4	40.3	2.1	30
K15-5	pink	0.36435	0.11462	0.0012	0.00023	0.05774	0.01499	0.00028	0.00029	7.8	1.54	57	14.39	DISCORDANT			
K15-6	pink	0.15725	0.12781	0.00091	0.00026	0.01813	0.01392	0.00088	0.00064	5.9	1.66	18.2	13.88	32	0.98	4.4	0.82
K15-7	pink	0.17889	0.09389	0.00132	0.00028	0.03284	0.016	0.00121	0.00081	8.5	1.83	32.8	15.73	9	2.9	5.8	0.87
K15-8	pink	0.16343	0.10109	0.00107	0.00025	0.02431	0.01411	0.00015	0.00037	6.9	1.59	24.4	13.99	17	1.9	5	0.78
K15-9	pink	0.11035	0.08847	0.0009	0.00022	0.0132	0.01015	0.0005	0.00035	5.8	1.39	13.3	10.17	40	0.7	4.8	0.7
K15-10	pink	0.22142	0.09935	0.0009	0.00019	0.02625	0.01062	0.00045	0.00029	5.8	1.21	26.3	10.5	3.2	4.6	3.5	16
K15-11	pink	0.11262	0.11195	0.00085	0.00022	0.01373	0.01324	0.00003	0.00027	5.4	1.4	13.8	13.26	49	0.48	4.6	0.68
K15-12	pink	0.43126	0.15578	0.00134	0.00031	0.08528	0.02496	0.00003	0.00049	8.6	2.01	83.4	23.35	DISCORDANT			
K15-13	pink	0.10813	0.09348	0.00092	0.00022	0.01507	0.01259	0.00075	0.00046	5.9	1.42	15.2	12.59	42	0.66	4.9	0.69
K15-14	pink	0.05253	0.01614	0.0083	0.00066	0.06147	0.01908	0.00428	0.00109	53.3	4.24	60.6	18.25	62	0.25	51.5	2.3
K15-15	pink	0.1035	0.05859	0.00143	0.00024	0.02077	0.01135	0.00102	0.00041	9.2	1.54	20.9	11.29	24	1.4	7.6	0.77
K15-16	pink	0.58055	0.1066	0.00265	0.00034	0.22078	0.03446	0.00388	0.00082	17	2.22	202.6	28.66	DISCORDANT			
K15-17	pink	0.73256	0.14641	0.00464	0.00071	0.47657	0.08407	0.01346	0.00282	29.8	4.56	395.7	57.84	DISCORDANT			
K15-18	pink	0.44328	0.10073	0.00329	0.00049	0.19889	0.04	0.01377	0.00307	21.2	3.12	184.2	33.87	DISCORDANT			
K15-19	pink	0.23413	0.13543	0.00111	0.0003	0.03416	0.01771	0.00095	0.00054	7.4	1.96	34.4	17.39	9.4	2.9	4.3	0.93
K15-20	pink	0.36238	0.14827	0.00108	0.00026	0.05056	0.0174	0.00078	0.0005	7	1.67	50.1	16.84	0.6	7.5	2.9	28
K15-21	pink	0.10621	0.07106	0.00172	0.00034	0.02812	0.01822	0.00287	0.001	11.1	2.17	28.2	18	29	1.11	9.1	1.1
K15-22	pink	0.40887	0.14989	0.00123	0.00029	0.07578	0.02284	0.0003	0.00047	7.9	1.84	74.2	21.56	0.4	40.3	2.6	36
K15-23	pink	0.4084	0.23672	0.0006	0.00021	0.03486	0.01651	0.00331	0.00088	3.9	1.34	34.8	16.2	4.3	4.4	4.4	16
K15-24	pink	0.80029	0.156	0.00625	0.00094	0.58323	0.10436	0.03924	0.00854	40.2	6	466.5	66.93	DISCORDANT			
K15-25	light pink	0.45521	0.13387	0.00145	0.00028	0.09368	0.02243	0.00205	0.00073	9.4	1.83	90.9	20.83	DISCORDANT			
K15-26	light pink	0.76133	0.15737	0.00323	0.0005	0.33508	0.05854	0.01056	0.00243	20.8	3.22	293.4	44.52	DISCORDANT			
K15-27	light pink	0.11809	0.10743	0.00121	0.00032	0.01965	0.01726	0.00011	0.00031	7.8	2.03	19.8	17.18	44	0.6	6.4	1
K15-28	light pink	0.57079	0.11531	0.00334	0.00048	0.28177	0.05056	0.01011	0.00236	21.5	3.05	252.1	40.05	DISCORDANT			
K15-29	light pink	0.143	0.11625	0.00072	0.0002	0.01302	0.01004	0.00046	0.00031	4.6	1.26	13.1	10.06	34	0.9	3.6	0.63
K15-30	light pink	0.16647	0.04683	0.00103	0.00013	0.02479	0.00652	0.00068	0.00024	6.6	0.83	24.9	6.47	0.2	9.9	4.34	16
K15-31	light pink	0.17712	0.08769	0.00092	0.00019	0.02296	0.01052	0.00082	0.00036	5.9	1.23	23.1	10.44	7	3.3	4	0.59
K15-32	light pink	0.46981	0.13815	0.00226	0.00043	0.14821	0.03716	0.00556	0.00173	14.5	2.79	140.3	32.86	DISCORDANT			
K15-33	light pink	0.11197	0.08295	0.00109	0.00023	0.01664	0.01192	0.00072	0.00042	7	1.49	16.8	11.91	36	0.83	5.8	0.72
K15-34	light pink	0.91917	0.31604	0.00147	0.0004	0.21943	0.05417	0.00587	0.00172	9.5	2.59	201.4	45.4	DISCORDANT			
K15-35	light pink	0.50292	0.17821	0.001	0.00023	0.06419	0.01865	0.00113	0.00052	6.4	1.45	63.2	17.79	DISCORDANT			
K15-36	light pink	0.1415	0.07016	0.00112	0.0002	0.02209	0.01045	0.00105	0.00037	7.2	1.27	22.2	10.38	11	2.6	5.4	0.63
K15-37	light pink	0.30443	0.19719	0.00084	0.00028	0.03662	0.02077	0.0021	0.00099	5.4	1.8	36.5	20.35	40	2.7	2.8	0.85

K15-38	light pink	0.54971	0.31445	0.00049	0.00019	0.03863	0.01686	0.0004	0.00038	3.2	1.22	38.5	16.49	2.4	5.4	0.7	16
K15-39	light pink	0.12655	0.11581	0.00078	0.00022	0.01421	0.01249	0.00045	0.00032	5	1.39	14.3	12.5	44	0.68	4	0.69
K15-40	pink	0.95362	0.26592	0.00101	0.00022	0.13968	0.02783	0.00603	0.00162	6.5	1.45	132.8	24.8	DISCORDANT			
K15-41	pink	0.08311	0.02538	0.00586	0.00057	0.07433	0.02308	0.00404	0.0011	37.7	3.64	72.8	21.81	6.5	3.4	31.9	1.9
K15-42	pink	0.25722	0.1238	0.00134	0.00031	0.05462	0.0239	0.00093	0.00066	8.6	2.02	54	23.01	3.7	4.3	5	25
K15-43	pink	0.20478	0.11529	0.00091	0.00023	0.02992	0.01548	0.00024	0.00028	5.9	1.46	29.9	15.26	8.9	2.9	3.6	0.71
K15-44	pink	0.65068	0.16026	0.00208	0.00037	0.20126	0.04154	0.005	0.0015	13.4	2.39	186.2	35.14	DISCORDANT			
K15-45	pink	0.31805	0.10245	0.00146	0.00026	0.07031	0.02037	0.00201	0.00074	9.4	1.69	69	19.33	0.1	10.4	4.6	32
K15-46	pink	0.14975	0.12679	0.00087	0.00025	0.01774	0.0143	0.00051	0.00037	5.6	1.6	17.9	14.26	34	0.9	4.3	0.78
K15-48	pink	0.44908	0.19048	0.0008	0.00022	0.05097	0.01745	0.00088	0.00044	5.1	1.41	50.5	16.86	0.5	8	1.6	24
K15-49	pink	0.27986	0.10173	0.00087	0.00017	0.03577	0.01158	0.006	0.0003	5.6	1.1	35.7	11.35	0.4	8.1	2.9	19
K15-50	pink	0.27374	0.19429	0.00056	0.0002	0.02199	0.0138	0.00076	0.00046	3.6	1.27	22.4	13.74	45	2.1	2	0.61
K15-51	pink	0.07336	0.06275	0.00116	0.00023	0.01273	0.0107	0.0009	0.00038	7.5	1.45	12.8	10.73	57	0.32	6.7	0.73
K15-52	pink	0.1598	0.07368	0.00134	0.00025	0.03066	0.01341	0.00037	0.00028	8.6	1.61	30.7	13.21	6.5	3.4	6	0.78
K15-53	pink	0.13025	0.06867	0.00126	0.00025	0.0235	0.01179	0.00067	0.00035	8.1	1.62	23.6	11.7	14	2.2	6	0.8

Table VIII. 14: Whale Bone Bay Dome W110866

Spot No.	Colour	Measured isotope ratios and 1 σ (%) internal errors						Estimated ages and 1 σ absolute internal errors (My)				$^{206}\text{Pb}/^{238}\text{U}$ & $^{207}\text{Pb}/^{235}\text{U}$	Concordance (%)	Selected age and 1 σ absolute external error (My)			
		$^{207}\text{Pb}/^{206}\text{Pb}$	\pm	$^{206}\text{Pb}/^{238}\text{U}$	\pm	$^{207}\text{Pb}/^{235}\text{U}$	\pm	$^{208}\text{Pb}/^{232}\text{Th}$	\pm	$^{206}\text{Pb}/^{238}\text{U}$	\pm	$^{207}\text{Pb}/^{235}\text{U}$	\pm	Spot MSWD	1 σ absolute external error (My)		
K16-1	light pink	0.46623	0.32552	0.0006	0.00025	0.03772	0.02134	0.00084	0.00039	3.9	1.61	37.6	20.88	8.9	2.9	1.4	0.75
K16-2	light pink	0.23805	0.24675	0.00052	0.00021	0.01849	0.01762	0.00056	0.00032	3.3	1.38	18.6	17.57	36	0.85	2.2	0.63
K16-3	light pink	0.69586	0.11544	0.00589	0.00074	0.51704	0.0769	0.0187	0.00357	37.9	4.75	423.2	51.47	DISCORDANT			
K16-4	light pink	0.11213	0.22108	0.0005	0.00019	0.007	0.01356	0.00005	0.00034	3.2	1.2	7.1	13.67	76	0.094	2.9	0.58
K16-5	light pink	0.29357	0.15904	0.00073	0.00018	0.03066	0.01488	0.00044	0.00027	4.7	1.17	30.7	14.65	6	3.5	2.8	0.54
K16-6	light pink	0.07291	0.06524	0.00144	0.00019	0.01496	0.01327	0.00009	0.00023	9.3	1.24	15.1	13.27	64	0.23	8.8	58
K16-7	light pink	0.12487	0.127	0.00134	0.00031	0.02565	0.0255	0.00071	0.00039	8.6	1.98	25.7	25.25	47	0.52	7.4	0.93
K16-8	light pink	0.26025	0.28421	0.00079	0.00032	0.02781	0.02833	0.00072	0.00062	5.1	2.04	27.9	27.99	39	0.74	3.5	0.96
K16-9	light pink	0.40995	0.12312	0.0016	0.00029	0.09286	0.02339	0.00166	0.00045	10.3	1.85	90.2	21.73	DISCORDANT			
K16-10	light pink	0.06091	0.06232	0.00091	0.00013	0.0075	0.00761	0.001	0.00035	5.9	0.82	7.6	7.67	80	0.062	5.68	0.4
K16-12	light pink	0.36721	0.14516	0.0008	0.00016	0.04058	0.01394	0.00061	0.00049	5.2	1.06	40.4	13.6	0.6	7.4	2.67	47
K16-13	light pink	0.12935	0.16819	0.00114	0.00031	0.02085	0.02656	0.00137	0.00057	7.3	2.02	21	26.41	58	0.3	6.4	0.93
K16-15	light pink	0.2841	0.10754	0.00172	0.00031	0.06985	0.02401	0.00165	0.00051	11.1	1.97	68.6	22.78	0.8	7	6.4	32
K16-18	pink	0.12726	0.11648	0.00089	0.00019	0.01639	0.01463	0.00014	0.00025	5.8	1.23	16.5	14.62	43	0.63	4.9	0.58
K16-19	pink	0.2596	0.1836	0.00095	0.00027	0.03058	0.01993	0.00057	0.00043	6.1	1.74	30.6	19.64	18	1.8	4.1	0.82
K16-20	pink	0.40914	0.07943	0.00167	0.00019	0.09878	0.01673	0.00161	0.0004	10.7	1.24	95.6	15.46	DISCORDANT			
K16-21	pink	0.21969	0.28078	0.00064	0.00028	0.01697	0.02044	0	0.00053	4.1	1.78	17.1	20.41	49	0.47	3	0.85
K16-22	pink	0.16764	0.17344	0.00111	0.00032	0.02837	0.02832	0.00011	0.00047	7.2	2.04	28.4	27.97	42	0.65	5.7	0.96
K16-23	pink	0.43654	0.22175	0.00085	0.00024	0.04865	0.02091	0.00142	0.0006	5.5	1.55	48.2	20.24	2.7	4.9	2.5	20

K16-24	pink	0.47538	0.25398	0.00076	0.00025	0.04818	0.02088	0.00096	0.00041	4.9	4.59	47.8	20.23	2.6	5	4.7	24
K16-25	pink	0.32112	0.17518	0.00078	0.00021	0.03434	0.01654	0.00023	0.00015	5	4.33	34.3	16.24	5.6	3.7	2.7	0.64
K16-26	pink	0.2513	0.11232	0.00109	0.00021	0.03985	0.01633	0.00186	0.00058	7	4.36	39.7	15.95	3	4.7	4.4	18
K16-27	pink	0.32911	0.17682	0.00098	0.00026	0.04612	0.02188	0.00023	0.00035	6.3	4.67	45.8	21.23	5.4	3.8	3.4	0.78
K16-28	pink	0.63422	0.24392	0.00124	0.00034	0.10924	0.03086	0.00102	0.00059	8	2.2	105.3	28.25	DISCORDANT			
K16-29	pink	0.05941	0.2017	0.00119	0.00037	0.0089	0.03011	0.00125	0.00069	7.6	2.39	9	30.3	96	0.0022	7.6	1.1
K16-30	pink	1.51317	1.26538	0.00029	0.00023	0.05804	0.01975	0.0003	0.00024	4.9	4.45	57.3	18.95	0.2	9.3	2.4	27
K16-31	pink	0.12415	0.12128	0.00183	0.00037	0.03208	0.03082	0.00016	0.00053	11.8	2.39	32.1	30.32	48	0.51	10.3	1.1
K16-32	pink	8.63846	46.67915	0.00014	0.00077	0.15538	0.06947	0.00216	0.00141	0.9	4.94	146.7	61.05	4.8	5.6	9.5	70
K16-33	pink	0.36141	0.21275	0.00079	0.00024	0.04092	0.02094	0.00026	0.00028	5.1	4.54	40.7	20.43	6.7	3.4	2.6	0.72
K16-34	pink	0.76874	0.38886	0.00068	0.00025	0.06413	0.02264	0.00146	0.00054	4.4	4.63	63.4	24.6	0.5	7.9	0.4	27
K16-35	pink	0.4146	0.14592	0.00092	0.00019	0.05357	0.01592	0.00071	0.00035	5.9	4.21	53	45.34	0.4	10.3	2.4	23
K16-36	pink	0.20476	0.10403	0.00176	0.00032	0.05077	0.02449	0.00031	0.00033	11.3	2.07	50.3	23.66	8.1	3	8.2	0.97
K16-38	pink	0.21349	0.11515	0.00102	0.0002	0.03205	0.01631	0.00076	0.00037	6.6	1.29	32	16.04	9.2	2.8	4.7	0.6
K16-39	pink	0.6928	0.24599	0.00079	0.00021	0.0809	0.02076	0.00044	0.00031	5.1	4.32	79	49.5	DISCORDANT			
K16-40	pink	0.39308	0.1446	0.00072	0.00015	0.03776	0.01185	0.00014	0.00014	4.6	0.95	37.6	11.6	0.3	9.1	2.07	17
K16-41	pink	0.36283	0.11951	0.00111	0.00018	0.05122	0.01509	0.00048	0.00027	7.1	4.19	50.7	14.57	0.2	9.9	3.9	22
K16-42	pink	0.19702	0.14892	0.00082	0.00021	0.02066	0.01476	0.00044	0.00028	5.3	4.37	20.8	14.68	26	4.3	3.9	0.64
K16-43	pink	0.06157	0.10737	0.00093	0.00018	0.00791	0.01371	0.00044	0.00029	6	1.18	8	13.81	88	0.025	5.8	0.55
K16-44	pink	0.24619	0.1427	0.00123	0.00027	0.04217	0.02293	0.00006	0.00034	7.9	1.75	41.9	22.34	11	2.6	5.5	0.81
K16-45	pink	0.25494	0.13883	0.00112	0.00023	0.03947	0.02016	0.00052	0.00034	7.2	1.51	39.3	19.69	8.6	2.9	5	0.69
K16-46	pink	0.80744	0.18263	0.00403	0.00069	0.52002	0.10423	0.01143	0.00348	26	4.4	425.2	69.63	DISCORDANT			
K16-47	pink	0.34854	0.17159	0.00087	0.00022	0.04492	0.01942	0.00121	0.00046	5.6	4.42	44.6	18.87	3	4.7	2.9	48
K16-48	pink	0.35575	0.31116	0.00064	0.00026	0.02716	0.02123	0.00172	0.00074	4.1	4.67	27.2	20.99	24	1.4	2.4	0.78
K16-49	pink	0.41995	0.30732	0.00232	0.00083	0.16835	0.11232	0.00415	0.00268	14.9	5.33	158	97.61	15	2	8.4	24
K16-50	pink	0.40141	0.25208	0.00079	0.00025	0.04545	0.025	0.00098	0.00054	5.1	4.62	45.1	24.28	8.6	2.9	2.6	0.74

Table VIII.15: Shark Bay Dome W110867

Spot No.	Colour	Measured isotope ratios and 1 σ (%) internal errors						Estimated ages and 1 σ absolute internal errors (My)						$^{206}\text{Pb}/^{238}\text{U}$ & $^{207}\text{Pb}/^{235}\text{U}$		Selected age and 1 σ absolute external error (My)	
		$^{207}\text{Pb}/^{206}\text{Pb}$	\pm	$^{206}\text{Pb}/^{238}\text{U}$	\pm	$^{207}\text{Pb}/^{235}\text{U}$	\pm	$^{208}\text{Pb}/^{232}\text{Th}$	\pm	$^{206}\text{Pb}/^{238}\text{U}$	\pm	$^{207}\text{Pb}/^{235}\text{U}$	\pm	Concordance (%)	Spot MSWD		
K17-1	pink	0.07494	0.14842	0.00113	0.00027	0.01213	0.02387	0.00024	0.0004	7.3	1.71	12.2	23.95	83	0.049	6.9	0.81
K17-3	pink	0.07664	0.11712	0.00089	0.00019	0.01082	0.01638	0.00104	0.00034	5.8	1.24	10.9	16.45	74	0.114	5.4	0.57
K17-4	pink	0.10723	0.07404	0.00091	0.00013	0.01268	0.0086	0.00011	0.00013	5.9	0.81	12.8	8.63	38	0.77	5.22	0.4
K17-5	pink	0.10799	0.0586	0.00093	0.00011	0.01427	0.00759	0.00018	0.00009	6	0.71	14.4	7.6	23	1.4	5.24	0.34
K17-6	pink	0.16545	0.2594	0.00077	0.00029	0.02017	0.03073	-0.00016	0.00037	5	1.88	20.3	30.59	60	0.28	4.1	0.86
K17-7	pink	0.26897	0.16376	0.0006	0.00015	0.02642	0.01479	0.00078	0.00024	3.9	0.97	26.5	14.63	10	2.6	2.48	0.45
K17-8	pink	0.4713	0.11055	0.00195	0.00027	0.134	0.02698	0.00317	0.00071	42.5	4.76	427.7	24.16	DISCORDANT			
K17-10	light pink	0.15733	0.13885	0.00129	0.00029	0.02368	0.02026	-0.00025	0.00039	8.3	1.89	23.8	20.1	41	0.69	6.9	0.89

K17-11	light pink	0.2469	0.10066	0.0007	0.00011	0.02494	0.00943	0.00029	0.00014	4.5	0.74	25	9.34	2	5.4	3.05	9.8
K17-12	light pink	0.27301	0.20016	0.00118	0.00033	0.04867	0.03325	0.00056	0.00057	7.6	2.14	48.2	32.2	19	1.7	5.1	0.98
K17-13	pink	0.09256	0.11875	0.00179	0.00037	0.02362	0.02999	0.00096	0.00049	11.5	2.35	23.7	29.75	66	0.19	10.6	1.1
K17-14	pink	0.59865	0.32132	0.00067	0.00024	0.05639	0.02261	0.00029	0.00037	4.3	1.57	55.7	21.73	1.4	6	4	22
K17-15	light pink	0.14838	0.25833	0.00087	0.00035	0.0178	0.03021	0.00061	0.00058	5.6	2.24	17.9	30.14	66	0.19	4.7	1.1
K17-16	light pink	0.31698	0.13639	0.00088	0.00019	0.03639	0.01384	0.00056	0.00024	5.7	4.2	36.3	13.56	1.6	5.8	3.1	48
K17-18	light pink	0.46334	0.3715	0.00067	0.00031	0.04199	0.02758	0.00064	0.00049	4.3	2.01	41.8	26.88	44	2.1	4.7	0.93
K17-19	light pink	0.44652	0.20433	0.00183	0.00048	0.10631	0.04118	-0.00022	0.00052	11.8	3.11	102.6	37.79	1.4	6.1	5.1	45
K17-22	light pink	0.13433	0.12422	0.00084	0.00018	0.01555	0.01404	0.00063	0.00022	5.4	1.14	15.7	14.04	43	0.61	4.6	0.55
K17-23	light pink	0.28751	0.14443	0.00099	0.00022	0.0424	0.01938	0.00007	0.00029	6.4	4.41	42.2	18.88	4.6	4	3.9	47
K17-24	light pink	0.20752	0.05383	0.00074	0.00008	0.0222	0.00544	0.00037	0.00012	4.7	0.49	22.3	5.4	DISCORDANT			
K17-26	light pink	0.33199	0.13224	0.00065	0.00013	0.03099	0.01101	0.00012	0.00018	4.2	0.81	34	10.84	0.9	6.8	2.25	43
K17-28	colourless	0.08817	0.02155	0.00081	0.00005	0.0101	0.00246	0.00019	0.00006	5.2	0.33	10.2	2.47	2.3	5.2	4.58	4.6
K17-29	colourless	0.05236	0.02093	0.00079	0.00005	0.00539	0.00215	0.00022	0.00007	5.1	0.32	5.5	2.17	85	0.038	5.04	0.16
K17-30	light pink	0.05778	0.06053	0.00101	0.00014	0.00809	0.00843	0.00037	0.00015	6.5	0.87	8.2	8.49	83	0.047	6.34	0.43
K17-31	light pink	0.13137	0.29701	0.00089	0.00038	0.01697	0.03772	-0.00019	0.00052	5.7	2.44	17.1	37.66	75	0.101	5	1.1
K17-32	pink	0.32167	0.41347	0.00075	0.00043	0.03526	0.04067	0.00064	0.00065	4.8	2.8	35.2	39.89	43	0.64	2.9	1.3
K17-33	pink	0.3092	0.14336	0.00075	0.00015	0.03367	0.01427	0.0004	0.00023	4.8	0.98	33.6	14.02	3.1	4.6	2.99	42

Table VIII.16: The Knob W110868

Spot No.	Colour	Measured isotope ratios and 1 σ (%) internal errors						Estimated ages and 1 σ absolute internal errors (My)			$^{206}\text{Pb}/^{238}\text{U}$ & $^{207}\text{Pb}/^{235}\text{U}$ Concordance (%)	Spot MSWD	Selected age and 1 σ absolute external error (My)				
		$^{207}\text{Pb}/^{206}\text{Pb}$	\pm	$^{206}\text{Pb}/^{238}\text{U}$	\pm	$^{207}\text{Pb}/^{235}\text{U}$	\pm	$^{208}\text{Pb}/^{232}\text{Th}$	\pm	$^{206}\text{Pb}/^{238}\text{U}$	\pm	$^{207}\text{Pb}/^{235}\text{U}$	\pm				
K18-1	light pink	0.30633	0.15643	0.00079	0.00019	0.03243	0.01469	0.00102	0.00038	5.1	1.23	32.4	14.45	4.4	4.1	2.9	45
K18-3	light pink	0.14653	0.05162	0.00078	0.00009	0.01611	0.00545	0.00041	0.00013	5.1	0.55	16.2	5.45	2.4	5.1	3.88	8
K18-4	light pink	0.14767	0.07528	0.00083	0.00012	0.01787	0.00877	0.00022	0.00016	5.4	0.8	18	8.75	12	2.4	4.29	0.37
K18-5	light pink	0.20128	0.07959	0.00083	0.00011	0.0233	0.00872	0.01031	0.00212	5.3	0.73	23.4	8.66	2.6	5	3.96	9.4
K18-6	pink	0.18473	0.05139	0.00094	0.0001	0.02443	0.00642	0.00048	0.00016	6	0.63	24.5	6.36	0.2	9.9	4.27	42
K18-7	pink	0.75055	0.0359	0.03091	0.0009	3.49448	0.27325	0.10177	0.02091	196.2	5.65	1526	61.73	DISCORDANT			
K18-8	pink	0.81591	0.0366	0.03977	0.00104	5.17997	0.40549	0.07134	0.01474	251.4	6.46	1849.3	66.62	DISCORDANT			
K18-9	pink	0.06182	0.08309	0.00161	0.00024	0.01469	0.01966	0.00142	0.00046	10.4	1.52	14.8	19.67	81	0.059	10	0.72
K18-10	pink	0.30042	0.20647	0.00112	0.00035	0.05048	0.03115	0.00262	0.00086	7.2	2.27	50	30.11	14	2.2	4.3	1
K18-11	pink	0.22371	0.06264	0.00119	0.00013	0.03658	0.00962	0.00031	0.00014	7.7	0.85	36.5	9.43	0.1	10.7	5.26	16
K18-12	pink	0.41695	0.16929	0.00104	0.00023	0.06422	0.02234	0.00011	0.00035	6.7	1.48	63.2	21.31	0.6	7.5	3.1	24
K18-13	pink	0.37962	0.14092	0.00141	0.00029	0.0748	0.02362	0.0013	0.0005	9.1	1.9	73.2	22.31	0.3	9	4.1	33
K18-14	pink	0.28631	0.21042	0.00076	0.00025	0.0323	0.02134	0.00035	0.00031	4.9	1.61	32.3	20.99	4.7	4.9	2.9	0.75
K18-15	pink	0.38009	0.03087	0.00115	0.00005	0.06203	0.00509	0.00126	0.00029	7.4	0.35	61.1	4.87	DISCORDANT			
K18-17	pink	0.18637	0.07719	0.00084	0.00012	0.02285	0.00894	0.00066	0.00021	5.4	0.8	22.9	8.88	3.4	4.5	3.97	9.8
K18-18	pink	0.44789	0.07591	0.00163	0.00017	0.10896	0.01621	0.00212	0.00057	10.5	1.08	105	14.84	DISCORDANT			

K18-19	pink	0.30737	0.0742	0.00087	0.00011	0.03883	0.00834	0.0003	0.00017	5.6	0.7	38.7	8.15	DISCORDANT			
K18-20	pink	0.08994	0.07882	0.00118	0.00017	0.01508	0.01307	0.00056	0.00035	7.6	1.11	15.2	13.07	53	0.39	7	0.52
K18-21	pink	1.01549	0.07194	0.00987	0.00048	1.49553	0.13407	0.01574	0.00392	63.3	3.08	928.6	54.55	DISCORDANT			
K18-22	pink	0.21246	0.06521	0.00105	0.00012	0.03332	0.00968	0.00043	0.00024	6.8	0.79	33.3	9.54	0.3	8.8	4.74	14
K18-23	pink	0.33999	0.07927	0.00133	0.00016	0.06482	0.01364	0.00055	0.00029	8.5	1.04	63.8	13.04	DISCORDANT			
K18-24	pink	0.56636	0.51874	0.00052	0.00032	0.04174	0.0287	0.00076	0.00045	3.3	2.04	41.5	27.97	45	2	0.7	0.96
K18-25	pink	0.14926	0.04844	0.00081	0.00008	0.01722	0.0054	0.00028	0.00011	5.2	0.54	17.3	5.39	4.5	6	4.11	7.6
K18-26	pink	0.24752	0.14252	0.00179	0.0004	0.06207	0.0335	0.00123	0.00062	11.5	2.55	61.1	32.02	10	2.6	7.8	1.2
K18-27	pink	0.51934	0.11729	0.00266	0.00039	0.2125	0.04184	0.00356	0.00112	17.1	2.49	195.6	35.04	DISCORDANT			
K18-28	pink	0.12226	0.06095	0.00084	0.0001	0.01469	0.00717	0.00032	0.00015	5.4	0.66	14.8	7.17	16	2	4.61	0.3
K18-29	pink	0.61522	0.28204	0.00091	0.00029	0.0775	0.02674	0.0016	0.00059	5.8	1.84	75.8	25.2	0.4	8.2	4.1	32
K18-31	light pink	0.61848	0.20097	0.00144	0.00033	0.11193	0.02751	0.00281	0.00091	9.3	2.13	107.7	25.12	DISCORDANT			
K18-32	light pink	0.05701	0.04782	0.00336	0.00037	0.02571	0.02148	0.00032	0.00033	21.6	2.4	25.8	21.27	83	0.047	21.2	1.2
K18-33	light pink	0.36236	0.11303	0.00119	0.0002	0.06145	0.0168	0.00134	0.00045	7.7	4.3	60.6	16.07	DISCORDANT			
K18-34	light pink	0.15168	0.04504	0.00087	0.00008	0.01893	0.00548	0.00049	0.00017	5.6	0.53	49	5.46	0.8	7.1	4.4	8.3
K18-35	light pink	0.24139	0.12314	0.00134	0.00026	0.04998	0.02405	0.00167	0.00063	8.6	1.67	49.5	23.26	6.6	3.4	5.9	0.78
K18-36	light pink	0.52057	0.23083	0.00113	0.00032	0.08011	0.02824	0.00197	0.00086	7.3	2.08	78.2	26.52	0.6	7.6	2.2	34
K18-37	light pink	0.60243	0.30081	0.00066	0.00023	0.06016	0.02177	0.00014	0.00028	4.2	4.5	59.3	20.85	0.6	7.5	0.7	24
K18-38	pink	0.34885	0.10951	0.00099	0.00016	0.05342	0.01485	0.00035	0.00025	6.4	1.06	52.8	14.32	DISCORDANT			
K18-39	pink	0.48577	0.18141	0.00093	0.00022	0.05961	0.01781	0.00236	0.00084	6	1.44	58.8	17.07	0.4	10.5	4.9	27
K18-40	pink	0.23089	0.11627	0.00145	0.00027	0.0507	0.02415	0.00043	0.00035	9.3	1.75	50.2	23.33	6.7	3.4	6.5	0.81
K18-41	pink	0.10041	0.10529	0.00099	0.00019	0.01542	0.01597	0.00077	0.00036	6.4	1.2	15.5	15.97	54	0.38	5.7	0.57
K18-42	pink	0.22653	0.09718	0.00085	0.00015	0.02863	0.01143	-0.00003	0.00019	5.5	0.98	28.7	11.28	2.8	4.8	3.61	13
K18-43	pink	0.6171	0.06375	0.00302	0.00019	0.27413	0.03188	0.00561	0.0019	19.4	1.25	246	25.41	DISCORDANT			
K18-44	pink	0.5277	0.08802	0.00265	0.00029	0.20765	0.03276	0.00179	0.00063	17.1	1.87	191.6	27.54	DISCORDANT			
K18-45	pink	1.43147	0.65677	0.00094	0.0004	0.19646	0.04073	0.00494	0.00181	6	2.55	182.1	34.57	DISCORDANT			
K18-46	pink	0.34255	0.11933	0.00196	0.00036	0.09656	0.03019	0.00095	0.00052	12.6	2.33	93.6	27.96	0.3	8.9	6.5	41
K18-47	pink	0.73782	0.20261	0.00128	0.00026	0.15837	0.03334	0.00087	0.00054	8.2	1.67	149.3	29.23	DISCORDANT			
K18-48	pink	0.30076	0.1431	0.00129	0.00028	0.06386	0.02784	0.00038	0.00033	8.3	1.84	62.9	26.55	3.4	4.5	4.9	22
K18-49	pink	0.25436	0.19121	0.00094	0.00027	0.04177	0.02936	0.0017	0.00071	6	1.74	41.5	28.62	20	1.7	4.1	0.8
K18-50	pink	0.43057	0.10625	0.00153	0.00023	0.09438	0.02066	0.00135	0.00054	9.8	1.47	91.6	19.17	DISCORDANT			

Table VIII.17: Te Karaka Rhyolite W110869

Spot No.	Colour	Measured isotope ratios and 1σ (%) internal errors						Estimated ages and 1σ absolute internal errors (My)				$^{206}\text{Pb}/^{238}\text{U}$ & $^{207}\text{Pb}/^{235}\text{U}$ Concordance (%)	Selected age and 1σ absolute external error (My)				
		$^{207}\text{Pb}/^{206}\text{Pb}$	\pm	$^{206}\text{Pb}/^{238}\text{U}$	\pm	$^{207}\text{Pb}/^{235}\text{U}$	\pm	$^{208}\text{Pb}/^{232}\text{Th}$	\pm	$^{206}\text{Pb}/^{238}\text{U}$	\pm	$^{207}\text{Pb}/^{235}\text{U}$	\pm				
K19-1	pink	0.10526	0.04959	0.00093	0.0001	0.01482	0.00686	0.00025	0.00009	6	0.63	14.9	6.86	16	2	5.19	0.31
K19-2	pink	0.07741	0.13483	0.00069	0.00017	0.00855	0.01476	0.00037	0.00026	4.4	1.06	8.6	14.86	76	0.091	4.2	0.51
K19-3	pink	0.13865	0.10343	0.00098	0.00018	0.01971	0.0143	0.00058	0.00025	6.3	1.18	19.8	14.23	31	1.03	5.3	0.54
K19-4	pink	0.1054	0.04812	0.00068	0.00007	0.01006	0.00451	0.00019	0.00007	4.4	0.45	10.2	4.53	16	1.9	3.83	0.22
K19-5	pink	0.63903	0.27798	0.00078	0.00024	0.07663	0.02446	0.00006	0.00032	5	1.55	75	23.07	0.2	9.6	0.8	28
K19-6	colourless	0.12796	0.1357	0.00099	0.00025	0.01828	0.01889	0.00022	0.00017	6.4	1.6	18.4	18.84	49	0.47	5.4	0.76
K19-7	colourless	0.08424	0.05993	0.00063	0.00008	0.00784	0.00551	0.00015	0.00009	4.1	0.51	7.9	5.55	45	0.57	3.72	0.24
K19-9	colourless	0.07609	0.06	0.00083	0.0001	0.0094	0.00735	0.00039	0.00013	5.3	0.64	9.5	7.39	54	0.37	5	0.3
K19-10	colourless	0.42667	0.21912	0.0015	0.00044	0.08896	0.03958	0.0002	0.0004	9.6	2.67	86.5	36.94	3.3	4.5	4.7	33
K19-12	colourless	0.07155	0.11144	0.00062	0.00012	0.00593	0.00918	0.00028	0.00011	4	0.75	6	9.27	82	0.055	3.84	0.36
K19-13	colourless	0.12909	0.06505	0.00079	0.0001	0.01337	0.00655	0.00031	0.00012	5.1	0.67	13.5	6.56	16	1.9	4.3	0.31
K19-14	colourless	0.05039	0.02395	0.00062	0.00004	0.0046	0.00218	0.00017	0.00004	4	0.27	4.7	2.2	74	0.113	3.92	0.13
K19-15	colourless	0.08647	0.02044	0.00065	0.00004	0.00804	0.00187	0.00019	0.00004	4.2	0.25	8.4	1.89	1.8	5.6	3.66	3.8
K19-17	light pink	0.18673	0.0725	0.00078	0.0001	0.02019	0.00745	0.0002	0.00011	5	0.67	20.3	7.42	2.7	4.9	3.77	8.5
K19-19	light pink	0.04717	0.01558	0.00068	0.00004	0.00459	0.00151	0.00018	0.00004	4.4	0.23	4.6	1.53	84	0.042	4.34	0.13
K19-20	light pink	0.08365	0.05679	0.00075	0.00009	0.00849	0.0057	0.00019	0.00007	4.8	0.57	8.6	5.74	47	0.51	4.47	0.28
K19-21	light pink	0.29403	0.14269	0.00069	0.00015	0.0277	0.01214	0.00095	0.00019	4.4	0.98	27.7	42	3.9	4.3	2.68	42
K19-22	light pink	0.11078	0.05173	0.00076	0.00009	0.01139	0.0052	0.00026	0.00009	4.9	0.55	11.5	5.22	16	2	4.19	0.28
K19-23	light pink	0.04608	0.07929	0.00072	0.00011	0.00494	0.00847	0.0002	0.00009	4.7	0.73	5	8.56	96	0.0021	4.61	0.33
K19-24	light pink	0.2547	0.22671	0.00096	0.00032	0.03307	0.02748	0.00073	0.00041	6.2	2.06	33	27.01	29	1.1	4.3	0.96
K19-25	light pink	0.07585	0.0223	0.0007	0.00004	0.00735	0.00215	0.00015	0.00004	4.5	0.29	7.4	2.17	13	2.3	4.17	0.13
K19-26	light pink	0.18577	0.09654	0.0012	0.0002	0.03461	0.01724	0.00056	0.00023	7.7	1.3	34.5	16.92	9.4	2.8	5.8	0.6
K19-28	light pink	0.12843	0.04286	0.00065	0.00006	0.01171	0.0038	0.00024	0.00007	4.2	0.41	11.8	3.82	2.9	4.8	3.45	5.1
K19-29	light pink	0.07691	0.07568	0.00089	0.00014	0.00974	0.00949	0.0003	0.00012	5.8	0.9	9.8	9.54	64	0.22	5.36	0.43
K19-30	light pink	0.05569	0.12945	0.00105	0.00025	0.00854	0.01976	0.00069	0.00034	6.8	1.62	8.6	19.9	92	0.0102	6.6	0.76
K19-31	light pink	0.08934	0.16955	0.00057	0.00017	0.00714	0.01339	0.00027	0.00015	3.7	1.08	7.2	13.5	78	0.08	3.4	0.51
K19-32	light pink	0.09311	0.0831	0.00081	0.00013	0.00973	0.00856	0.00042	0.00014	5.2	0.85	9.8	8.61	56	0.34	4.79	0.4
K19-33	light pink	0.1648	0.10963	0.00082	0.00014	0.01824	0.01179	0.00012	0.00015	5.3	0.93	18.4	11.75	24	1.4	4.34	0.42
K19-34	light pink	0.11085	0.03109	0.00096	0.00005	0.00874	0.00242	0.00017	0.00005	3.9	0.29	8.8	2.43	2.2	5.2	3.23	4.6
K19-35	light pink	0.05791	0.02571	0.00075	0.00006	0.0058	0.00257	0.0002	0.00006	4.8	0.36	5.9	2.59	64	0.21	4.68	0.19
K19-36	light pink	0.25528	0.18001	0.00105	0.00028	0.03447	0.02268	0.00054	0.00033	6.8	1.83	34.4	22.26	19	1.7	4.7	0.85
K19-37	light pink	0.13697	0.07922	0.00069	0.00011	0.01305	0.00734	0.00001	0.00006	4.4	0.68	13.2	7.36	20	1.7	3.64	0.34
K19-38	light pink	0.46466	0.26168	0.00046	0.00016	0.02822	0.01281	0.00045	0.00019	3	1.02	28.3	12.65	3.4	4.5	4.03	43
K19-39	light pink	0.29908	0.09568	0.00082	0.00012	0.03323	0.00971	0.00042	0.00016	5.3	0.79	33.2	9.54	0.2	9.6	3.17	14
K19-40	light pink	0.12555	0.03682	0.00061	0.00005	0.01031	0.00296	0.00018	0.00005	3.9	0.35	10.4	2.98	1.6	5.8	3.25	4.7
K19-41	light pink	0.09664	0.03683	0.00083	0.00007	0.00925	0.00349	0.00017	0.00005	5.4	0.46	9.3	3.51	20	1.6	4.84	0.22
K19-42	light pink	0.13884	0.12632	0.00085	0.0002	0.01561	0.01379	0.00023	0.00023	5.5	1.27	15.7	13.79	42	0.65	4.6	0.61

K19-45	light pink	0.2643	0.08858	0.00074	0.00011	0.02544	0.00779	0.00018	0.00008	4.7	0.74	25.5	7.71	0.4	8.4	2.96	42
K19-46	light pink	0.08703	0.04416	0.00067	0.00007	0.00802	0.00403	0.00019	0.00007	4.3	0.43	8.1	4.06	30	1.07	3.91	0.22
K19-47	light pink	0.51656	0.18002	0.00123	0.00027	0.07886	0.02253	0.00074	0.00034	7.9	1.75	77.1	21.2	DISCORDANT			
K19-48	light pink	0.07731	0.02122	0.00073	0.00005	0.0073	0.00202	0.00016	0.00005	4.7	0.29	7.4	2.03	13	2.3	4.28	0.16
K19-49	light pink	0.19982	0.2088	0.00045	0.00016	0.01302	0.01285	0.00039	0.00017	2.9	1.03	13.1	12.88	39	0.72	2.13	0.48
K19-50	light pink	0.10235	0.04959	0.00069	0.00008	0.00849	0.00406	0.00013	0.00005	4.5	0.49	8.6	4.09	26	1.3	3.94	0.25
K19-51	light pink	0.06082	0.03932	0.00062	0.00006	0.00483	0.00311	0.00011	0.00004	4	0.38	4.9	3.14	75	0.103	3.89	0.19
K19-52	light pink	3.8185	6.4961	0.00019	0.00032	0.0838	0.02721	0.00008	0.00033	4.2	2.04	81.7	25.5	DISCORDANT			
K19-53	light pink	0.13465	0.05914	0.00071	0.00008	0.01281	0.00552	0.00028	0.0001	4.6	0.53	12.9	5.54	10	2.7	3.83	0.24
K19-54	light pink	0.38869	0.25163	0.00089	0.00028	0.04256	0.02438	0.0001	0.00028	5.7	1.82	42.3	23.75	11	2.6	3.2	0.84
K19-55	light pink	0.12795	0.06636	0.00088	0.00011	0.01426	0.00726	0.00018	0.00007	5.6	0.73	14.4	7.27	19	1.7	4.86	0.34

Table VIII.18: Staircase Dome W110870

Spot No.	Colour	Measured isotope ratios and 1 σ (%) internal errors						Estimated ages and 1 σ absolute internal errors (My)			$^{206}\text{Pb}/^{238}\text{U}$ & $^{207}\text{Pb}/^{235}\text{U}$		Concordance (%)	Spot MSWD	Selected age and 1 σ absolute external error (My)		
		$^{207}\text{Pb}/^{206}\text{Pb}$	\pm	$^{206}\text{Pb}/^{238}\text{U}$	\pm	$^{207}\text{Pb}/^{235}\text{U}$	\pm	$^{208}\text{Pb}/^{232}\text{Th}$	\pm	$^{206}\text{Pb}/^{238}\text{U}$	\pm	$^{207}\text{Pb}/^{235}\text{U}$	\pm				
K20-1	pink	0.12151	0.26727	0.00099	0.0004	0.01941	0.042	0.00002	0.0004	6.4	2.58	19.5	41.84	74	0.109	5.6	1.2
K20-2	pink	0.06007	0.25932	0.00153	0.00063	0.01238	0.05321	0.00054	0.00097	9.9	4.05	12.5	53.37	96	0.0028	9.7	1.9
K20-3	pink	0.50436	0.03168	0.00194	0.00008	0.12386	0.00726	0.00113	0.00014	12.5	0.51	118.6	6.56	DISCORDANT			
K20-4	pink	0.18014	0.10853	0.00116	0.00024	0.02894	0.0165	0.00054	0.00027	7.5	1.53	29	16.28	45	2	5.5	0.73
K20-5	pink	0.08645	0.02646	0.00113	0.00008	0.01379	0.00414	0.00039	0.00008	7.3	0.52	13.9	4.15	7.4	3.2	6.48	0.25
K20-7	pink	0.2541	0.12602	0.00129	0.00026	0.04712	0.02155	0.00051	0.00029	8.3	1.69	46.7	20.9	5.3	3.8	5.7	0.78
K20-9	light pink	0.07515	0.02671	0.00111	0.00008	0.01159	0.00406	0.00039	0.00008	7.2	0.5	11.7	4.08	21	1.6	6.59	0.25
K20-10	light pink	2.53904	0.18308	0.0012	0.00008	0.423	0.02166	0.00038	0.00008	7.7	0.49	358.2	15.45	DISCORDANT			
K20-11	light pink	0.35604	0.17791	0.00141	0.00035	0.06999	0.03083	0.00105	0.00042	9.1	2.27	68.7	29.25	3.4	4.5	4.9	28
K20-12	light pink	0.08098	0.01744	0.00113	0.00006	0.01288	0.00273	0.00044	0.00006	7.3	0.39	43	2.74	1.7	5.7	6.48	5.8
K20-13	light pink	0.06094	0.02221	0.00101	0.00007	0.00901	0.00325	0.00029	0.00006	6.5	0.42	9.1	3.27	37	0.82	6.15	0.22
K20-16	light pink	0.06679	0.0277	0.00128	0.0001	0.01224	0.00502	0.00051	0.00011	8.2	0.62	12.3	5.03	36	0.84	7.73	0.32
K20-17	light pink	0.40147	0.52082	0.00122	0.00084	0.07319	0.08132	0.00007	0.0011	7.9	5.44	71.7	76.94	39	0.73	3.8	2.5
K20-19	light pink	0.45142	0.19893	0.00145	0.00038	0.10103	0.03715	0.00113	0.00044	9.4	2.43	97.7	34.26	0.9	6.9	3.6	38
K20-20	light pink	0.07798	0.03273	0.00127	0.0001	0.01422	0.0059	0.00062	0.00014	8.2	0.66	14.3	5.9	25	1.3	7.53	0.31
K20-21	light pink	0.06799	0.01966	0.00122	0.00007	0.01162	0.00332	0.00034	0.00007	7.8	0.47	11.7	3.33	19	1.7	7.34	0.22
K20-22	light pink	0.43555	0.02492	0.0022	0.00008	0.14427	0.00869	0.00203	0.00027	14.2	0.5	136.8	7.71	DISCORDANT			
K20-23	pink	0.06823	0.03405	0.00127	0.00011	0.01291	0.00638	0.00038	0.00012	8.2	0.69	13	6.39	40	0.7	7.66	0.34
K20-25	colourless	0.06156	0.03581	0.001	0.00009	0.00895	0.00516	0.00044	0.00011	6.4	0.56	9	5.2	58	0.31	6.16	0.28
K20-26	colourless	0.10692	0.02442	0.00103	0.00007	0.01624	0.00362	0.00034	0.00007	6.7	0.44	16.3	3.61	0.3	9	5.46	8.4
K20-27	colourless	0.08039	0.02413	0.00117	0.00008	0.01341	0.00397	0.00037	0.00009	7.5	0.52	13.5	3.97	9	2.9	6.78	0.25
K20-29	colourless	0.33116	0.26934	0.00213	0.00084	0.11123	0.08084	0.00184	0.001	13.7	5.41	107.1	73.87	20	1.6	7.6	2.5
K20-30	colourless	0.56007	1.04569	0.0004	0.00051	0.02681	0.03681	0.00079	0.00073	2.6	3.29	26.9	36.4	47	0.51	0.5	1.6

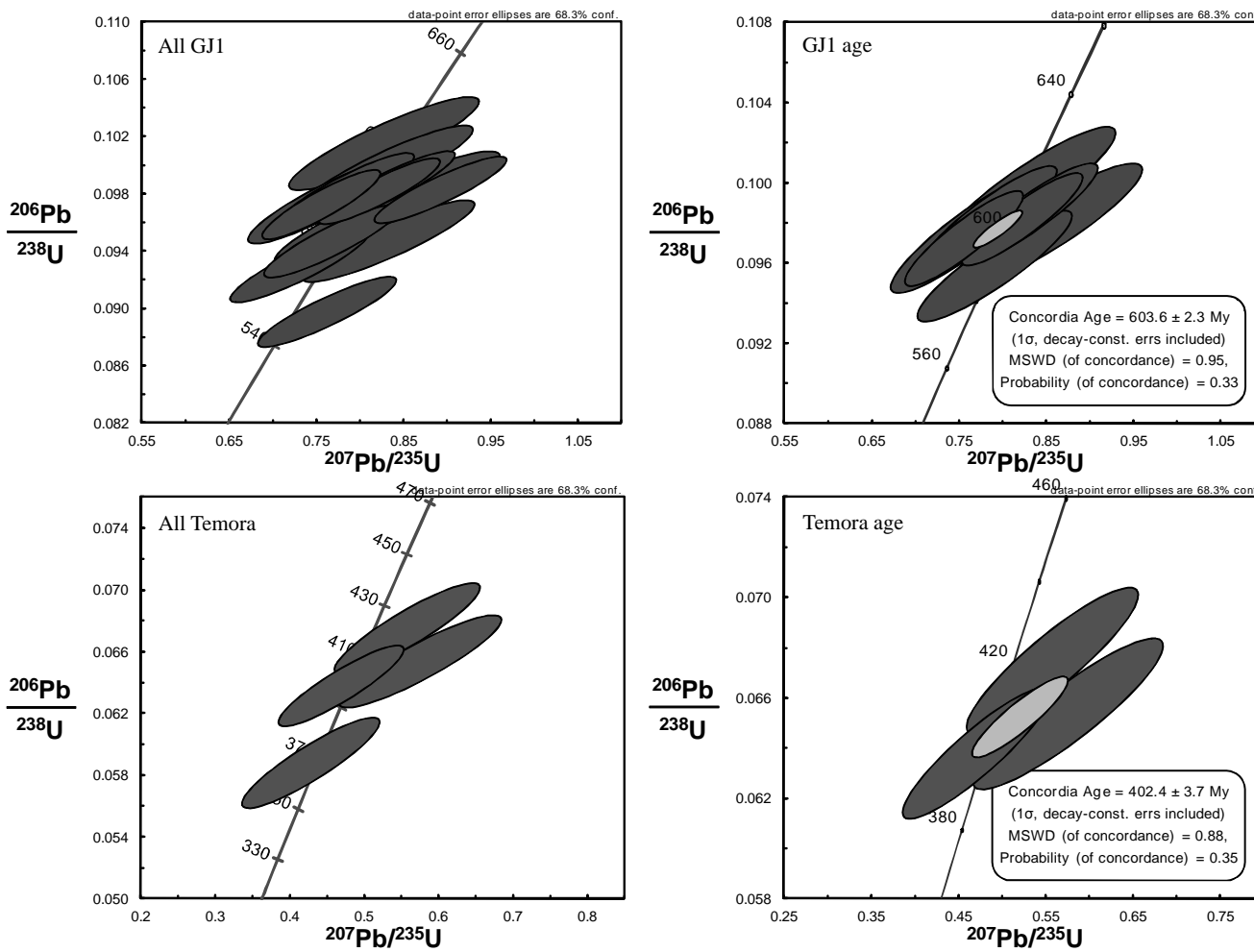
K20-31	colourless	0.06697	0.01727	0.00109	0.00006	0.01084	0.00277	0.00025	0.00005	7	0.4	10.9	2.79	11	2.6	6.48	0.19		
K20-32	ee colourless	0.08408	0.0193	0.00441	0.00026	0.05375	0.01236	0.00151	0.00032	28.3	1.65	53.2	41.94	DISCORDANT	4.8	6.72	2.8		
K20-33	ee colourless	0.05747	0.00672	0.0011	0.00003	0.00903	0.00109	0.00028	0.00004	7.1	0.22	9.1	1.1	2.8	4.8	6.72	2.8		
K20-36	colourless	0.06399	0.01888	0.00121	0.00007	0.01117	0.00328	0.00027	0.00006	7.8	0.44	11.3	3.3	23	1.4	7.33	0.22		
K20-38	colourless	0.06533	0.0146	0.00106	0.00005	0.00971	0.00217	0.00023	0.00005	6.8	0.35	9.8	2.18	12	2.5	6.39	0.16		
K20-39	colourless	0.07191	0.02534	0.00123	0.00008	0.01285	0.0045	0.00035	0.00009	7.9	0.55	13	4.51	22	1.5	7.37	0.25		
K20-40	ee colourless	0.08371	0.02222	0.00124	0.00008	0.0156	0.0041	0.00026	0.00007	8	0.52	45.7	4.1	3.5	4.5	7.04	6.8		
K20-41	colourless	0.05574	0.02718	0.00119	0.00009	0.0096	0.00466	0.00027	0.00008	7.6	0.56	9.7	4.68	63	0.24	7.42	0.28		
K20-43	ee colourless	0.08048	0.01956	0.00127	0.00008	0.01539	0.00372	0.00029	0.00006	8.2	0.49	45.5	3.72	2.5	5	7.18	7.3		
K20-44	colourless	0.07449	0.01976	0.00111	0.00007	0.01207	0.00319	0.00025	0.00006	7.2	0.44	12.2	3.2	7.3	3.2	6.45	0.22		
K20-45	colourless	0.05924	0.01769	0.00119	0.00007	0.01033	0.00308	0.00031	0.00007	7.7	0.45	10.4	3.1	31	1.05	7.27	0.23		
K20-46	ee colourless	0.17834	0.07096	0.00094	0.00013	0.02476	0.00936	0.0002	0.00013	6	0.85	24.8	9.27	2.9	4.7	4.45	44		
K20-47	colourless	0.05498	0.01142	0.00121	0.00005	0.00982	0.00207	0.0003	0.00006	7.8	0.35	9.9	2.08	24	1.4	7.47	0.16		
K20-48	colourless	0.05506	0.0151	0.00118	0.00006	0.00925	0.00255	0.00028	0.00006	7.6	0.4	9.4	2.56	43	0.62	7.34	0.19		
K20-49	colourless	0.0476	0.02191	0.00118	0.00008	0.00829	0.00381	0.00015	0.00007	7.6	0.51	8.4	3.84	82	0.053	7.5	0.25		
K20-50	ee colourless	0.09977	0.02304	0.00107	0.00007	0.01506	0.00346	0.00037	0.00009	6.9	0.44	45.2	3.46	0.7	7.2	5.84	7.6		
K20-51	ee colourless	0.12841	0.18684	0.00203	0.00065	0.03398	0.0484	-0.00038	0.00061	13.1	4.19	33.9	47.53	64	0.22	11.3	2		

Appendix IX: Concordia and probability density plots

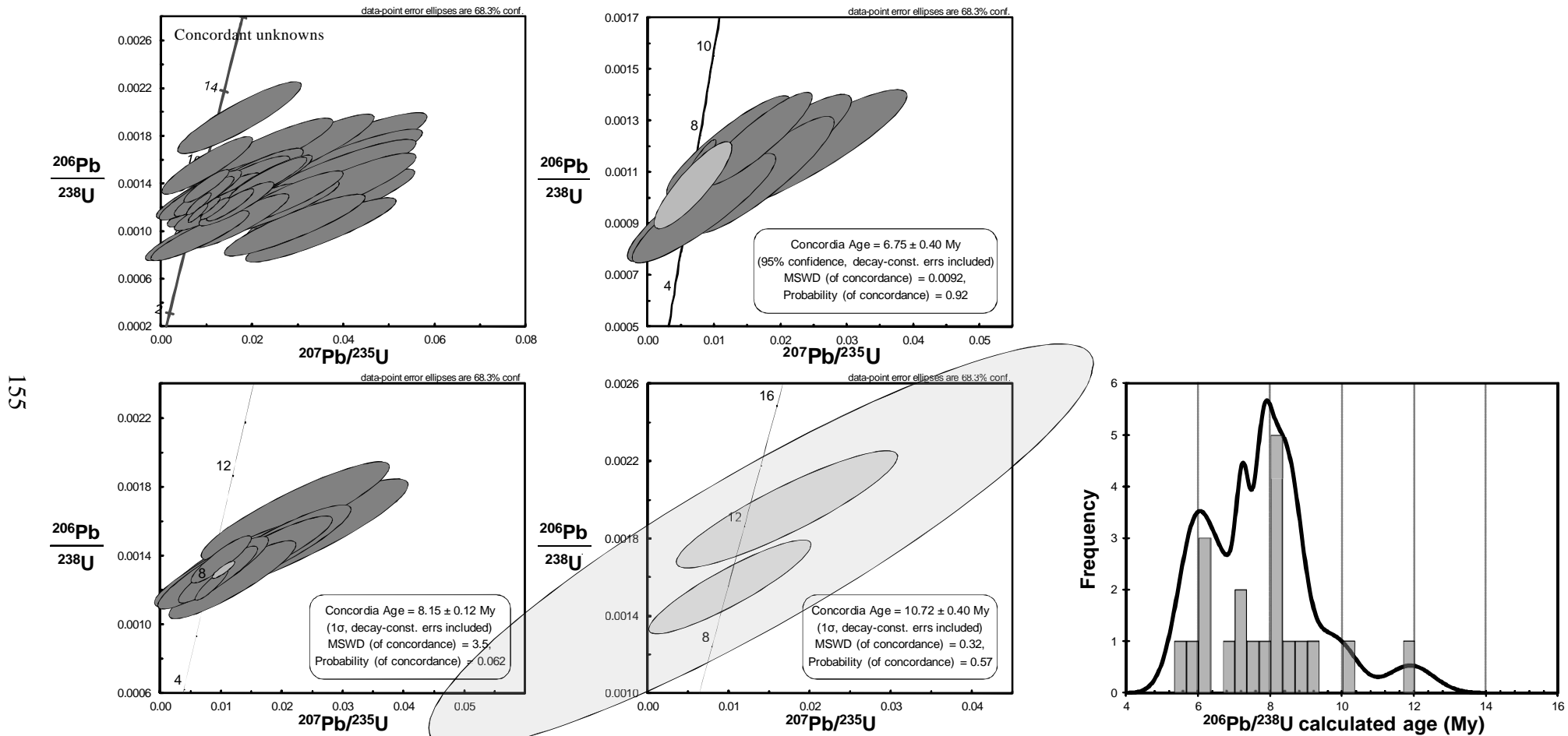
The following figures contain output from Isoplot:

- Concordia plots of all GJ1 analyses from each session;
- Concordia plots of the GJ1 age determined from each session;
- Concordia plots of all Temora2 analyses from each session;
- Concordia plots of the Temora2 age determined from each session;
- Concordia plots of the concordant unknowns from each session (i.e. one sample);
- Concordia plots of the determined eruption age for each sample;
- Concordia plots of older age peaks from each sample if present and if based on more than 1 zircon;
- Probability density plots of all concordant unknowns from each session; and
- Concordia plot of all concordant analyses from the four individual samples of Broken Hills Rhyolite.

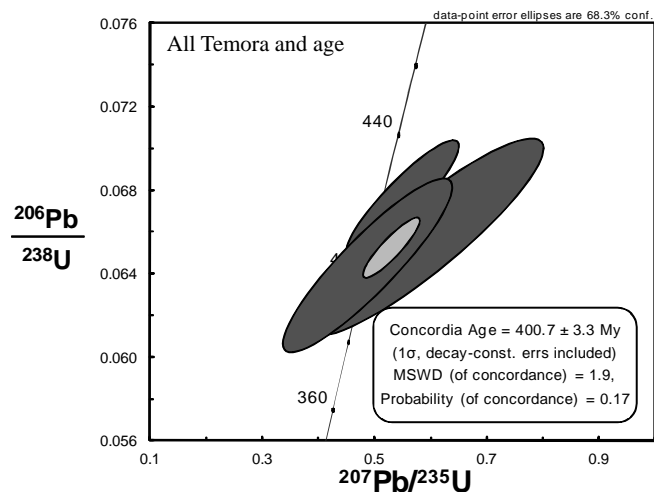
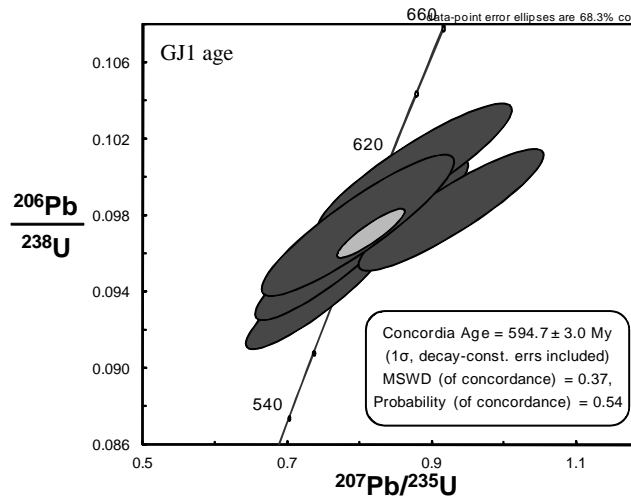
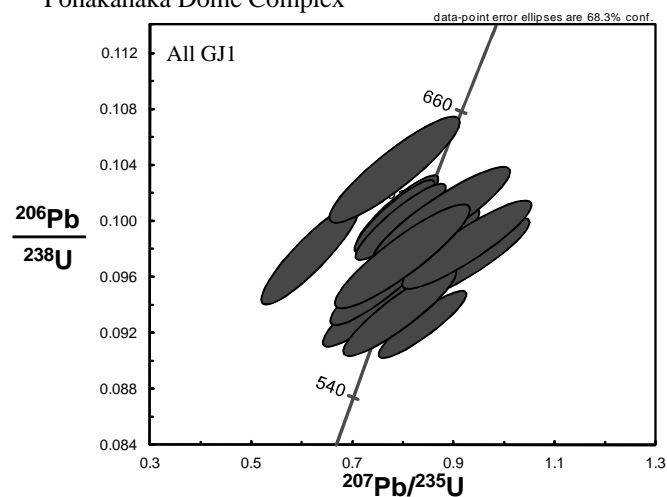
Timata Dome



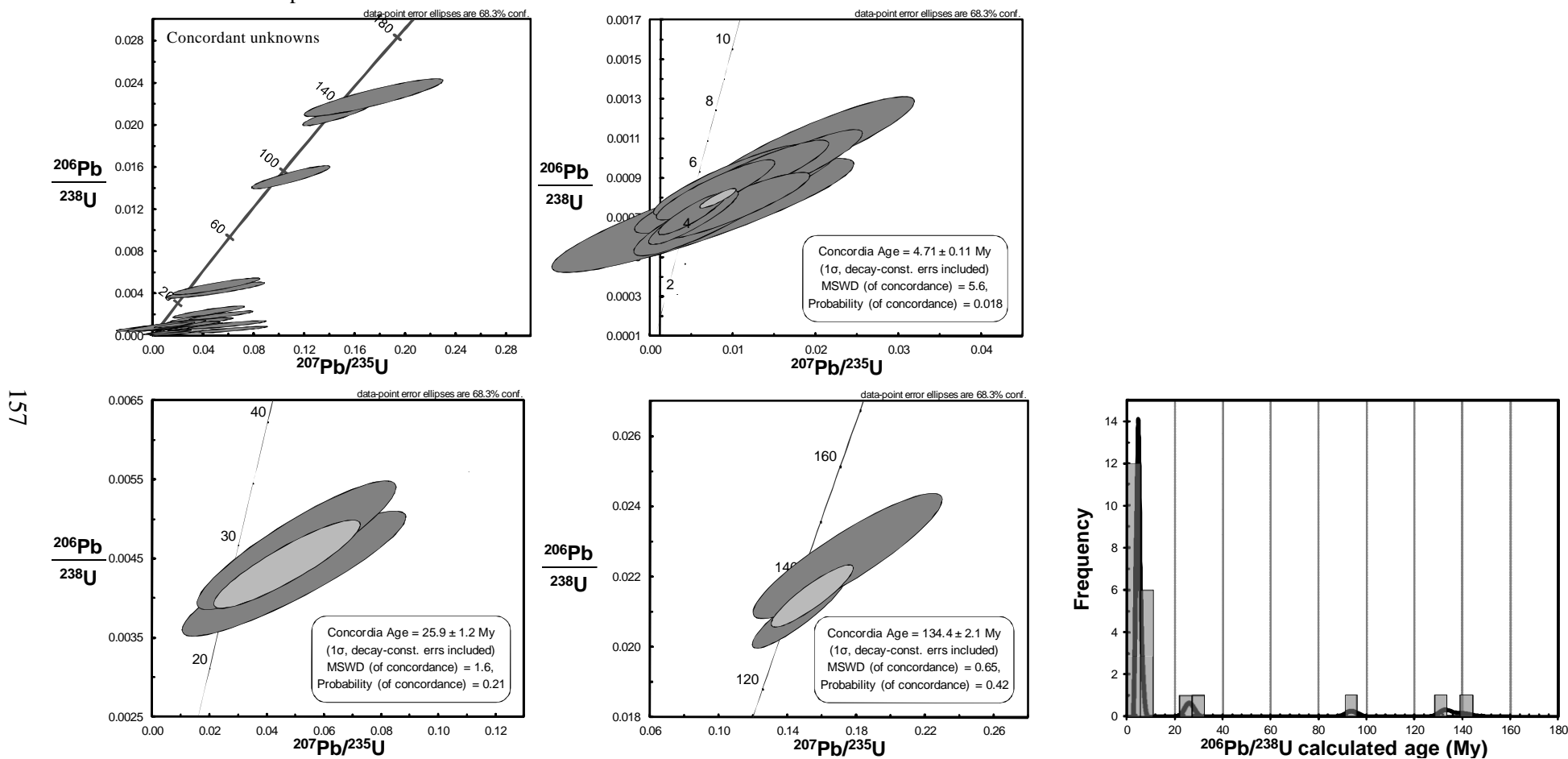
Timata Dome



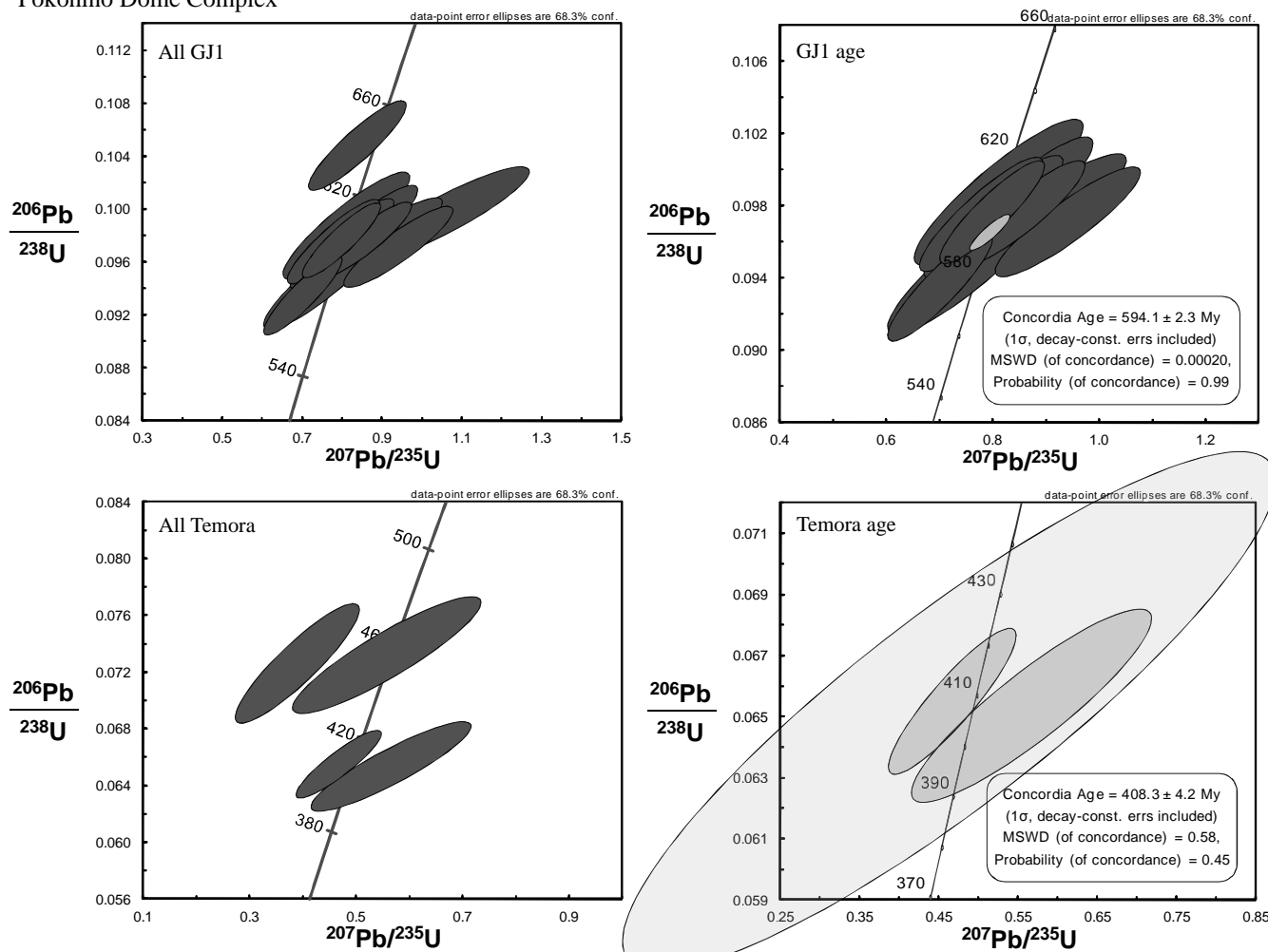
Pohakahaka Dome Complex



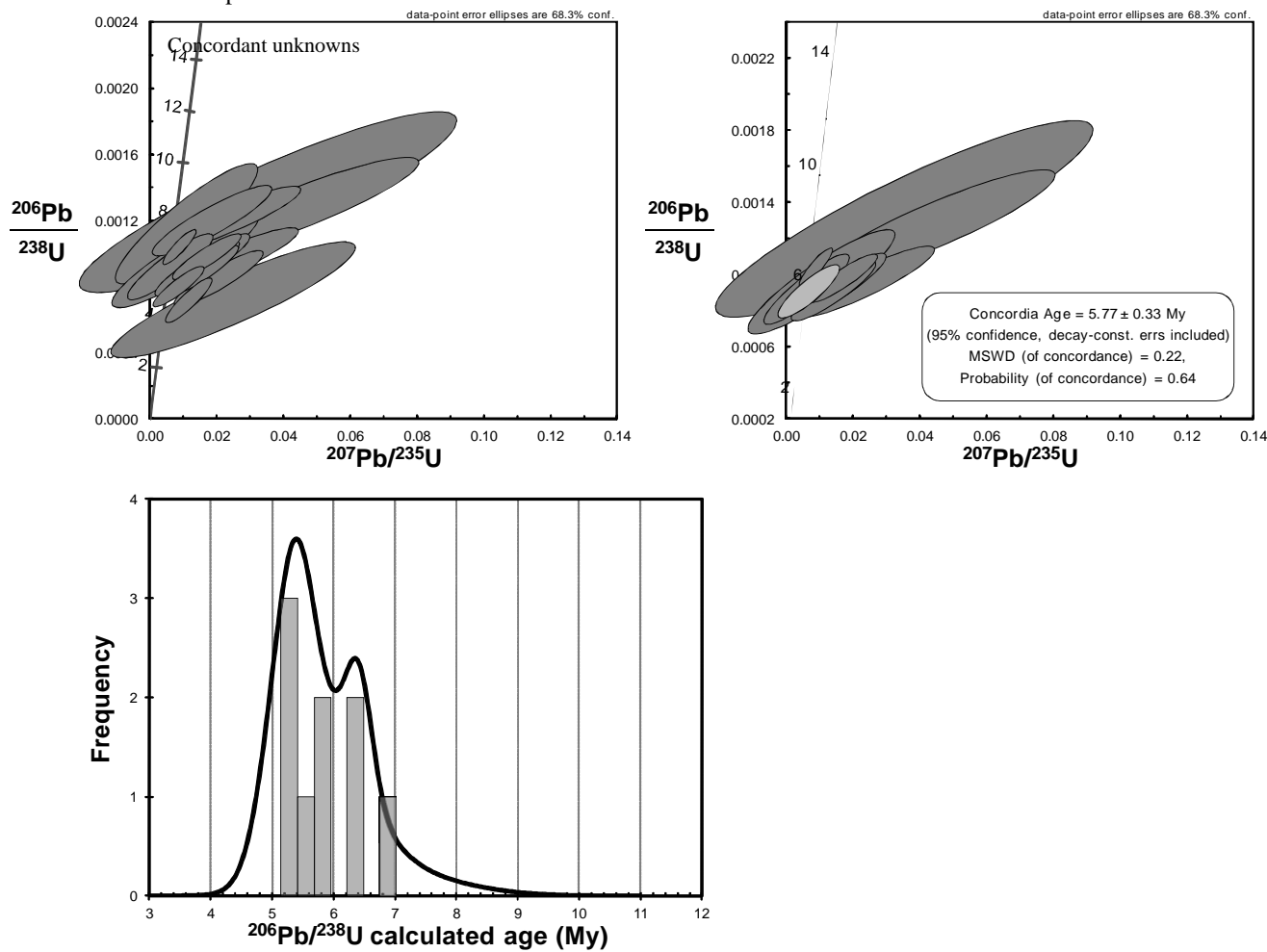
Pohakahaka Dome Complex



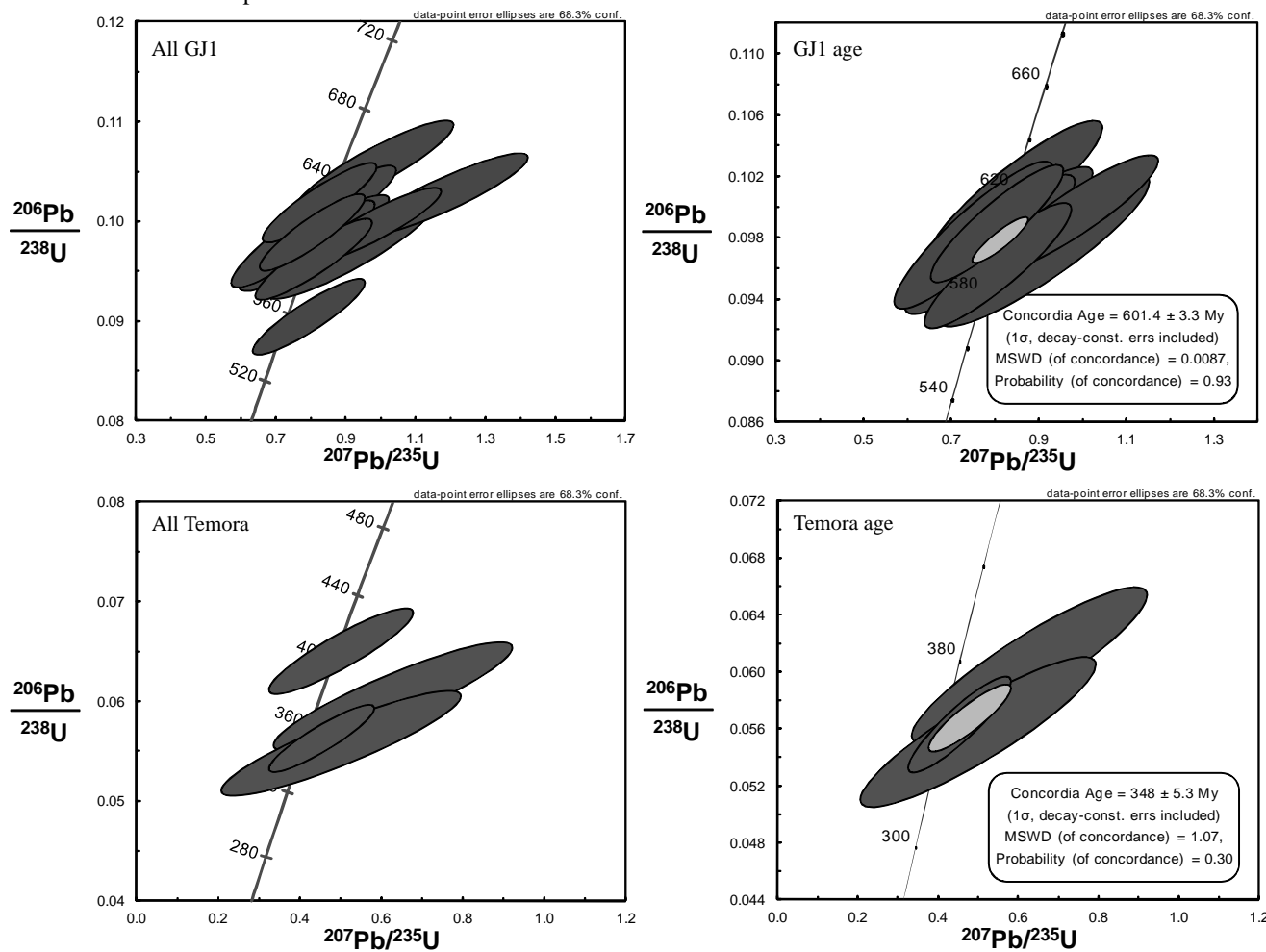
Pokohino Dome Complex



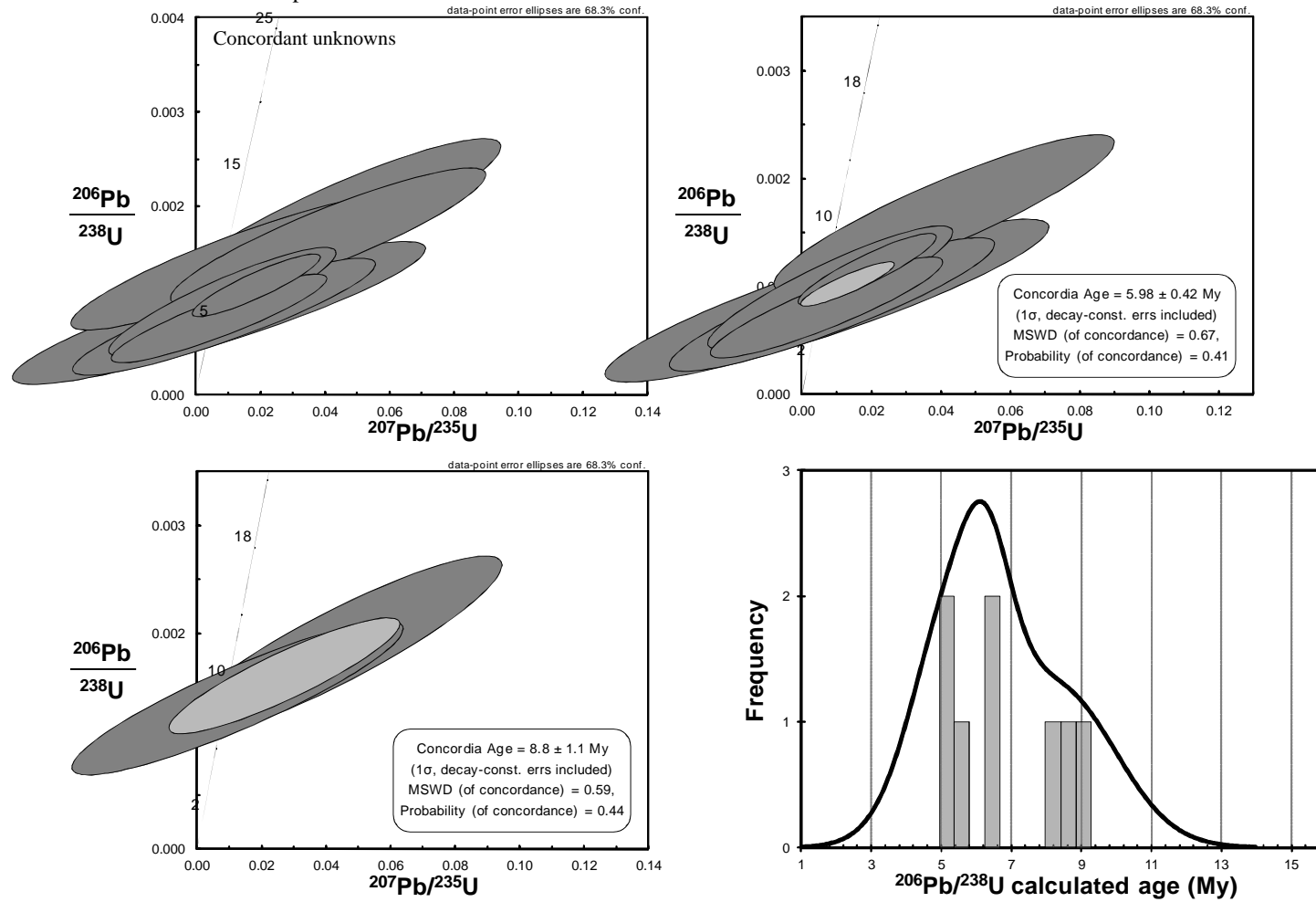
Pokohino Dome Complex



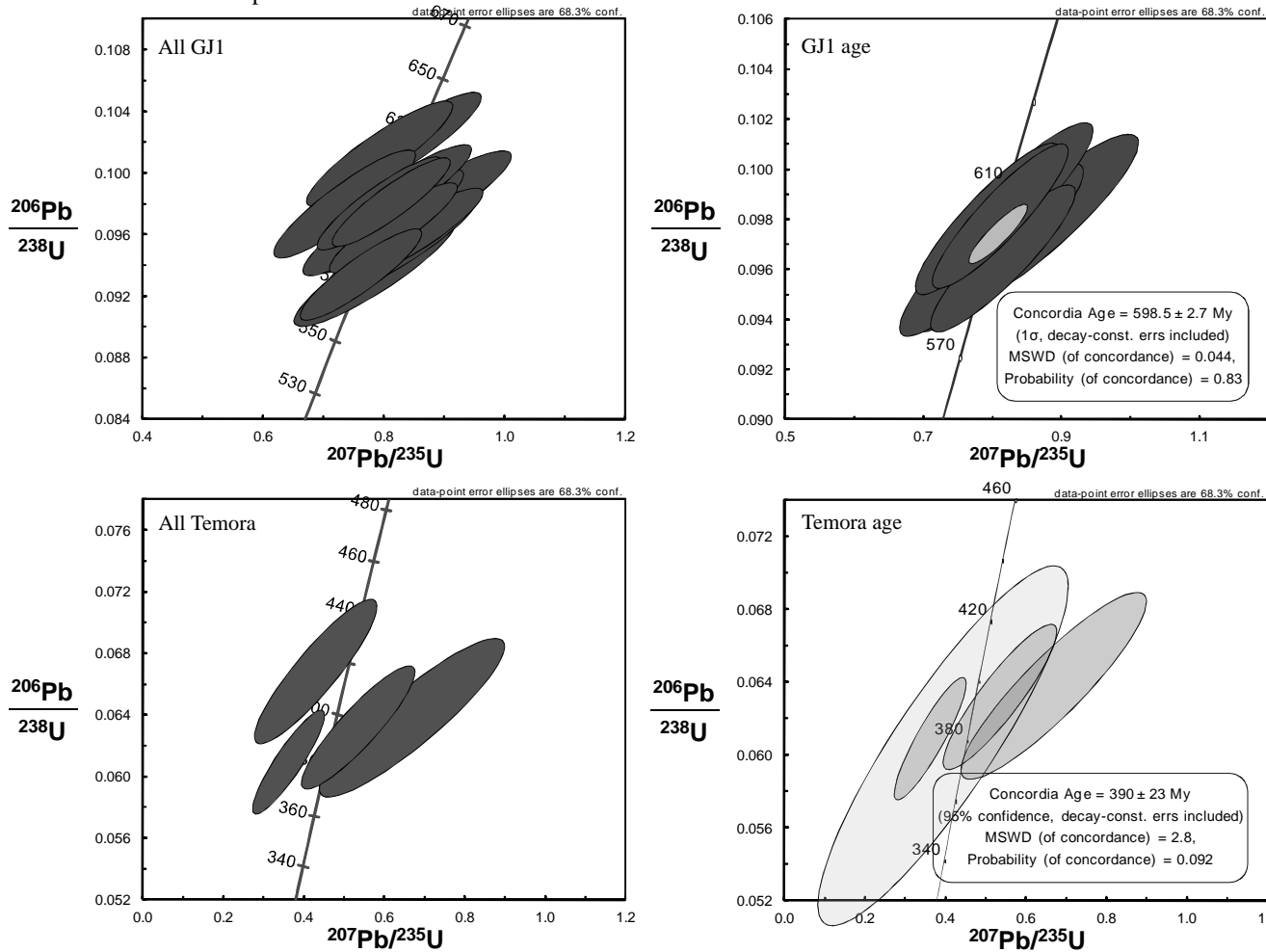
Broken Hills Mine sample 1



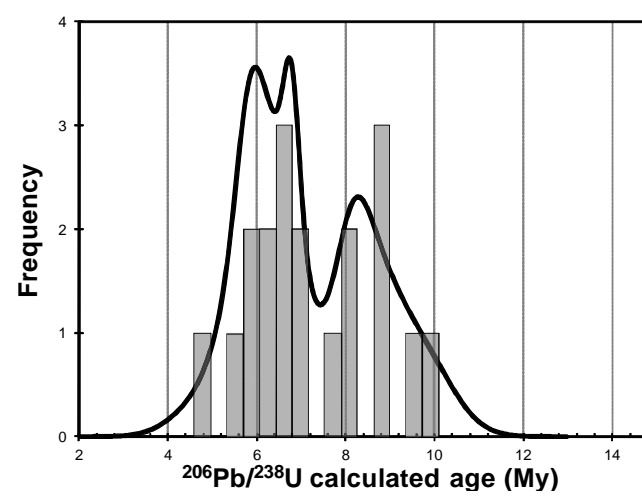
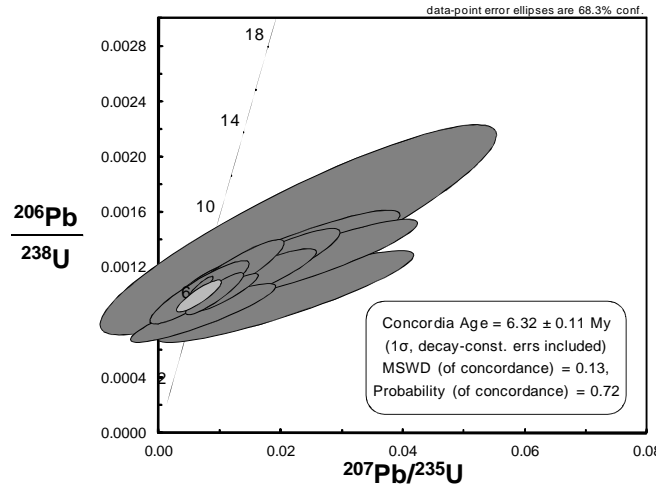
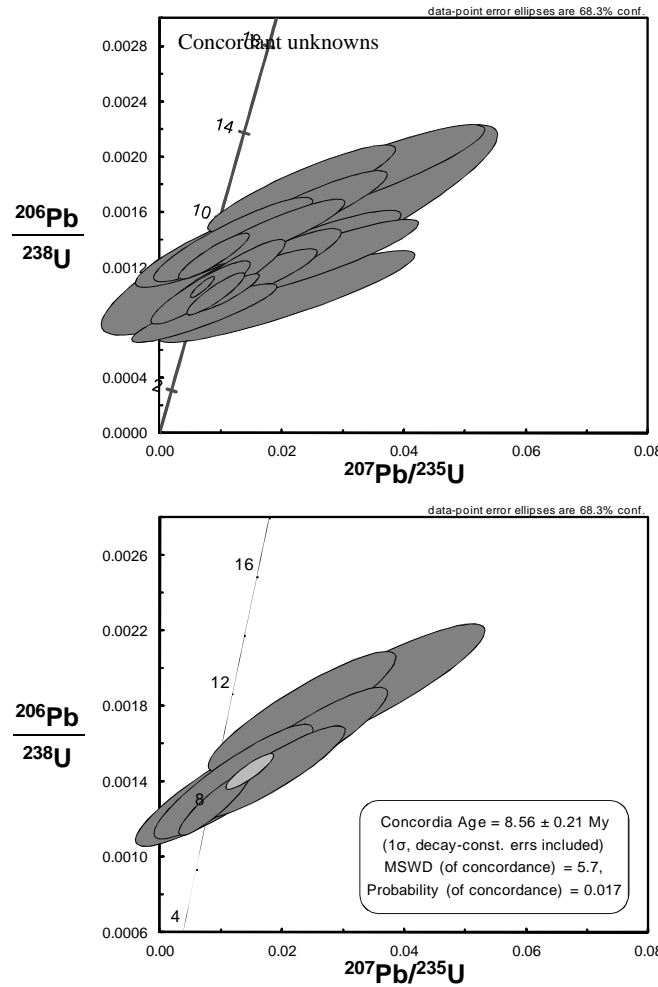
Broken Hills Mine sample 1



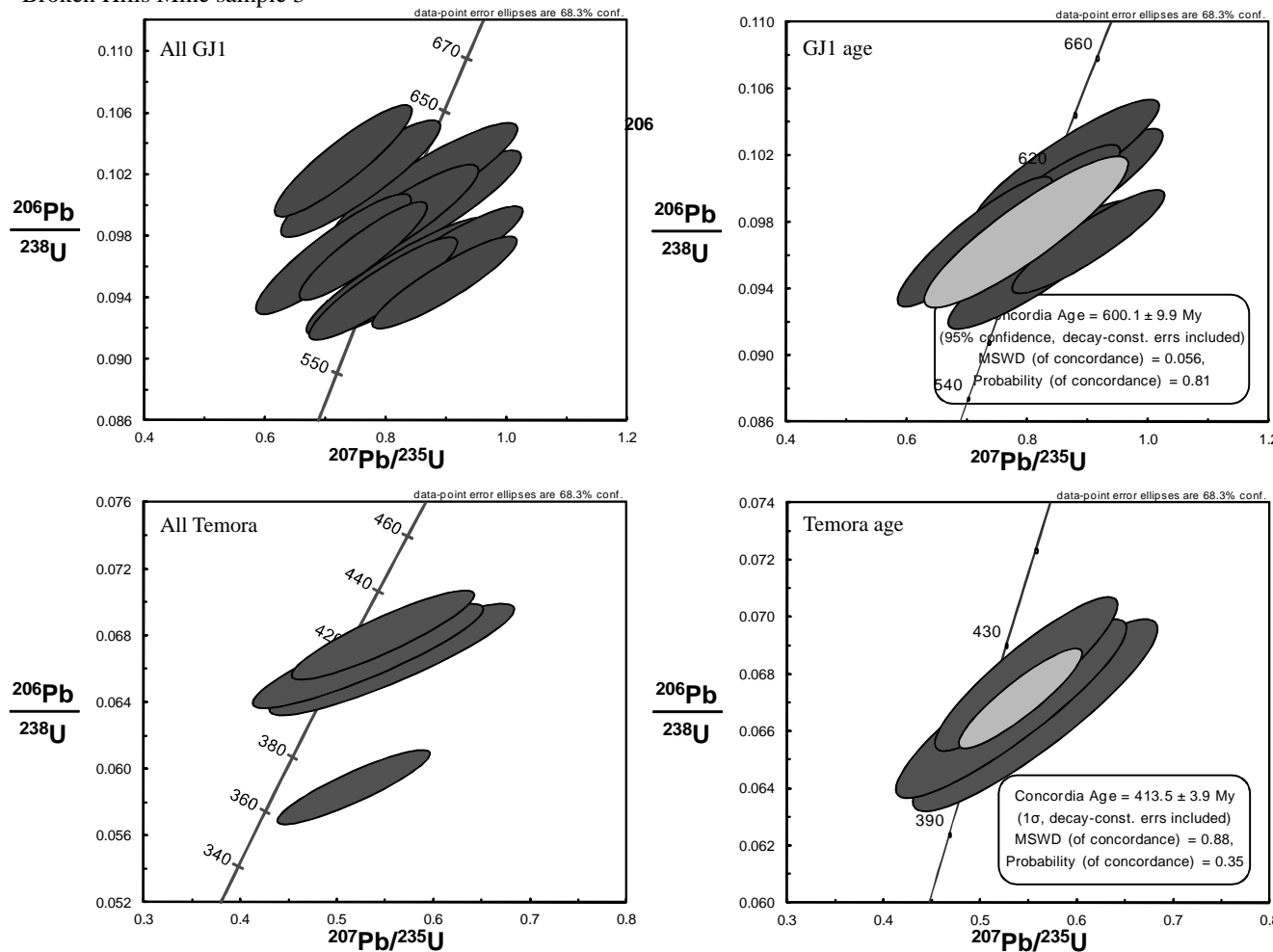
Broken Hills Mine sample 2



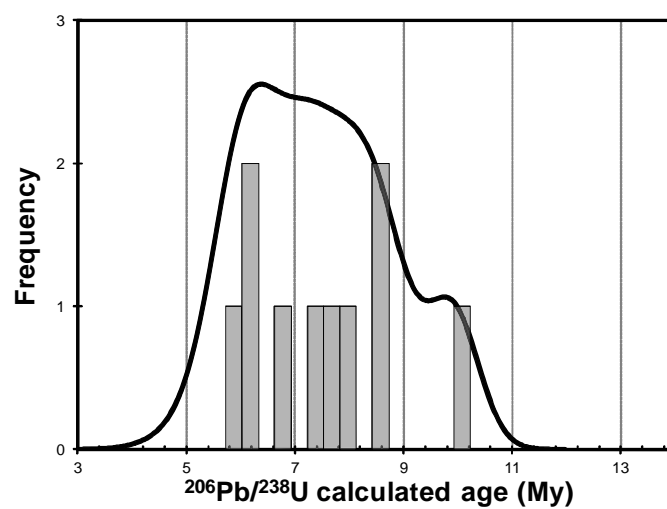
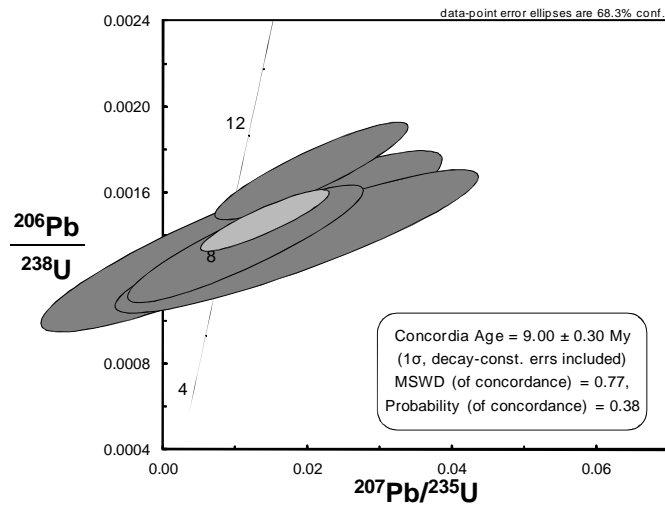
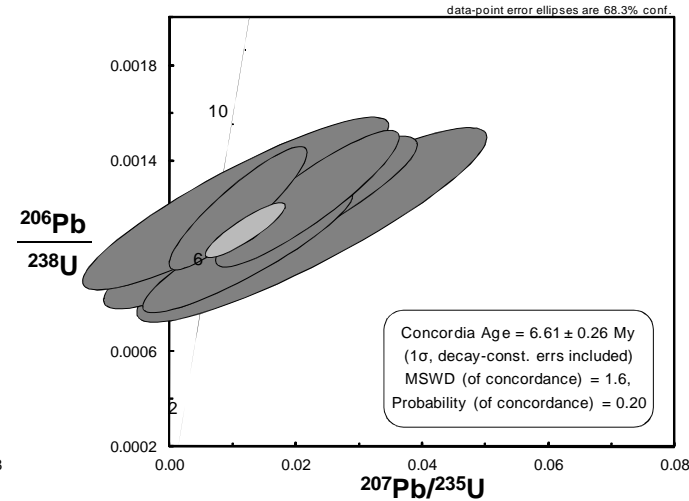
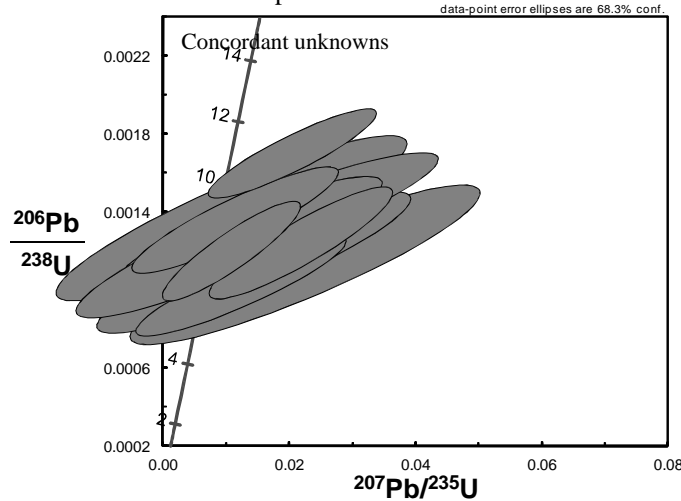
Broken Hills Mine sample 2



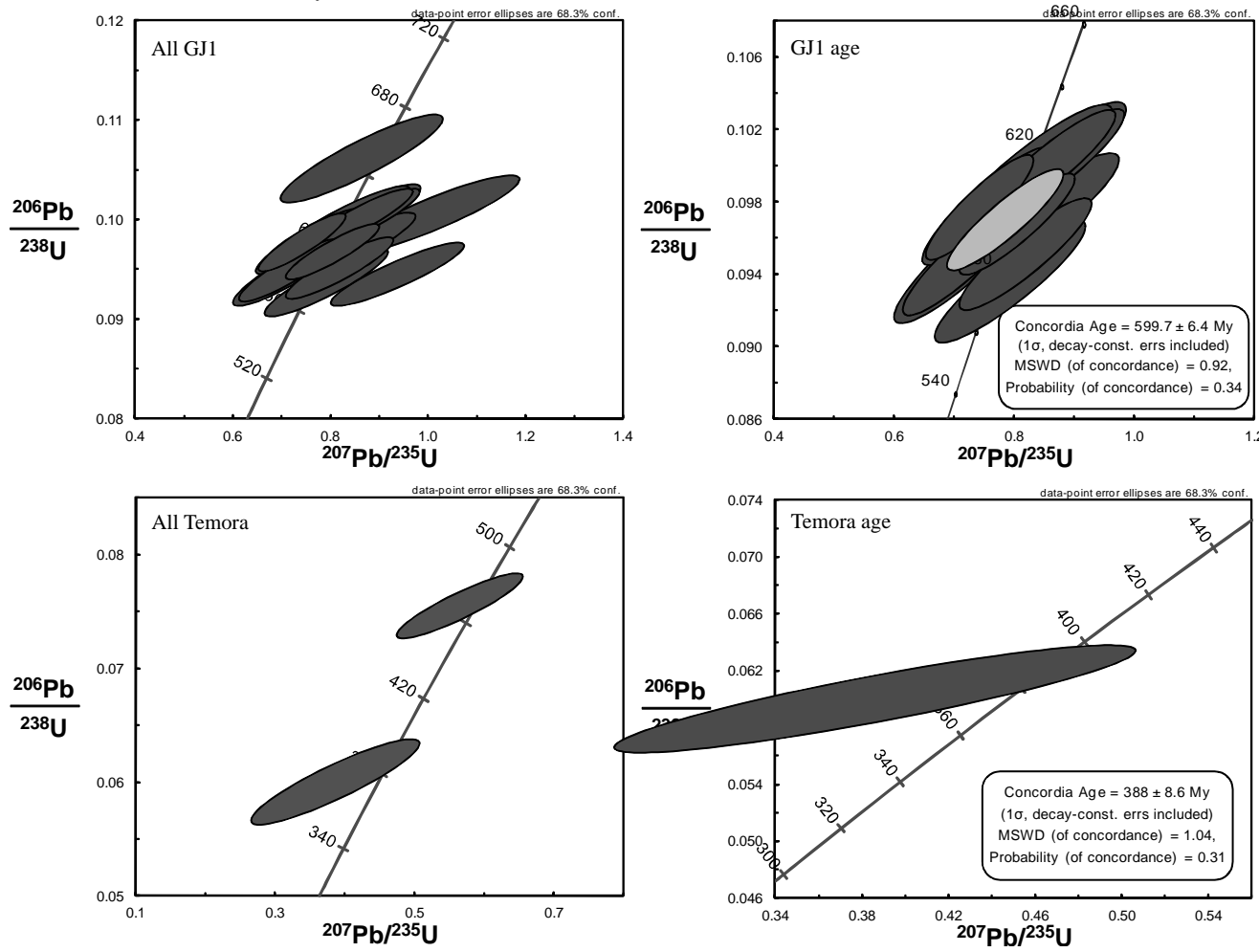
Broken Hills Mine sample 3



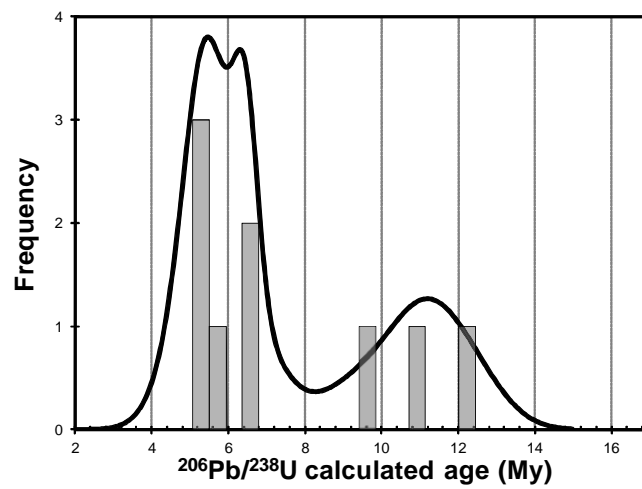
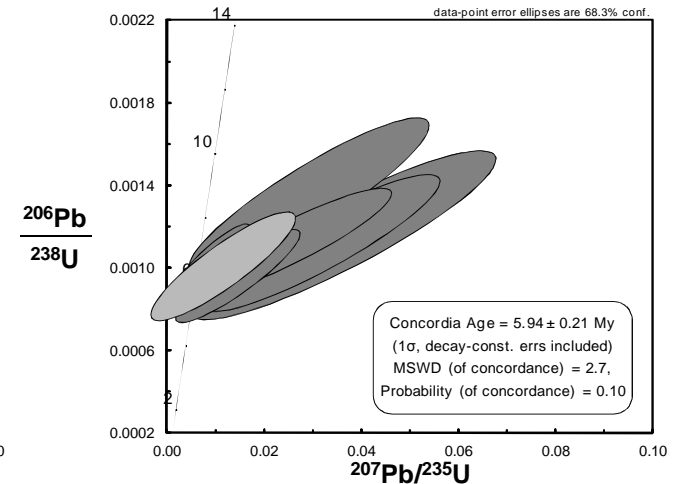
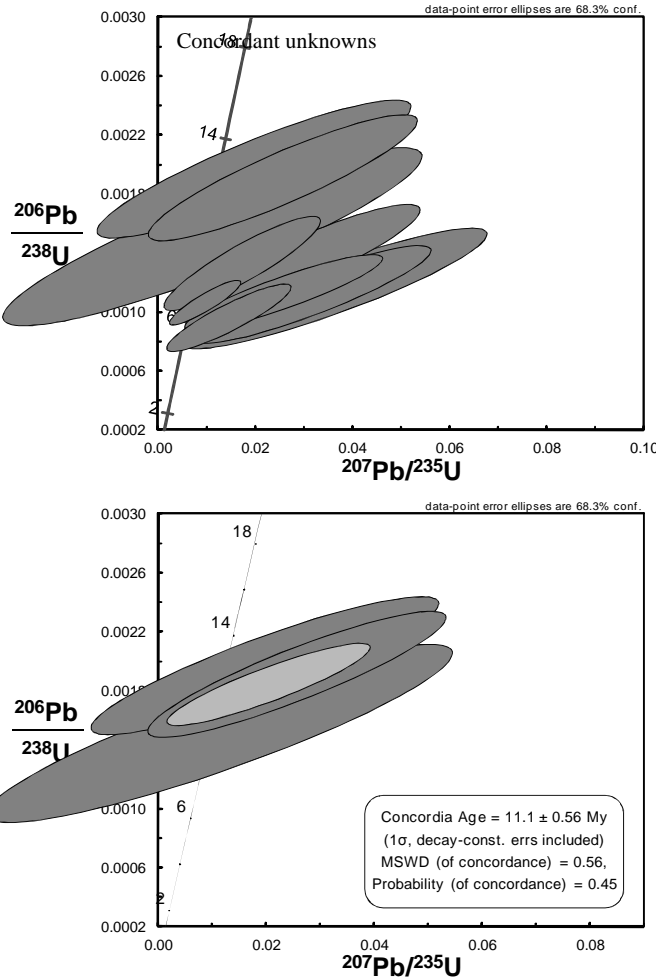
Broken Hills Mine sample 3



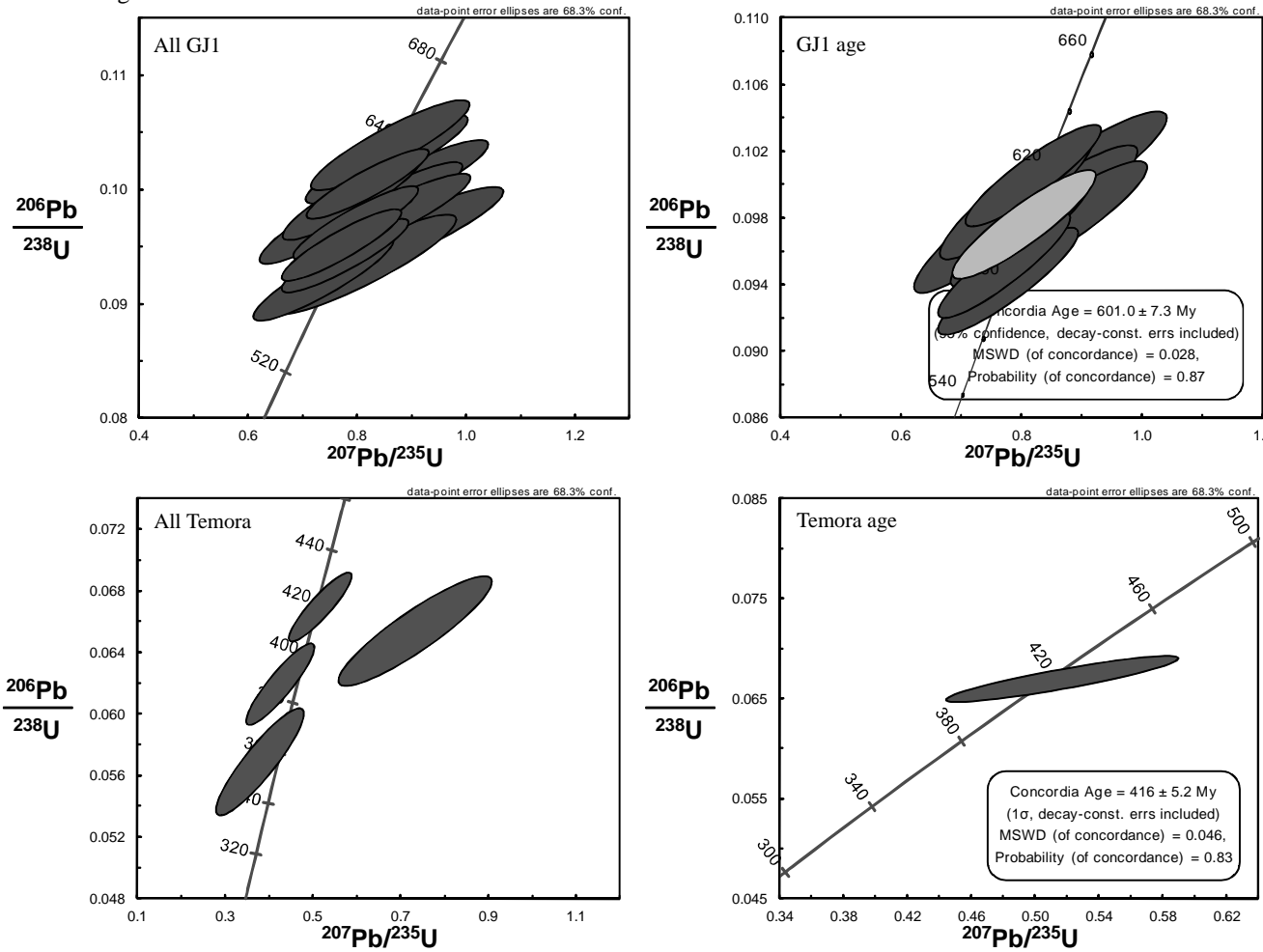
Broken Hills Flow Banded Rhyolite



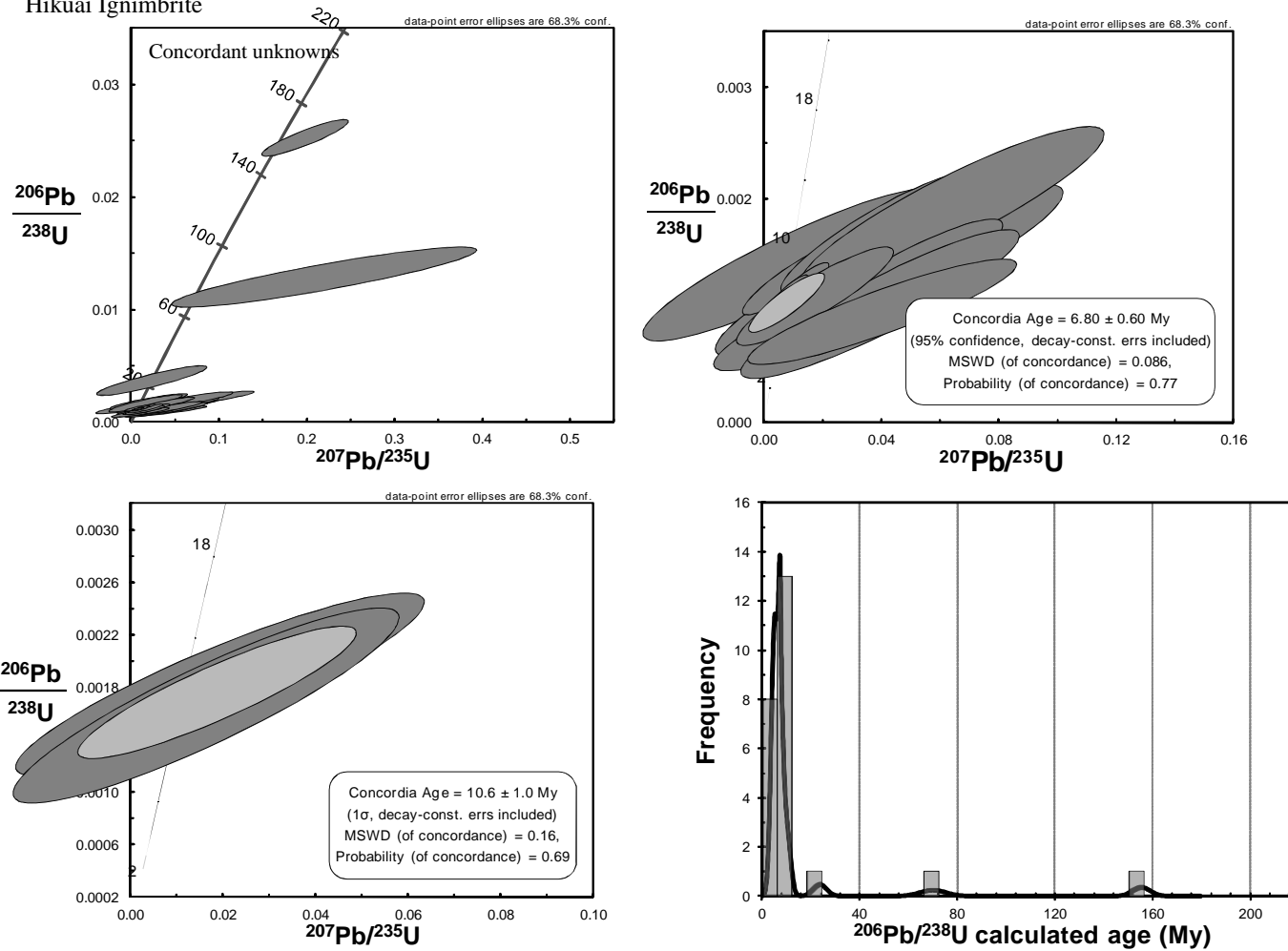
Broken Hills Flow Banded Rhyolite



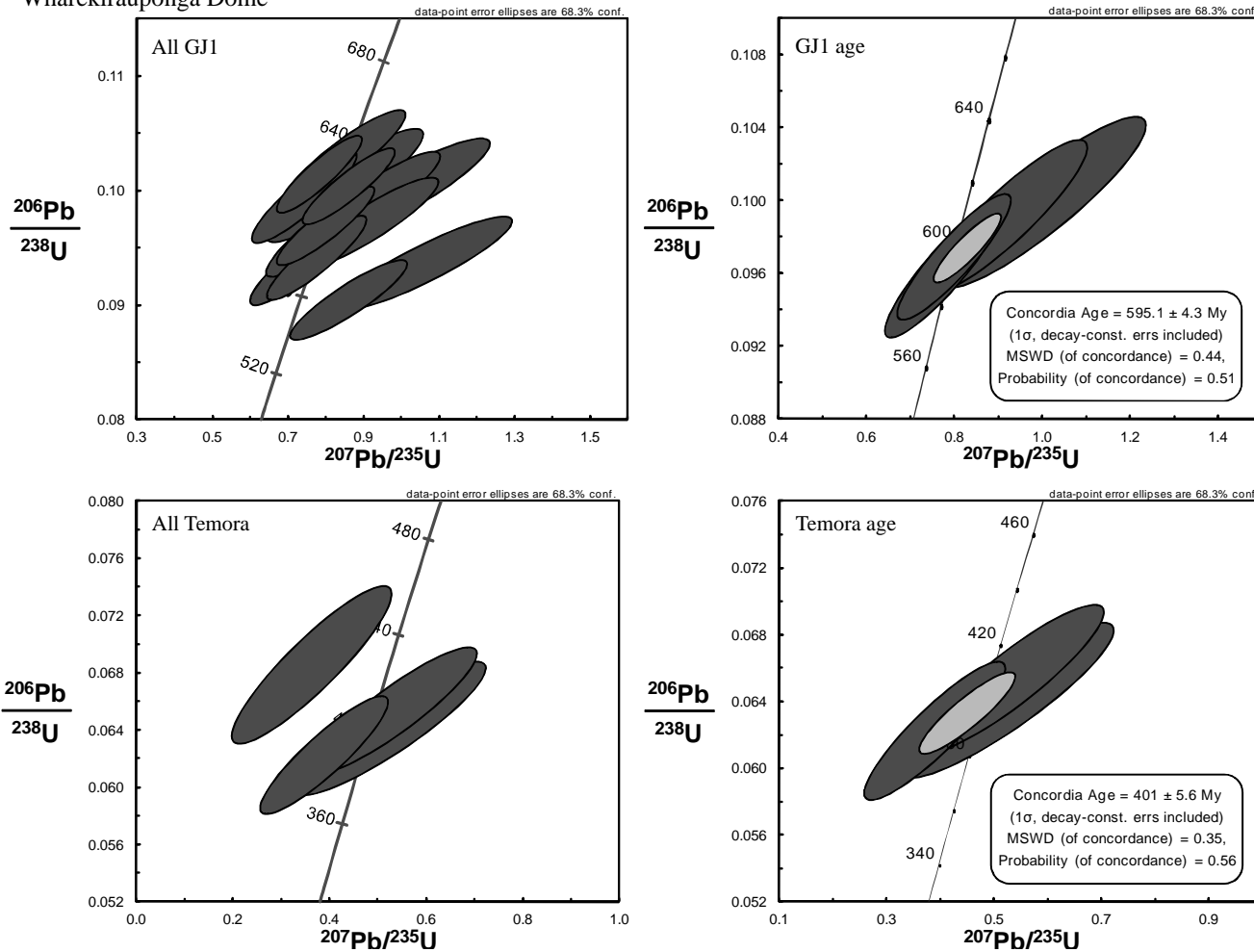
Hikuai Ignimbrite



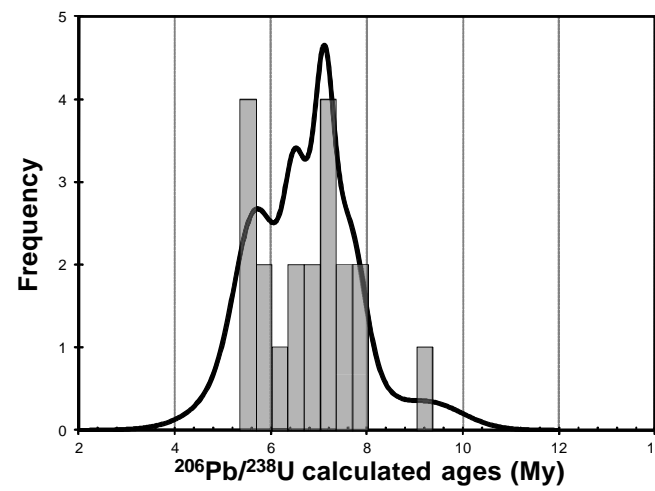
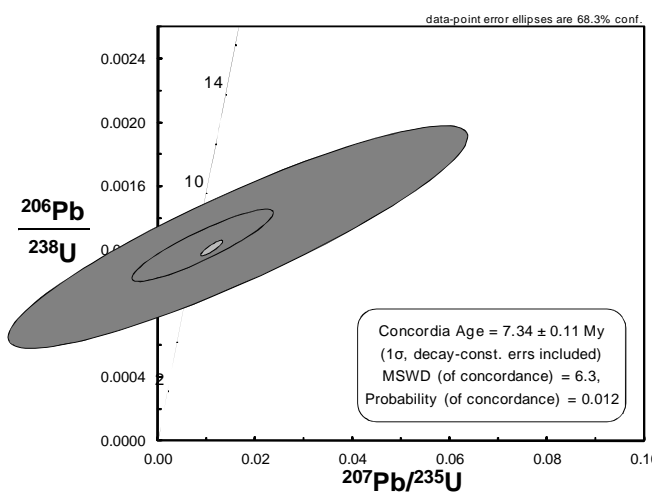
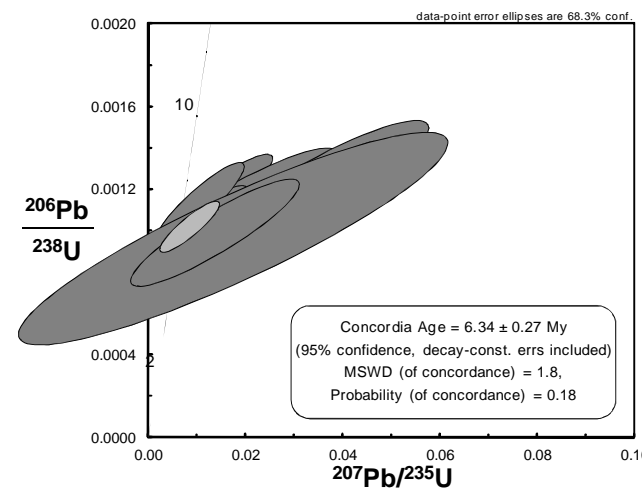
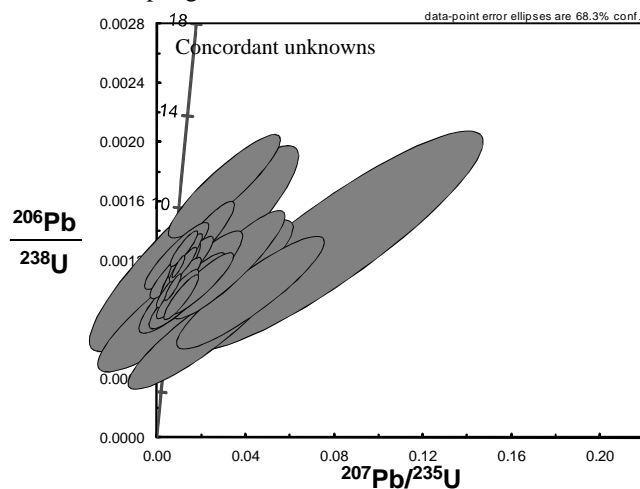
Hikuai Ignimbrite



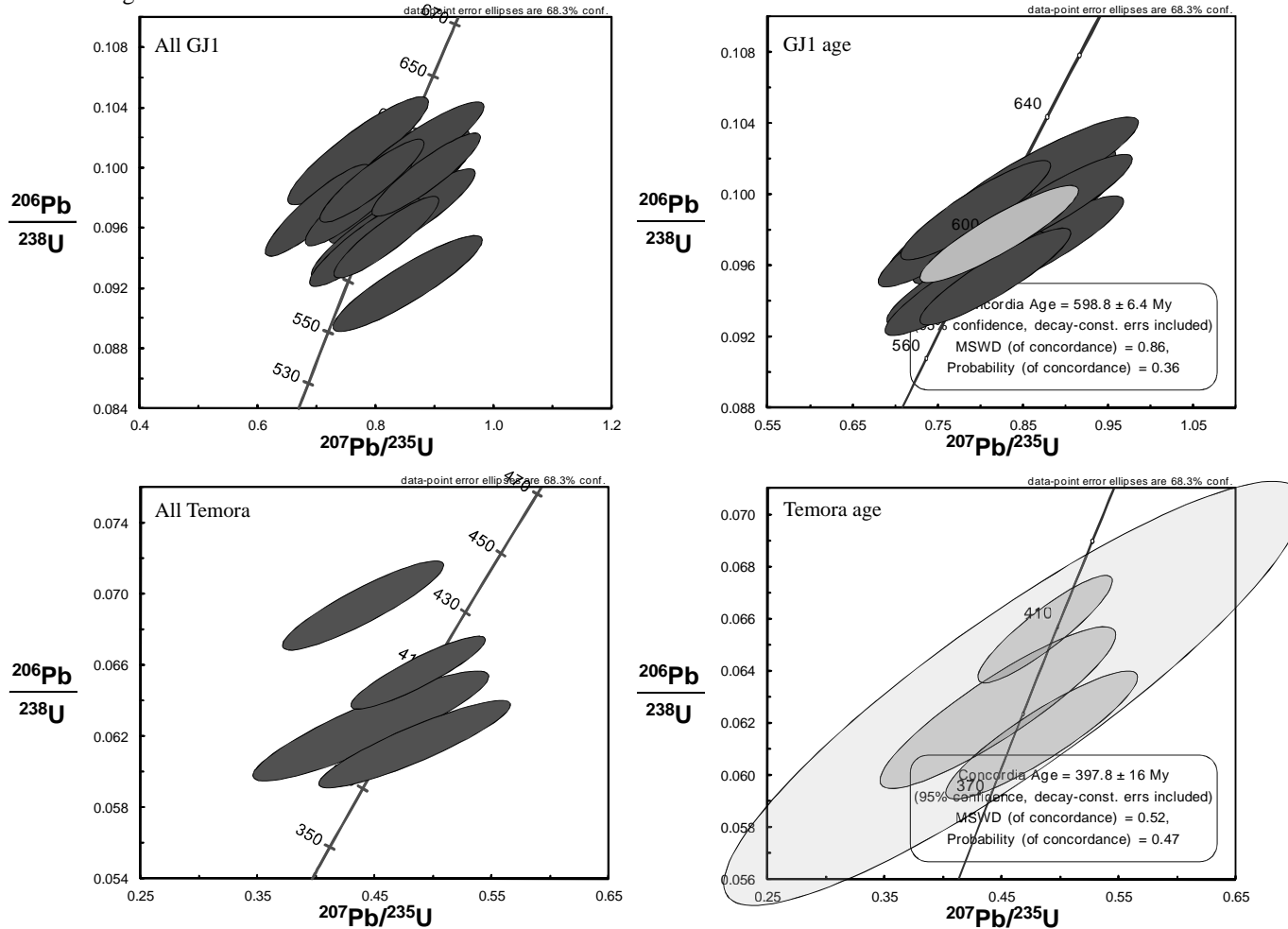
Wharekirauponga Dome



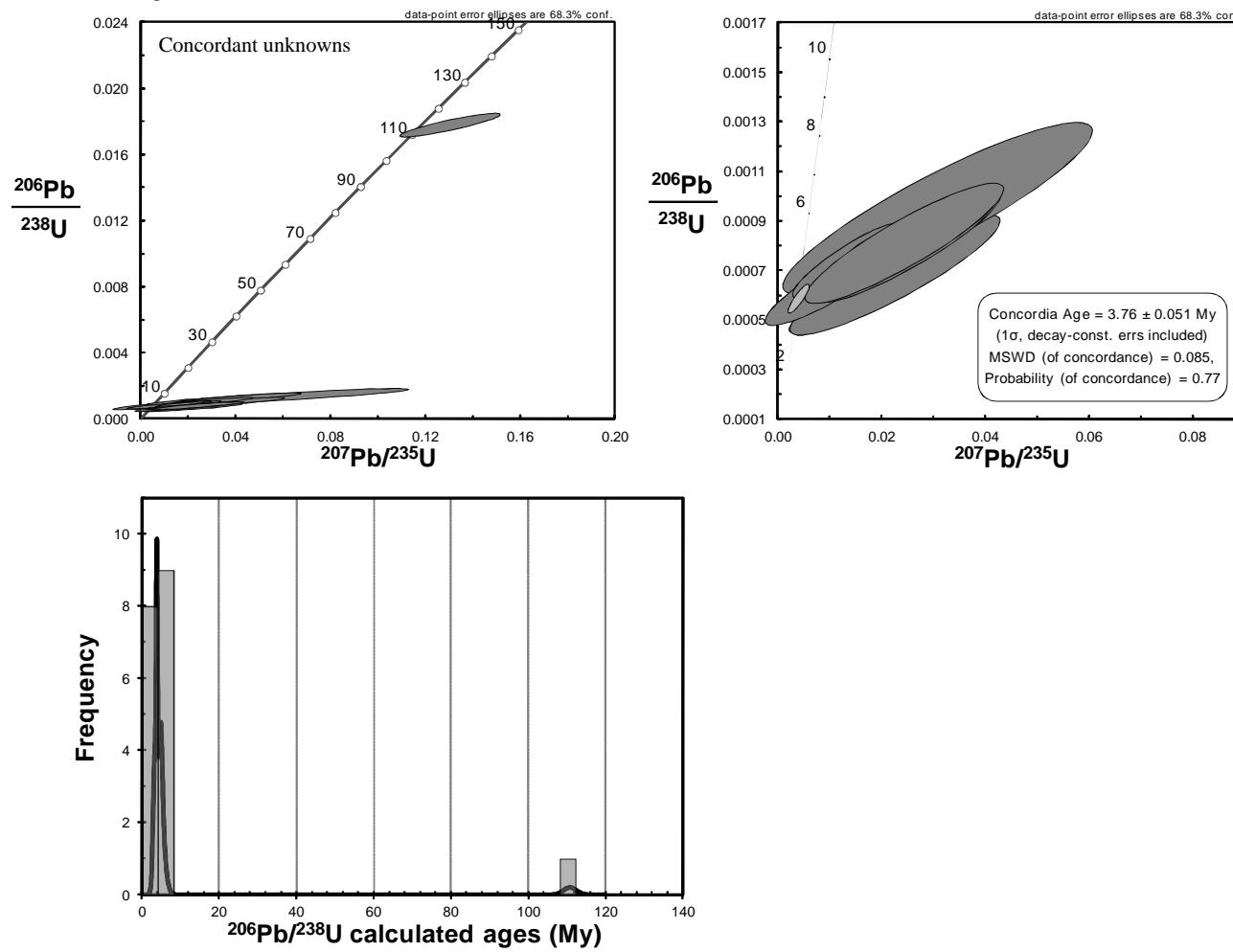
Wharekirauponga Dome



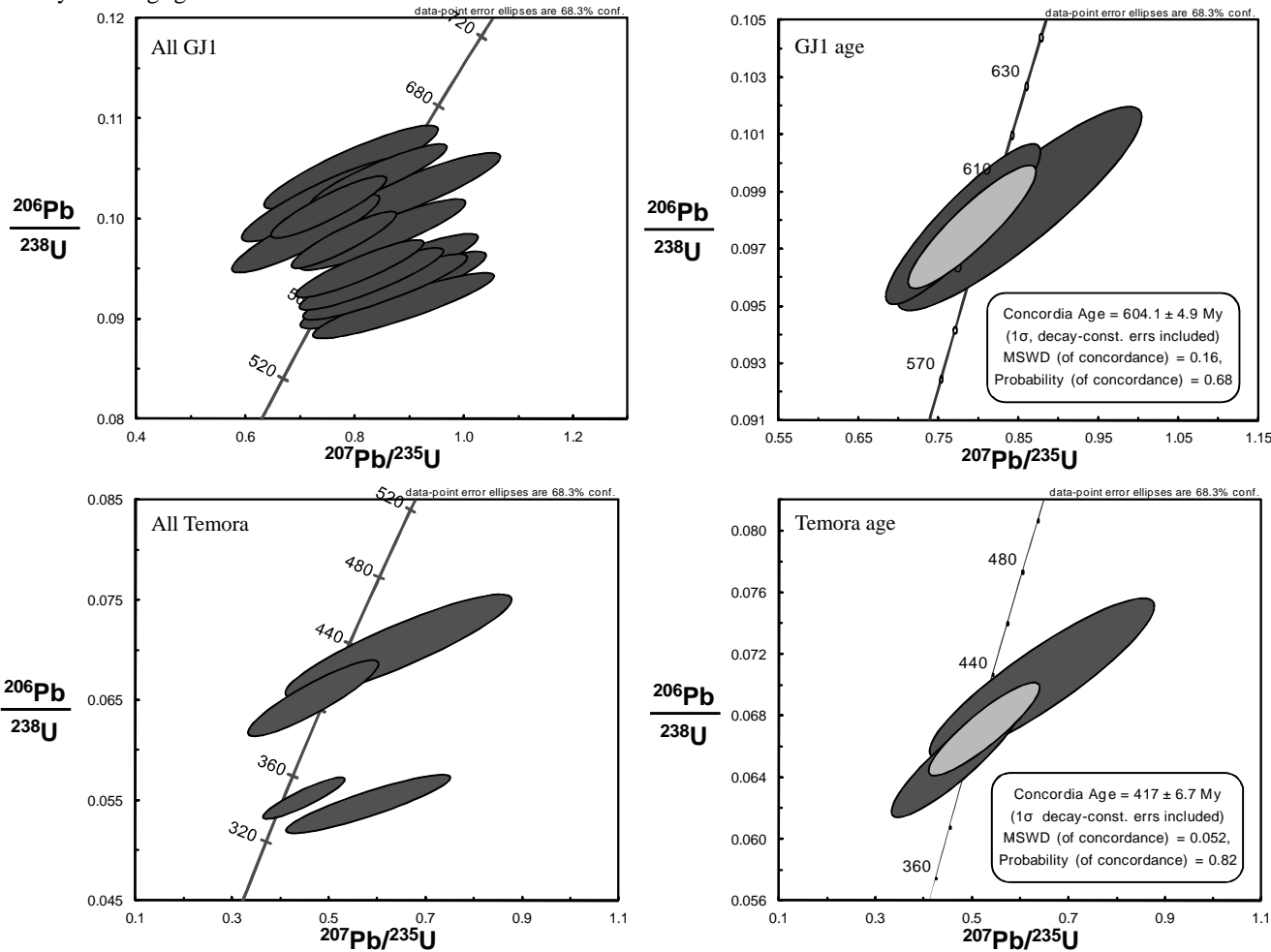
Owharoa Ignimbrite



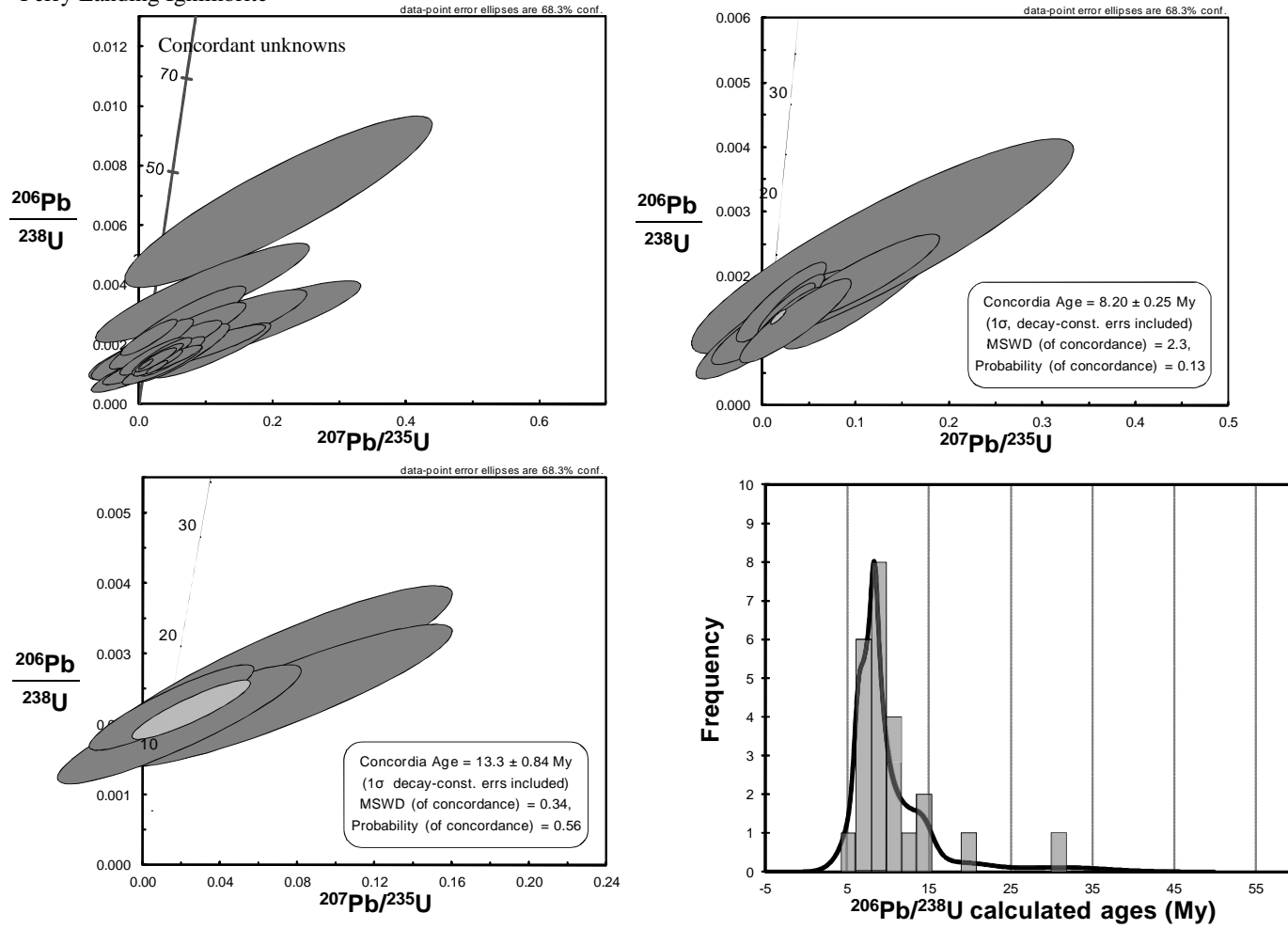
Owharoa Ignimbrite



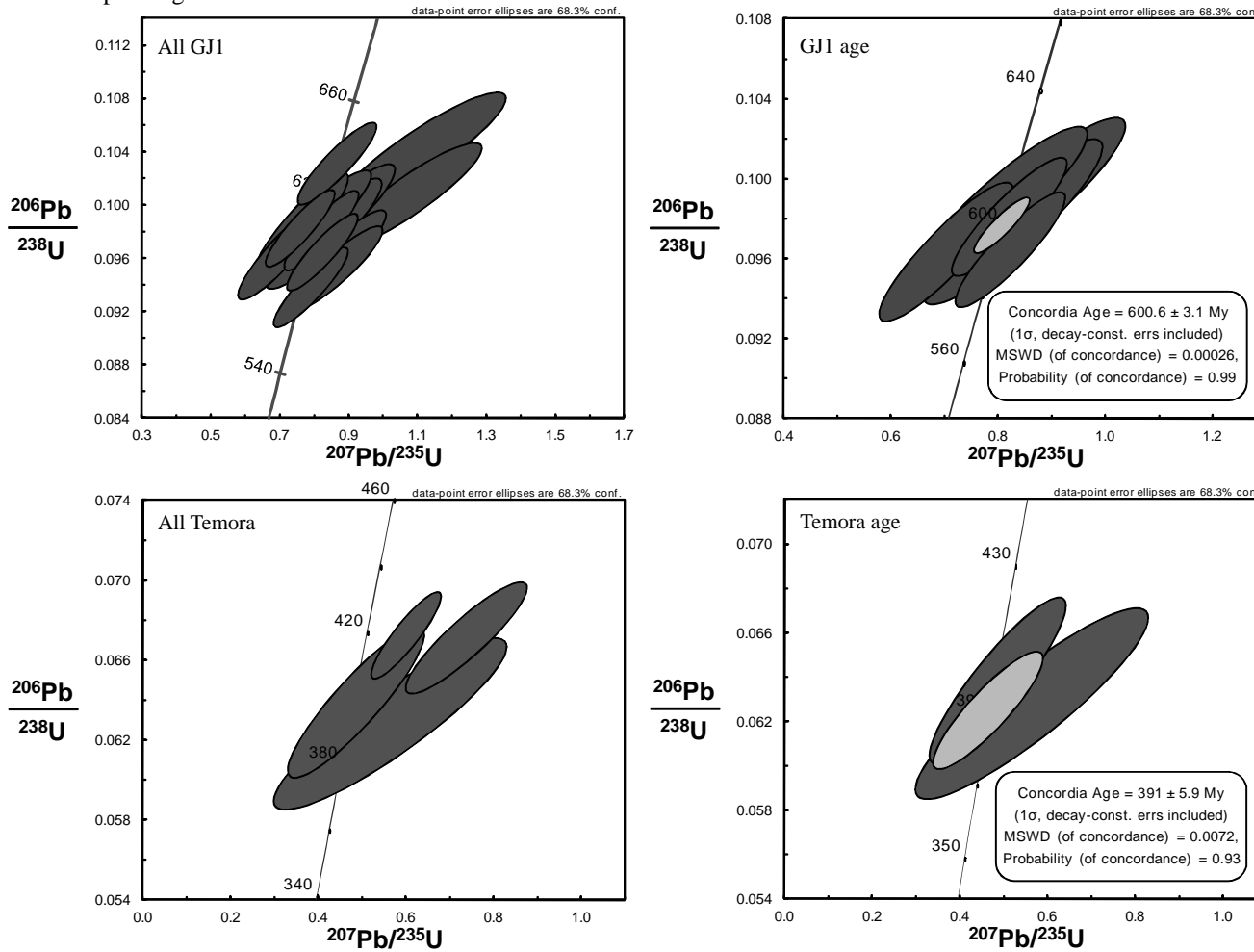
Ferry Landing Ignimbrite



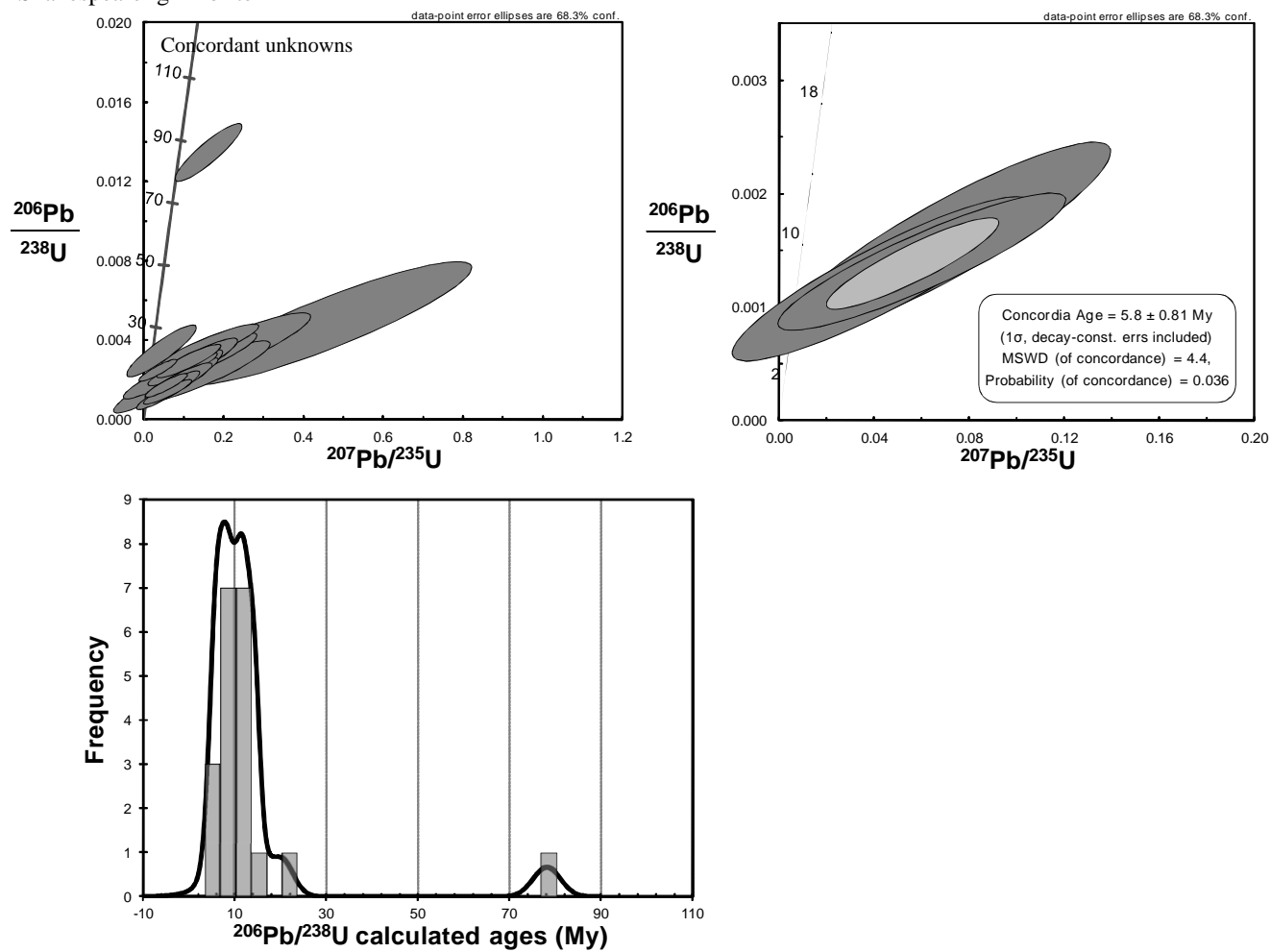
Ferry Landing Ignimbrite



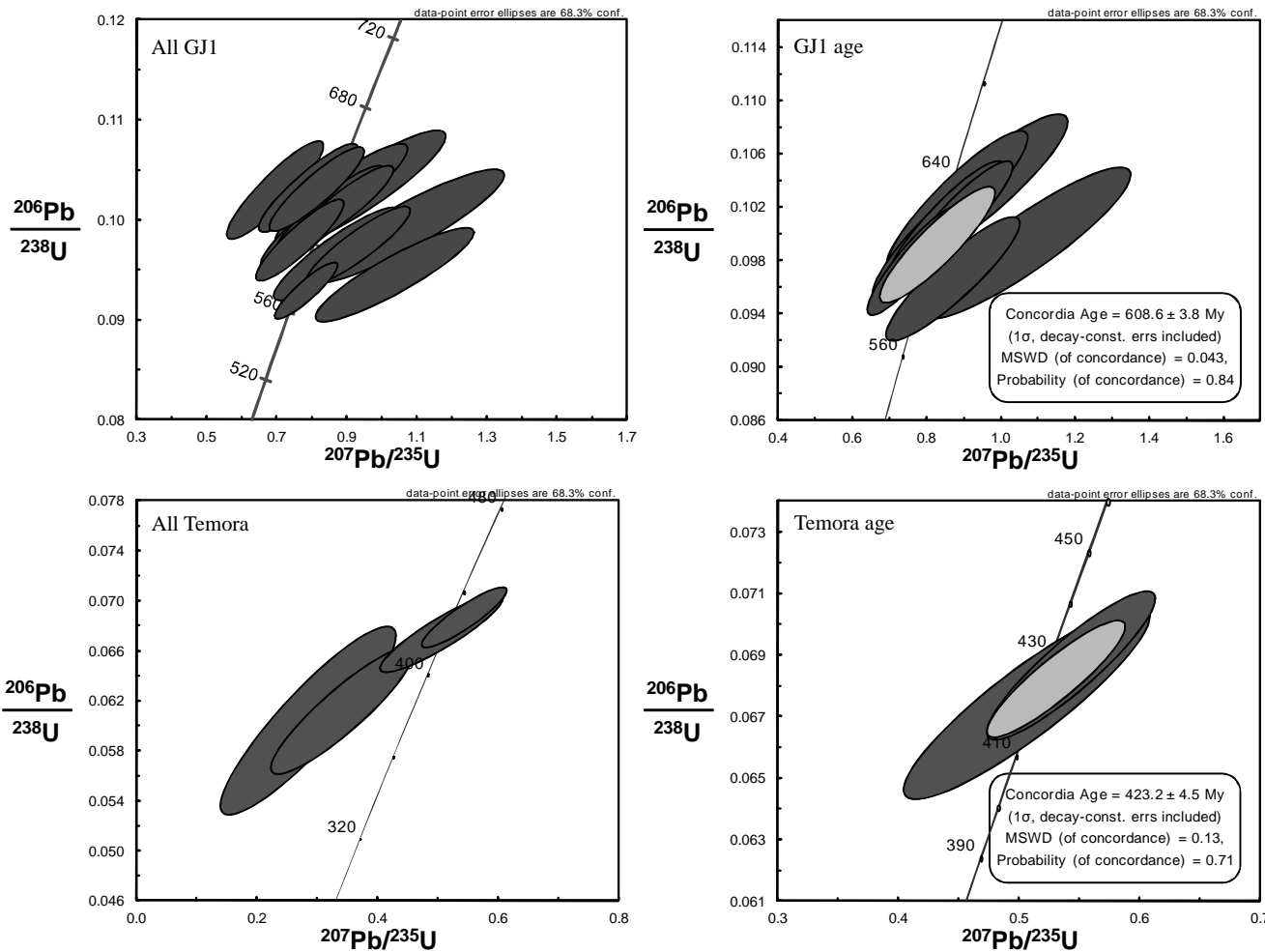
Shakespeare Ignimbrite



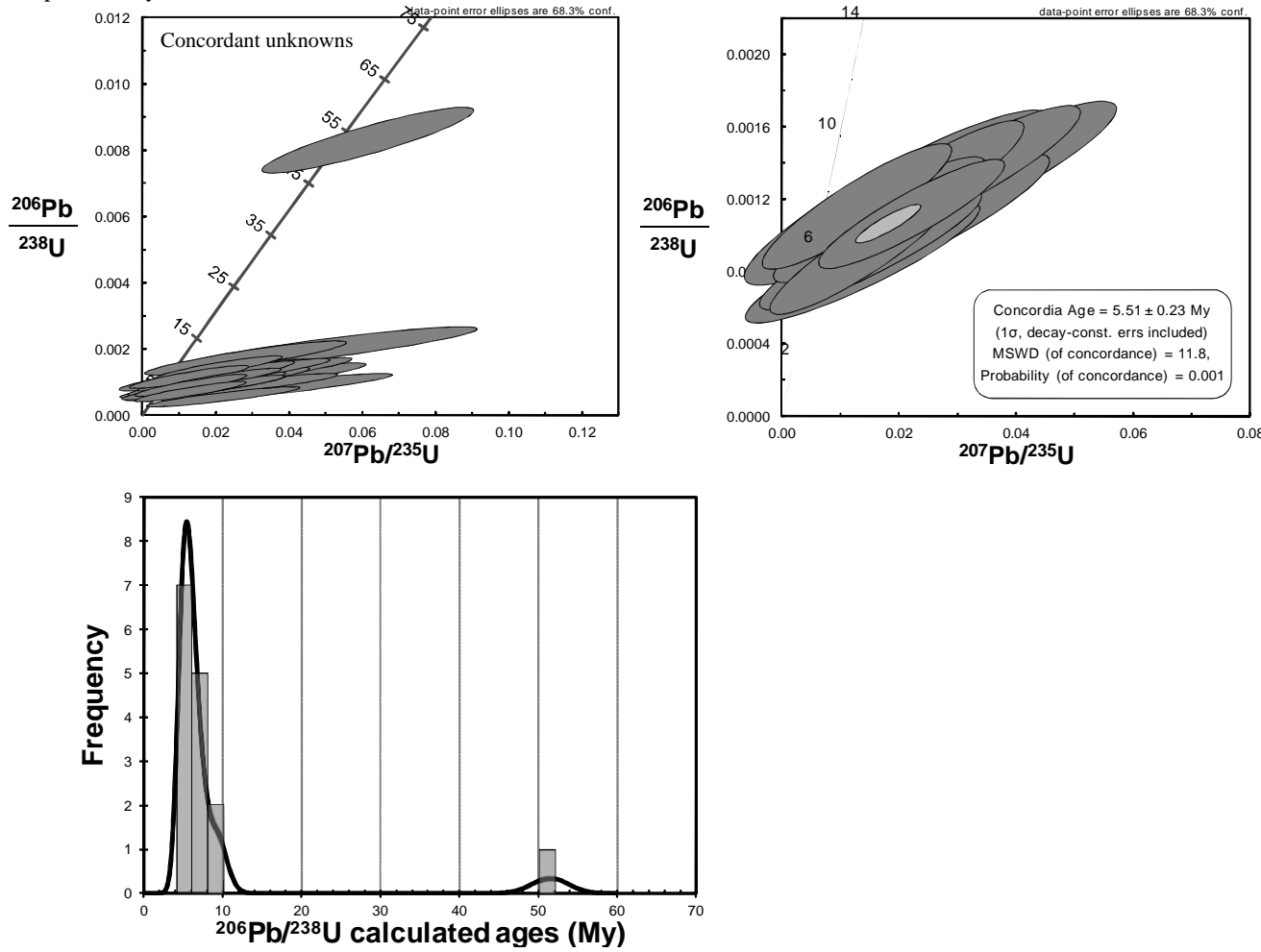
Shakespeare Ignimbrite



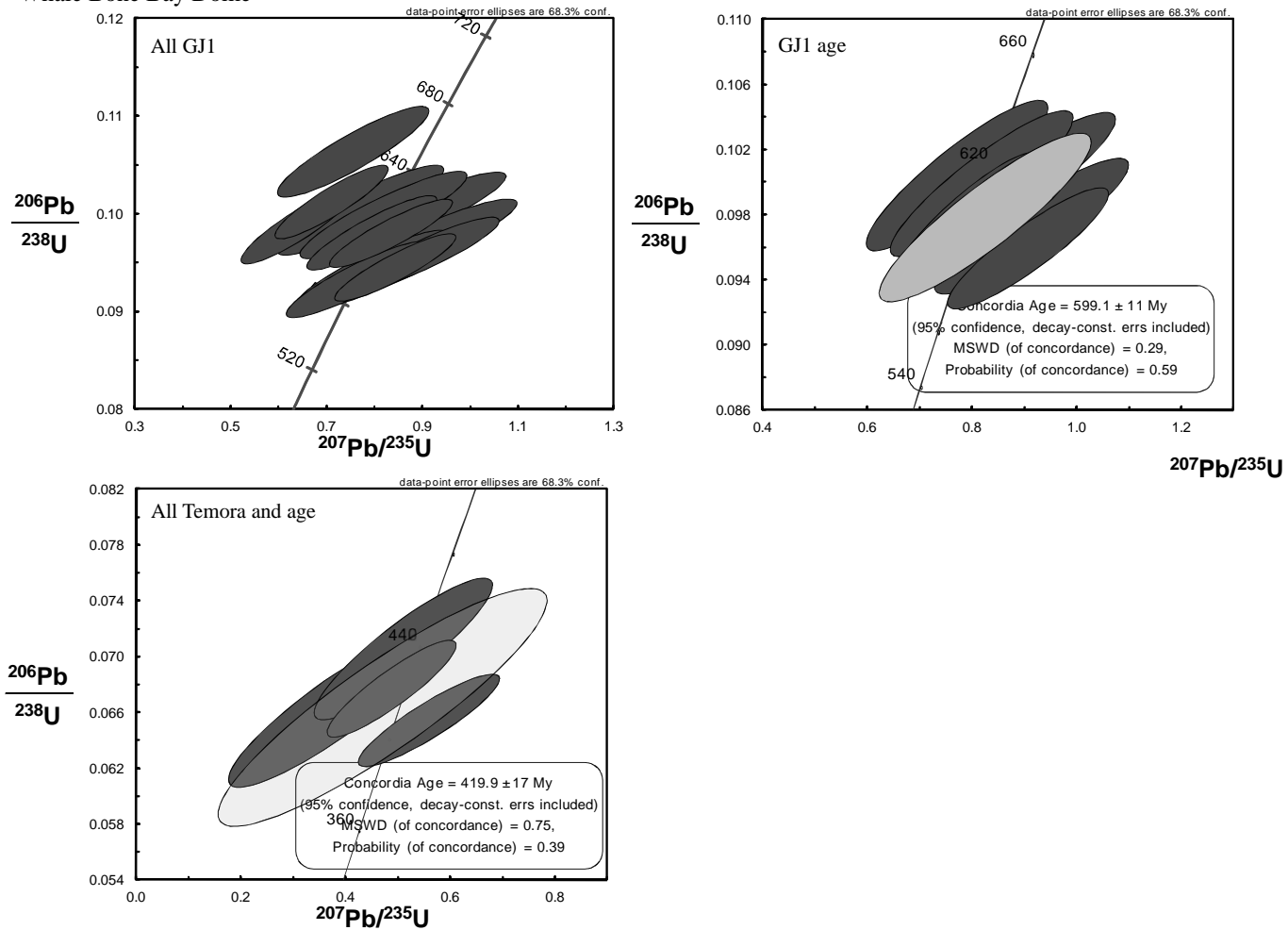
Papakura Bay Dome



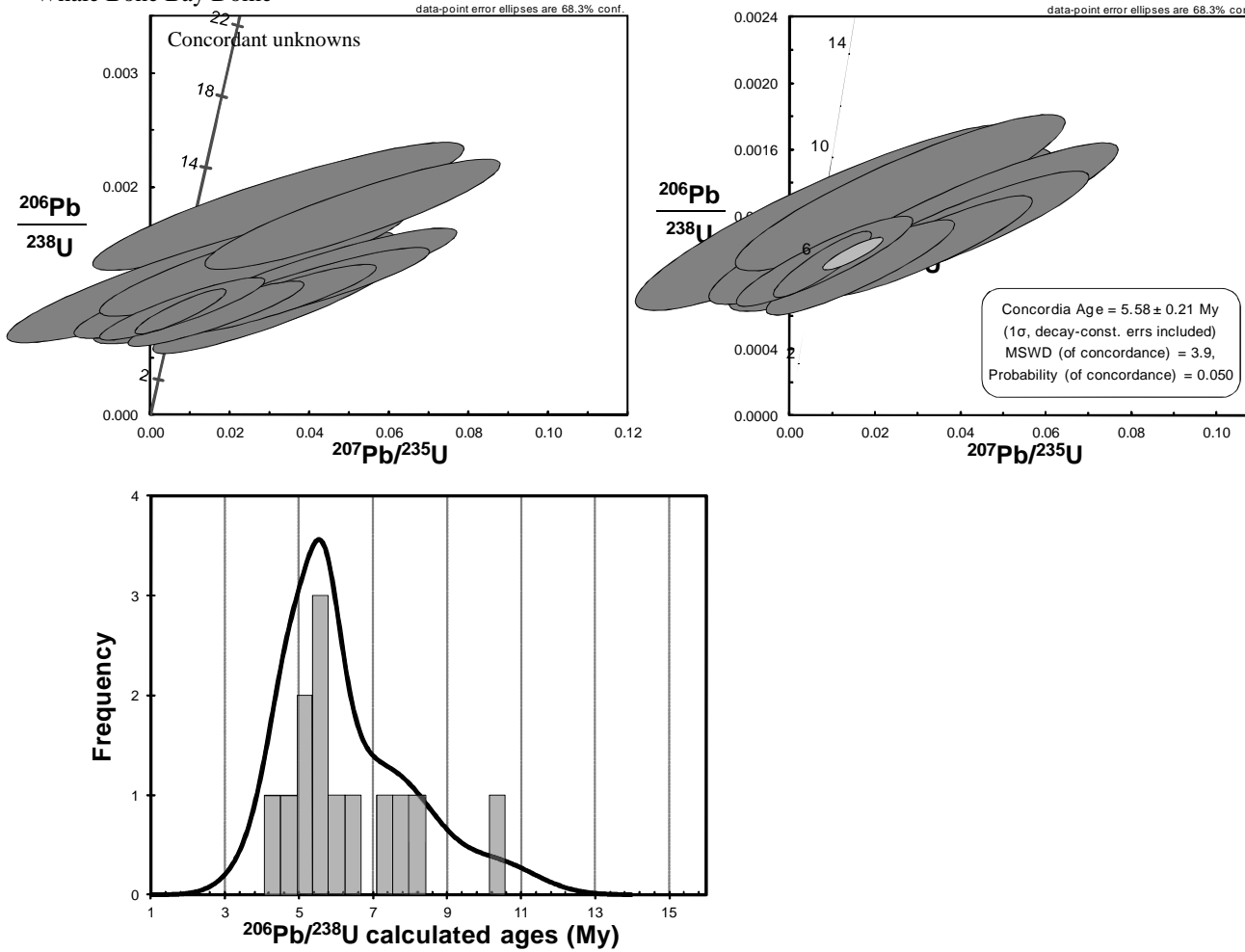
Papakura Bay Dome



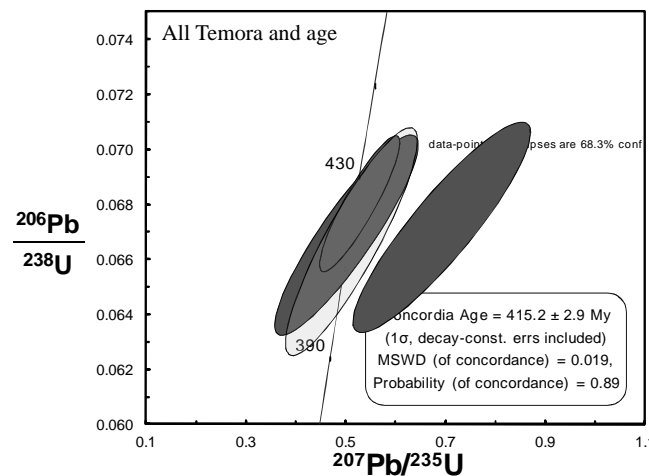
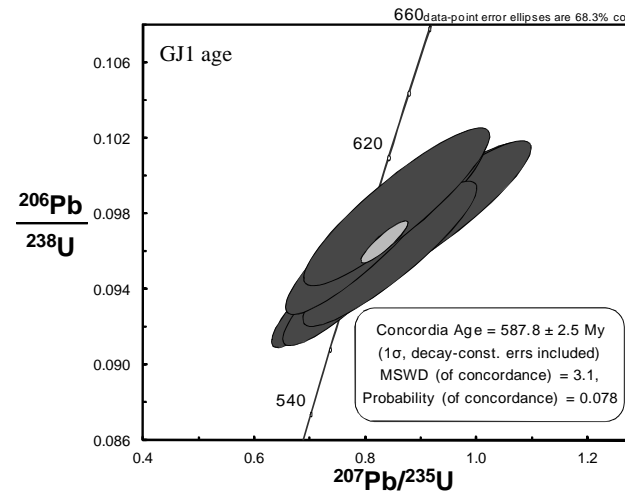
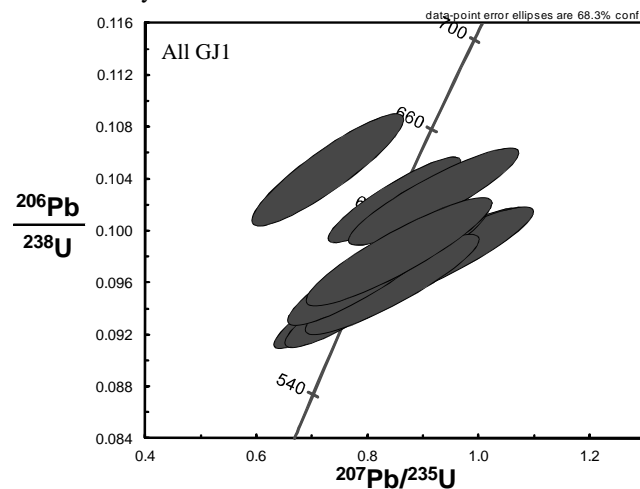
Whale Bone Bay Dome



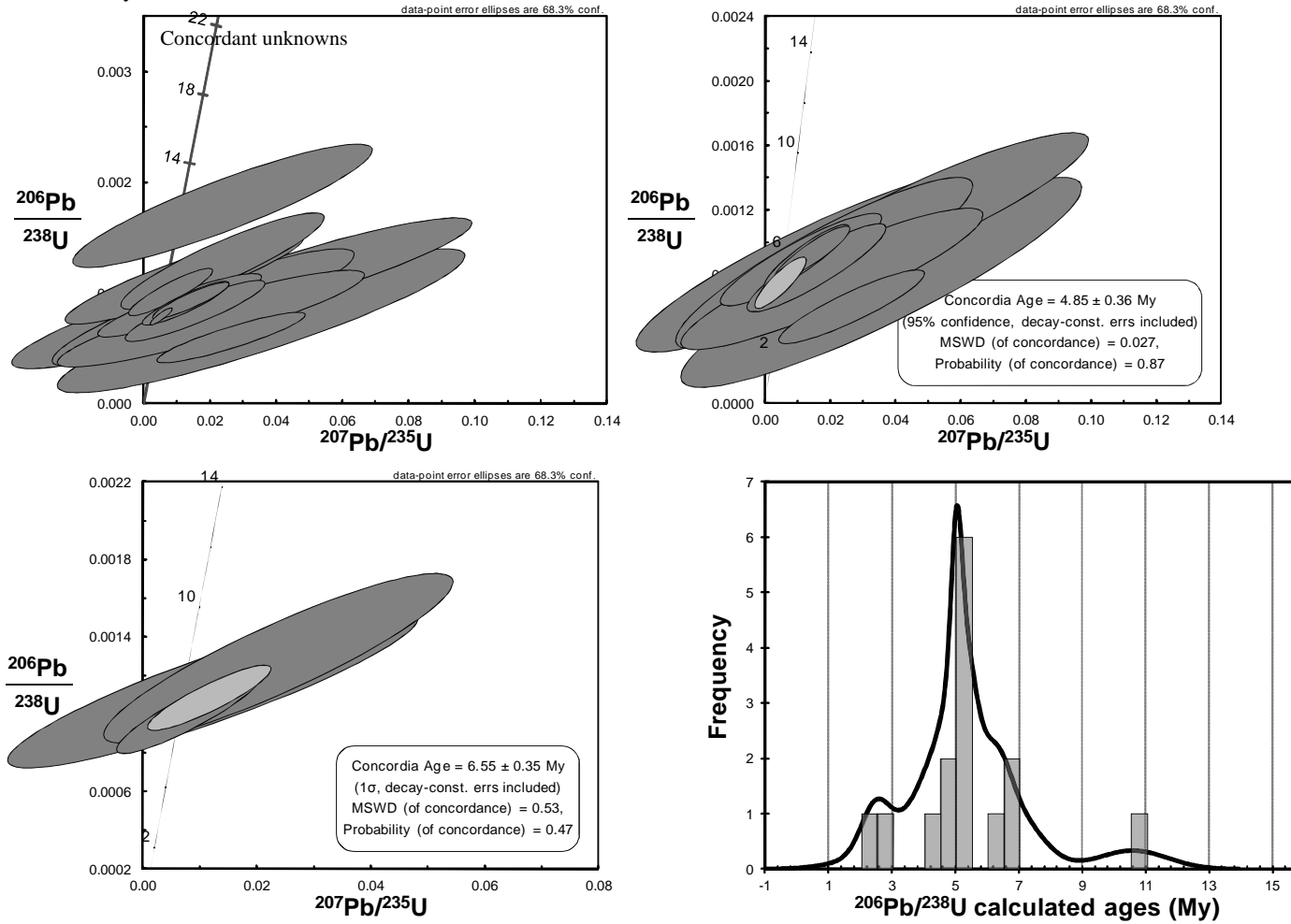
Whale Bone Bay Dome



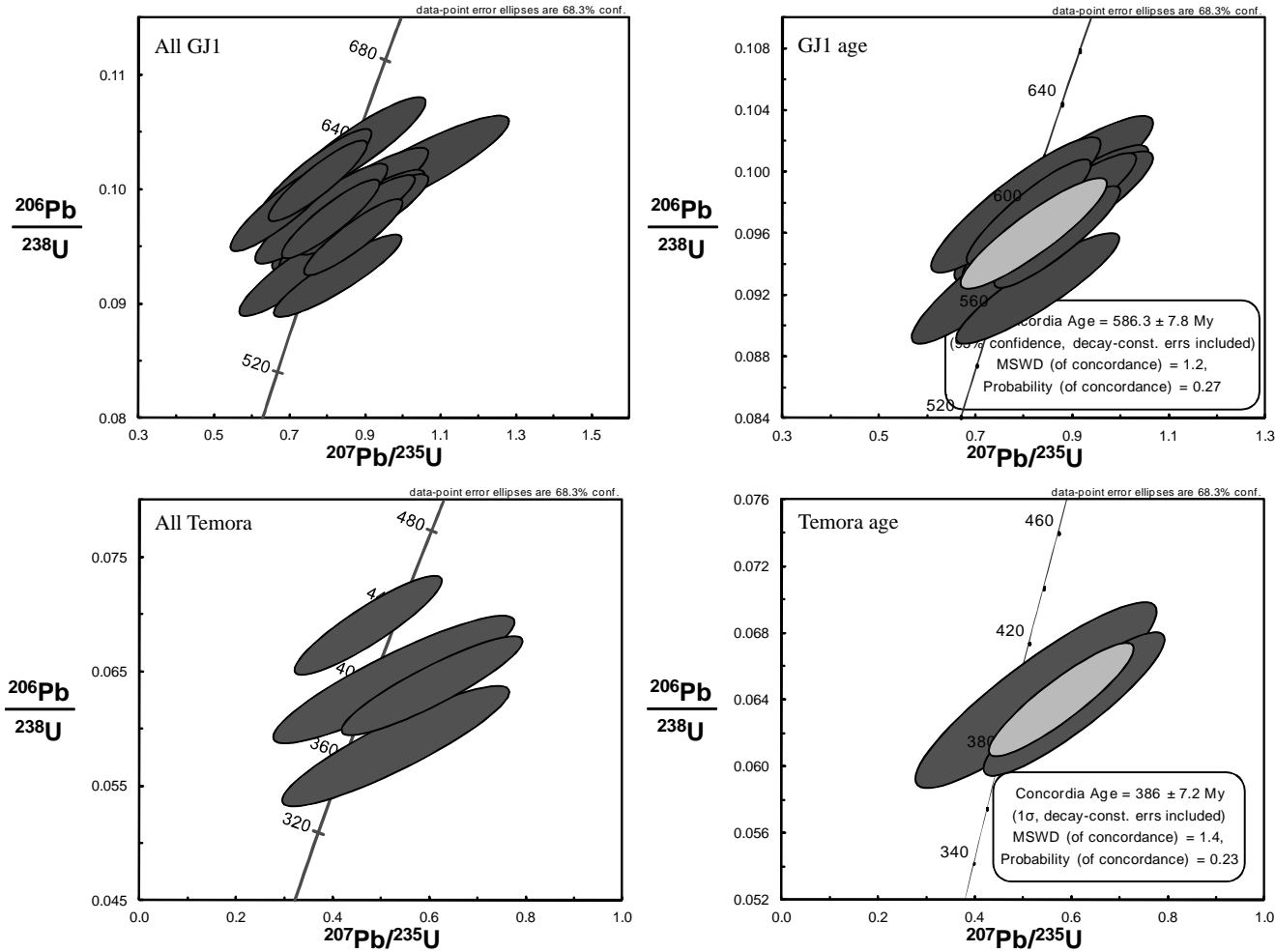
Shark Bay Dome



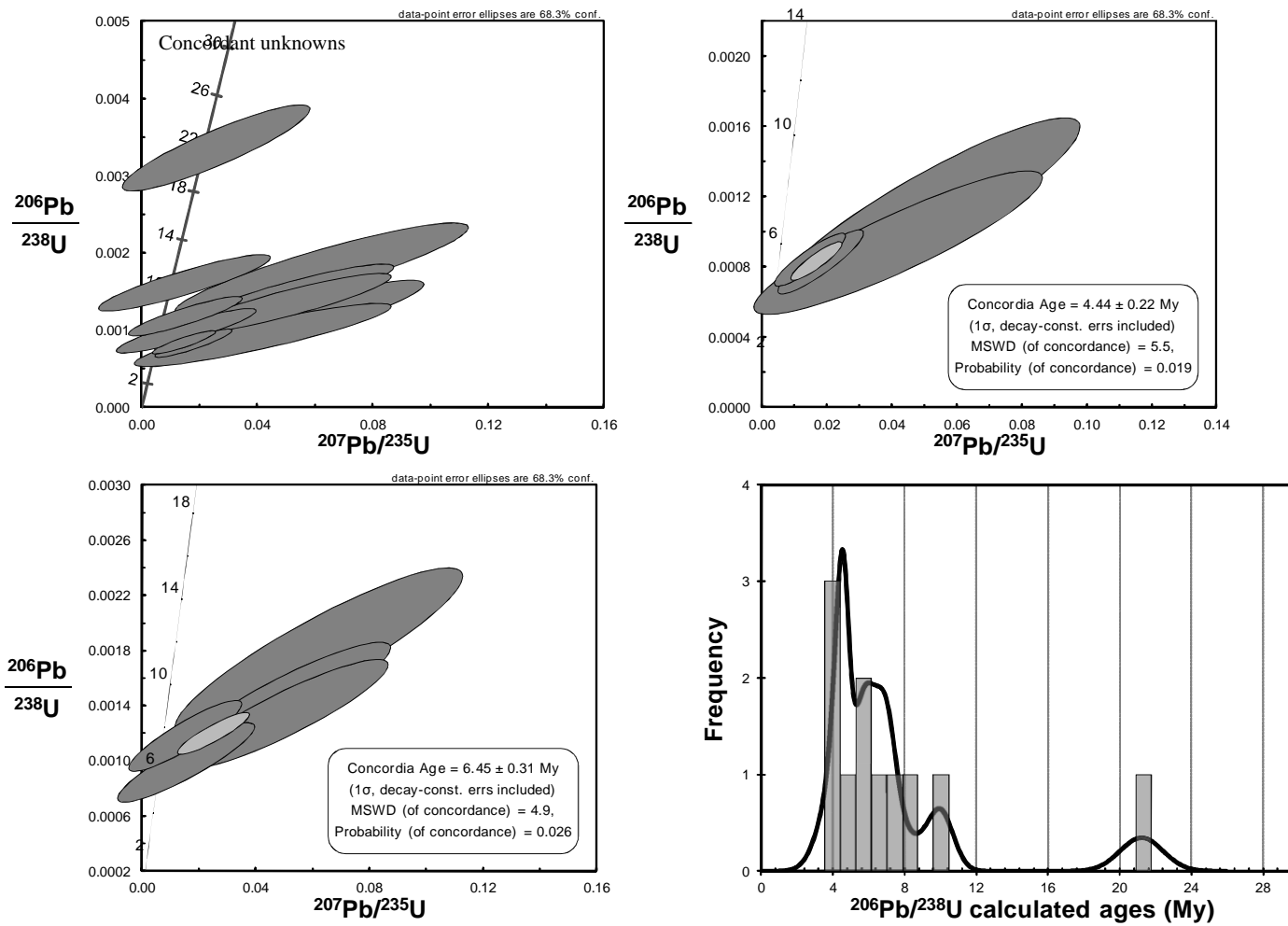
Shark Bay Dome



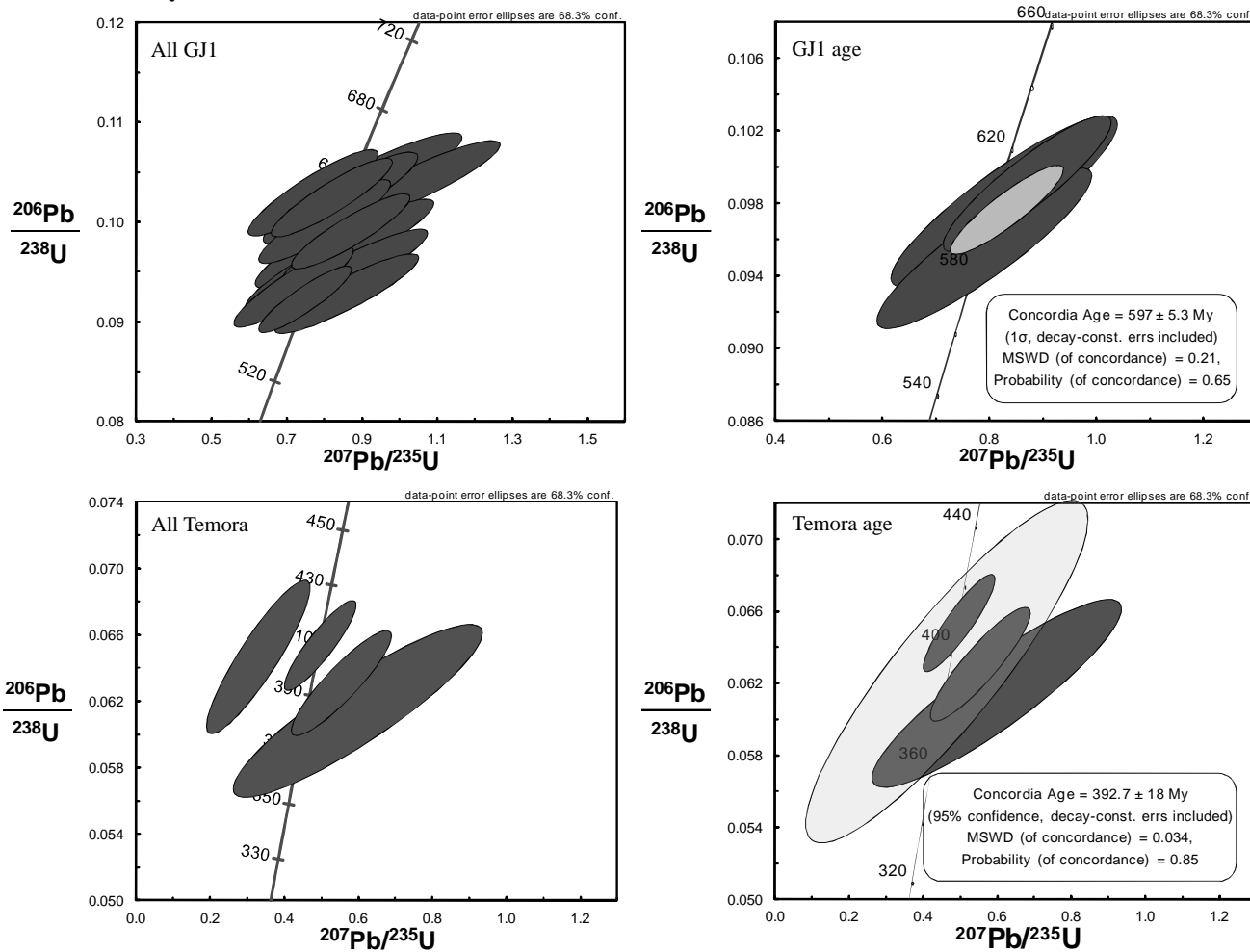
The Knob



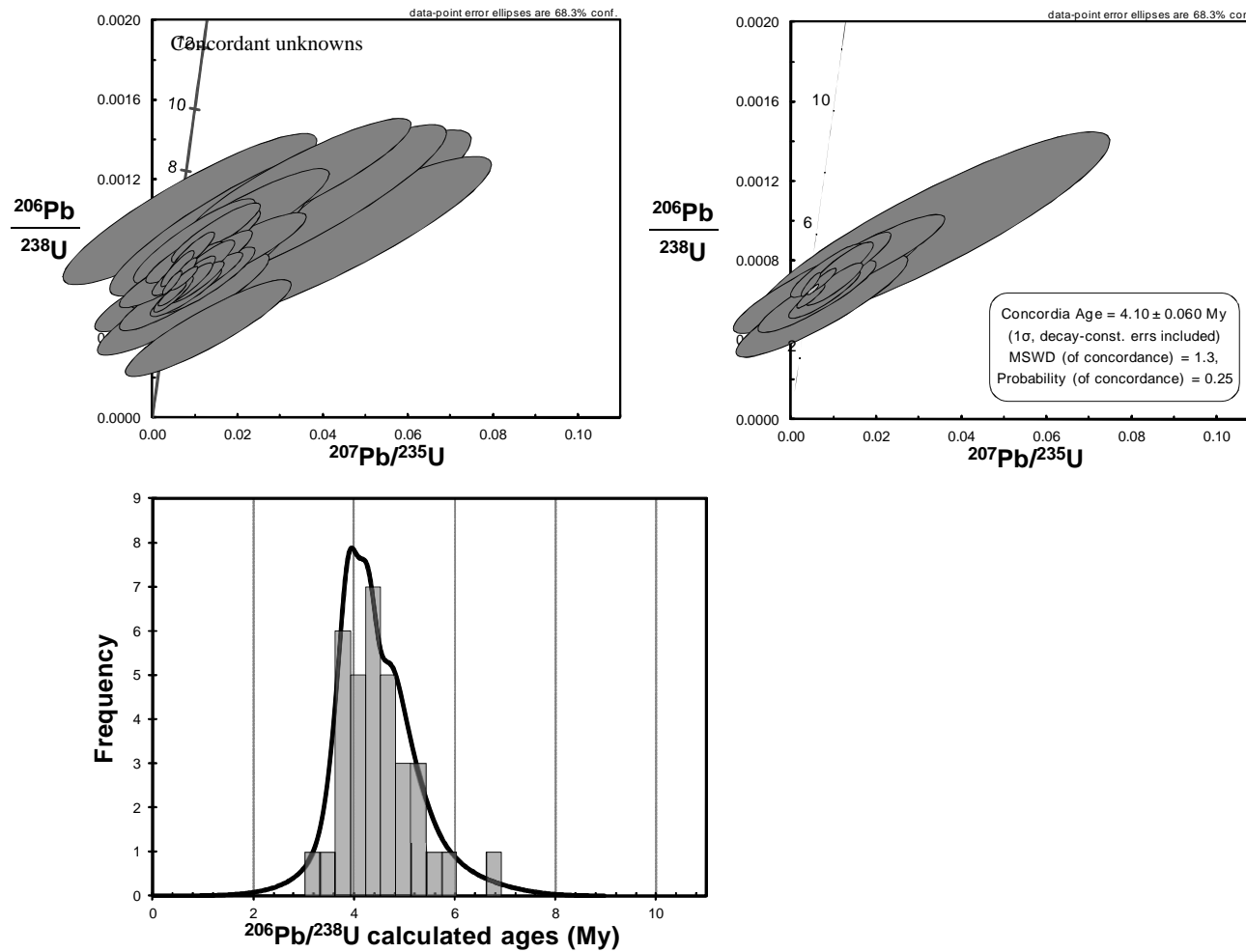
The Knob



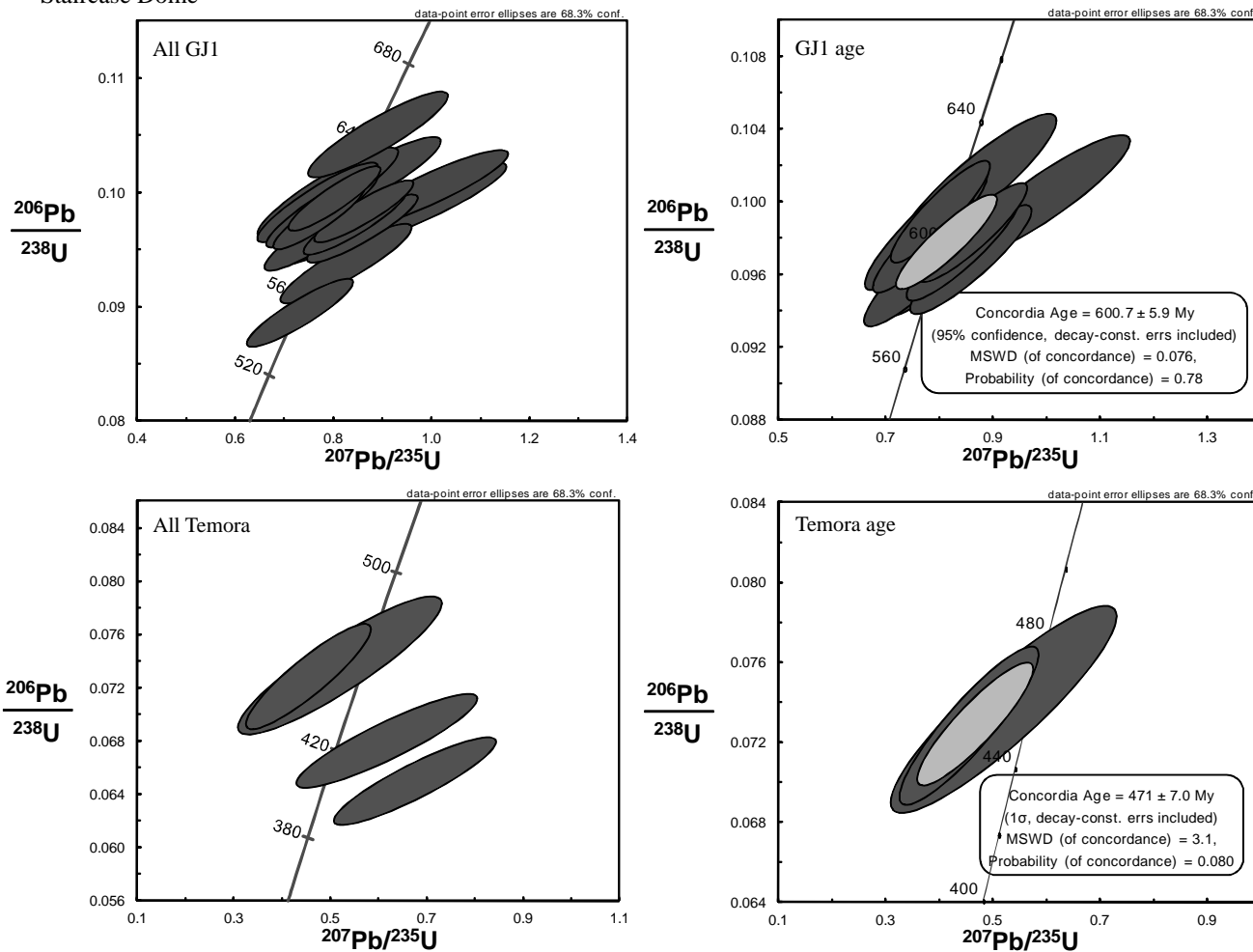
Te Karaka Rhyolite



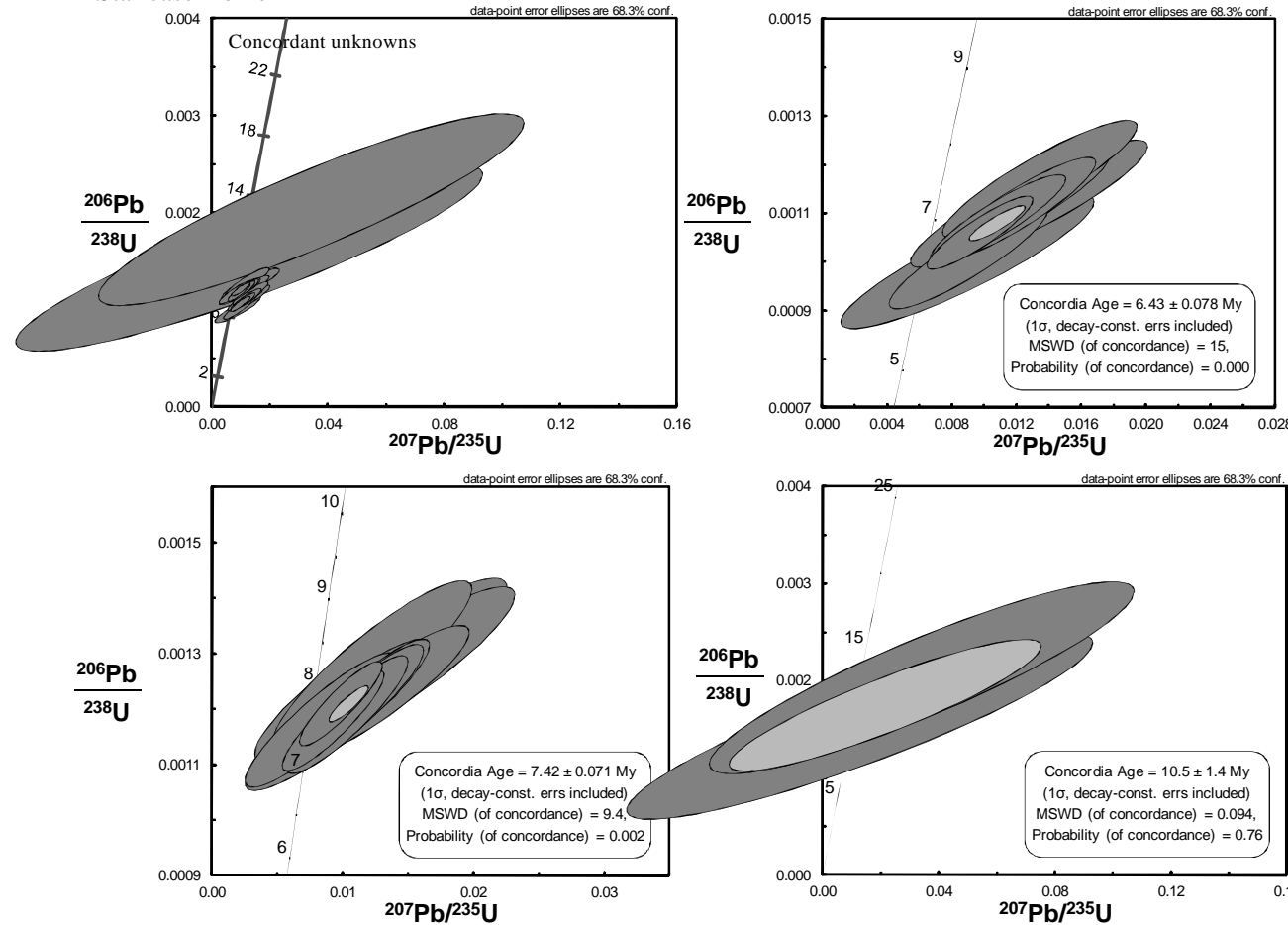
Te Karaka Rhyolite



Staircase Dome

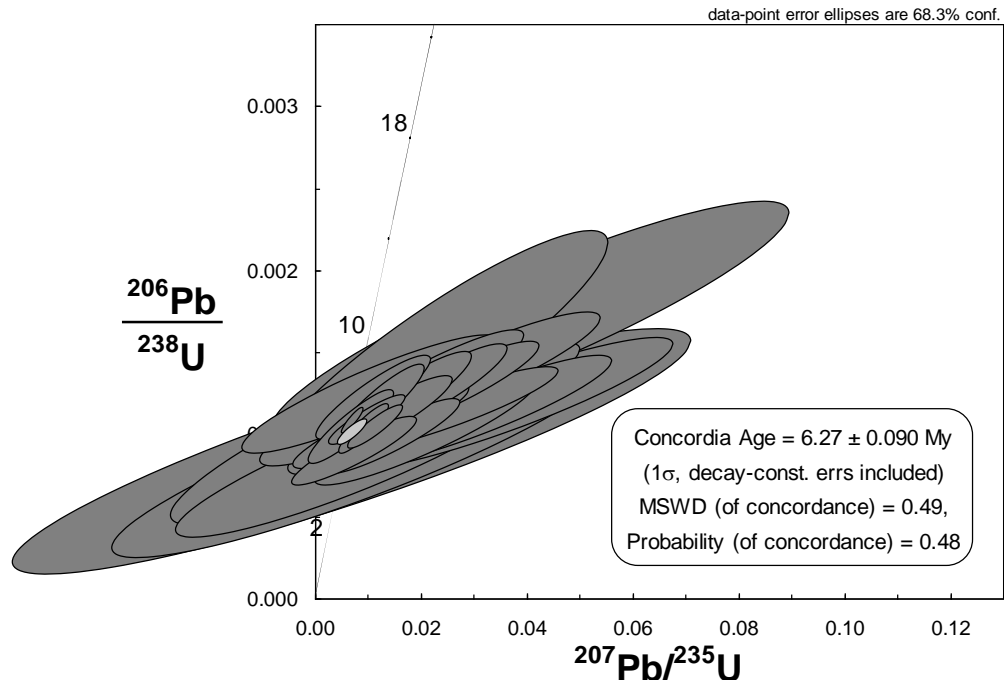


Staircase Dome



189

Broken Hills Rhyolite (concordia age using all concordant analyses that were used to determine the age of the four individual samples of Broken Hills Rhyolite)



Appendix X: CVZ age data

Table X.1: Compilation of age data from previous geochronological studies of CVZ volcanics, as used in Fig. 5.4 and 5.5.

Sample no. (from respective studies)	Rock type	NZTM coordinates		Method (FT = fission track)	Age (My)	\pm
		Easting	Northing			
Table 2, p. 108, Seward & Moore (1987)						
1 TA-6	obsidian Woody Hill	1848323	5898584	FT	7.28	0.95
2 TA-2	obsidian Woody Hill	1849024	5898285	FT	7.36	0.90
3 HA-3	obsidian ~2 km W of Gemstone Bay, Bluff Centre	1848278	5920092	FT	7.65	0.85
4 HA-5	obsidian ~1 km W of Cathedral Cove, Bluff Centre	1848377	5920693	FT	7.77	0.91
5 CB-4	obsidian Motutapere Dome	1844881	5917984	FT	7.38	0.90
6 CB-8	obsidian Motutapere Dome	1843580	5918381	FT	7.37	0.82
7 ON-1	obsidian Onemana	1855856	5884093	FT	7.21	0.84
Table 1, p. 364-367, Adams <i>et al.</i> (1994)						
8 12394TR PC4	basalt cobble in volc mudflow, slightly altered Fletcher Bay	1814979	5960728	K-Ar	17.6	0.6
9 12395TR PF1	pale grey basaltic andesite flow Carey Bay	1821291	5955841	K-Ar	18.0	0.4
10 12391TR PC1	grey andesite flow (upper part) Sugarloaf	1816178	5961130	K-Ar	17.5	0.9
11 12392TR PC2	grey basaltic andesite flow (lower part) Sugarloaf	1815979	5961030	K-Ar	17.4	0.9
12 12393TR PC3	grey andesite dike Sugarloaf	1815378	5961129	K-Ar	16.0	0.3
13 7182Bi PP1	biotite diorite intrusive Ongohi Stream	1812798	5952422	K-Ar	16.9	0.4
14 12396TR TU1	dark grey andesite flow Tuateawa Stream	1830025	5941558	K-Ar	14.5	0.3
15 12397TR BE1	grey andesite breccia Colville Bay	1819218	5943635	K-Ar	14.3	1.0
16 12398TR BE2	dark grey andesite flow Papaaroa Beach	1817035	5935929	K-Ar	14.2	0.8
17 12403TR BE4	pale grey andesite flow Te Kouma Peninsula	1818962	5923530	K-Ar	13.9	1.2
18 12404TR BE5	dark grey andesite flow Te Kouma Peninsula	1818962	5923530	K-Ar	14.9	1.0
19 12405TR BE6	dark grey dacite flow Kouri-Te Kouma Rd junction	1821062	5923935	K-Ar	14.9	0.6
20 12406TR BE7	dark grey andesite plug Kirita Hill	1818678	5916128	K-Ar	15.5	0.7
21 12399TR WO1	black basaltic andesite flow Waiau River Valley	1825569	5920844	K-Ar	13.6	0.6
22 12400TR BE3	grey basaltic andesite flow Waiau Falls	1827170	5920647	K-Ar	12.9	0.6
23 10432TR H31	pale grey andesite flow Whangapoua Beach	1833141	5934764	K-Ar	13.4	0.4
24 10433TR H32	grey andesite flow Whangapoua; Punga Punga quarry	1831243	5933759	K-Ar	13.1	0.1
25 12389TR MA1	dark grey andesite flow Matatranghi Bluff	1839749	5931978	K-Ar	13.1	0.5
26 12401TR MA2	pale grey dacite plug Motutere	1827868	5921949	K-Ar	13.2	0.2
27 10403TR H2	grey andesite plug Five Mile Stream	1833505	5904956	K-Ar	10.9	0.2
28 12388TR MM1	pale grey andesite flow Kaimarama	1836680	5917266	K-Ar	12.3	0.7
29 12415TR MPK1	silicic andesite flow Te Mata Valley	1829199	5906948	K-Ar	12.2	0.5
30 12416TR MPK2	grey andesite plug Te Mata Valley	1829600	5906948	K-Ar	11.0	0.4

31	12417TR MPK3	grey andesite clast-breccia Te Mata Valley	1827699	5907145	K-Ar	12.1	0.5
32	17820TR N44/749	dark grey andesite flow Buffalo Beach Stream	1838170	5922371	K-Ar	13.8	0.2
33	17821TR N44/718	grey andesite flow Owera Stream	1836964	5924769	K-Ar	13.4	0.2
34	12390TR TT1	dark grey andesite clast Te Tutu Trig	1840752	5930779	K-Ar	13.7	0.2
35	10428TR H27	pale grey andesite plug Whaoeai Bay	1848046	5934697	K-Ar	11.5	0.5
36	7173TR 12C	grey andesite Wataia Bay	1846459	5928391	K-Ar	11.4	0.2
37	10404TR H3	grey andesite flow Five Mile Stream	1834903	5906159	K-Ar	9.8	0.6
38	12767TR 871/2	platy basaltic andesite flow Taurahuue Stream	1837799	5908366	K-Ar	9.4	0.7
39	12769TR 871/1	platy basaltic andesite flow Rangihau Rd	1838602	5907267	K-Ar	9.2	0.9
40	12382TR TA1	grey andesite flow Hot Water Beach	1851993	5913698	K-Ar	8.2	0.5
41	12383TR TA2	dark grey andesite flow Whenuakite Quarry	1848904	5908189	K-Ar	8.9	0.5
42	12414TR K1	grey andesite flow Upper Kaueranga Valley	1838523	5896863	K-Ar	9.0	0.40
43	12387TR T1	dark grey andesite flow Haukawakawa track	1837406	5904964	K-Ar	7.6	0.4
44	12413TR T2	grey andesite flow Moss Creek Track	1838121	5897863	K-Ar	8.1	0.2
45	10577Hb 586	ignimbrite Coroglen	1838894	5910969	K-Ar	10.0	0.4
46	12384TR PBR1	pale grey-cream slightly banded rhyolite flow Hahei Beach Rd	1847783	5917490	K-Ar	7.7	0.2
47	12380TR HB1	cream-grey, flow-banded rhyolite Hereheretaura Point	1851282	5918898	K-Ar	8.1	0.1
48	12381TR HB2	cream-grey, flow-banded rhyolite Hereheretaura Point	1851181	5918998	K-Ar	7.9	0.1
49	12385TR RH1	pale, devitrified rhyolite flow Knight's farm	1844080	5918583	K-Ar	8.0	0.4
50	12386TR RH2	pale, glassy rhyolite flow Red Hill trig	1841880	5917978	K-Ar	8.0	0.1
51	12771TR/Bi 84/105	perlite-glassy rhyolite flow Hahei	1849581	5918995	K-Ar	7.7	0.1
52	10414TR H13	pumiceous, well-bedded, lithic-rich rhyolite ash Stanley Island	1857433	5941820	K-Ar	5.3	0.2
53	7169TR 4C	dark grey basalt flow Opito Bay	1851352	5932503	K-Ar	9.0	0.4
54	10420TR H19	pale grey basaltic andesite flow Opito Point	1851952	5932705	K-Ar	8.4	0.4
55	10421TR H20	grey basaltic andesite plug Opito Point	1851852	5932504	K-Ar	9.2	1.1
56	10423TR H22	grey basaltic andesite flow Opito Bay	1851152	5932303	K-Ar	8.8	0.3
57	10425TR H24	dark grey basalt flow Tamaihu	1849544	5935600	K-Ar	7.8	0.4
58	10426TR H25	dark grey basalt flow Tamaihu	1848445	5935298	K-Ar	8.6	0.3
59	10429TR H28	grey dolerite plug New Chums Beach	1833440	5935165	K-Ar	8.5	0.2
60	10430TR H29	grey dolerite plug New Chums Beach	1833640	5935265	K-Ar	9.1	0.2
61	10405TR H4	dark grey basalt flow overlying rhyolite ash Red Mercury Island	1862832	5943033	K-Ar	5.2	0.6
62	10406TR H5	dark grey basalt flow overlying rhyolite ash Red Mercury Island	1862832	5943033	K-Ar	4.8	0.2
63	10407TR H6	dark grey basalt flow overlying rhyolite ash Red Mercury Island	1862832	5943033	K-Ar	4.6	0.3
64	10409TR H8	grey dolerite intrusive into basalt Red Mercury Island	1863433	5942734	K-Ar	4.8	0.3
65	10411TR H10	grey dolerite intrusive into basalt Double Island	1859632	5942826	K-Ar	4.2	0.4
66	10412TR H11	grey dolerite intrusive into rhyolite ash Stanley Island	1857833	5941821	K-Ar	5.8	0.3
67	10413TR H12	grey dolerite unconformably under rhyolite ash Stanley Island	1857433	5941820	K-Ar	4.9	0.3
68	10415TR H14	basalt flow beneath ash Stanley Island	1857635	5941021	K-Ar	6.0	0.4
69	10416TR H15	grey, platy andesite flow Middle Island	1855733	5941616	K-Ar	5.6	0.2
70	10417TR H16	pale grey basaltic andesite flow Green Island	1854637	5939513	K-Ar	5.6	0.4

71	10418TR H17	silicic andesite flow Koropuki Island	1854734	5940814	K-Ar	4.5	0.2	
72	12770TR 871/6	grey basaltic andesite flow Woody Hill	1848624	5898184	K-Ar	5.1	0.3	
73	12768TR 871/7	grey basaltic andesite flow Woody Hill	1848524	5898284	K-Ar	5.5	0.2	
Table 2, p. 368, Adams <i>et al.</i> (1994)								
74	10576(584)	Carina Rock Ignimbrite	1838894	5910969	FT	10.4	1.5	
75	10577(586)	Carina Rock Ignimbrite	1839093	5911570	FT	11.0	1.2	
76	10566(573)	Wharepapa Ignimbrite	1849986	5916595	FT	8.2	0.7	
77	10567(574)	Wharepapa Ignimbrite	1849589	5915093	FT	9.2	1.9	
78	10578(587)	Pumpkin Rock Ignimbrite	1841776	5920178	FT	7.0	1.2	
79	10580(591)	Pumpkin Rock Ignimbrite	1843285	5916180	FT	5.6	1.7	
80	10582(593)	Pumpkin Rock Ignimbrite	1843285	5916180	FT	6.0	0.6	
81	10584(589)	Pumpkin Rock Ignimbrite	1845186	5915684	FT	5.6	0.5	
82	10572(579)	Whenuakite Rhyolite dome	1847601	5908987	FT	6.8	1.8	
Appendix I, Adams <i>et al.</i> (1994)								
83	10596TR GB24B	andesite dike Paradise Bay	1816872	6005536	K-Ar	17.1	0.3	
84	10597TR GB38	quartz-porphyry dike Rangiwahakaera Bay	1810872	6005421	K-Ar	16.7	0.4	
85	6987TR MH7	quartz-porphyry dike Miners Head mine shaft	1810872	6005421	K-Ar	16.3	0.3	
86	6314Bi Pb19	quartz-porphyry dike Miners Head	1811073	6005222	K-Ar	18.5	0.4	
87	6980TR ORR2	basaltic andesite Oreville Battery	1817716	5987637	K-Ar	12.3	0.4	
88	6994TR ORR3	basaltic andesite Whangaparapara Rd	1817216	5987636	K-Ar	13.8	0.4	
Table 1 and 3, p. 55-58 and 69-72, Takagi (1995)								
89	S26-45	44373	basaltic andesite Red Mercury Island	1863033	5942733	K-Ar	3.89	0.23
90	S25-326	45375	basaltic andesite Red Mercury Island	1862933	5942733	K-Ar	4.15	0.26
91	S25-327	44378	basaltic andesite Red Mercury Island	1862832	5942933	K-Ar	4.40	0.21
92	S25-324	44380	basaltic andesite Red Mercury Island	1862832	5943133	K-Ar	3.93	0.26
93	S25-325	44382	basaltic andesite Double Island	1860232	5942827	K-Ar	3.82	0.22
94	S25-282	44389	basaltic andesite Stanley (Kawithiu) Island	1858235	5941022	K-Ar	4.85	0.29
95	S26-46	44390	basaltic andesite Stanley (Kawithiu) Island	1858335	5940922	K-Ar	4.93	0.30
96	S25-290	44391	basaltic andesite Stanley (Kawithiu) Island	1858436	5940822	K-Ar	5.38	0.16
97	S25-291	44393	basaltic andesite Stanley (Kawithiu) Island	1858135	5941122	K-Ar	5.55	0.17
98	S25-286	44394	basaltic andesite Stanley (Kawithiu) Island	1858135	5941222	K-Ar	5.61	0.28
99	S25-285	44395	andesite Stanley (Kawithiu) Island	1858432	5942623	K-Ar	5.48	0.35
100	S25-284	44398	basaltic andesite Stanley (Kawithiu) Island	1857935	5941121	K-Ar	4.60	0.28
101	S25-288	44399	basaltic andesite Korapuke Island	1858039	5939221	K-Ar	5.43	0.16
102	S25-287	44400	basaltic andesite Korapuke Island	1854838	5939113	K-Ar	5.26	0.40
103	S25-289	44402	basaltic andesite Korapuke Island	1854838	5939113	K-Ar	5.44	0.14
104	S26-48	14594	rhyolite Ohena Island	1857256	5931616	K-Ar	5.79	0.13
105	S26-47	14593	basaltic andesite Ohena Island	1860950	5934826	K-Ar	5.30	0.61
106	S25-331	14607	andesite Ohena Island	1856048	5934815	K-Ar	5.44	0.14
107	S25-329	14602	basaltic andesite Ohena Island	1856252	5933315	K-Ar	5.63	0.14
108	S25-330	14604	basaltic andesite Ohena Island	1856252	5933315	K-Ar	5.67	0.35
109	S25-338	44405	rhyolite Great Mercury Island	1851131	5941806	K-Ar	6.99	0.16
110	S25-337	44406	dacite Great Mercury Island	1849426	5943803	K-Ar	7.44	0.22
111	S25-335	44407	dacite Great Mercury Island	1848618	5947002	K-Ar	5.76	0.52

112	S25-334	44408	andesite Great Mercury Island		1848416	5947802	K-Ar	8.36	0.26
113	S25-336	44409	dacite Great Mercury Island		1846619	5946497	K-Ar	9.08	0.22
114	S25-328	44384	basalt Opito Bay		1851652	5932704	K-Ar	8.39	0.23
115	S26-49	44387	basalt Opito Bay		1849145	5935099	K-Ar	7.92	0.43
116	S25-333	44410	basaltic andesite Whangapoua		1833342	5934364	K-Ar	8.39	0.21
117	S25-332	44411	basaltic andesite Whangapoua		1833340	5935264	K-Ar	7.88	0.20
118	S31-150	45520	andesite Colville		1815278	5961128	K-Ar	16.16	0.44
119	S30-145	45355	andesite Te Whau Point		1818318	5943833	K-Ar	14.78	0.43
120	S30-341	45362	andesite Matariki Bay		1814773	5918120	K-Ar	12.54	0.33
121	S30-376	45378	andesite Ruffins Peninsula		1824393	5955448	K-Ar	13.86	0.38
122	S31-152	45378	andesite Ruffins Peninsula		1824393	5955448	K-Ar	13.56	0.38
123	S31-149	45376	andesite Puriora Point		1826306	5949952	K-Ar	13.11	0.38
124	S30-144	45359	dacite Ruffins Peninsula		1819952	5928434	K-Ar	14.25	0.77
125	S31-151	45359	dacite Ruffins Peninsula		1819952	5928434	K-Ar	13.90	0.40
126	S30-170	45361	andesite Te Kouma Rd		1820163	5923233	K-Ar	13.92	0.40
127	S30-146	45360	andesite Rangihau Rd		1821261	5924135	K-Ar	14.15	0.34
128	S30-354	45368	andesite Rangihau Rd		1838802	5907168	K-Ar	9.90	0.24
129	S30-362	45366	rhyolite Kaipowai Rd		1839002	5907068	K-Ar	9.18	1.10
130	S30-142	45369	rhyolite Maungatawhiri		1841596	5910675	K-Ar	8.00	0.36
131	S30-165	45352	rhyolite Dalmeny		1843766	5924684	K-Ar	10.82	0.25
132	S30-336	45351	rhyolite Purangi Dome		1847093	5913087	K-Ar	7.85	0.18
133	S30-347	45346	rhyolite Purangi Dome		1848383	5917692	K-Ar	7.26	0.17
134	S31-144	45346	rhyolite Purangi Dome		1848383	5917692	K-Ar	6.54	0.34
135	S31-145	45346	rhyolite dacite		1848383	5917692	K-Ar	7.10	0.17
136	S30-143	45372	Cathedral Cove dacite		1849278	5920094	K-Ar	7.85	0.18
137	S30-355	45372	dacite Cathedral Cove		1849278	5920094	K-Ar	7.67	0.17
138	S30-335	45345	rhyolite Cathedral Cove		1848477	5920793	K-Ar	7.93	0.19
139	S30-169	45371	andesite Hot Water Beach		1851993	5913798	K-Ar	8.75	0.20
140	S30-166	45349	andesite Te Karo Bay		1853211	5905697	K-Ar	8.62	0.22
141	S30-375	45471	andesite Kauaerange Valley		1833135	5889850	K-Ar	9.58	0.23
142	S31-147	45470	andesite Kauaerange Valley		1834132	5891453	K-Ar	10.45	0.27
143	S31-146	45469	andesite Kauaerange Valley		1835330	5892656	K-Ar	13.39	0.31
144	S30-167	45463	dacite Whiritoa (Parakiwai Quarry)		1851477	5872179	K-Ar	5.88	0.14
145	S30-163	45464	rhyolite Te Ananui Beach		1856364	5880192	K-Ar	4.88	0.11
146	S30-164	45464	rhyolite Te Ananui Beach		1856364	5880192	K-Ar	4.87	0.11
147	S30-168	45461	rhyolite Papakura Bay		1856880	5871989	K-Ar	5.45	0.15
148	S31-142	45404	andesite Dohertys Creek (Paeroa)		1840202	5855951	K-Ar	4.03	0.97
149	S31-138	45411	basalt S of Waihi		1847014	5850860	K-Ar	3.96	0.16
150	S31-143	45414	andesite Waitete Hill, Waihi		1849704	5857268	K-Ar	5.89	0.14
151	S31-141	45406	rhyolite Golden Valley		1856301	5860682	K-Ar	5.34	0.13
152	S31-140	45406	rhyolite Golden Valley		1856301	5860682	K-Ar	5.51	0.31

153	S31-139	45416	andesite 2 Rd (Athenree)	1857521	5849879	K-Ar	4.35	0.11
154	S31-133	45467	dacite Waioteariki Ig. (Matamata)	1853973	5818155	K-Ar	2.18	0.15
155	S31-130	45467	dacite Waioteariki Ig. (Matamata)	1853973	5818155	K-Ar	2.13	0.17
156	S31-134	45417	andesite Wharawhara Rd (Katikati)	1852238	5838764	K-Ar	4.34	0.10
157	S31-137	45392	rhyolite Bowentown Heads	1864526	5849391	K-Ar	2.51	0.25
158	S31-135	45392	rhyolite Bowentown Heads	1864526	5849391	K-Ar	2.77	0.31
159	S31-129	45429	dacite Te Puna	1868574	5822682	K-Ar	1.52	0.23
160	S31-132	45421	dacite Mangatawa Quarry	1885985	5822710	K-Ar	2.36	0.08
161	S31-131	45421	dacite Mangatawa Quarry	1885985	5822710	K-Ar	2.28	0.15
Table A1, p. 57-59, Brathwaite & Christie (1996)								
162	17878TR		pyroxene andesite Whakamoehau Stream	1846684	5867067	K-Ar	6.67	0.14
163	17868TR		pyroxene andesite Edmonds Stream	1849385	5867072	K-Ar	6.61	0.12
164	17881TR		pyroxene andesite Golden Cross	1846590	5864166	K-Ar	6.70	0.14
165	17877TR		pyroxene andesite, weak alteration Waiharakeke Stream	1850088	5865973	K-Ar	6.25	0.14
166	17856TR		pyroxene andesite Right Branch Stream	1851390	5865375	K-Ar	5.59	0.21
167	17865R		pyroxene andesite Seaview Bay	1859896	5864191	K-Ar	6.03	0.14
168	17882TR		pyroxene-plagioclase inclusion Seaview Bay	1859896	5864191	K-Ar	5.66	0.20
169	17874TR		pyroxene andesite Bellamys Farm quarry	1854396	5862880	K-Ar	6.16	0.28
170	17866TR		pyroxene andesite Willows Rd	1853696	5862378	K-Ar	6.68	0.13
171	17855bi		hornblende-biotite dacite Cascade Stream	1848793	5862669	K-Ar	7.25	0.20
172	17851hb		hornblende dacite weak alteration Mangakara Stream	1845200	5858161	K-Ar	6.90	0.50
173	17873TR		pyroxene andesite Kurerere Quarry	1836981	5866649	K-Ar	6.96	0.30
174	17872TR		pyroxene andesite Bradshaw Rd	1838886	5864352	K-Ar	7.50	0.28
175	17864TR		pyroxene andesite Komata Reefs Rd	1840590	5862554	K-Ar	7.78	0.17
176	17879TR		pyroxene andesite Kapukapu Stream	1839792	5861452	K-Ar	7.20	0.14
177	17869TR		pyroxene andesite Taraiki Stream	1840297	5858852	K-Ar	6.12	0.18
178	17831TR		pyroxene andesite Tirohia	1835406	5852240	K-Ar	7.06	0.20
179	17862TR		pyroxene andesite Waitoki Stream	1839313	5849646	K-Ar	7.62	0.16
180	17858TR		pyroxene andesite, moderate alteration McBrinn Stream	1843983	5867062	K-Ar	6.68	0.14
181	17863TR		pyroxene andesite, weak alteration Waitekauri Rd	1846091	5863264	K-Ar	7.89	0.14
182	17876TR		pyroxene andesite, weak alteration Grace Darling Stream	1845391	5863063	K-Ar	7.36	0.31
183	17880TR		pyroxene andesite, moderate alteration Barneys Quarry	1846794	5862065	K-Ar	7.94	0.15
184	17867TR		pyroxene andesite Huanui Stream	1844796	5860461	K-Ar	6.59	0.12
185	17837TR		pyroxene andesite, weak alteration Ohinemuri River, Karangahake	1840604	5854851	K-Ar	6.31	0.20
186	17857TR		pyroxene andesite, moderate alteration Mataura Stream	1850594	5862773	K-Ar	6.81	0.14
187	13564TR		pyroxene andesite, weak alteration Gladstone Hill, UW20/140.5	1853204	5857775	K-Ar	6.76	0.25
188	13563TR		pyroxene andesite, weak alteration Bulltown Road Quarry	1851799	5860174	K-Ar	6.54	0.18
189	17836TR		pyroxene andesite, weak alteration Martha Hill Mine, footwall	1851702	5858673	K-Ar	7.36	0.12
190	7873ad		altered andesite with adularia Martha Hill Mine, WHD10/271.2	1851702	5858673	K-Ar	7.23	0.38
191	7872ad		altered andesite with adularia Martha Hill Mine, WHD10/291.5	1851702	5858673	K-Ar	6.58	0.54

192	7874ad	altered andesite with adularia Martha Hill Mine, WHD9/129	1851702	5858673	K-Ar	6.92	0.30
193	17832TR	pyroxene andesite Romaru Stream	1838909	5851546	K-Ar	7.72	0.13
194	17830TR	pyroxene andesite Hotahaka Stream	1840814	5849449	K-Ar	7.28	
195	17861TR	pyroxene andesite, moderate alteration Haehaenga Stream	1842028	5841748	K-Ar	6.65	0.12
Table A2, p. 60-61, Brathwaite & Christie (1996)							
196	17847TR	pyroxene andesite Waitawheta River	1849622	5847263	K-Ar	4.51	0.11
197	17828TR	pyroxene andesite Ananui Stream	1850524	5846164	K-Ar	4.43	0.10
198	19796TR	pyroxene andesite Wharawhara Quarry	1852238	5838563	K-Ar	4.01	0.09
199	19794TR	pyroxene andesite Waihi Stream	1859107	5857986	K-Ar	5.47	0.13
200	17833TR	hornblende andesite Golden Valley	1857101	5860784	K-Ar	5.10	0.12
201	17849hb	hornblende dacite Black Hill	1853305	5857275	K-Ar	4.92	0.50
202	17826TR	pyroxene andesite Trig 1406, Athenree	1858119	5851280	K-Ar	4.70	0.11
203	17845TR	hornblende dacite Athenree	1858922	5849781	K-Ar	4.30	0.19
204	17825TR	hornblende dacite 4 km SW of Waihi	1847706	5855664	K-Ar	5.53	0.09
205	17848hb	hornblende dacite Mangakino Stream	1843815	5849254	K-Ar	5.56	0.35
206	17860TR	pyroxene andesite Waiorongomai Stream	1844326	5843052	K-Ar	5.43	0.12
207	17853hb	hornblende dacite Waipapa Stream	1846926	5843857	K-Ar	5.05	0.25
208	17853bi	hornblende dacite Waipapa Stream	1846926	5843857	K-Ar	4.96	0.22
209	17870TR	pyroxene andesite Waipapa Stream	1846630	5841856	K-Ar	4.72	0.20
210	17871TR	pyroxene andesite Waipapa Stream	1846530	5841555	K-Ar	4.89	0.32
211	17829TR	pyroxene andesite Pohomihhi Stream	1846731	5840755	K-Ar	4.87	0.11
212	17827TR	pyroxene andesite Waitawheta River	1848133	5840257	K-Ar	4.75	0.16
213	17846hb	hornblende andesite Woodlands Rd	1855529	5844872	K-Ar	4.33	0.11
Table A3, p. 62, Brathwaite & Christie (1996)							
214	17850TR	glassy hypersthene rhyolite Bowentown Heads	1864226	5848990	K-Ar	2.89	0.07
215	19795TR	felsitic hypersthene rhyolite Waimata Stream	1851017	5849967	K-Ar	4.06	0.09
216	17834TR	spherulitic biotite rhyolite Homunga Bay	1860301	5861390	K-Ar	5.16	0.20
217	17835TR	spherulitic biotite rhyolite Homunga Bay	1860301	5861390	K-Ar	5.51	0.20
218	19686bi	spherulitic biotite rhyolite Waihi Beach Rd	1858111	5855483	K-Ar	5.30	0.12
219	13652TR	spherulitic biotite rhyolite Baxter Rd, Waihi, PS4/141.6	1854908	5856577	K-Ar	5.28	0.16
Table 3.2, p 49, Krippner (2000)							
220	W99614	ignimbrite Wharepapa Ignimbrite	1840712	5902770	K-Ar	5.38	0.29
221	W99886	ignimbrite Wharepapa Ignimbrite	1844706	5906380	K-Ar	6.18	0.34
222	W99612	ignimbrite Oteao Ignimbrite	1843007	5905476	K-Ar	5.68	0.32
223	W99693	ignimbrite Webb Creek Ignimbrite	1838225	5895662	K-Ar	5.39	0.32
224	W99600	rhyolite Rangihau Rhyolite	1839509	5903868	K-Ar	6.89	0.37
225	W99912	rhyolite Precipice Rhyolite	1841809	5904473	K-Ar	5.12	0.28
226	W99908	rhyolite Precipice Rhyolite	1841809	5904473	K-Ar	5.19	0.42
227	W991002	rhyolite Kokonga Rhyolite	1845211	5903880	K-Ar	6.51	0.36
228	W991005	rhyolite Ruahine Rhyolite	1846113	5903281	K-Ar	5.86	0.31

229	W99835	rhyolite Welcome Jack Rhyolite	1840716	5900769	K-Ar	8.42	0.22
230	W99876	rhyolite Kauaeranga Rhyolite	1838523	5896763	K-Ar	4.90	0.60
231	W99994	rhyolite Camp Rhyolite	1840025	5896266	K-Ar	5.30	0.30
232	W99706	andesite Tauraikau Andesite	1838020	5898063	K-Ar	8.50	0.60
233	W99816	andesite Tauraikau Andesite	1838010	5903165	K-Ar	7.60	0.50
234	W99691	andesite Taurahuehue Andesite	1837825	5895662	K-Ar	6.60	0.30
235	W99733	andesite Tauraikau Andesite	1838012	5902064	K-Ar	6.40	0.40
Table 1, p. 463, Briggs <i>et al.</i> (2005)							
236	411	rhyolite Minden Peak	1868574	5822482	Ar-Ar	2.16	0.03
237	405	rhyolite Kaikaikaroro	1863687	5812568	Ar-Ar	2.39	0.06
238	408	rhyolite Mount Maunganui	1879968	5830406	Ar-Ar	2.35	0.06
239	407	rhyolite Mangatawa	1885985	5822710	Ar-Ar	2.39	0.13
240	410	dacite Upuhue	1887489	5821312	Ar-Ar	2.69	0.04
241	409	rhyolite Papamoa Dome	1889894	5819014	Ar-Ar	2.50	0.03
242	433	dacite Kopukairua	1885091	5819206	Ar-Ar	2.20	
243	416	rhyolite Otanewainuku	1881519	5799486	Ar-Ar	1.95	0.02
244	420	rhyolite Puwhenua	1874116	5797774	Ar-Ar	2.14	0.04
245	431	rhyolite Mount Misery	1880601	5810893	Ar-Ar	2.69	0.03
246	439	dacite/rhyolite Lower Papamoa Ignimbrite	1886891	5819509	Ar-Ar	2.40	0.02
247	432	dacite/rhyolite Upper Papamoa Ignimbrite	1887597	5816508	Ar-Ar	1.90	0.10
248	435	rhyolite Kaimai Dome	1857796	5804354	Ar-Ar	2.86	0.08
249	415	rhyolite Kakahu	1857612	5793447	Ar-Ar	2.87	0.02
250	507	dacite/rhyolite Waiteariki Ignimbrite	1868092	5811374	Ar-Ar	2.09	0.03
251	421	dacite Aongatete Ignimbrite	1855561	5826162	Ar-Ar	3.55	0.05
252	428	dacite Aongatete Ignimbrite	1855561	5826162	Ar-Ar	3.93	0.06